TP 10217E

SUBGRADE DESIGN MODEL EXTENSION

for Canadian Pacific Railways Ltd.
and the Transportation Development Centre
Policy and Coordination Group
Transport Canada

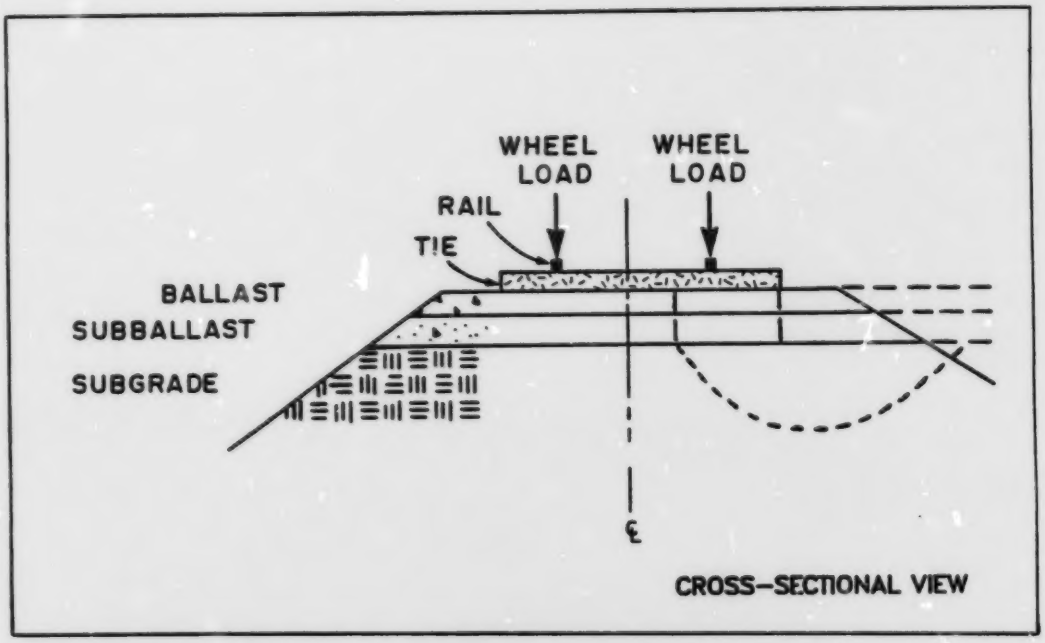

CA1
DTC800-
90
S72

by P.J. Sattler, D.G. Fredlund and V.V. Neis
University of Saskatchewan

41.D

March 1990

DATE DUE

JUL 1 3 1991

TP 10217E

SUBGRADE DESIGN MODEL EXTENSION

FINAL REPORT

CA1
DTC800-
90
S72

458960

41.D

Prepared for

Canadian Pacific Railways Ltd.

and the Transportation Development Centre
Policy and Coordination Group
Transport Canada

by

Pamela J. Sattler
Research Engineer

and

D.G. Fredlund
Professor of Civil Engineering

and

V.V. Neis
Professor of Civil Engineering
University of Saskatchewan
Saskatoon, Saskatchewan
CANADA S7N 0W0

Library and Information Centre / Centre de Documentation (GSLA)
RECEIVED - REÇU LE
JUL 13 1990
Transport Canada / Transports Canada

March 1990

458960

DSU 44178

91-03638/

DISCLAIMER

The contents of this report reflect the current views of the research team at the University of Saskatchewan and not necessarily the official view or opinions of Canadian Pacific Railways or the Transportation Development Centre of Transport Canada.

Un sommaire en français de ce rapport est inclus avant la Table des matières.

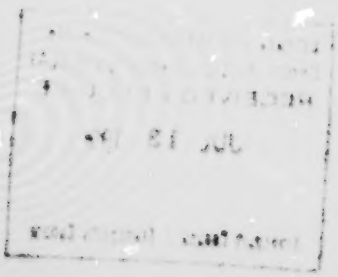

Transport Canada / Transports Canada

PUBLICATION DATA FORM

1. Transport Canada Publication No.	2. Project No.	3. Recipient's Catalogue No.
TP 10217E	7271	

4. Title and Subtitle	5. Publication Date
SUBGRADE DESIGN MODEL EXTENSION	March 1990
	6. Performing Organization Document No.

7. Author(s)	8. Transport Canada File No.
Pamela J. Sattler, D.G. Fredlund and V.V. Neis	D1465-438-4

9. Performing Organization Name and Address	10. DSS File No.
University of Saskatchewan Department of Civil Engineering Saskatoon, Saskatchewan S7N 0W0	15SD.T8200-8-8567
	11. DSS or Transport Canada Contract No.
	T8200-8-8567/01SD

12. Sponsoring Agency Name and Address		13. Type of Publication and Period Covered
Transportation Development Centre 200 René-Lévesque Blvd. West West Tower, Suite 601 Montreal, Quebec H2Z 1X4	CP Rail Gare Windsor C.P. 6042 "A" Montreal,Quebec	Final
		14. Project Officer W.G. Rowan

15. Supplementary Notes (Funding programs, titles of related publications, etc.)

See also **TP 9523E**, "USER'S MANUAL - GEOTRACK AND GEOPLOT STRESS, BEARING AND COMPARE", Second Edition.

16. Abstract

The objective of this third stage of a four-stage research program is to extend the subgrade design model to accommodate embankment side slopes. The previous two stages of the overall program were devoted to the measurement of the matric suction in the subgrade of a track structure and the incorporation of the matric suction term into a bearing capacity design procedure. The current study investigates the effect of embankment side slope on bearing capacity employing slope stability analyses for soils with negative pore-water pressures. A parametric study revealed that side slopes have little effect on the vertical, horizontal and shear stress distributions beneath the loaded structure.

Three observations were noted with respect to bearing capacity:

1) bearing capacity decreases with a large inclination of slope, particularly in granular materials;
2) bearing capacity decreases with overall height of a slope, particularly in cohesive materials; and
3) bearing capacity becomes independent of slope height at greater distances from the edge of the slope.

Slope stability analysis should be used to complement bearing capacity analyses when designing railway embankments.

17. Key Words	18. Distribution Statement
Rail track ballast; subballast; subgrade; soil mechanics; soil suction; modelling; load bearing capacity	Limited number of copies available on request from the Transportation design Development Centre.

19. Security Classification (of this publication)	20. Security Classification (of this page)	21. Declassification (date)	22. No. of Pages	23. Price
Unclassified	Unclassified	-	131+App.	-

TDC/CDT 79-003
Rev 88

Canada

Transports Canada Transport Canada

FORMULE DE DONNÉES POUR PUBLICATION

1. N° de la publication de Transports Canada	2. N° de l'étude	3. N° de catalogue du destinataire
TP 10217E	7271	

4. Titre et sous-titre	5. Date de la publication
SUBGRADE DESIGN MODEL EXTENSION	mars 1990
	6. N° du document de l'organisme exécutant

7. Auteur(s)	8. N° de dossier — Transports Canada
Pamela J. Sattler, D.G. Fredlund et V.V. Neis	D1465-438-4

9. Nom et adresse de l'organisme exécutant	10. N° de dossier — ASC
University of Saskatchewan Department of Civil Engineering Saskatoon (Saskatchewan) S7N 0W0	15SD.T8200-8-8567
	11. N° de contrat — ASC ou Transports Canada T8200-8-8567/01SD

12. Nom et adresse de l'organisme parrain		13. Genre de publication et période visée
Centre de développement des transports 200 ouest, boul. René-Lévesque Tour ouest, suite 601 Montréal (Québec) H2Z 1X4	CP Rail Gare Windsor C.P. 6042 "A" Montréal(Québec)	final
		14. Agent de projet W.G. Rowan

15. Remarques additionnelles (Programmes de financement, titres de publications connexes, etc.)
Voir aussi **TP 9523E**, "USER'S MANUAL - GEOTRACK AND GEOPLOT STRESS, BEARING AND COMPARE, Second Edition".

16. Résumé

Le présent rapport concerne la troisième étape d'un programme de recherche en quatre étapes, dont le but a été d'intégrer un modèle de calcul en remblai le facteur déclivité des talus de plates-formes ferroviaires. Les deux étapes précédentes auraient permis de mesurer la succion capillaire d'un sol support et de développer une méthode de calcul de la portance qui tienne compte de cette succion. Le présent rapport concerne l'étude de l'influence de la déclivité d'un talus sur la portance, utilisant des analyses de stabilité à des pressions d'eau interstitielle négatives. Une étude paramétrique a montré que la déclivité des talus a peu d'influence sur la distribution des contraintes verticales, horizontales et de cisaillement sous l'infrastructure de la voie ferrée.

En ce qui concerne la portance des sols supports, trois observations ont été faites:

1) la portance diminue lorsque la déclivité est forte, surtout dans le cas d'un sol à cohésion faible
2) la portance diminue avec la hauteur du talus, surtout dans le cas d'un sol à cohésion forte, et
3) la portance s'affranchit de la hauteur du talus d'antant plus que l'on s'éloigne de ce dernier.

Il est recommandé que les études sur la portance des sols supports tiennent compte de la stabilité des talus lorsqu'il s'agit de dimensionner des plates-formes ferroviaires en remblai.

17. Mots clés	18. Diffusion
Ballast, sous-couche, sol support, mécanique des sols, modélisation, portance.	Le Centre de développement des transports dispose d'un nombre limité d'exemplaires.

19. Classification de sécurité (de cette publication)	20. Classification de sécurité (de cette page)	21. Déclassification (date)	22. Nombre de pages	23. Prix
Non classifiée	Non classifiée	-	131+App.	-

CDT/TDC 79-005
Rev 88

Canada

ACKNOWLEDGEMENTS

The authors wish to acknowledge the financial contributions provided by Canadian Pacific Railways and the Transportation Development Centre which have made this research possible.

The authors wish to acknowledge the co-operation of Harry E. Stewart in the modification of the GEOTRACK computer program.

Sincere thanks are extended to Julian Gan for his assistance in operating the PC-SIGMA computer program. The efforts of Leonard Lam and Darrell McClarty in making the enhancements to the GEOTRACK computer program are gratefully appreciated.

Sincere appreciation is extended to Mr. M.J. Klassen of Canadian Pacific Railways for the contribution of his time and effort toward the completion of this study.

The suggestions and recommendations for computer model enhancements by Mr. W.G. Rowan of the Transportation Development Centre are gratefully acknowledged.

EXECUTIVE SUMMARY

This report presents the third stage of a four-stage research program proposed by Dr. D.G. Fredlund at the University of Saskatchewan to investigate the role played by soil suction in the behavior and design of track systems. The first stage was devoted to the investigation of suitable methods for the measurement of soil suction. A bearing capacity approach to the design of railway subgrades was developed in the second phase of the research program. The primary objective of the current research is to extend the subgrade design model to accommodate embankment side-slopes.

The bearing capacity design procedure utilizes a comparison between subgrade bearing capacity (i.e., computed from subgrade shear strength parameters) and stress distribution beneath the loaded track structure (i.e., computed by the GEOTRACK computer program) to provide a measure of the factor of safety against a bearing capacity type failure.

Originally, the emphasis was to be placed on modification of the GEOTRACK computer program to accommodate embankment side-slopes. However, a parametric study revealed that embankment side-slopes have little effect on the vertical, horizontal and shear stress distributions beneath the loaded structure. Therefore, the study was extended to more completely investigate the effect of embankment side-slope on bearing capacity. Slope stability

analyses for soils with negative pore-water pressures were used to complement the study.

Three observations were noted with respect to bearing capacity: 1) bearing capacity decreases with a large inclination of slope, particularly in granular materials; 2) bearing capacity decreases with overall height of a slope, particularly in cohesive materials; and 3) bearing capacity becomes independent of slope height at greater distances from the edge of the slope. Early approaches which have been taken to account for embankment side-slopes include the modification of the bearing capacity factors applied to the individual terms of the conventional bearing capacity equation. Recent research suggests the use of a completely new approach using elasto-plastic soil mechanics theory. Both approaches are presented and discussed in this report.

Slope stability analyses should be used to complement bearing capacity analyses when designing railway embankments. Slope stability analyses can be conducted for embankments with either positive or negative pore-water pressures or a combination thereof. Saturated-unsaturated seepage analyses can also be used to play an important role in embankment design.

SOMMAIRE

Le rapport présente le résultat de la troisième des quatre étapes du programme de recherche proposé par le professeur D.G. Fredlund du groupe géotechnique de l'Université de la Saskatchewan à Saskatoon dans le but d'approfondir l'influence de la succion capillaire sur le comportement des sols supports des voies ferrées et, partant, sur la conception de celles-ci. La première étape du programme avait porté sur l'étude de méthodes permettant de mesurer la succion in situ. Cette étape a été suivie d'une deuxième portant, elle, sur une méthode de calcul de la portance des sous-couches des voies ferrées. Quant à la troisième étape, elle a pour but d'étendre ce concept aux talus des plates-formes.

En comparant la portance du sol support, calculée à partir des paramètres de résistance au cisaillement, à la courbe de distribution des contraintes qui sollitent la voie ferrée chargée, connue grâce au programme informatique GEOTRACK, il est possible de tirer un ordre de grandeur de la marge de sécurité contre le dépassement de la portance du sol support.

Au départ, on avait pensé modifier le programme informatique GEOTRACK dans ce but, mais une étude paramétrique a montré que la déclivité des talus avait peu d'influence sur la distribution des contraintes verticales, horizontales et de cisaillement sollicitant la voie ferrée. D'où la décision d'infléchir la recherche vers l'étude approfondie de l'influence de la déclivité des talus sur la portance des sol supports. Des analyses sur la stabilité des talus de remblais ayant des pressions d'eau interstitielle négatives ont étayé la présente recherche.

En ce qui concerne la portance des sols supports, trois observations ont été faites:

1) la portance diminue lorsque la déclivité est forte, surtout dans le cas d'un sol à cohésion faible;
2) la portance diminue avec la hauteur du talus, surtout dans le cas d'un sol à cohésion forte, et
3) la portance s'affranchit de la hauteur du talus d'antant plus que l'on s'éloigne de ce dernier.

Les méthodes antérieures qui prenaient en compte la déclivité des talus ont été affinées en modifiant les facteurs de sécurité compris dans l'équation classique sur la portance des sols supports. Les recherches récentes favorisent une méthode complètement différente faisant appel à la théorie d'élastoplasticité des sols. Le rapport aborde ces deux rapports méthodes et les explique.

Il est recommandé que les études sur la portance des sols supports tiennent compte de la stabilité des talus lorsqu'il s'agit de dimensionner des plates-formes ferroviaires en remblai, les études correspondantes devant être menées à des pressions d'eau interstitielle tant positives que négatives, voire une combinaison des deux. Des analyses de la succion dans des sols saturés ou non saturés pourront également servir au dimensionnement des remblais.

TABLE OF CONTENTS

1.0 INTRODUCTION.....1

2.0 OBJECTIVES.....5

3.0 SCOPE.....6

4.0 STRESS ANALYSES.....7
- 4.1 Use of the GEOTRACK Program for Computation of Stress.....15
- 4.2 Results of 2-D Stress Analysis.....24
- 4.3 Comparison of 2-D Stress Analyses and GEOTRACK Results.....40
- 4.4 Conclusions of the Stress Analysis Study.....54

5.0 BEARING CAPACITY ANALYSES.....56
- 5.1 Modification of Conventional Bearing Capacity for Layered Systems.....64
- 5.2 Incorporation of Unsaturated Soil Mechanics in Conventional Bearing Capacity Theory.....76
- 5.3 Influence of Embankment Side-Slopes on the Computation of Conventional Bearing Capacity.....82
- 5.4 Conclusions Based on the Bearing Capacity Analysis.....101

6.0 SLOPE STABILITY ANALYSES.....103
- 6.1 Slope Stability Analyses for Soils with Negative Pore-Water Pressures.....110
- 6.2 Slope Stability Analyses for Railway Embankments.....119
- 6.3 Conclusions of Slope Stability Analyses.....123

7.0 CONCLUSIONS.....124

References.....127

Appendix A: Comparison of GEOTRACK Stress Distribution at Various Embankment Side-Slopes, Computer Output

Appendix B: Slope Stability with Negative Pore-Water Pressures, Computer Output

LIST OF FIGURES

Fig. 4.1 Stress distribution for a particulate system (Spangler and Handy, 1982).....8

Fig. 4.2 Distribution of vertical pressure below a concentrated load at the ground surface (Spangler and Handy, 1982).....10

Fig. 4.3 Contours of equal vertical stress under a loaded area of width B according to Boussinesq analysis (Spangler and Handy, 1982).....11

Fig. 4.4 Contours of equal vertical pressure in relation to a 2:1 slope (Spangler and Handy, 1982).....13

Fig. 4.5 The 2:1 method for computing stress distribution beneath an applied load (Broms, 1965).....14

Fig. 4.6 Forces and elements in the GEOTRACK model (Chang, Adegoke and Selig, 1980).....18

Fig. 4.7 Vertical stress distribution computed by the GEOTRACK model.....20

Fig. 4.8 Horizontal stress distribution computed by the GEOTRACK model.....21

Fig. 4.9 Shear stress distribution computed by the GEOTRACK model.....22

Fig. 4.10 Bulk stress computed by the GEOTRACK model.....23

Fig. 4.11 Vertical stress distribution for zero embankment side-slope by PC-SIGMA computer model.....25

Fig. 4.12 Horizontal stress distribution for zero embankment side-slope by PC-SIGMA computer model.....26

Fig. 4.13 Shear stress distribution for zero embankment side-slope by PC-SIGMA computer model.....27

Fig. 4.14 Vertical stress distribution for 1:1 embankment side-slope by PC-SIGMA computer model.....28

Fig. 4.15 Horizontal stress distribution for 1:1 embankment side-slope by PC-SIGMA computer model.....29

Fig. 4.16 Shear stress distribution for 1:1 embankment side-slope by PC-SIGMA computer model.....30

Fig. 4.17 Vertical stress distribution for 0.5:1 embankment side-slope by PC-SIGMA computer model.....32

Fig. 4.18 Horizontal stress distribution for 0.5:1 embankment side-slope by PC-SIGMA computer model.....33

Fig. 4.19 Shear stress distribution for 0.5:1 embankment side-slope by PC-SIGMA computer model.....34

Fig. 4.20 Vertical stress distribution for 0.25:1 embankment side-slope by PC-SIGMA computer model.....35

Fig. 4.21 Horizontal stress distribution for 0.25:1 embankment side-slope by PC-SIGMA computer model.....36

Fig. 4.22 Shear stress distribution for 0.25:1 embankment side-slope by PC-SIGMA computer model.....37

Fig. 4.23 Comparison of vertical stress distribution for various slope angles.....38

Fig. 4.24 Comparison of horizontal stress distribution for various slope angles.....39

Fig. 4.25 Comparison of shear stress distribution for various slope angles.....41

Fig. 4.26 Comparison of GEOTRACK vertical stress distribution to PC-SIGMA for zero embankment slope.....42

Fig. 4.27 Comparison of GEOTRACK horizontal stress distribution to PC-SIGMA for zero embankment slope.....43

Fig. 4.28 Comparison of GEOTRACK shear stress distribution to PC-SIGMA for zero embankment slope.....44

Fig. 4.29 Comparison of GEOTRACK vertical stress distribution to PC-SIGMA for 1:1 embankment slope.....45

Fig. 4.30 Comparison of GEOTRACK horizontal stress distribution to PC-SIGMA for 1:1 embankment slope.....46

Fig. 4.31 Comparison of GEOTRACK shear stress distribution to PC-SIGMA for 1:1 embankment slope.....47

Fig. 4.32 Comparison of GEOTRACK vertical stress distribution to PC-SIGMA for 0.5:1 embankment slope.....48

Fig. 4.33 Comparison of GEOTRACK horizontal stress distribution to PC-SIGMA for 0.5:1 embankment slope.....49

Fig. 4.34 Comparison of GEOTRACK shear stress distribution to PC-SIGMA for 0.5:1 embankment slope.....50

Fig. 4.35 Comparison of GEOTRACK vertical stress distribution to PC-SIGMA for 0.25:1 embankment slope.....51

Fig. 4.36 Comparison of GEOTRACK horizontal stress distribution to PC-SIGMA for 0.25:1 embankment slope.....52

Fig. 4.37 Comparison of GEOTRACK shear stress distribution to PC-SIGMA for 0.25:1 embankment slope.....53

Fig. 5.1 Modes of bearing capacity failure - general shear failure (after Vesic, 1973).....57

Fig. 5.2 Modes of bearing capacity failure - local shear failure (after Vesic, 1973).....58

Fig. 5.3 Modes of bearing capacity failure - punching shear failure (after Vesic, 1973).....59

Fig. 5.4 Idealized bearing capacity failure geometry for Prandtl log-spiral (Spangler and Handy, 1982)...61

Fig. 5.5 Cross-sectional view of the track system showing the geometry perpendicular to the track.....66

Fig. 5.6 Longitudinal view of the track system showing the geometry parallel to the track.....67

Fig. 5.7 Failure geometry for the complete tie-track system for the length of the track.....68

Fig. 5.8 Failure geometry for the heavily stressed outer third of the tie and the distance of a double truck loading.....69

Fig. 5.9 Failure geometry for the local failure of an individual tie punching into a weak subgrade....70

Fig. 5.10 Failure geometry for a portion of the track beneath a double truck arrangement for weak subgrades.....71

Fig. 5.11 Broms' approach to computing bearing capacity (after Broms, 1965).....73

Fig. 5.12 Hanna and Meyerhof approach to computing bearing capacity (Hanna and Meyerhof, 1980).....75

Fig. 5.13 Effect of partial submergence on bearing capacity (Meyerhof, 1955).....77

Fig. 5.14 Typical schematic pore-water pressure profiles.79

Fig. 5.15 Components of the total cohesion term for unsaturated soils.....80

Fig. 5.16 Schematic of the failure zone for a footing at the crest of slope (Graham, Andrews and Shields, 1988).....83

Fig. 5.17 Bearing capacity of a foundation on the **face** of a slope (Meyerhof, 1957).....85

Fig. 5.18 Bearing capacity of a foundation on the **top** of a slope (Meyerhof, 1957).....86

Fig. 5.19 Bearing capacity factor for a strip foundation on the **face** of a slope of purely **cohesive** material (Meyerhof, 1957).....88

Fig. 5.20 Bearing capacity factor for a strip foundation on the **face** of a slope of purely **cohesionless** material (Meyerhof, 1957).....89

Fig. 5.21 Bearing capacity factor for a strip foundation on the **top** of a slope of purely **cohesive** material (Meyerhof, 1957).....90

Fig. 5.22 Bearing capacity factor for a strip foundation on the **top** of a slope of purely **cohesionless** material (Meyerhof, 1957).....91

Fig. 5.23 Contours of theoretical N_q values (Shields et al, 1977).....94

Fig. 5.24 Contours of experimental N_q values (Shields et al, 1977).....95

Fig. 5.25 Experimental N_q contours for vertical loading (Bauer et al, 1981).....96

Fig. 5.26 Schematic of failure zone for embedment and set-back (Graham, Andrews and Shields, 1988)...98

Fig. 5.27 Predicted N_q values (Graham, Andrews and Shields, 1988).....99

Fig. 5.28 Comparison of predicted and experimental N_q values for B = 300 m (Graham, Andrews and Shields, 1988).....100

Fig. 6.1 Concept of slope stability in a purely frictional material.....104

Fig. 6.2 Concept of slope stability in a slope of infinite extent (Spangler and Handy, 1982).....105

Fig. 6.3 Forces acting upon an individual slice of a sliding mass of soil.....108

Fig. 6.4 Three-dimensional failure surface for an unsaturated soil.....112

Fig. 6.5 Mohr circles at failure for an unsaturated soil.....113

Fig. 6.6 Relationship between cohesion, matric suction and the angle ϕ^b (Fredlund, 1987).....115

1.0 INTRODUCTION

In 1982, Professor D.G. Fredlund of the Geotechnical Group at the University of Saskatchewan, Saskatoon, Saskatchewan proposed a four-stage research program to develop a better understanding of the role played by soil suction in the behavior and design of track system subgrades.

The first stage was undertaken jointly with Clifton Associates Ltd., Regina, Saskatchewan, for the Transportation Development Centre, Canadian National Railways, and Canadian Pacific Railways. This stage of the four-stage research program was devoted to the investigation of suitable methods for measuring soil suction in the field (van der Raadt and Clifton, 1985). Soil suction data was collected on a continuing basis from five field sites in western Canada using a thermal conductivity sensor[1].

Each site was instrumented with six thermal conductivity sensors at pre-determined horizontal locations below the top of the subgrade. A corrugated metal culvert which was installed vertically and directly adjacent to the track structure served to house the data acquisition system and to provide access to the sensor ports. Results indicated that

[1] manufactured by Agwatronics Incorporated, Merced, California.

reliable measurements of matric suction up to a maximum of about 250 kPa could be obtained with the thermal conductivity sensor. A Masters thesis (van der Raadt, 1988) was produced which documents the complete results of the matric suction measurements.

Problems which were identified with the sensor installation procedure by van der Raadt (1988) (i.e., water accumulation in the culvert causing sensor malfunction) have been addressed in more recent sensor installations beneath the railway track system (Sattler and Fredlund, 1989b). Eighteen thermal conductivity sensors were installed beneath the Canadian Pacific Railways Ltd. Emerson Subdivision trackage during the fall of 1989 utilizing a backhoe trencher and small hand auger. Special precautions were exercised in the backfilling of the auger hole behind the sensor as well as the backhoe trench in order to eliminate water migration along the sensor lead wires (Sattler and Fredlund, 1989b).

Continuing research at the University of Saskatchewan is devoted to the measurement of matric suction both insitu and in the laboratory. The calibration procedure for the thermal conductivity sensor has been developed and documented at the University of Saskatchewan (Wong and Ho, 1987; Fredlund and Wong, 1988; Wong et al, 1990). Techniques for the measurement of soil suction in the laboratory on Shelby tube samples derived from the field have been examined (Sattler and Fredlund, 1989).

Improvements to the techniques for measuring soil suction is a topic of continuing interest at the University of Saskatchewan.

Having studied techniques and procedures for measuring soil suction in the first stage of the program as well as other related research activities, the second stage of the research concentrated on the incorporation of the soil suction term into a workable design procedure. A bearing capacity approach for design of railway subgrades was developed during the second stage (Sattler and Fredlund, 1988) as part of a joint research contract between the University of Saskatchewan, Transportation Development Centre, Canadian Pacific Railways, and Canadian National Railways. This approach to the design of railway subgrades utilized a comparison between stress analysis techniques for railway tie-track-subgrade systems and conventional bearing capacity modified for layered systems. Analyses of laboratory matric suction measurements on Shelby tube samples derived from the Canadian Pacific Railways Ltd. Emerson Subdivision Floodway Trackage near Winnipeg, Manitoba illustrated the significance of utilizing matric suction in the bearing capacity design procedure (Clifton, Lam and Sattler, 1988).

The design approach which was developed utilized a bearing capacity approach in which the strength of the unsaturated soil subgrade is related to the stress state, material parameters, soil suction and failure geometry. Two

methods were proposed for the estimation of the bearing capacity beneath a loaded tie-track system: 1) the Meyerhof and Hanna approach (1980) applying primarily to weak clay subgrades, and 2) the Broms' approach (1965) applicable to stronger clay, glacial till, silt and sand subgrades (Sattler and Fredlund, 1988).

The stresses beneath the loaded track system were calculated from the computer program, GEOTRACK, which combines the stiffness matrix of the tie-track system with a Boussinesq stress distribution in the ballast-subballast-subgrade system. The estimated bearing capacity of the subgrade system was compared to an average stress value representing the vertical stress distribution beneath the loaded track structure. The result was bearing capacity factor of safety design charts for various combinations of axle load, loading configuration, soil parameters and soil suction (Sattler and Fredlund, 1988). The design approach did not consider side-slopes on embankments.

The objective of the current research contract between the University of Saskatchewan, Canadian Pacific Railways and the Transportation Development Centre was to extend the subgrade bearing capacity design approach to accommodate steep embankment slopes. Originally, it was decided that the emphasis would be placed on the stress analysis part of the bearing capacity approach. Initial results of the research in the area of stress analysis showed that the magnitude of the embankment slope had little effect on the

stress analysis results. At the same time, the magnitude of the embankment slope significantly affects the computation of bearing capacity. In order to accomplish the stated objective to modify the approach for embankment slopes, bearing capacity and slope stability analyses considering side-slopes on embankments were investigated in further detail.

2.0 OBJECTIVES

The objective of the current research was to extend the bearing capacity design approach for railway subgrades in order to accommodate embankment side-slopes. Originally, the emphasis was to be placed on the stress analysis portion of the bearing capacity approach, but initial research indicated that embankment side-slopes had little effect on the outcome of the stress analysis. Consequently, the final emphasis was placed upon investigation of effect of embankment side-slopes upon computed bearing capacity. Slope stability analyses for soils with negative pore-water pressures were also given consideration in this study.

3.0 SCOPE

In the extension of the bearing capacity design procedure for embankment side-slopes, three methods of analysis were utilized: 1) stress analysis, 2) bearing capacity analyses, and 3) slope stability analyses.

The GEOTRACK computer program was compared to two-dimensional finite element analyses in order to determine the significance of changes in the embankment side-slopes on the stress analysis. Modifications to the GEOTRACK computer program were made for the computation of stresses along sloped offsets (i.e., for comparison to embankment side-slopes).

An investigation was conducted into the methods for evaluating bearing capacity on sloped surfaces. The problems addressed were: 1) the separation of bearing capacity and slope stability problems, 2) the complementary relationship between slope stability and bearing capacity, 3) the theory of bearing capacity for sloped surfaces, and 4) the modifications required for the computation of bearing capacity on sloped surfaces.

Slope stability analyses were used to complement the bearing capacity analyses. Slope stability analyses for soils with negative pore-water pressures were investigated as a final addition to the research.

4.0 STRESS ANALYSES

The concept of stress distribution beneath the ground surface is illustrated for a particulate arrangement in Figure 4.1. A point load of an intensity equal to 1.0 is distributed 1/4 to each of the particles in the second layer and so on throughout the depth. By a process of successively distributing the load from layer to layer, the bell-shaped curve at the bottom of the diagram is developed to describe the spreading of the point load with depth. The highest stress intensity is located directly beneath the load (Spangler and Handy, 1982).

Although the concept described above (i.e., "particulate theory") is valid, classical soil mechanics assumes that although the soil is particulate it behaves as a homogeneous continuum with elastic properties. Results from the two theories are similar, but "continuum elastic theory" is the convention adopted in classical soil mechanics (Spangler and Handy, 1982).

The study of the distribution of stress through elastic media is credited to a French mathematician in 1885 known as Boussinesq. Boussinesq assumed an infinite half-space of ideally elastic, homogeneous, isotropic material. Although soil is known to be non-elastic, non-homogeneous, and non-isotropic, the classical Boussinesq solution serves as a reasonably good guide for the determination of stresses beneath a load, when properly applied in engineering

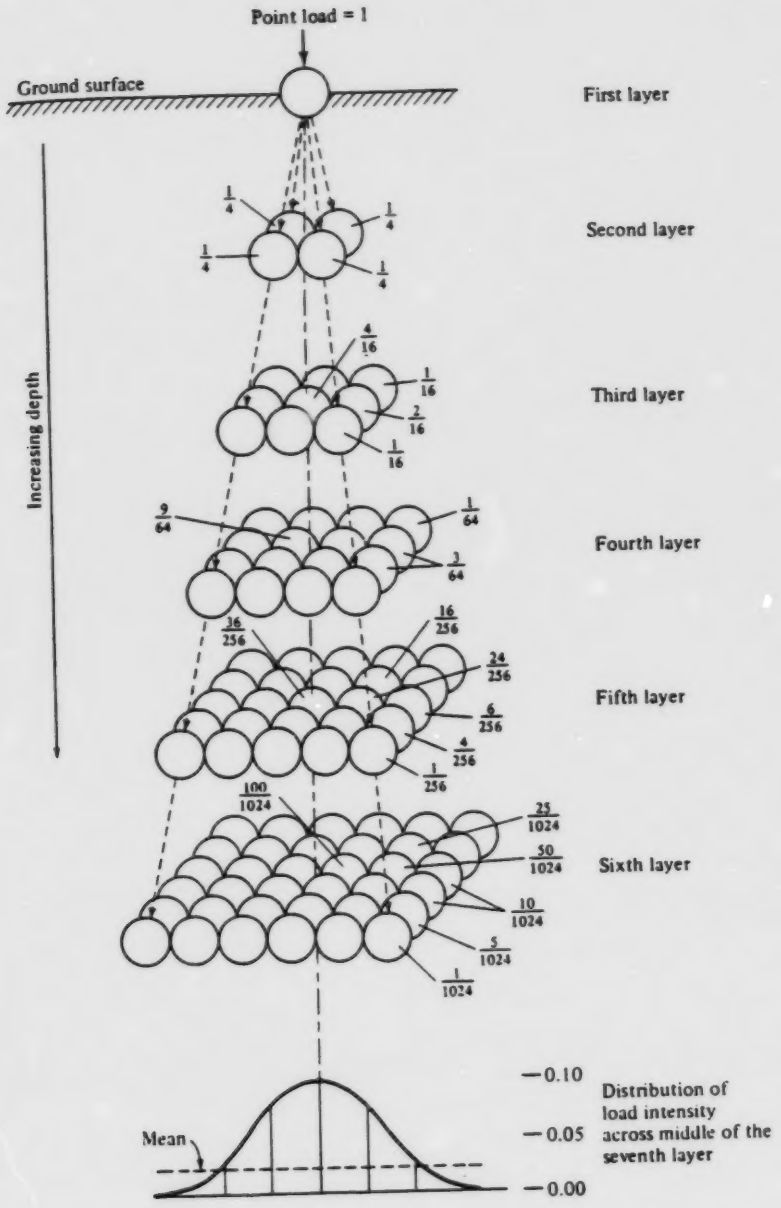

Fig. 4.1 Stress distribution for a particulate system (Spangler and Handy, 1982)

practice (Spangler and Handy, 1982). The Boussinesq solution has been extended to layered analyses by Burmister (1943) and was used for the formulation of the GEOTRACK computer program (Chang, Adegoke and Selig, 1980).

The distribution of the vertical pressure on any horizontal plane below a concentrated load at the ground surface is represented by a bell-shaped surface as shown in Figure 4.2. If the stress surface is plotted for a series of horizontal planes at various depths and if points of equal stress on the various planes are connected, a "pressure bulb" is developed. The pressure at each point on the bulb is the same. Pressures inside the bulb are greater than pressures on the bulb or pressures outside the bulb (Spangler and Handy, 1982).

Figure 4.3 illustrates a series of pressure bulbs for two types of foundations of width, B, with applied load, q: 1) an infinitely long foundation, and 2) a square foundation. The pressure bulbs for each example are symmetrical about the centerline (Spangler and Handy, 1982). The diagram for the infinitely long foundation (i.e., a strip footing) shows that at a distance 2B from the center of the footing and at a depth B, the stress has dissipated to 3% of q, the load applied at the surface. At a distance equal to 3B from the center of the footing and at a depth B, the stress has dissipated to less than 1% of the surface applied load, q. For the square foundation, the stress at

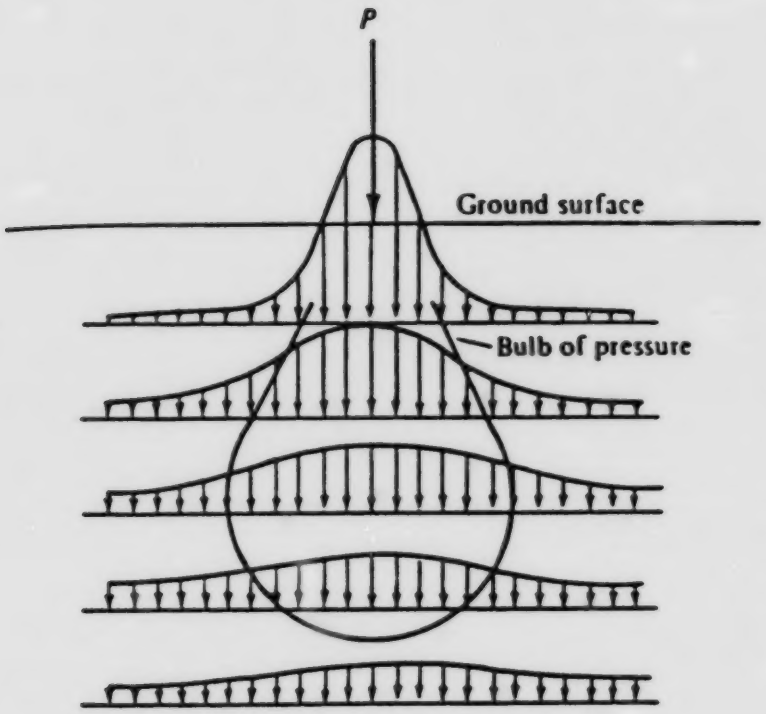

Fig. 4.2 Distribution of vertical pressure below a concentrated load at the ground surface (Spangler and Handy, 1982)

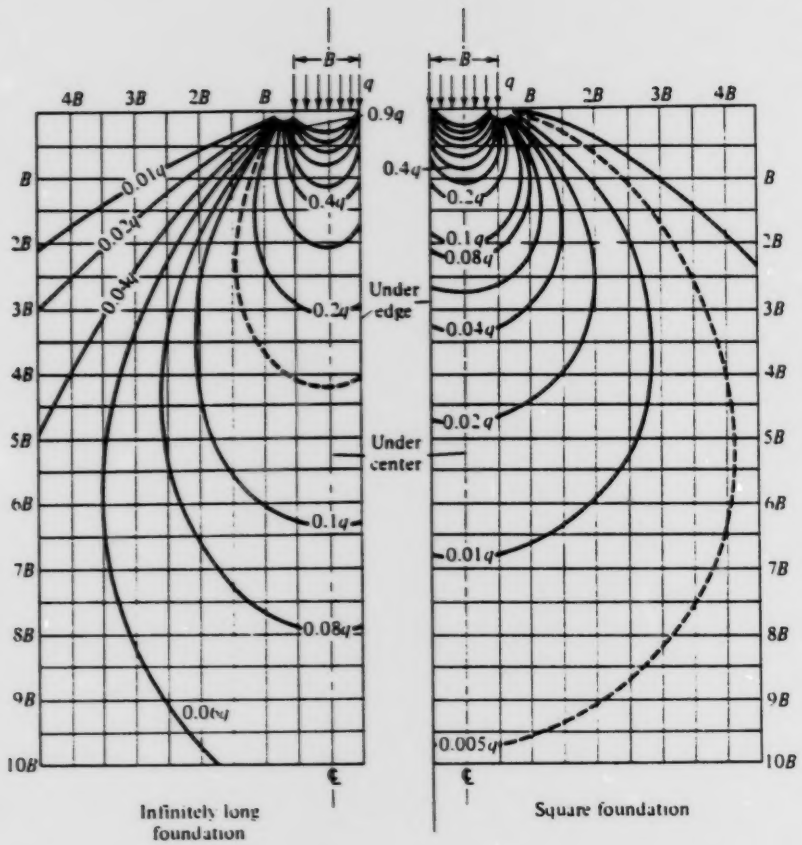

Fig. 4.3 Contours of equal vertical stress under a loaded area of width B according to Boussinesq analysis (Spangler and Handy, 1982)

depth B and distance 2B from the center of the footing is 1% of the surface applied load.

If a 2:1 slope (i.e., 2 horizontal to 1 vertical) were extended out from the edge of the infinitely long footing, only 3% of the applied load would be located above the sloped line (Figure 4.4). Therefore, 97% of the total applied load would be distributed to the soil within the area defined by an embankment slope with sides in the ratio of 2 horizontal to 1 vertical. For a square foundation, 99% of the total applied load would be distributed to the soil within the area defined by an embankment slope with sides in the ratio of 2:1. The 2:1 slope used for the example represents an embankment slope of 30 degrees, a relatively common embankment slope. The example illustrates the insignificance of typical embankment side-slopes on the computed stress distribution beneath an applied load.

Another approximate method for computing the stress distribution beneath an applied load is the 2:1 method (Figure 4.5) (Spangler and Handy, 1982). If the load is applied over an area with dimensions A and B, the stress on the soil at depth H is assumed to be uniformly distributed on an area with dimensions (A+H) by (B+H). The assumed angle of spreading corresponds to a slope somewhat greater than 60 degrees. Figure 4.3 indicates that for a square footing about 94% of the applied load is distributed within the area (A+H) multiplied by (B+H) at depth H. Since embankment side-slopes are typically less than 60 degrees,

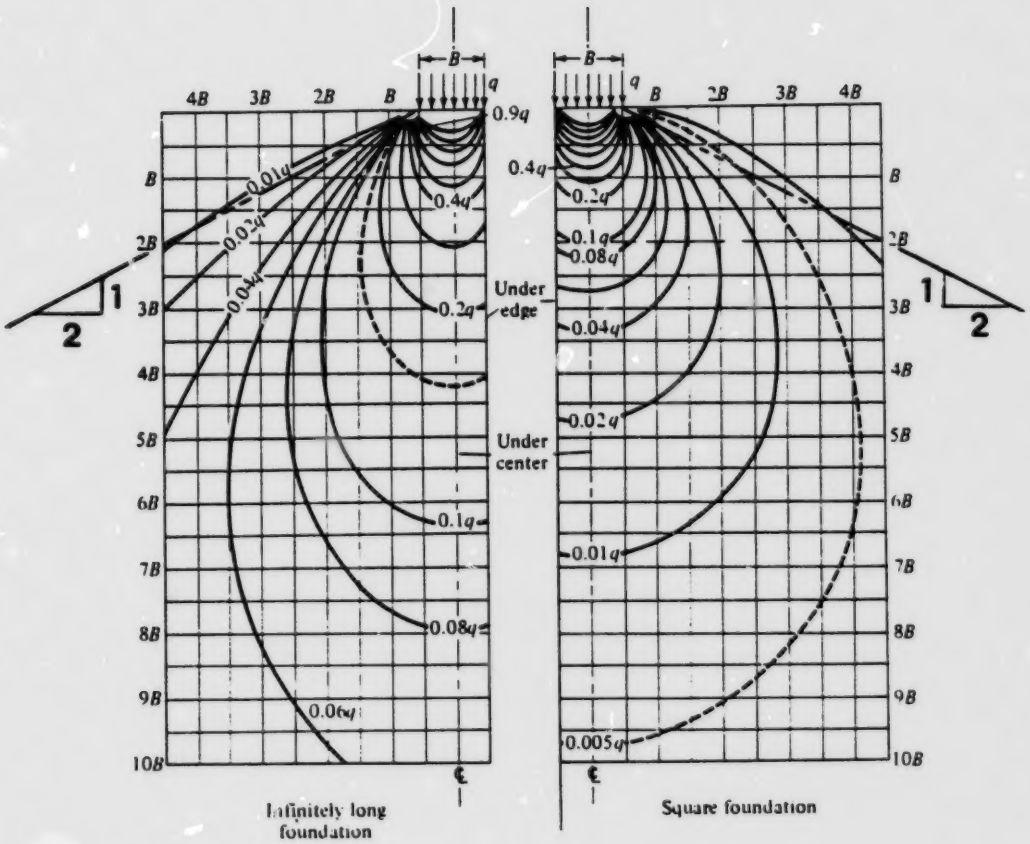

Fig. 4.4 Contours of equal vertical pressure in relation to a 2:1 slope (after Spangler and Handy, 1982)

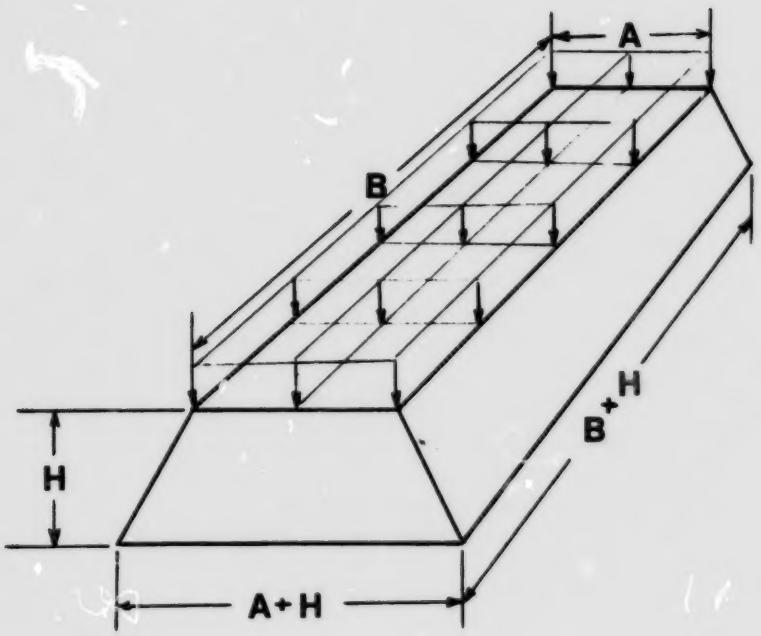

Fig. 4.5 The 2:1 method for computing stress distribution beneath an applied load (Broms, 1965)

greater than 94% of the applied load will be distributed to the depth H.

The simplified illustrations and examples from the preceding discussion illustrate that embankment side-slopes have little effect on stress distribution computations. In order to verify the simplified results, a parametric study was undertaken using a finite element computer program called PC-SIGMA (Fredlund, 1989). The results of the GEOTRACK stress analysis and the finite element stress analysis and their comparative results are presented in the following sections.

4.1 Use of the GEOTRACK Program for Computation of Stress

The 2:1 method for stress distribution (i.e., as presented in Chapter 4.0) was adopted by Broms (1965) in his approach to the computation of bearing capacity. In the application of the Broms' approach to the design of railway subgrades (Sattler and Fredlund, 1988), the GEOTRACK stress distribution was used rather than the conventional 2:1 method employed by Broms. Using the 2:1 method (i.e., which corresponds to an approximate slope of 60 degrees), Figure 4.3 illustrates that for a square foundation about 94% of the applied load is distributed to the enlarged area at depth H while for an infinitely long foundation about 80% of the applied load will be distributed at the depth H. This observation implies that as the shape of the foundation

becomes more like a strip footing and less like a square, the 2:1 method becomes less adequate in the distribution of stresses to greater depths. The dimensions used for the computation of bearing capacity for a rail-track system more closely resemble a strip footing than a square foundation. Therefore, the conventional 2:1 method for stress distribution could not be used.

In the application of the Broms' approach (1965) to the design of railway subgrades, Broms' **concept** of distributing the stress from the applied load through the ballast and subballast material and then computing bearing capacity from conventional equations was used (Sattler and Fredlund, 1988). The actual dimensions of the tie-track system were used with the computed stress distribution from the applied loads as calculated by the GEOTRACK computer program (Sattler and Fredlund, 1988).

The GEOTRACK computer program uses classical "elastic theory" in which the ballast, subballast, and subgrade soil are represented as linear, elastic layers each specified by a separate modulus of elasticity and Poisson's ratio. The soil layers are infinite in the horizontal plane and are situated on a half-space, which is infinite in both the horizontal and vertical directions. The rails and ties are represented by linear elastic beams with a specified modulus of elasticity, cross-sectional area, and moment of inertia (Chang, Adegoke and Selig, 1980).

Stress is distributed from the rail to the tie and from the tie to the ballast in the form of concentrated reactions as illustrated in Figure 4.6. The concentrated reactions at the ballast surface are then distributed throughout the ballast, subballast, and subgrade layers based on Burmister's (1943) adaption of the Boussinesq stress distribution for layered systems (Chang, Adegoke and Selig, 1980).

The railway embankment geometry cannot be input into the GEOTRACK computer program for computation of stress distribution beneath the tie-track system. It was originally anticipated that this limitation on the GEOTRACK computer program would seriously restrict its use in a bearing capacity design approach for railway subgrades. However, stress analyses conducted as a part of this study indicated otherwise.

A typical railway loading configuration was input into the GEOTRACK computer program for computation of stress distribution. A complete listing of the typical data file is located in Appendix A.

A loading configuration corresponding to a 119,000 kg (263,000 lb) railway car was assumed. The resultant axle loads were increased by 50% to account for dynamic impact. Wheel loads of 220 kN (49.4 kips) were distributed to tie numbers 1, 4, 8, and 11. A depth of granular (i.e., ballast and subballast combined) equal to 914 mm (36 in) was assumed to cover the subgrade. The modulus used to represent the

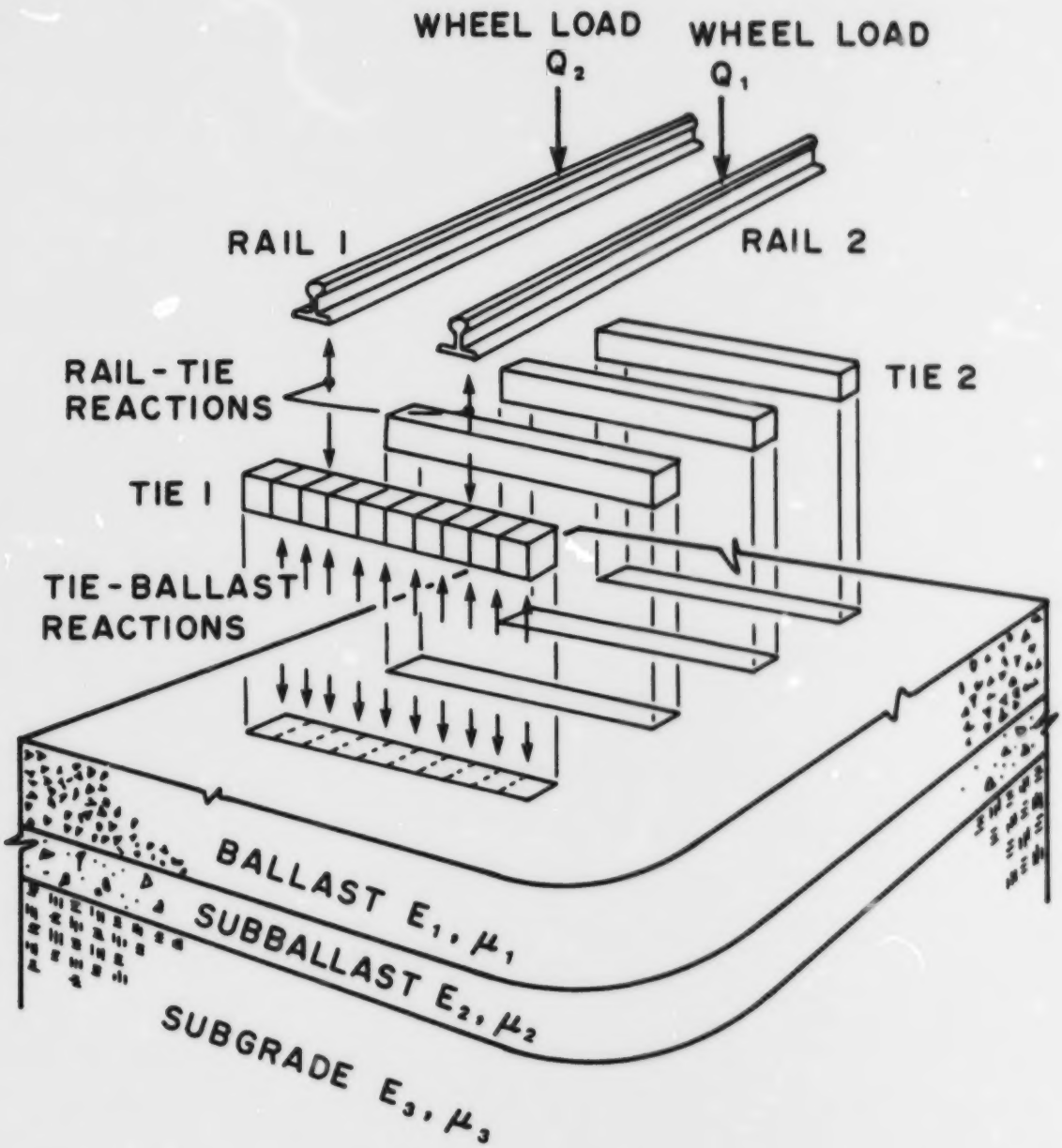

Fig. 4.6 Forces and elements in the GEOTRACK model (Chang, Adegoke and Selig, 1980)

granular material was 241.5 MPa (35,000 psi) whereas the value of modulus used to represent the subgrade was 69.0 MPa (10,000 psi).

Figures 4.7 through 4.10 illustrate the results of the GEOTRACK stress distribution for the typical railway loading configuration. Figure 4.7 illustrates the vertical stress below the track due to the applied loads whereas Figure 4.8 shows the horizontal stresses induced parallel to the tie within the subgrade soil. The shear stresses in the x-z plane are presented in Figure 4.9. The sum of the stresses in the x, y, and z planes is diagrammed in Figure 4.10 as the bulk stress.

On Figure 4.7, if a 2:1 slope were drawn through the soil from the edge of the tie, about 98% of the vertical stress from the applied load would be distributed to the soil below the line defining a 2:1 slope. The same statement can be made regarding horizontal stresses distributed below the applied load. With respect to shear stresses, the GEOTRACK computer program indicates a stress concentration at the end of the tie in Figure 4.9. The stress concentration which is illustrated is due to utilizing the GEOTRACK option which assumes that the ties do not lift off the ballast. If it had been assumed that the ties do separate from the ballast, the stress concentration would have been eliminated.

The preceding results from the GEOTRACK distribution of stress below the applied loading configuration confirm the

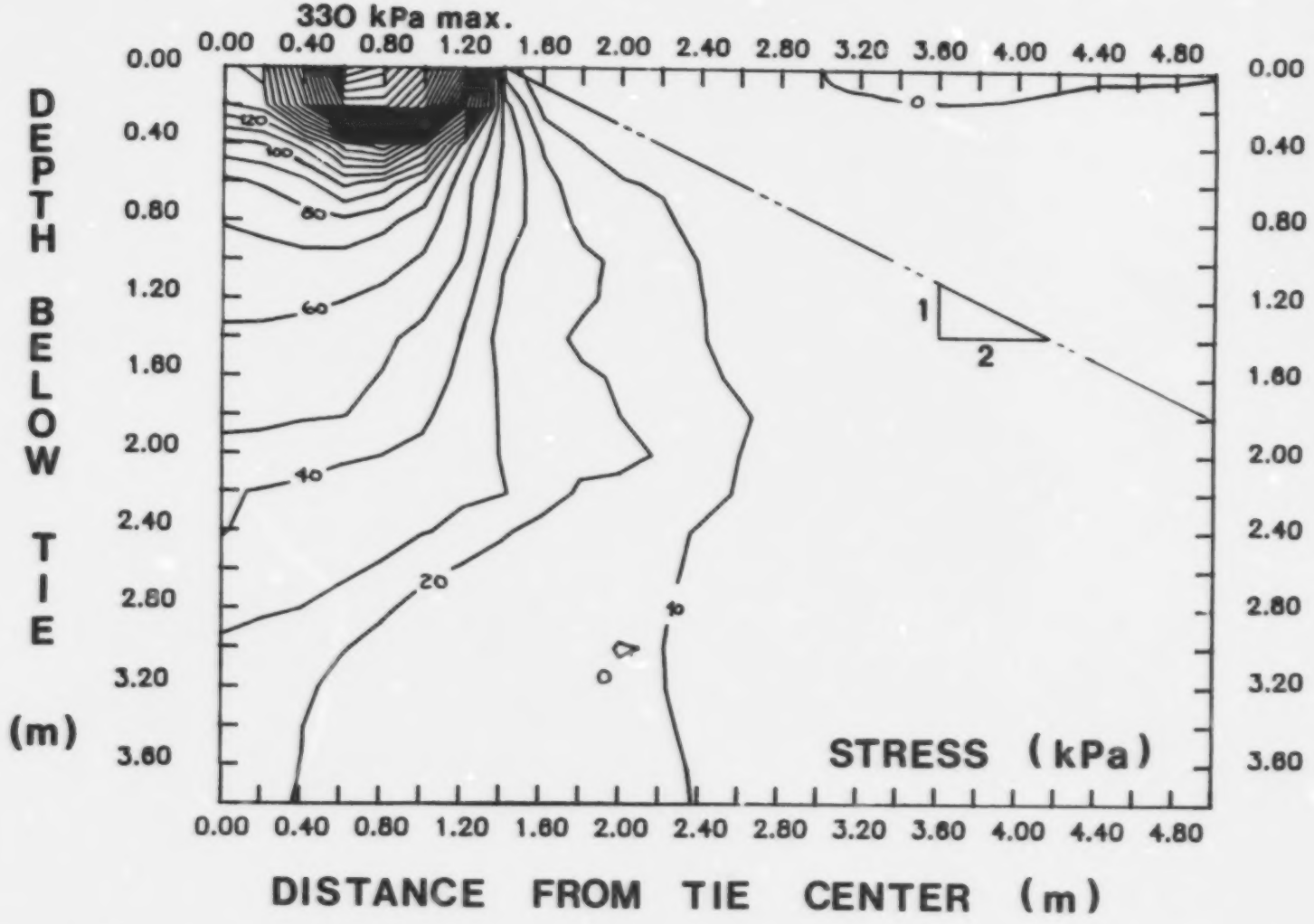

Fig. 4.7 Vertical stress distribution computed by the GEOTRACK model

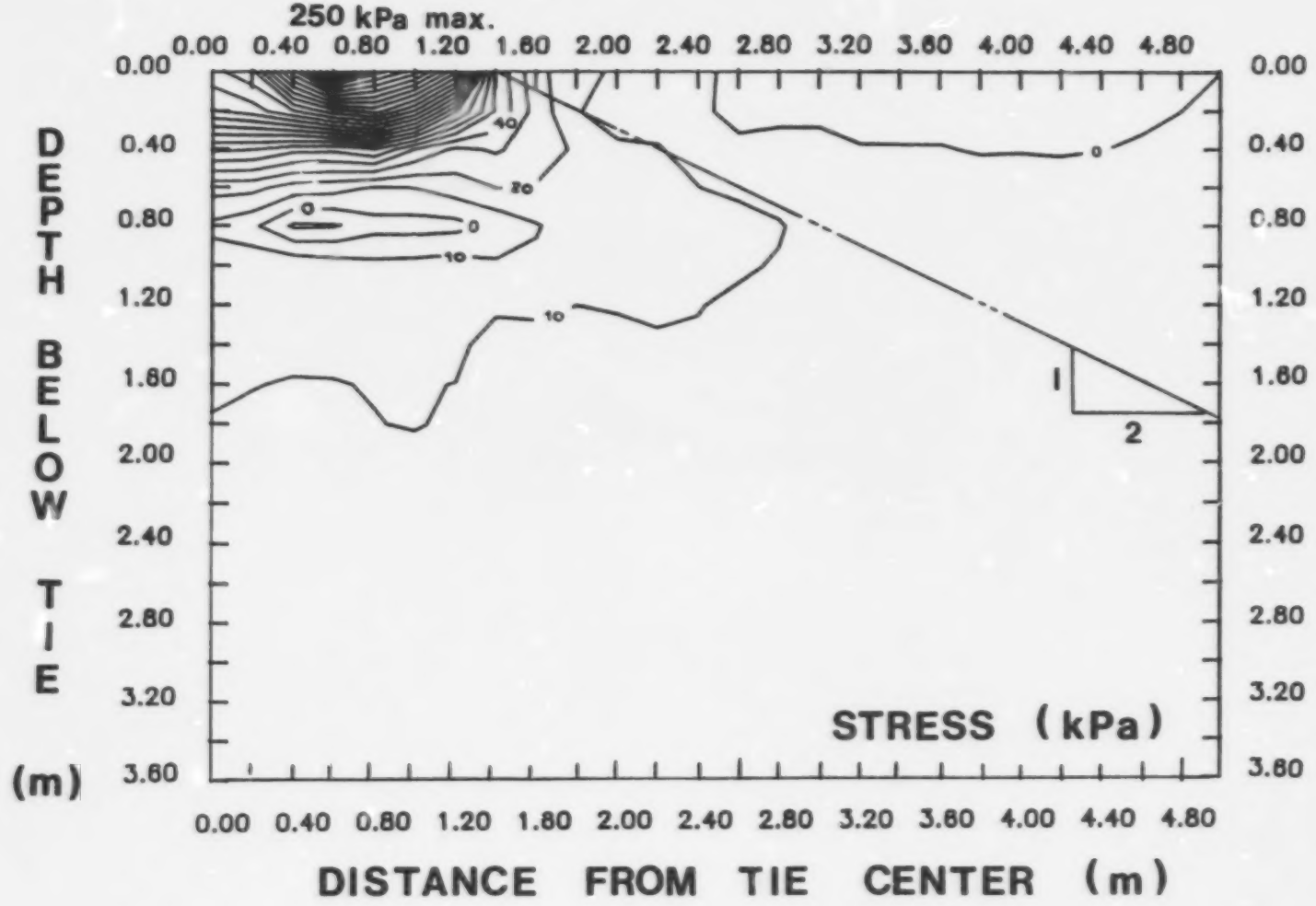

Fig. 4.8 Horizontal stress distribution computed by the GEOTRACK model

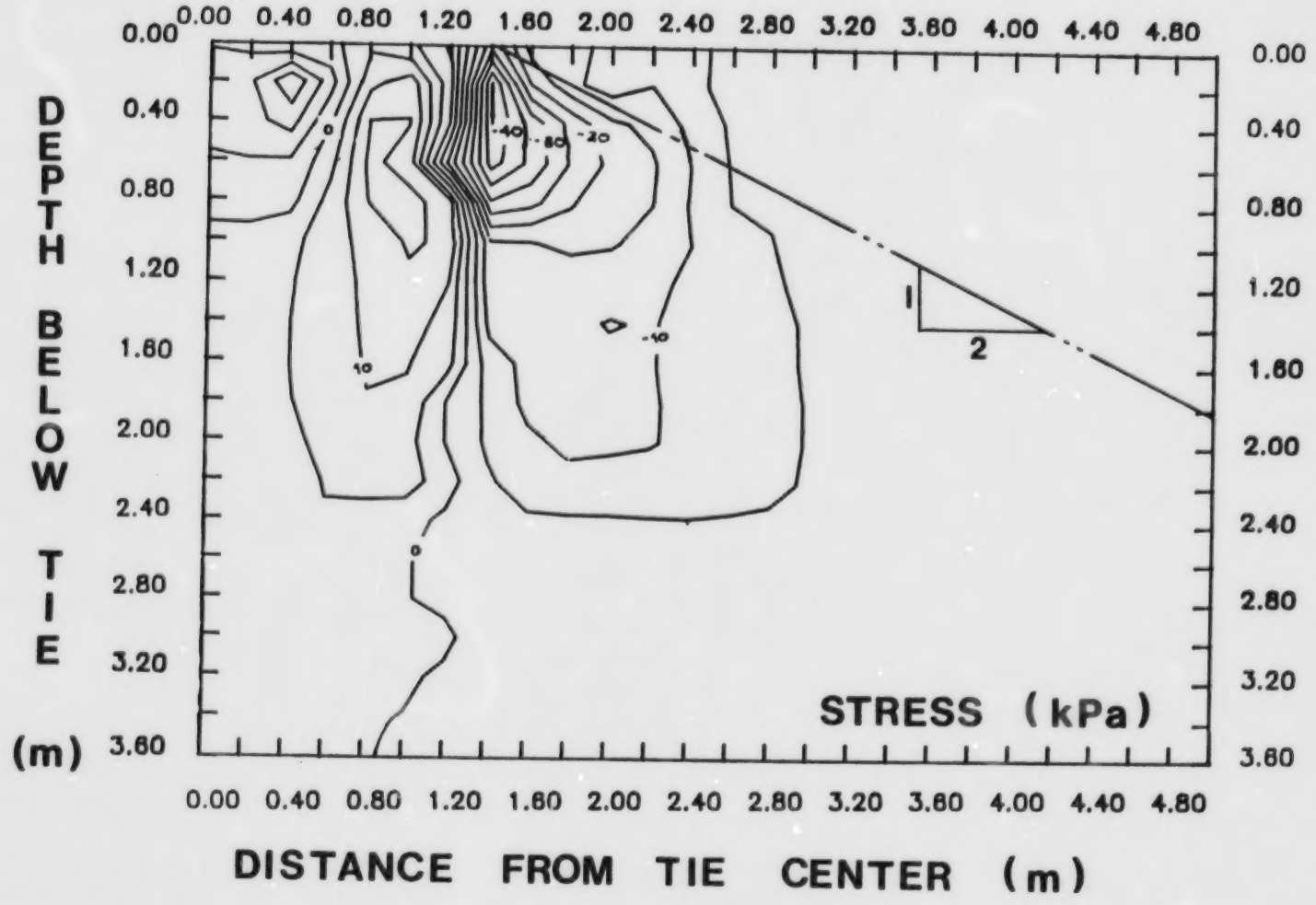

Fig. 4.9 Shear stress distribution computed by the GEOTRACK model

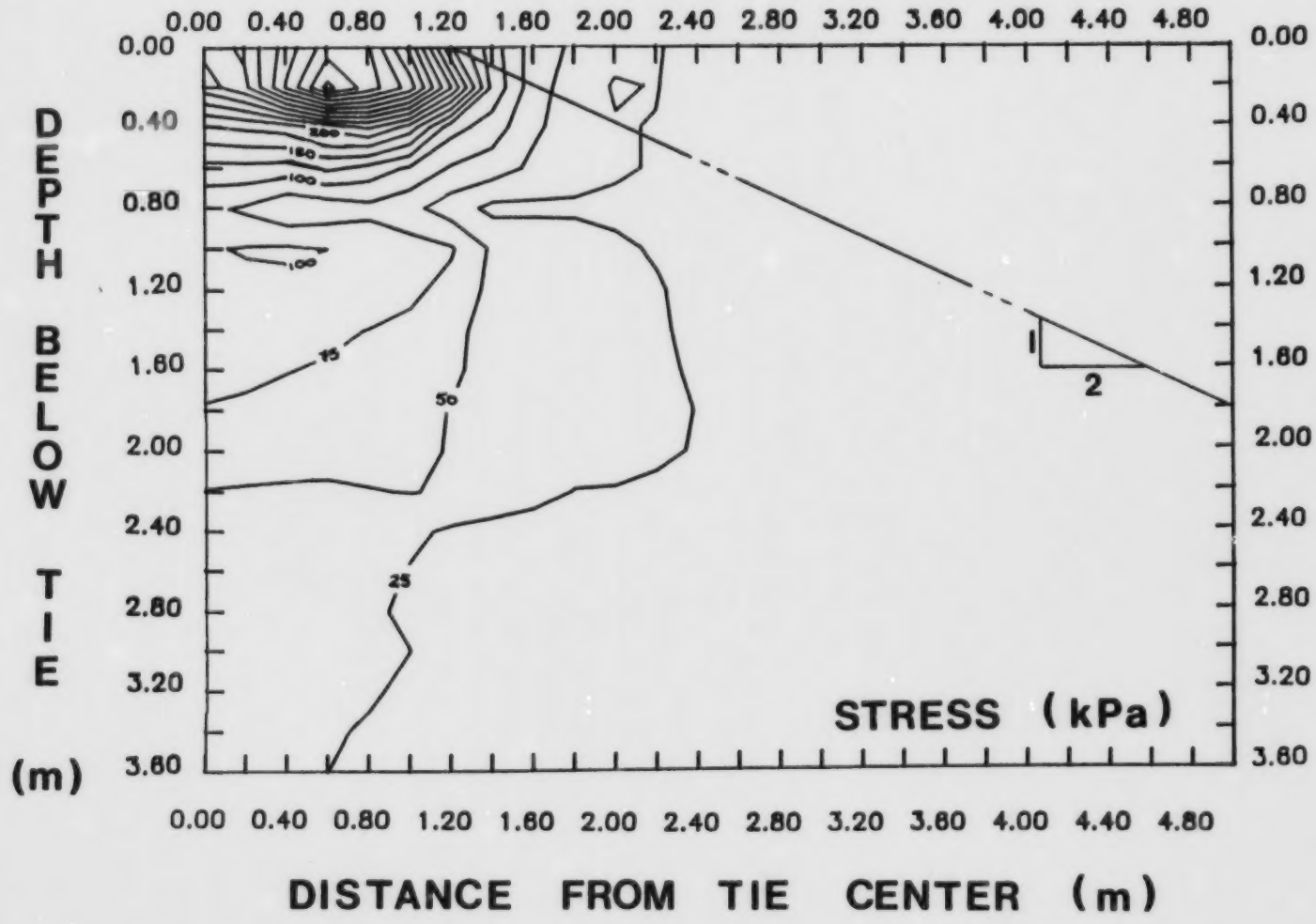

Fig. 4.10 Bulk stress computed by the GEOTRACK model

suggestions made previously that the effect of typical embankment slope on stress distribution is negligible. In order to further document the research, a two-dimensional finite element program, PC-SIGMA (Fredlund, 1989), was used to conduct a study on the effect of various slopes on the computed stress distribution beneath the loaded area.

4.2 Results of 2-D Stress Analysis

A previous study revealed that two-dimensional finite element analyses do not adequately represent the complex three-dimensional, rail - tie - ballast - subballast - subgrade system for purposes of computing stress distribution beneath the track loading configuration. However, since the actual computed values for stress are not as important as the comparisons between the various two-dimensional analyses, the two-dimensional analyses may be used to investigate the effect of embankment side-slopes on computed stress distribution.

Four different embankment slopes were considered: 1) zero embankment slope, 2) 1 horizontal : 1 vertical slope or 45 degrees, 3) 0.5:1 or about 60 degrees, and 4) 0.25:1 or 75 degrees. Figures 4.11, 4.12, and 4.13 illustrate the vertical, horizontal, and shear stresses, respectively, for the zero embankment slope. Figures 4.14, 4.15, and 4.16 show the vertical horizontal, and shear stresses for the 1:1 slope. The vertical, horizontal, and

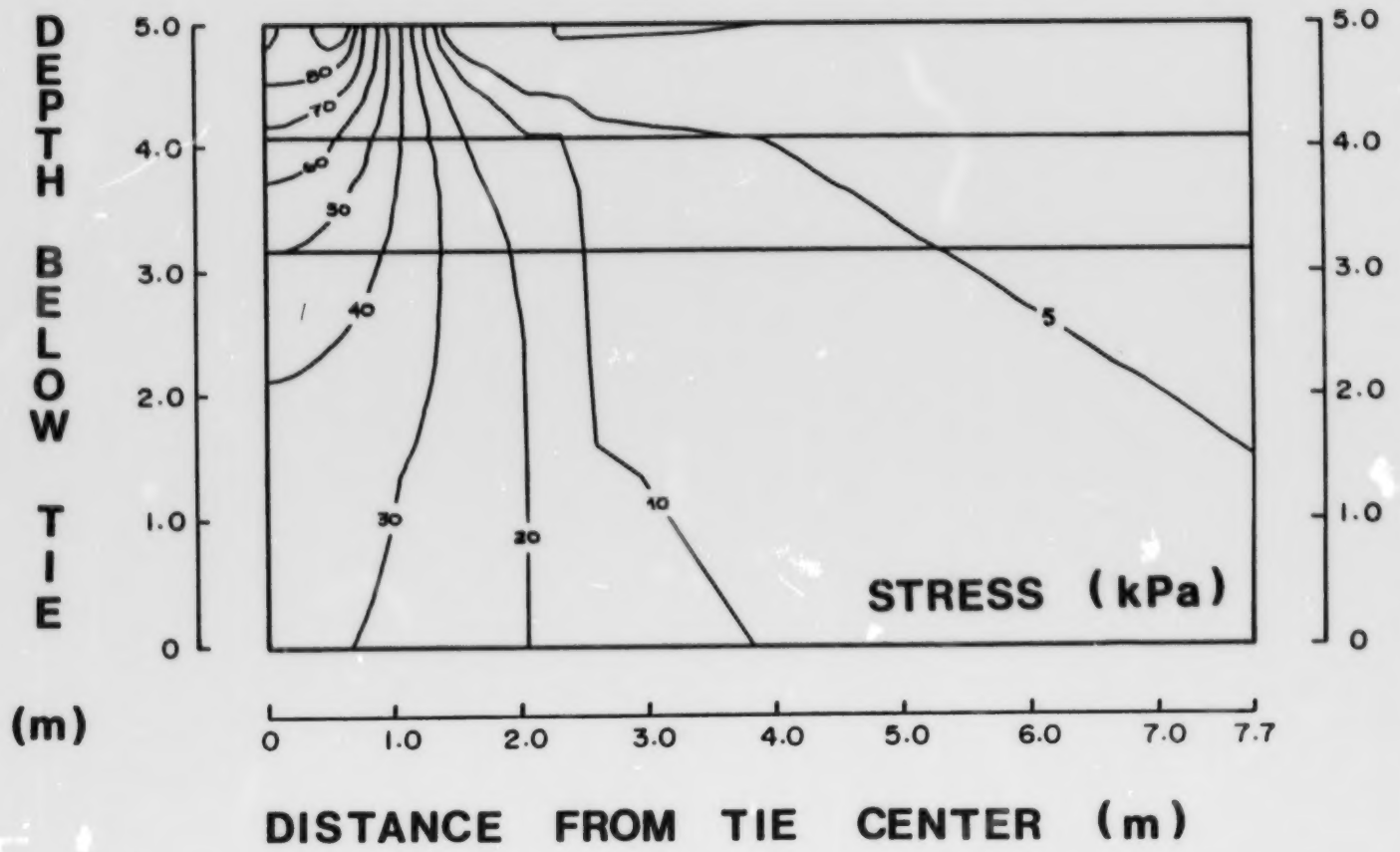

Fig. 4.11 Vertical stress distribution for zero embankment side-slope by PC-SIGMA computer model

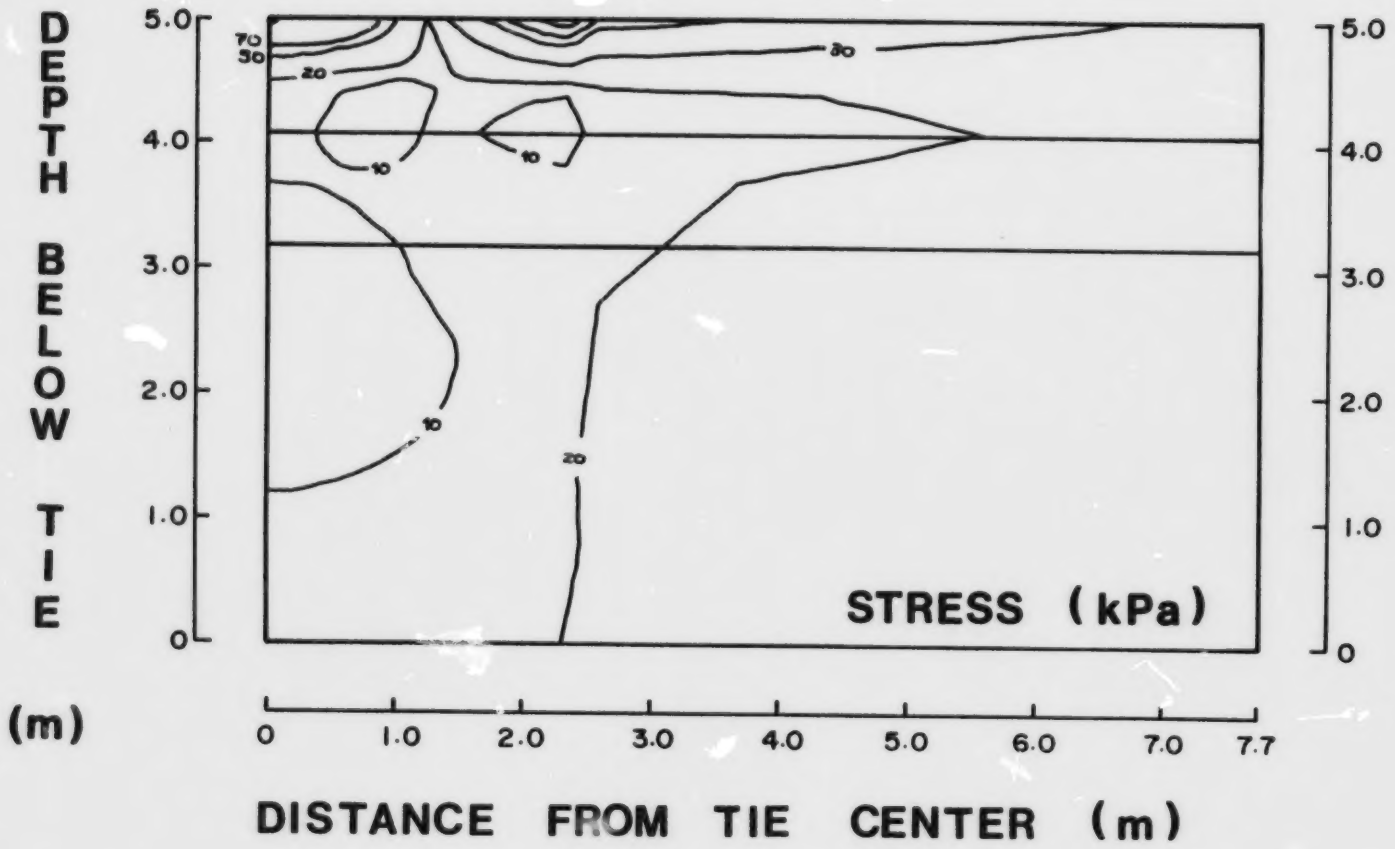

Fig. 4.12 Horizontal stress distribution for zero embankment side-slope by PC-SIGMA computer model

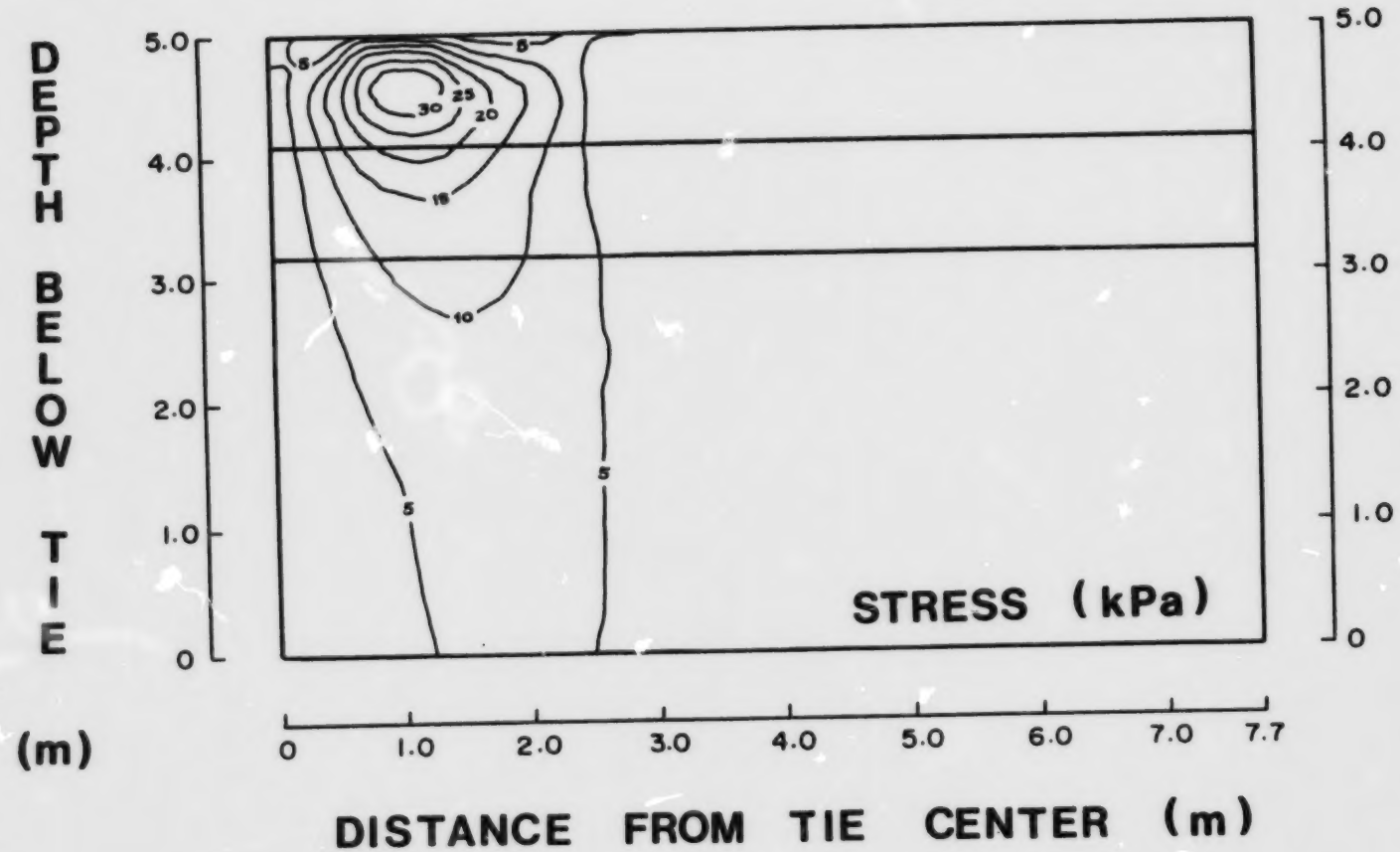

Fig. 4.13 Shear stress distribution for zero embankment side-slope by PC-SIGMA computer model

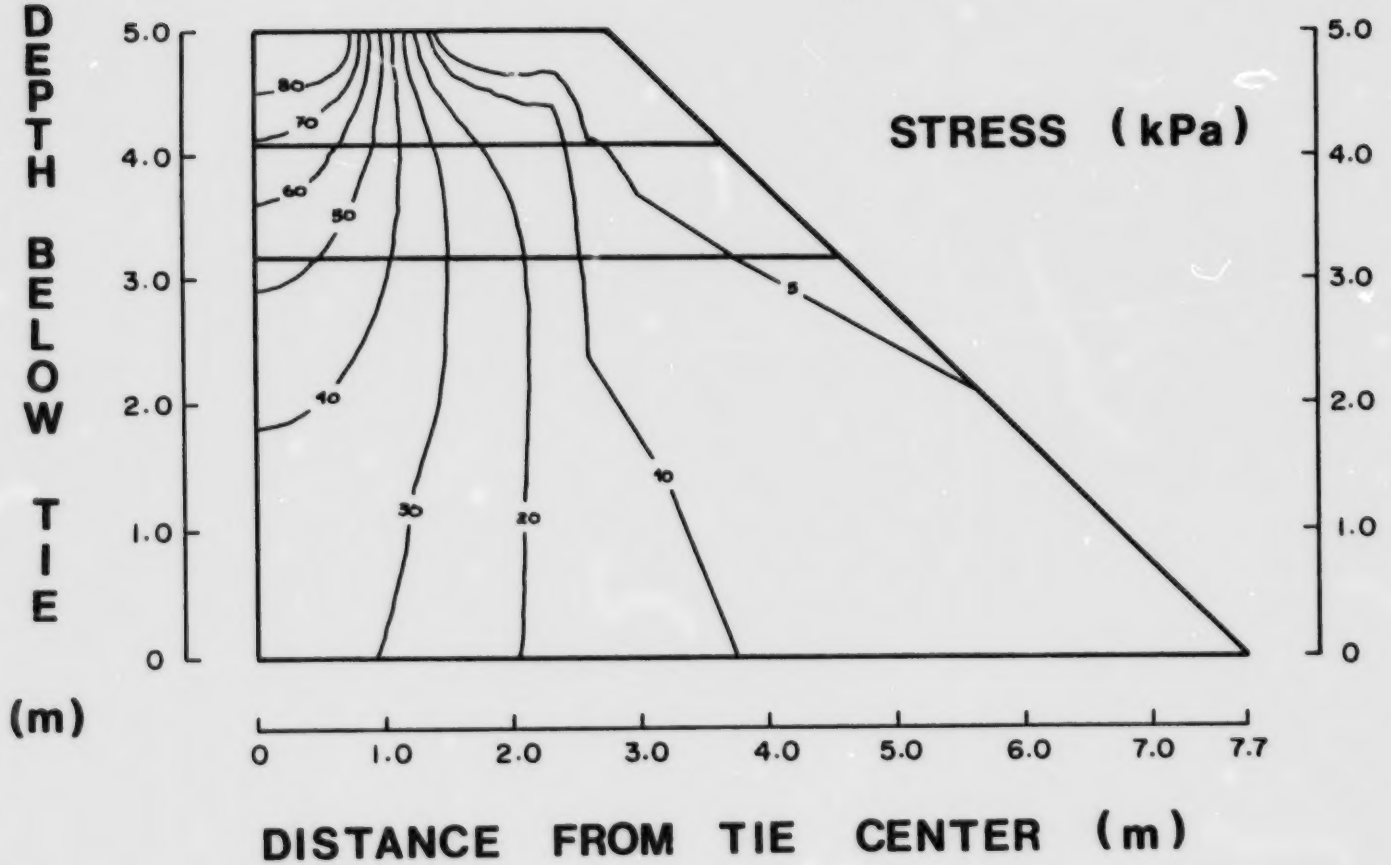

Fig. 4.14 Vertical stress distribution for 1:1 embankment side-slope by PC-SIGMA computer model

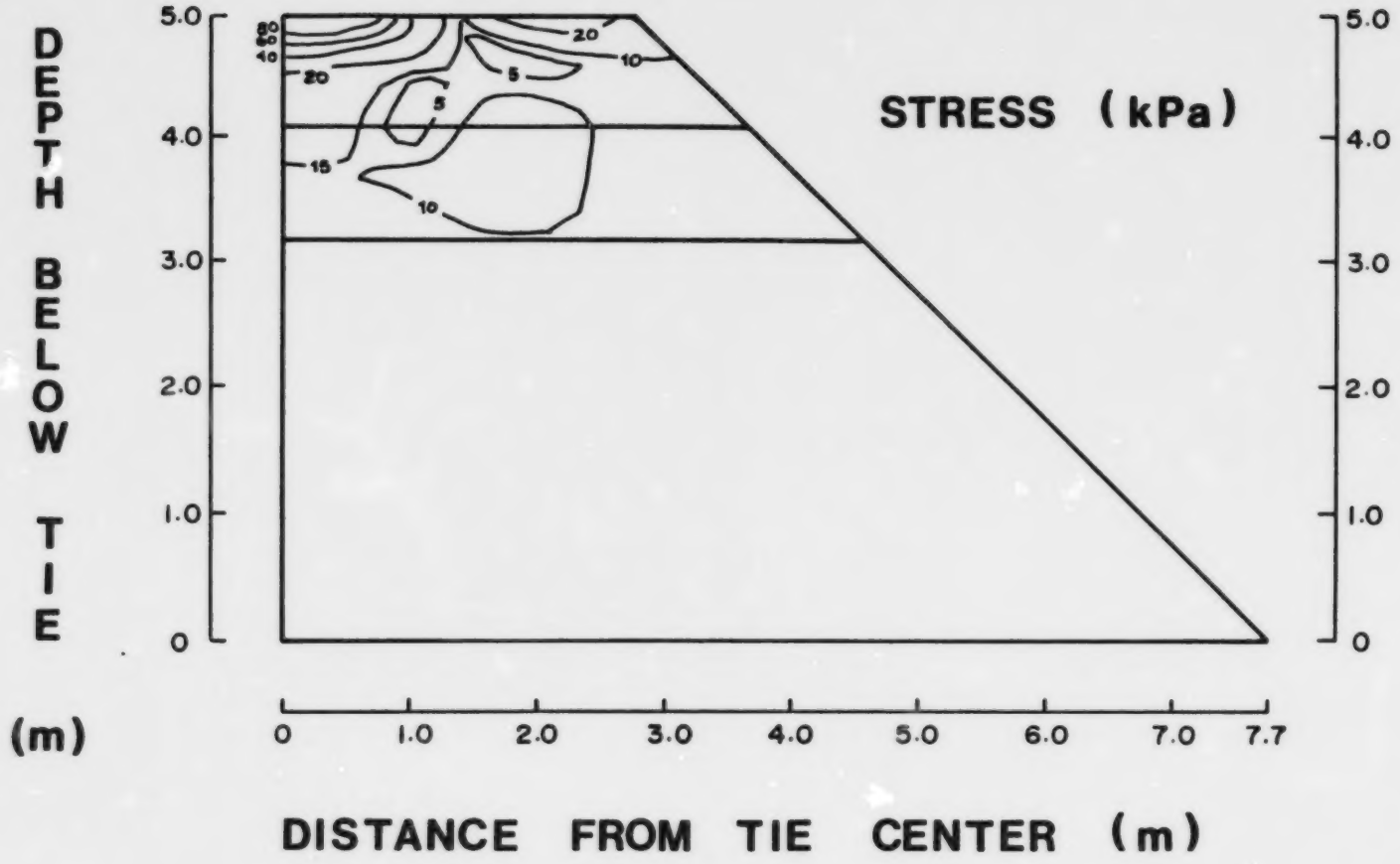

Fig. 4.15 Horizontal stress distribution for 1:1 embankment side-slope by PC-SIGMA computer model

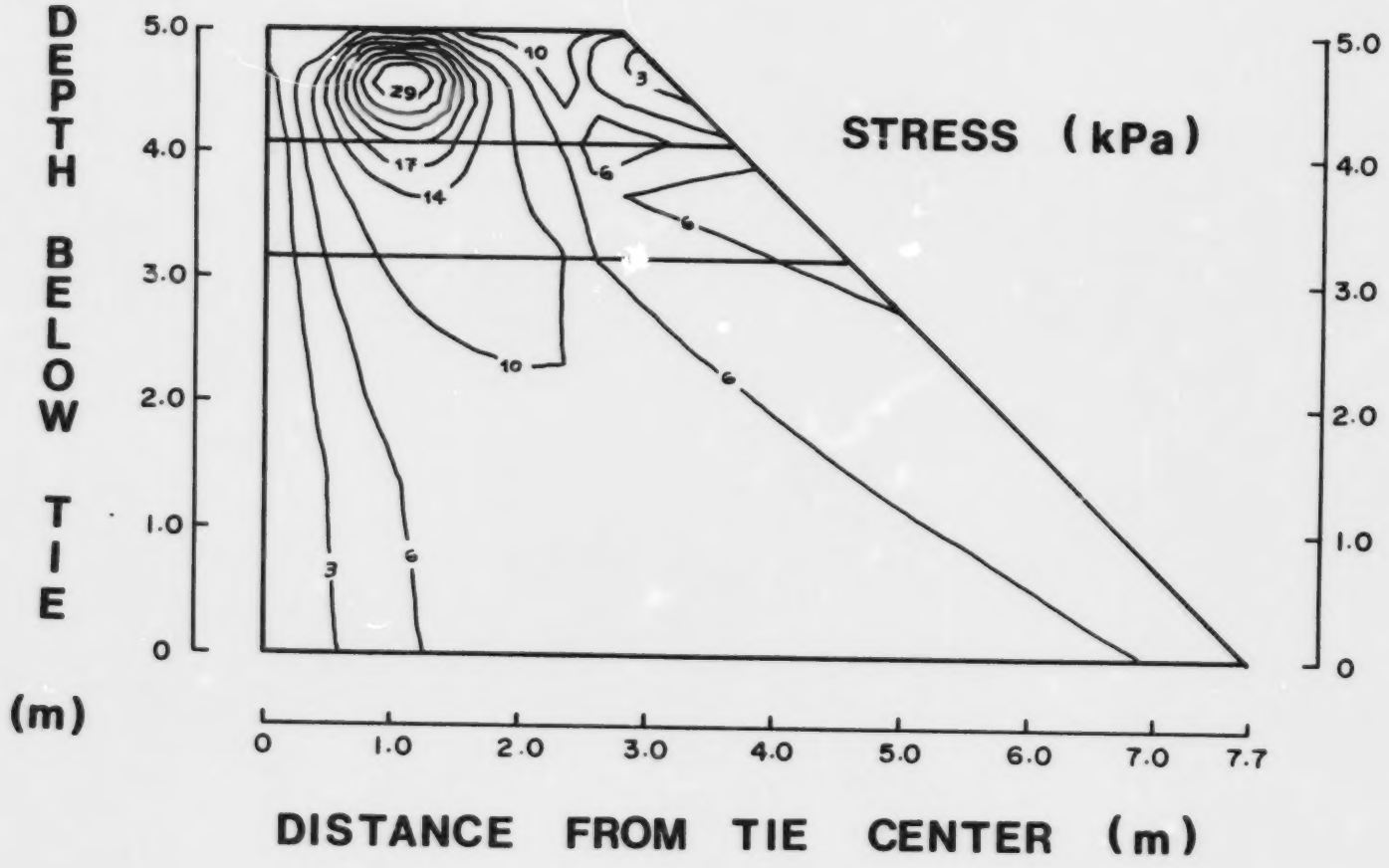

Fig. 4.16 Shear stress distribution for 1:1 embankment side-slope by PC-SIGMA computer model

shear stresses for the 0.5:1 slope are represented in Figures 4.17, 4.18, and 4.19, respectively. The vertical, horizontal, and shear stresses for the 0.25:1 slope are pictured in Figures 4.20, 4.21, and 4.22.

Figures 4.11, 4.12, and 4.13 represent the stress distribution which would result if there were no embankment side-slopes (i.e., the assumption of the GEOTRACK computer program). The 1:1 embankment side-slope represents a slope flatter than the 60 degree slope used by Broms for stress distribution whereas the 0.25:1 slope represents a slope steeper than the 60 degree slope.

For the vertical stresses shown in Figures 4.11, 4.14, 4.17, and 4.20, the analyses show that as the side-slopes are steepened, there is some crowding of the stress contours along the slope (Figure 4.23). However, the stresses along the side-slopes are still only about 5% of the stress applied at the surface. In other words, about 95% of the stress from the loading configuration is distributed to the area immediately beneath the load. It is the vertical stresses which are considered when analyzing the influence of the loading configuration on the subgrade. Since vertical stresses are minimally affected by embankment slope, it can be concluded that the use of the GEOTRACK analysis is adequate for use in the bearing capacity approach to design.

Figure 4.24 which is a combination of Figures 4.12, 4.15, 4.18, and 4.21 illustrates a more significant role of

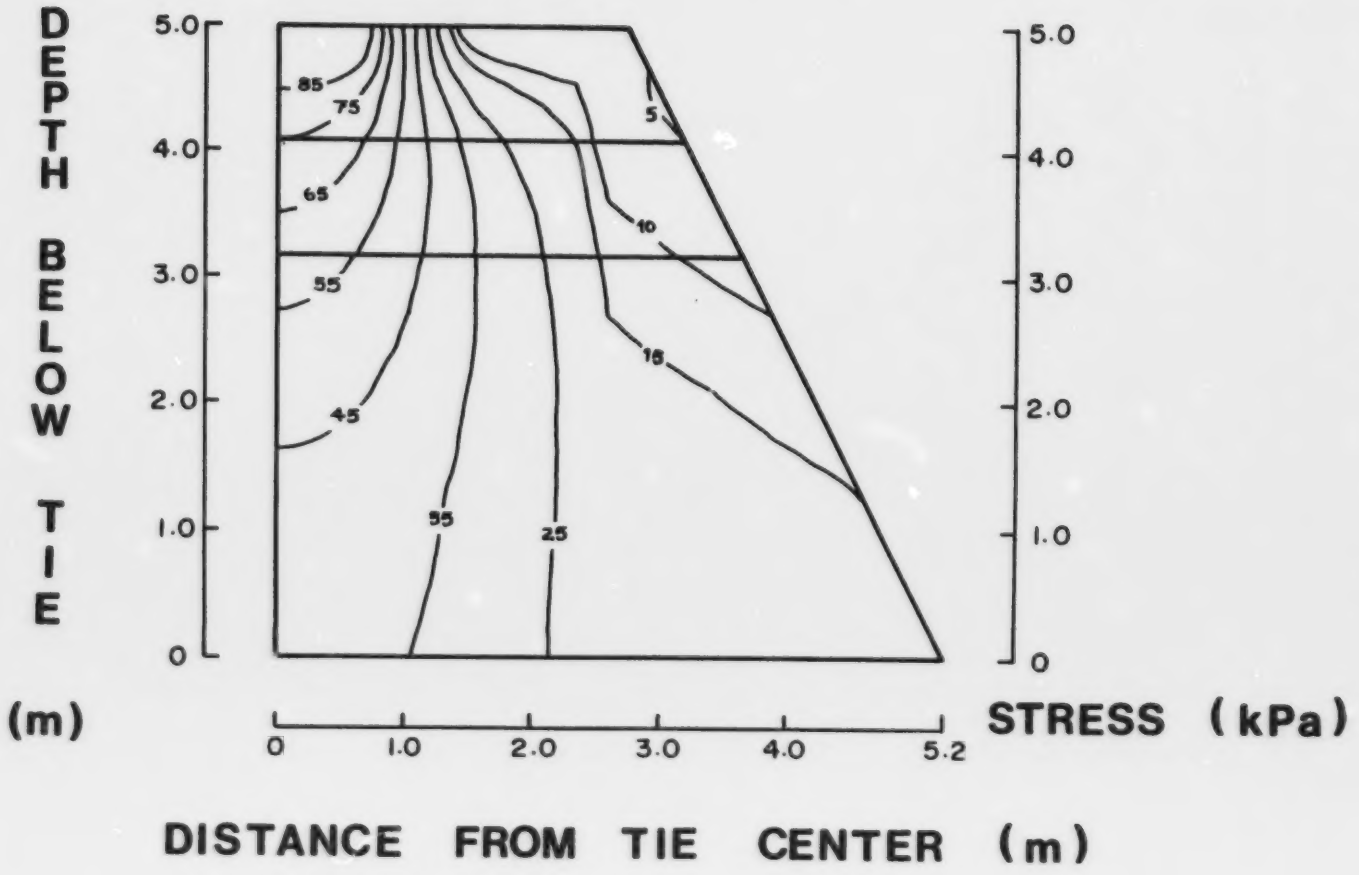

Fig. 4.17 Vertical stress distribution for 0.5:1 embankment side-slope by PC-SIGMA computer model

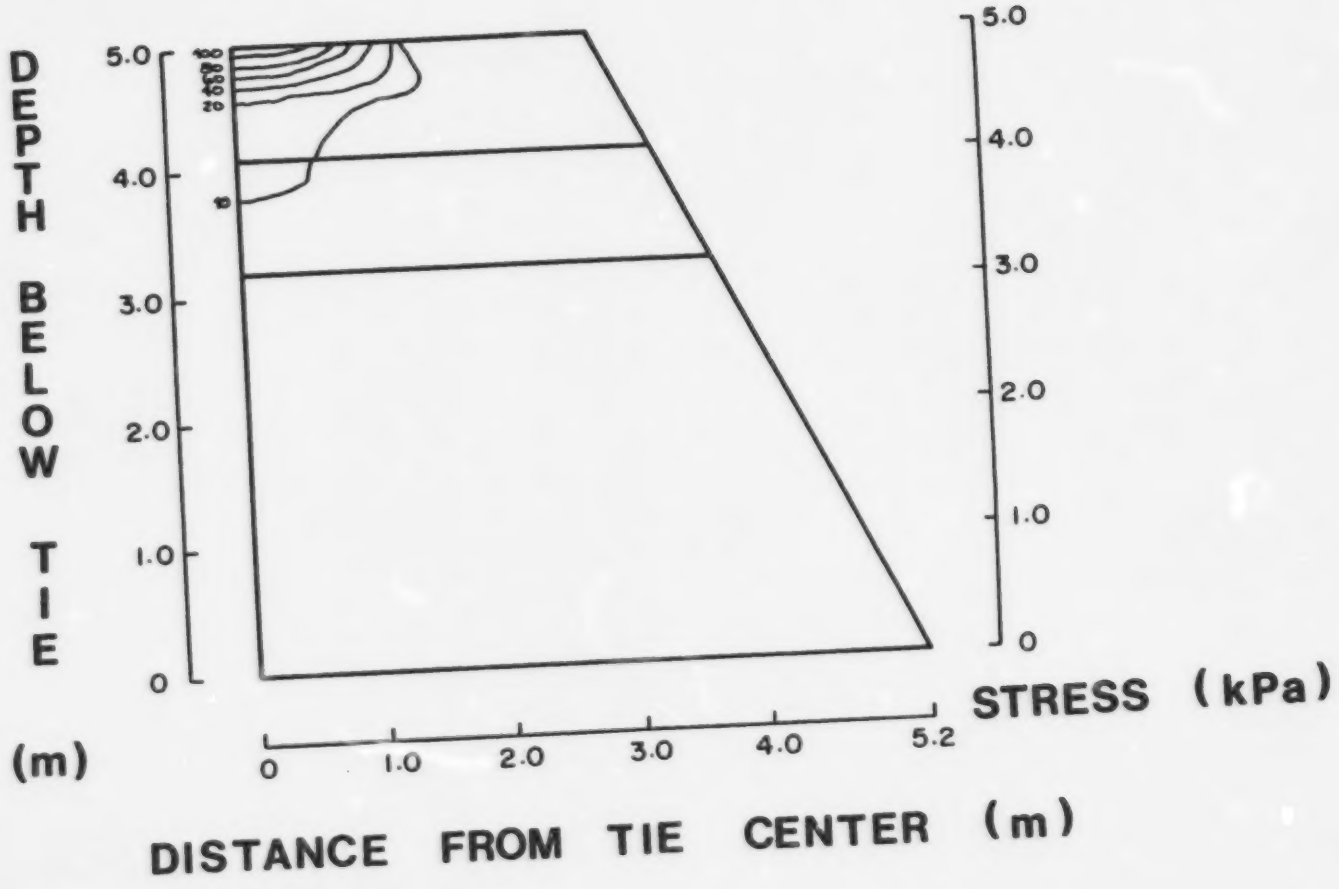

Fig. 4.18 Horizontal stress distribution for 0.5:1 embankment side-slope by PC-SIGMA computer model

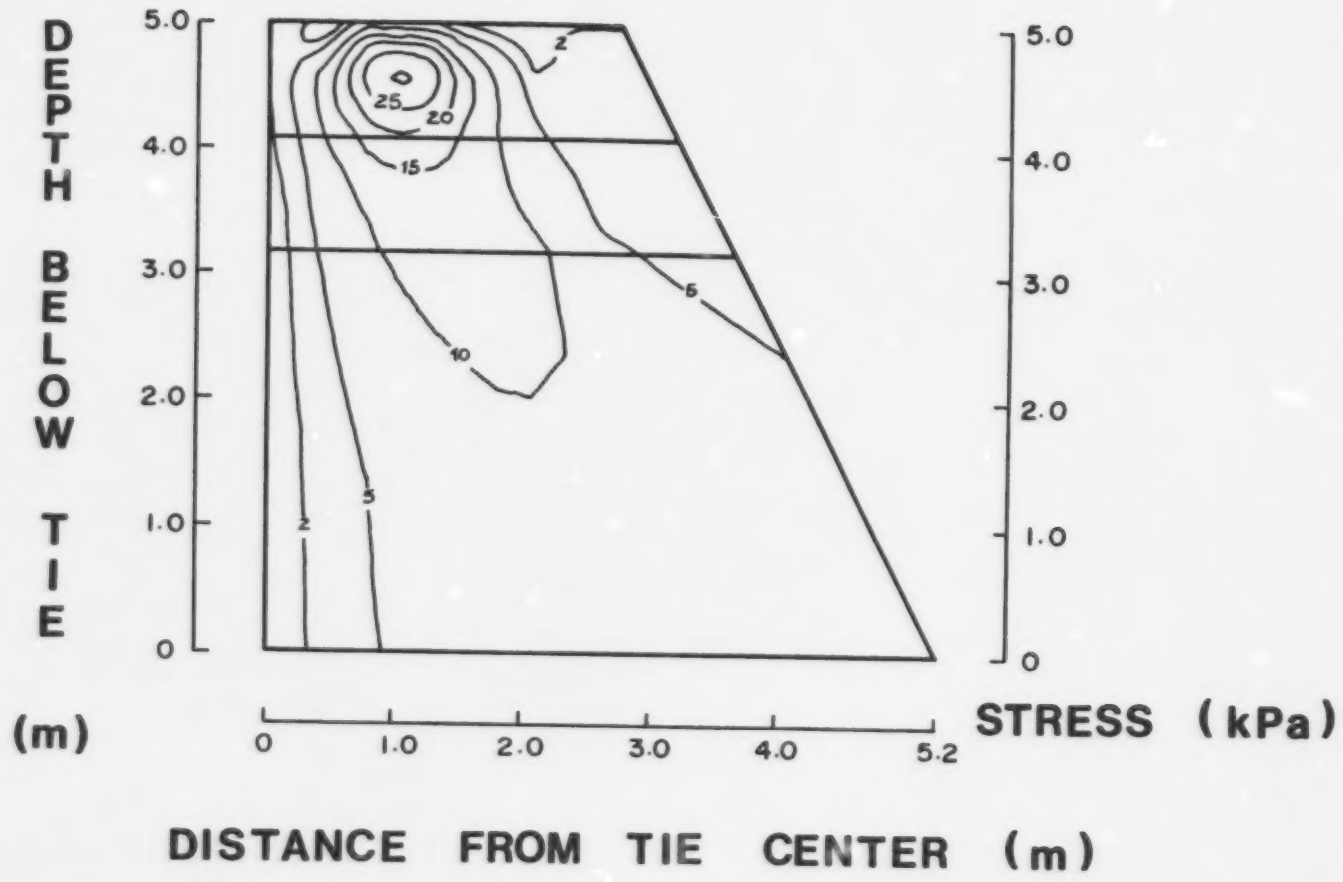

Fig. 4.19 Shear stress distribution for 0.5:1 embankment side-slope by PC-SIGMA computer model

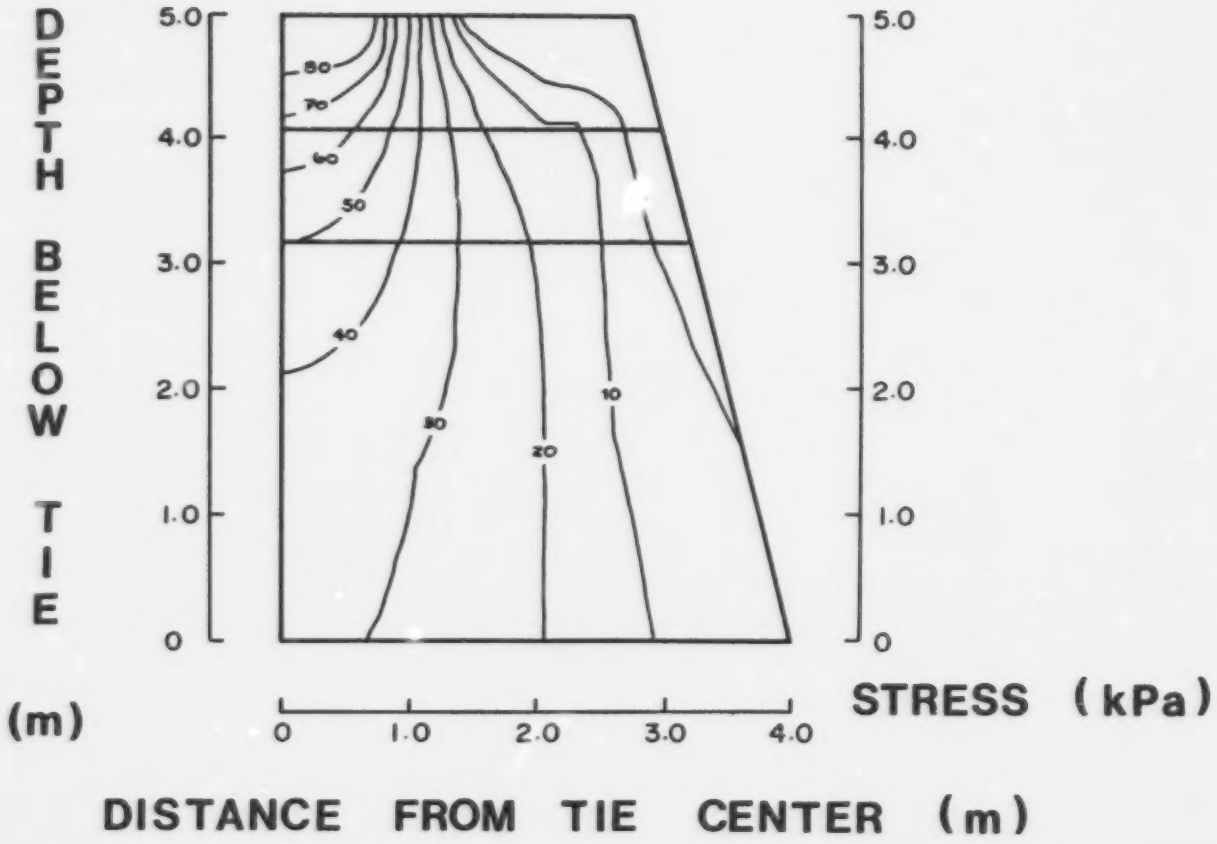

Fig. 4.20 Vertical stress distribution for 0.25:1 embankment side-slope by PC-SIGMA computer model

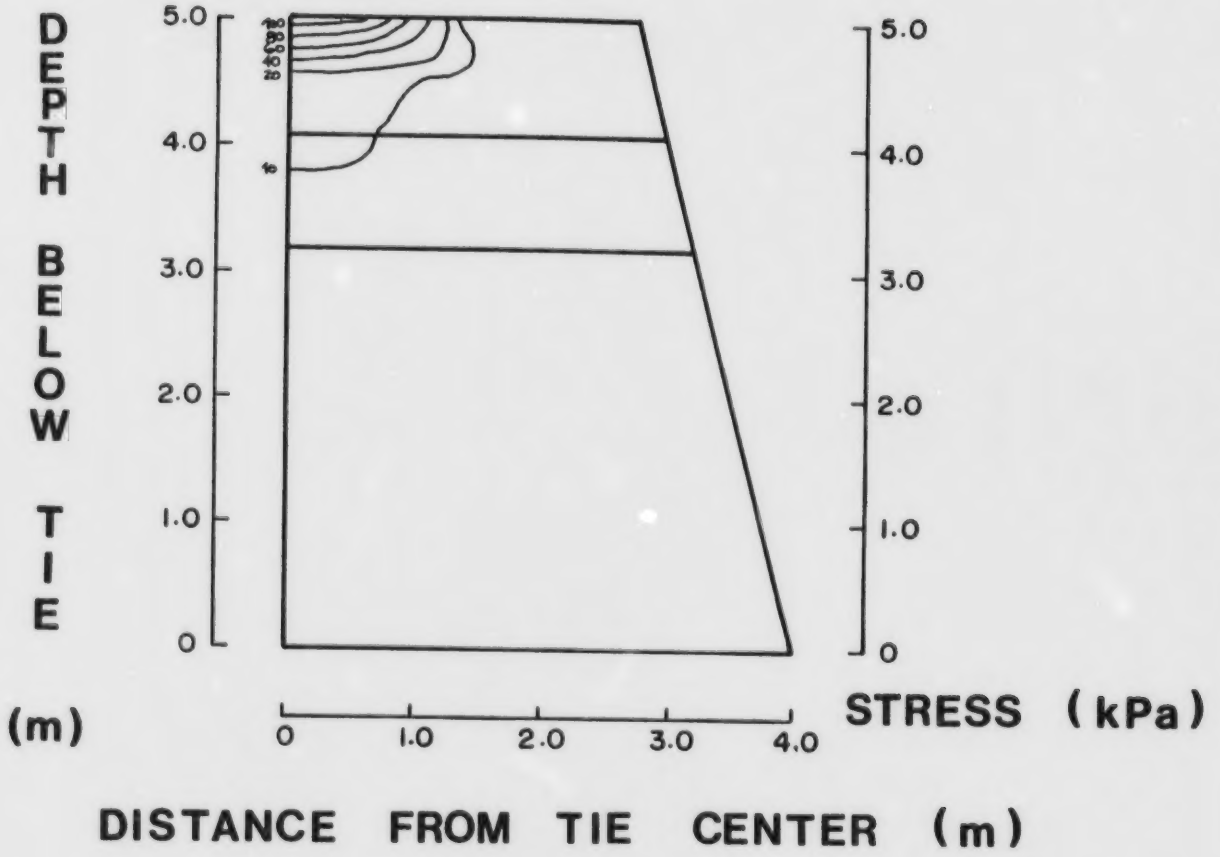

Fig. 4.21 Horizontal stress distribution for 0.25:1 embankment side-slope by PC-SIGMA computer model

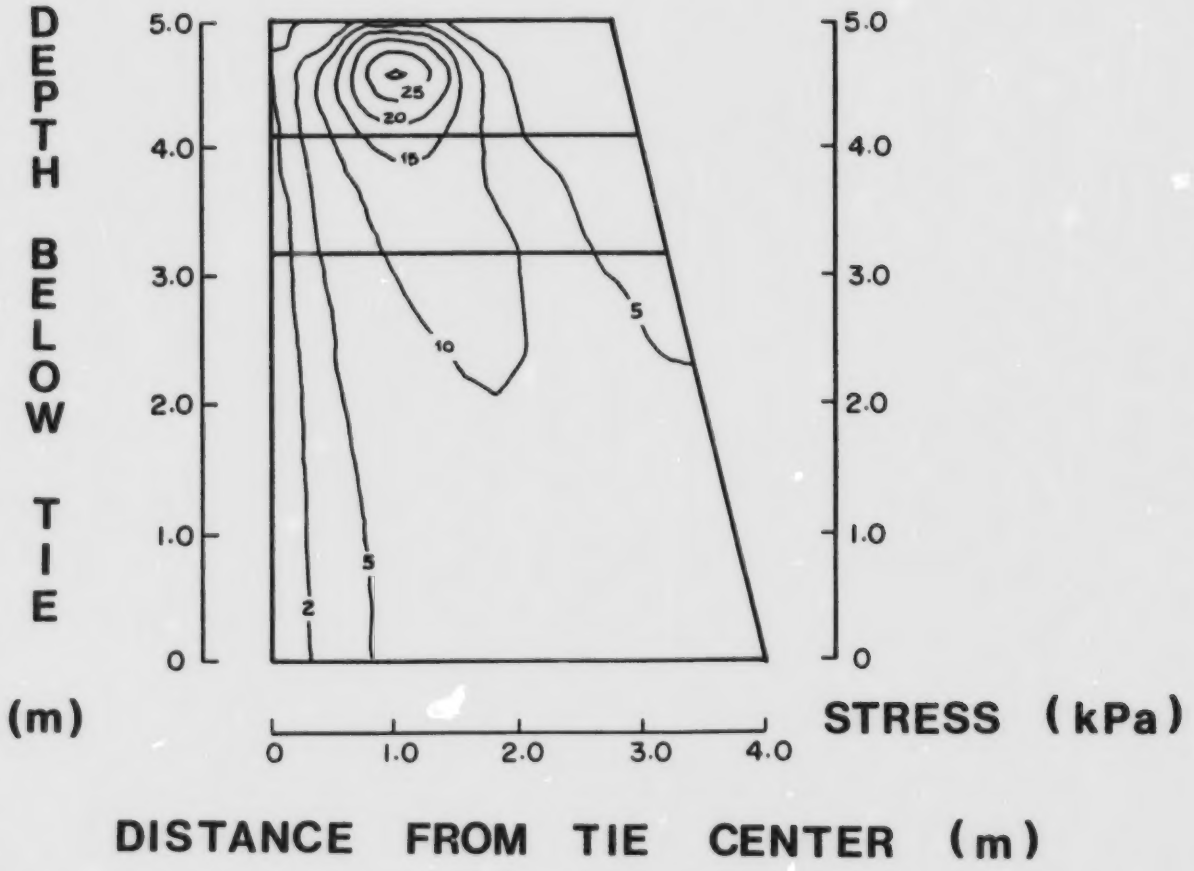

Fig. 4.22 Shear stress distribution for 0.25:1 embankment side-slope by PC-SIGMA computer model

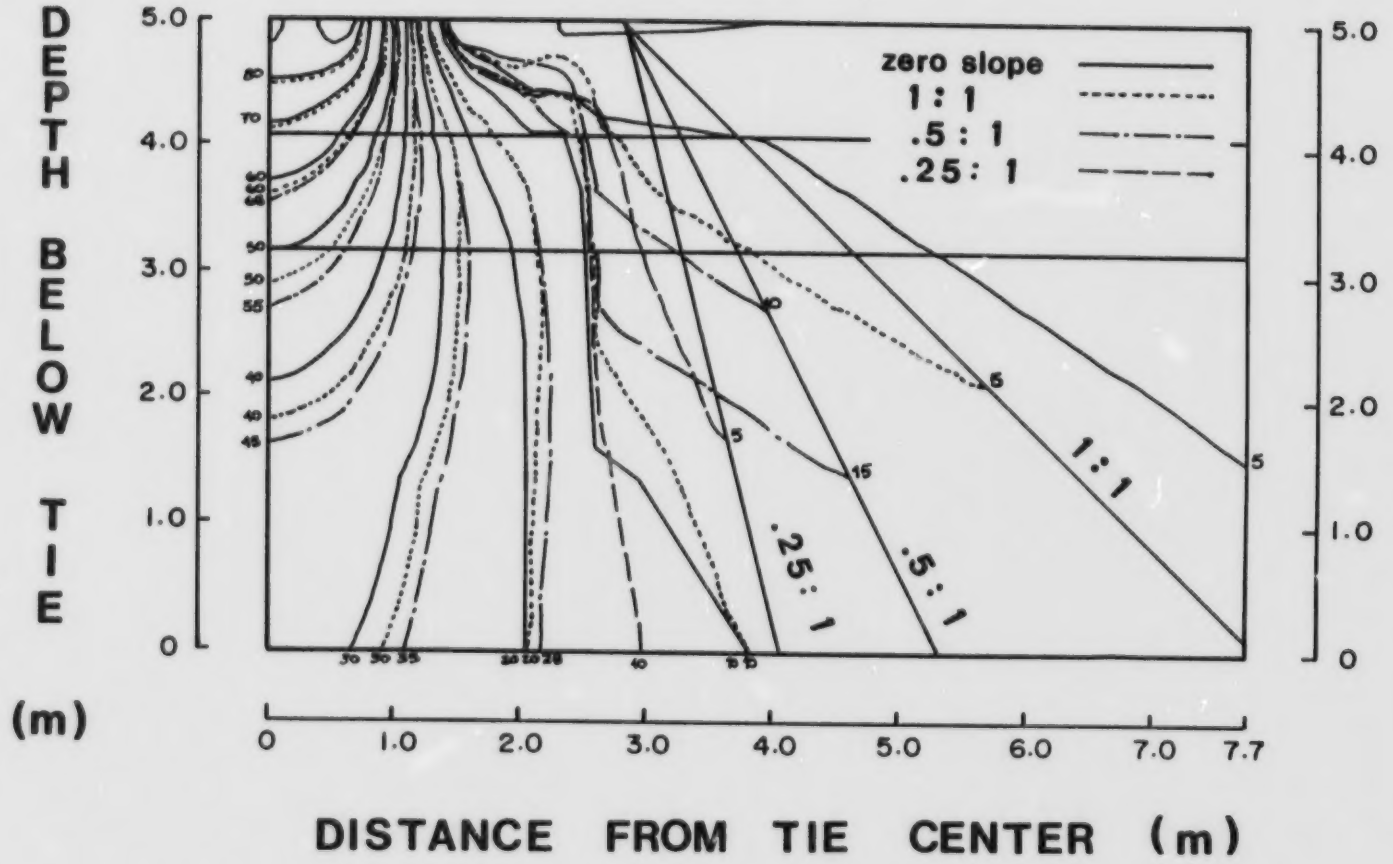

Fig. 4.23 Comparison of vertical stress distribution for various slope angles

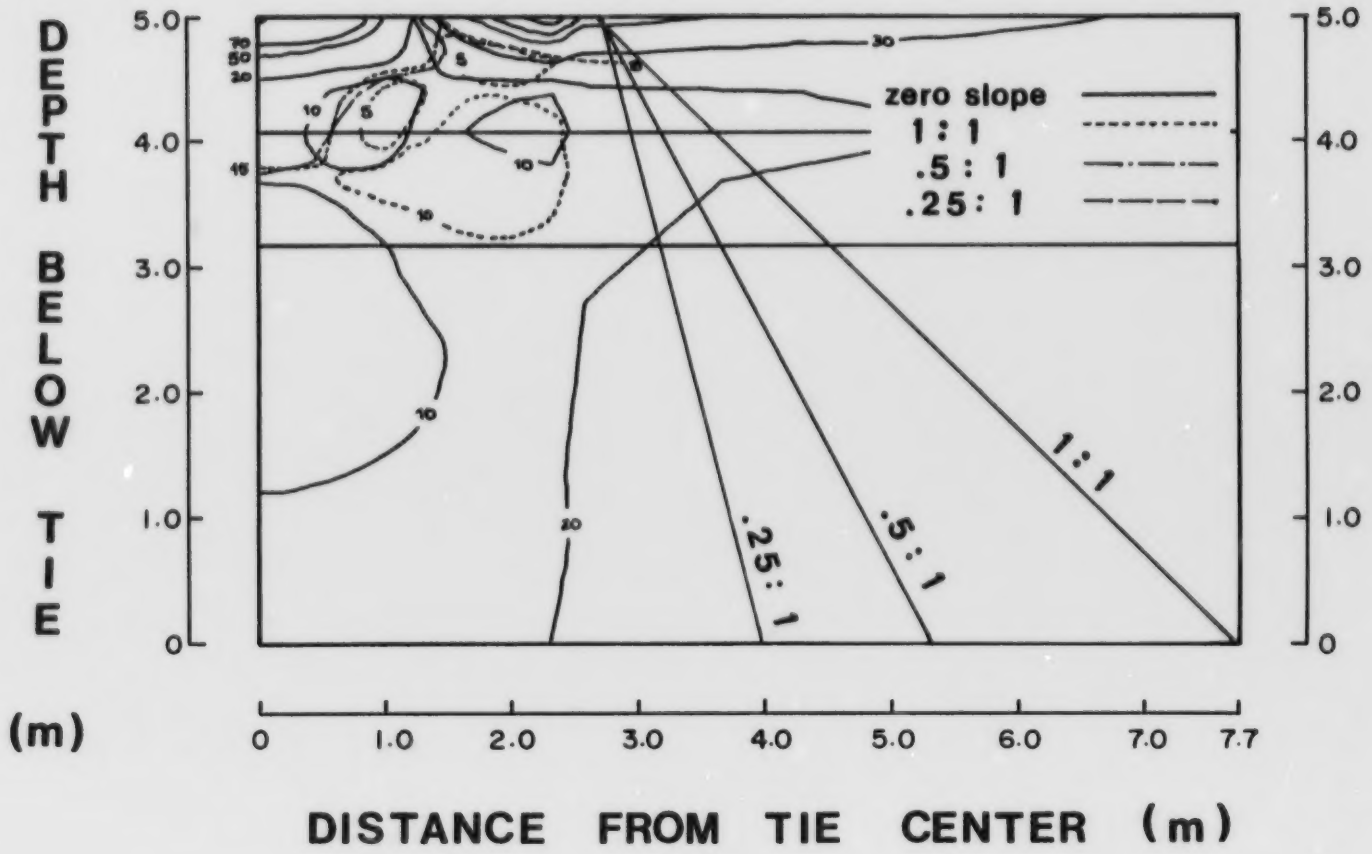

Fig. 4.24 Comparison of horizontal stress distribution for various slope angles

embankment slope on the magnitude and distribution of horizontal stresses beneath the track. Figure 4.25 which is a superposition of Figures 4.13, 4.16, 4.19, and 4.22 also illustrates some significance of embankment slope on the distribution and magnitude of shear stresses below the track. These latter two observations suggest the importance of applying slope stability analyses to problems with steep embankment slopes. Since bearing capacity is a shear strength calculation, the observations from Figure 4.25 suggest that modifications to the bearing capacity approach to railway design should be based upon modifying the bearing capacity rather than the vertical stress distribution.

4.3 Comparison of 2-D Stress Analyses and GEOTRACK Results

It has already been stated that two-dimensional finite element analyses are not adequate to compare to three-dimensional results from the GEOTRACK computer program; however, the comparisons have been made in this section for the sake of completeness.

The GEOTRACK vertical, horizontal, and shear stresses are compared to each of the vertical, horizontal, and shear stresses for each of the embankment side-slopes (i.e., zero slope, 1:1, 0.5:1, and 0.25:1). The comparisons are presented in Figures 4.26 through 4.37.

In each of Figures 4.26, 4.29, 4.32, and 4.35 which portray the vertical stress distributions, the comparisons

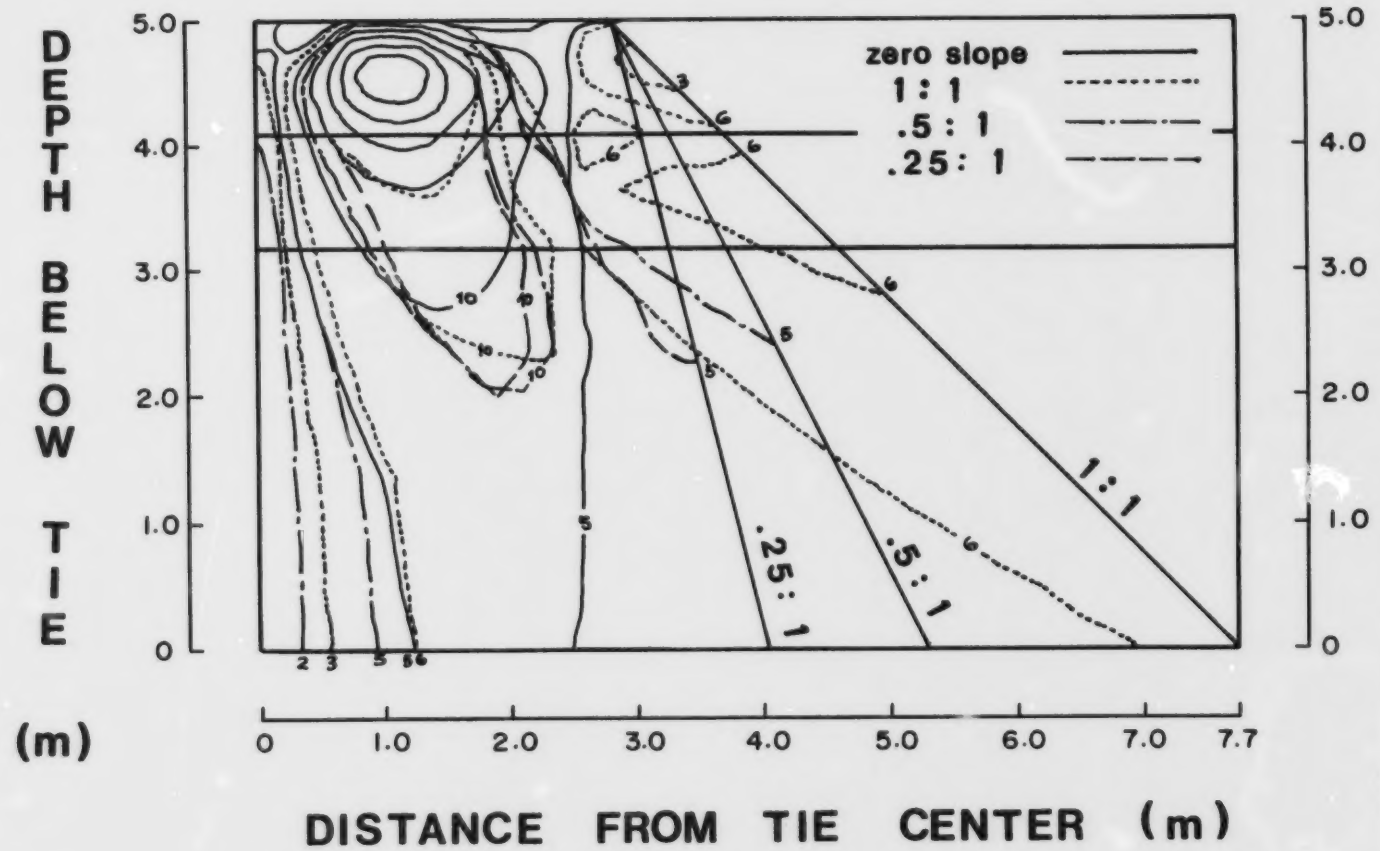

Fig. 4.25 Comparison of shear stress distribution for various slope angles

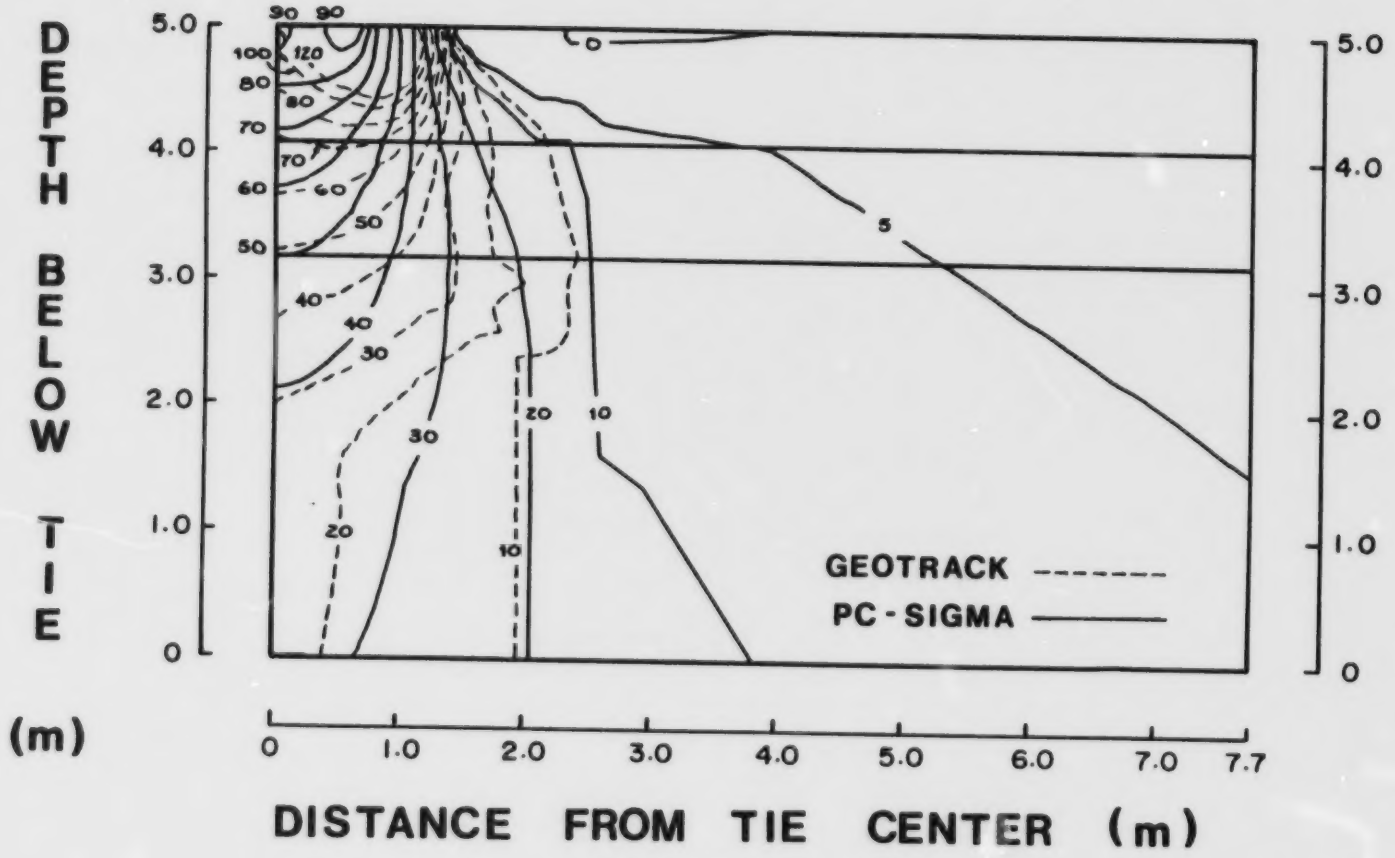

Fig. 4.26 Comparison of GEOTRACK vertical stress distribution to PC-SIGMA for zero embankment slope

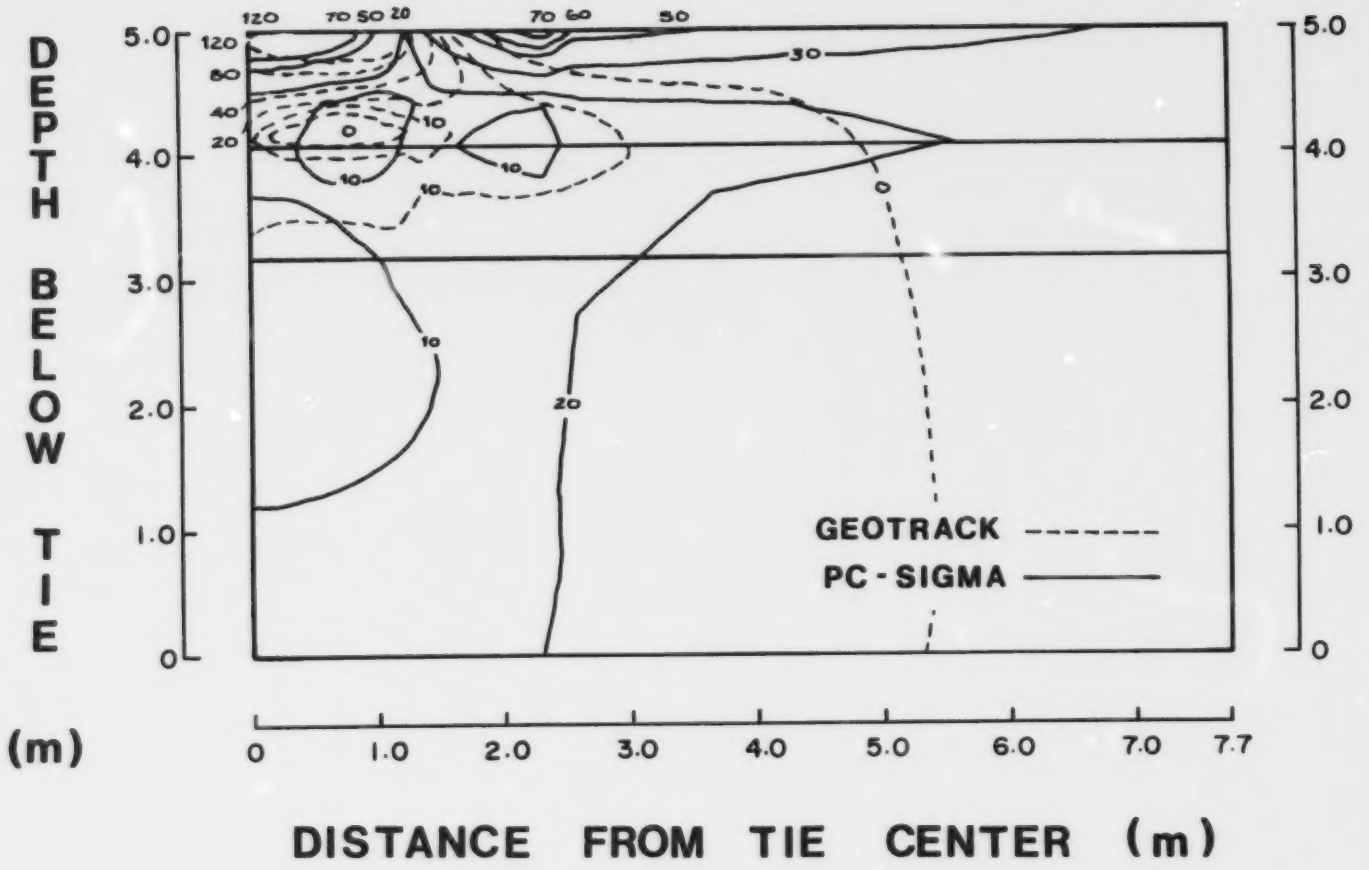

Fig. 4.27 Comparison of GEOTRACK horizontal stress distribution to PC-SIGMA for zero embankment slope

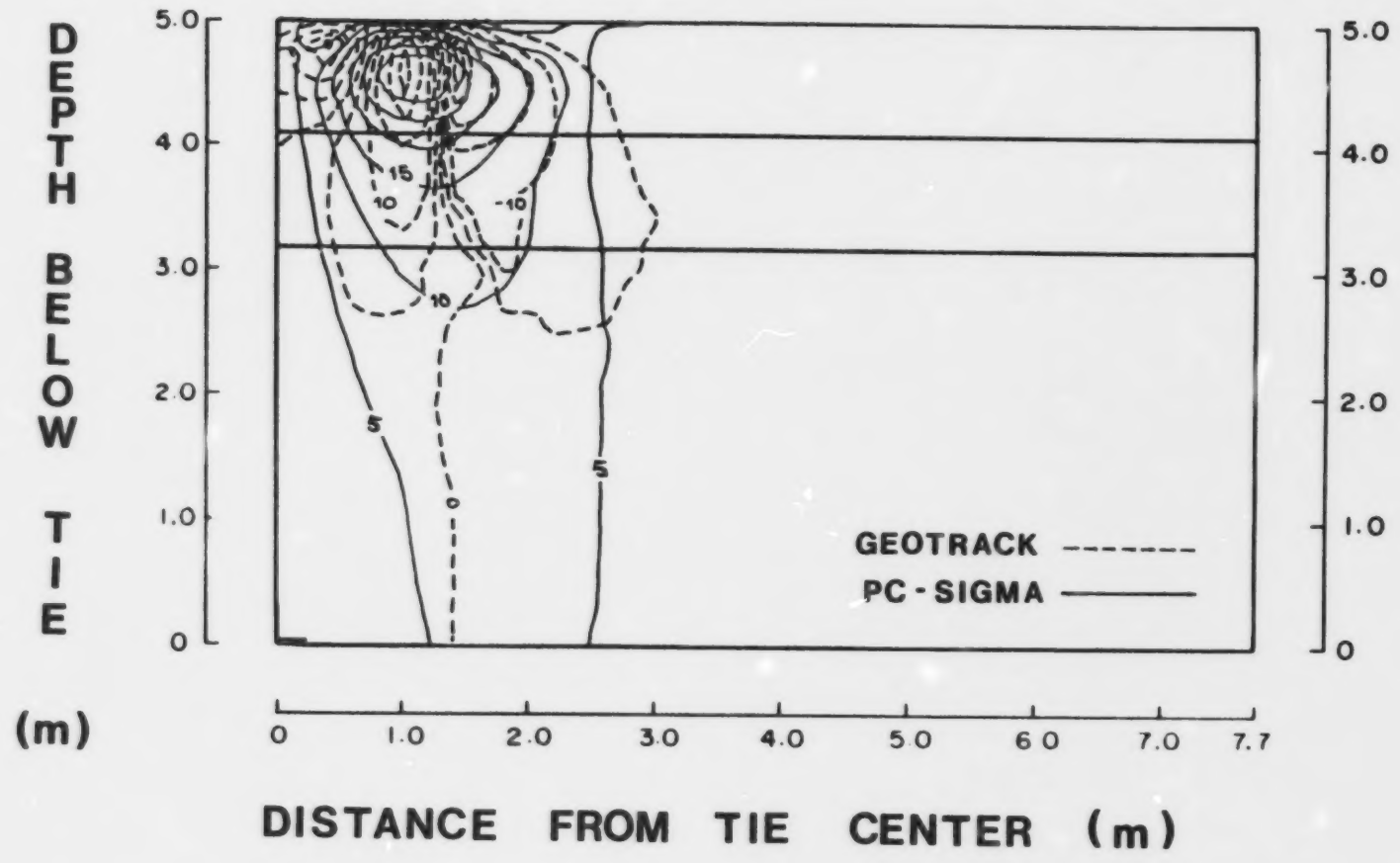

Fig. 4.28 Comparison of GEOTRACK shear stress distribution to PC-SIGMA for zero embankment slope

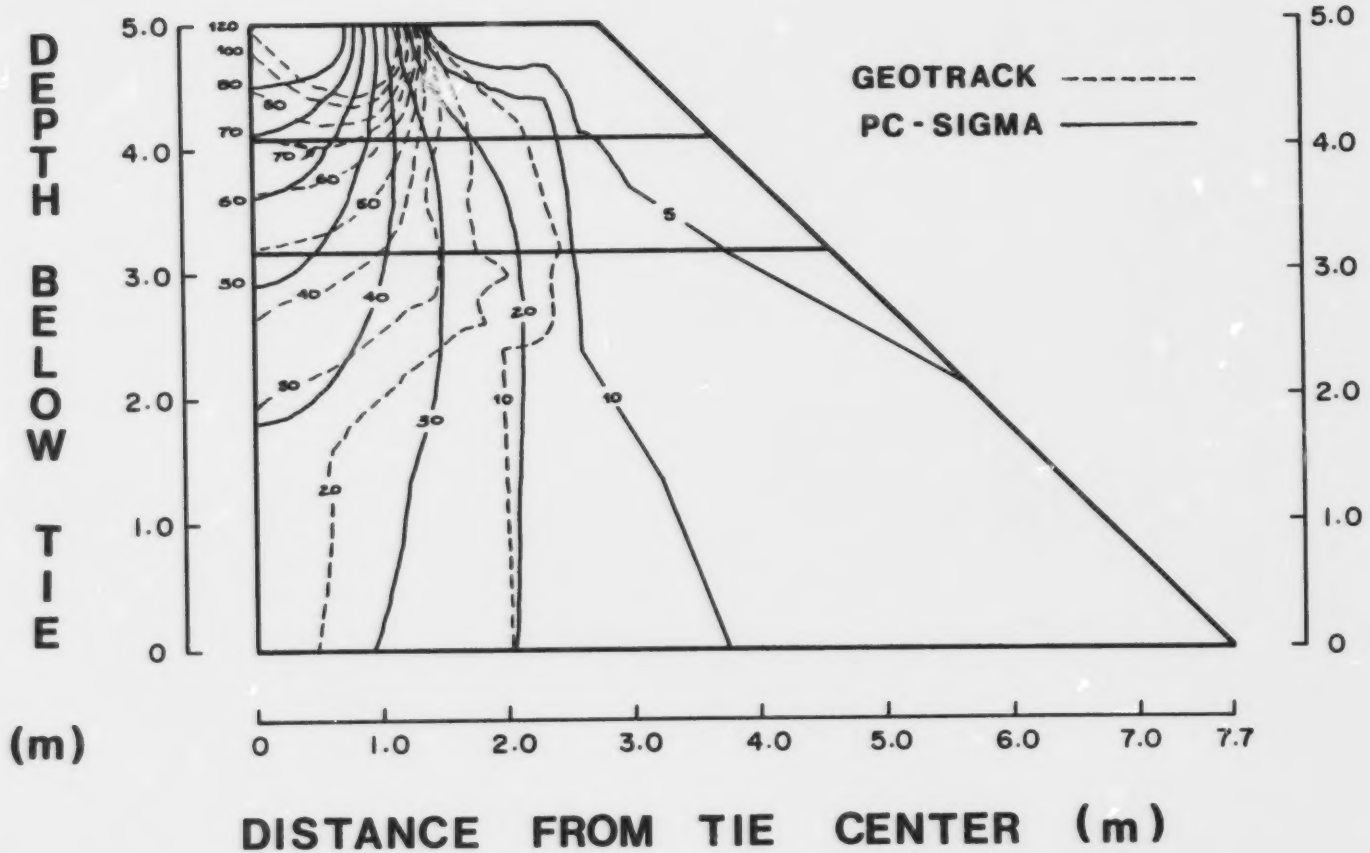

Fig. 4.29 Comparison of GEOTRACK vertical stress distribution to PC-SIGMA for 1:1 embankment slope

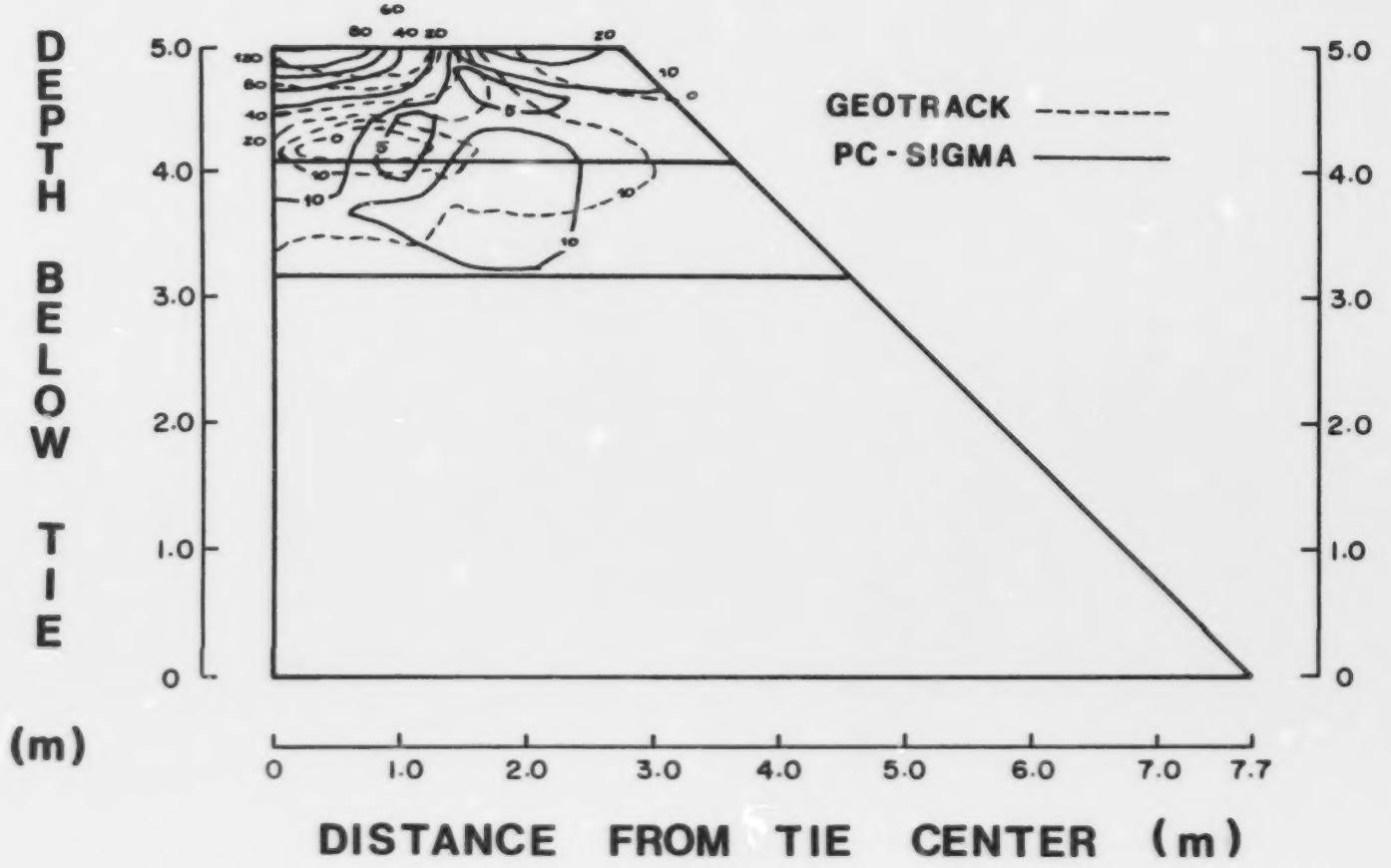

Fig. 4.30 Comparison of GEOTRACK horizontal stress distribution to PC-SIGMA for 1:1 embankment slope

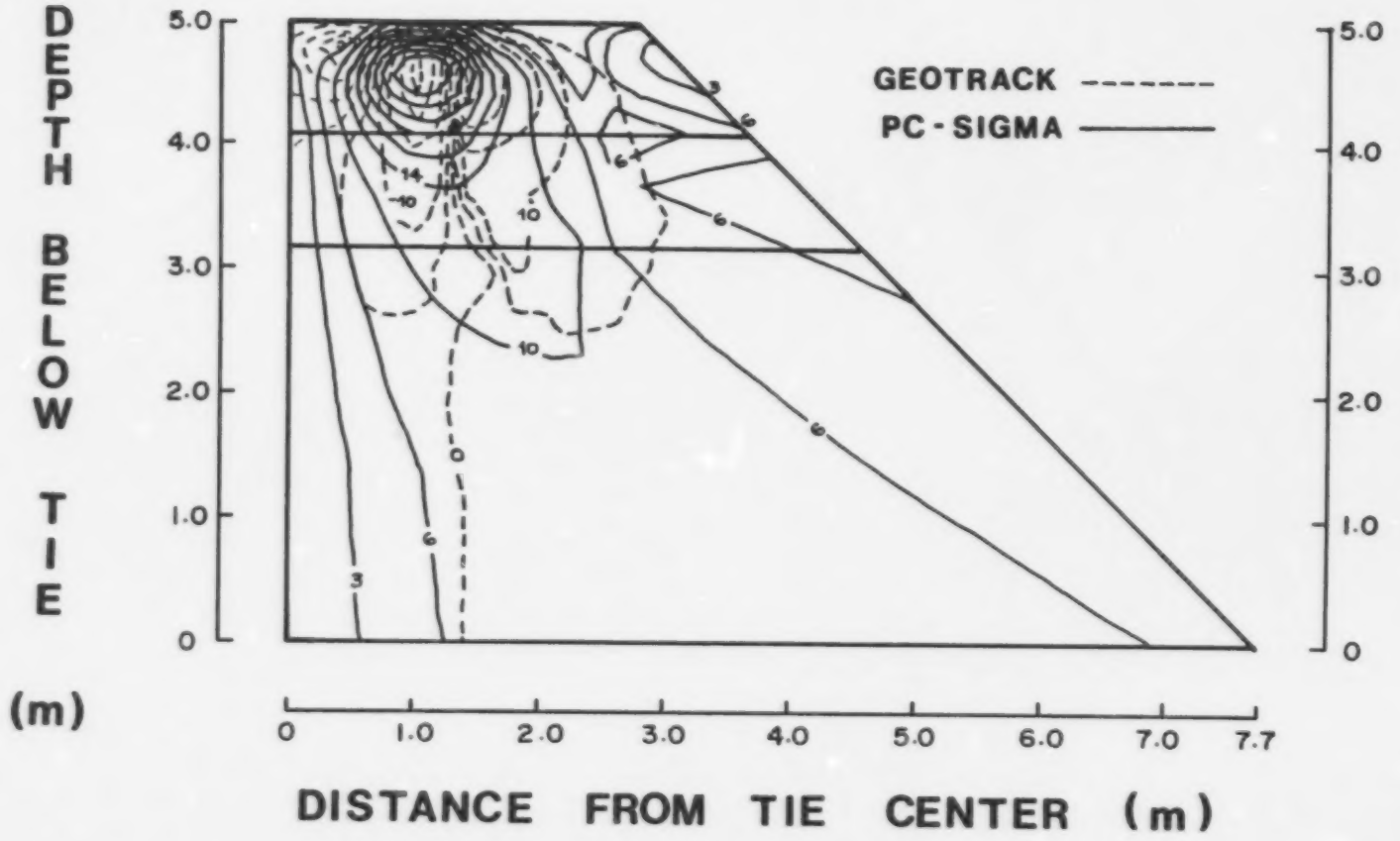

Fig. 4.31 Comparison of GEOTRACK shear stress distribution to PC-SIGMA for 1:1 embankment slope

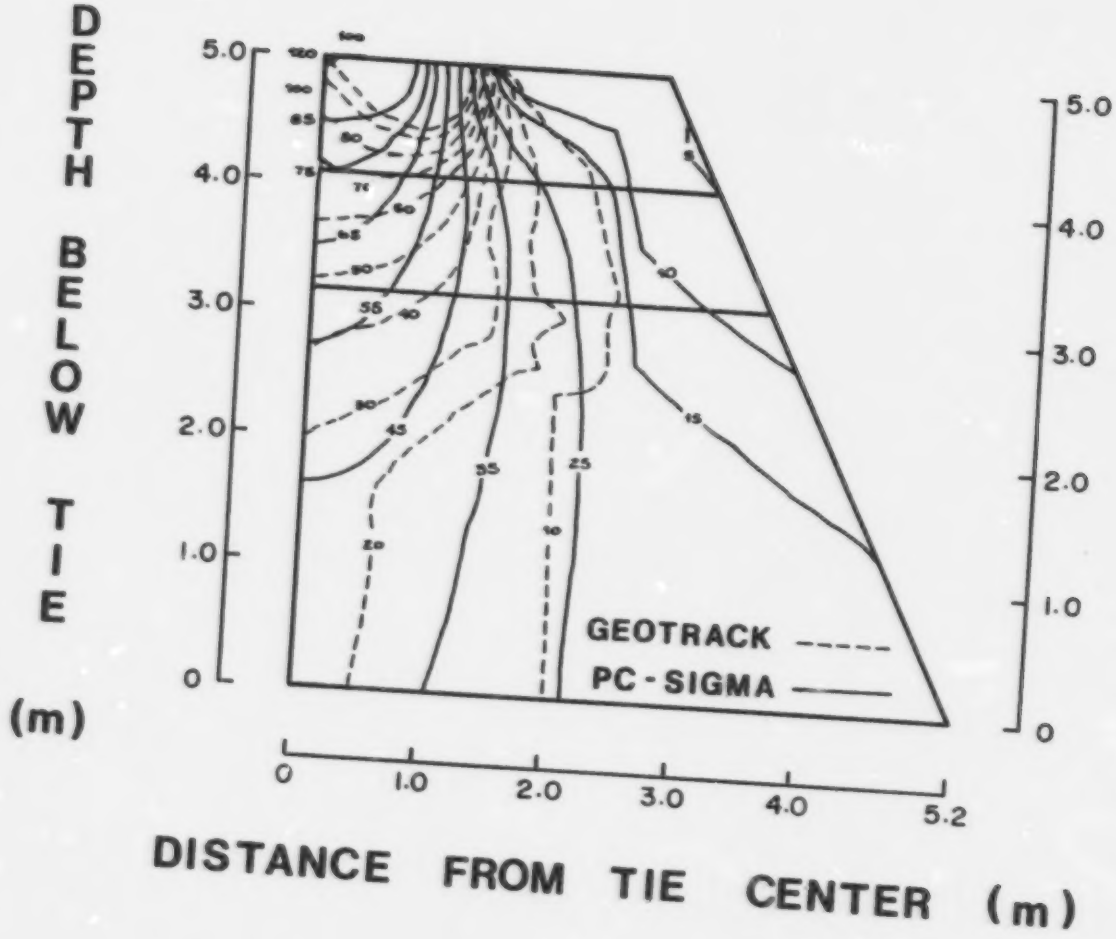

Fig. 4.32 Comparison of GEOTRACK vertical stress distribution to PC-SIGMA for 0.5:1 embankment slope

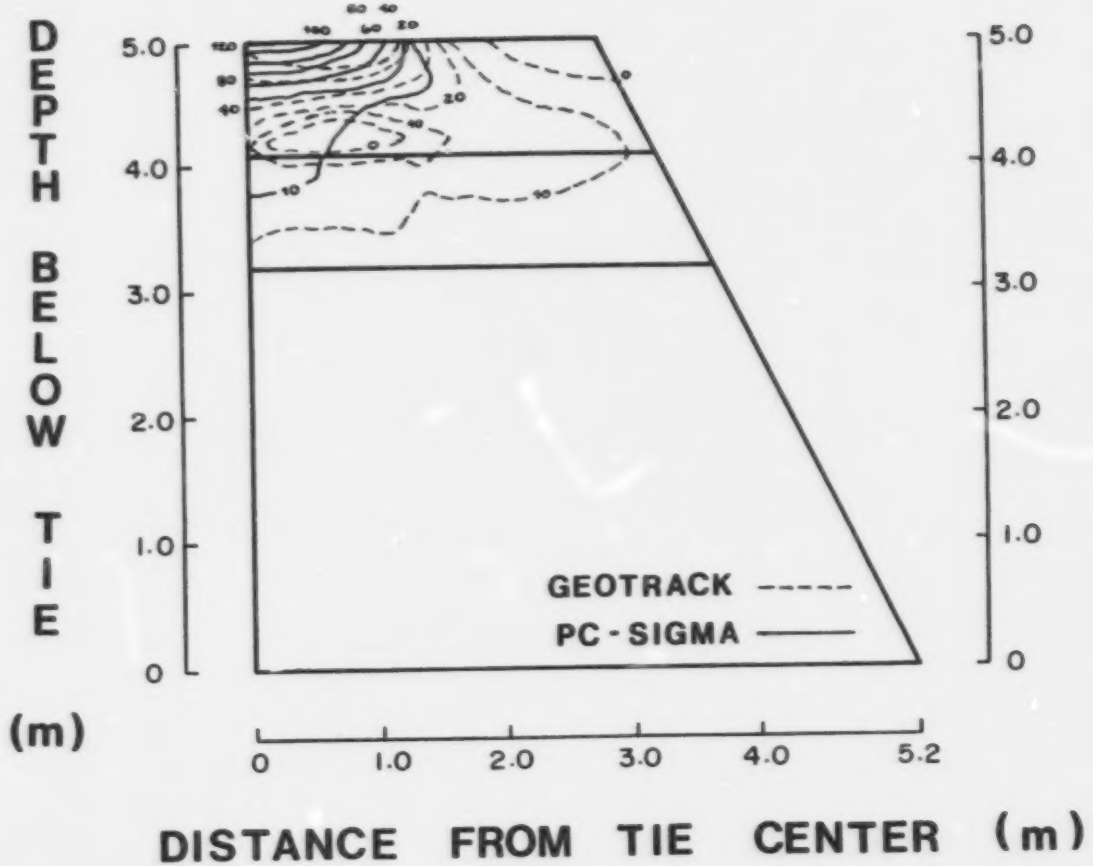

Fig. 4.33 Comparison of GEOTRACK horizontal stress distribution to PC-SIGMA for 0.5:1 embankment slope

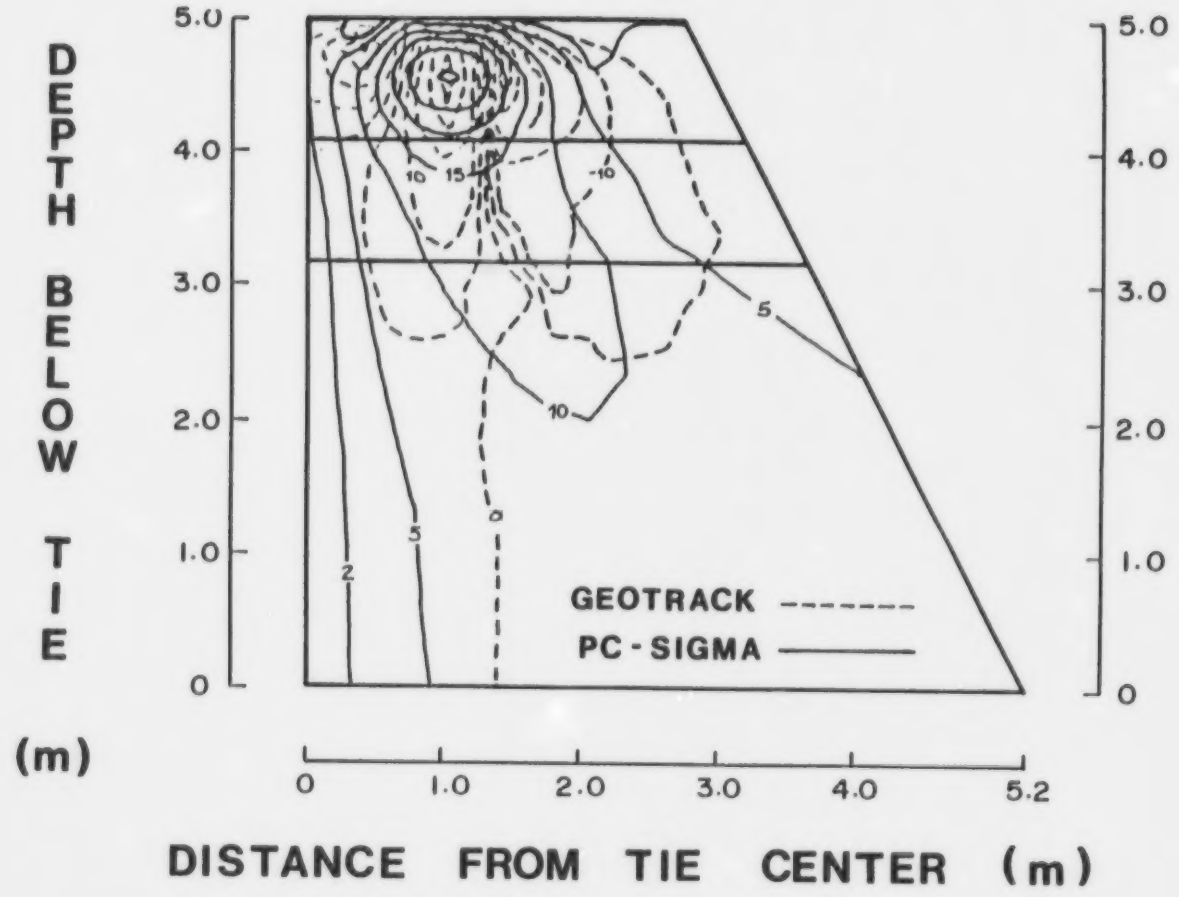

Fig. 4.34 Comparison of GEOTRACK shear stress distribution to PC-SIGMA for 0.5:1 embankment slope

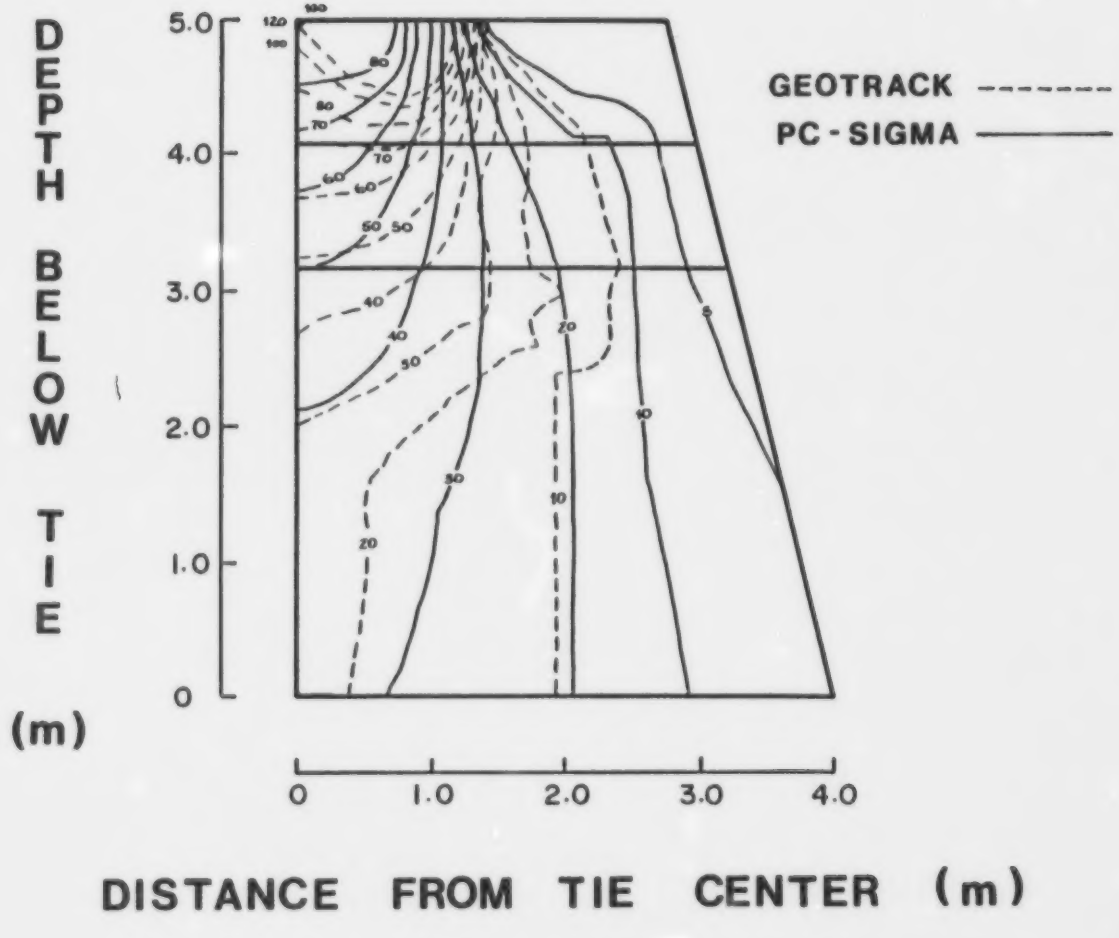

Fig. 4.35 Comparison of GEOTRACK vertical stress distribution to PC-SIGMA for 0.25:1 embankment slope

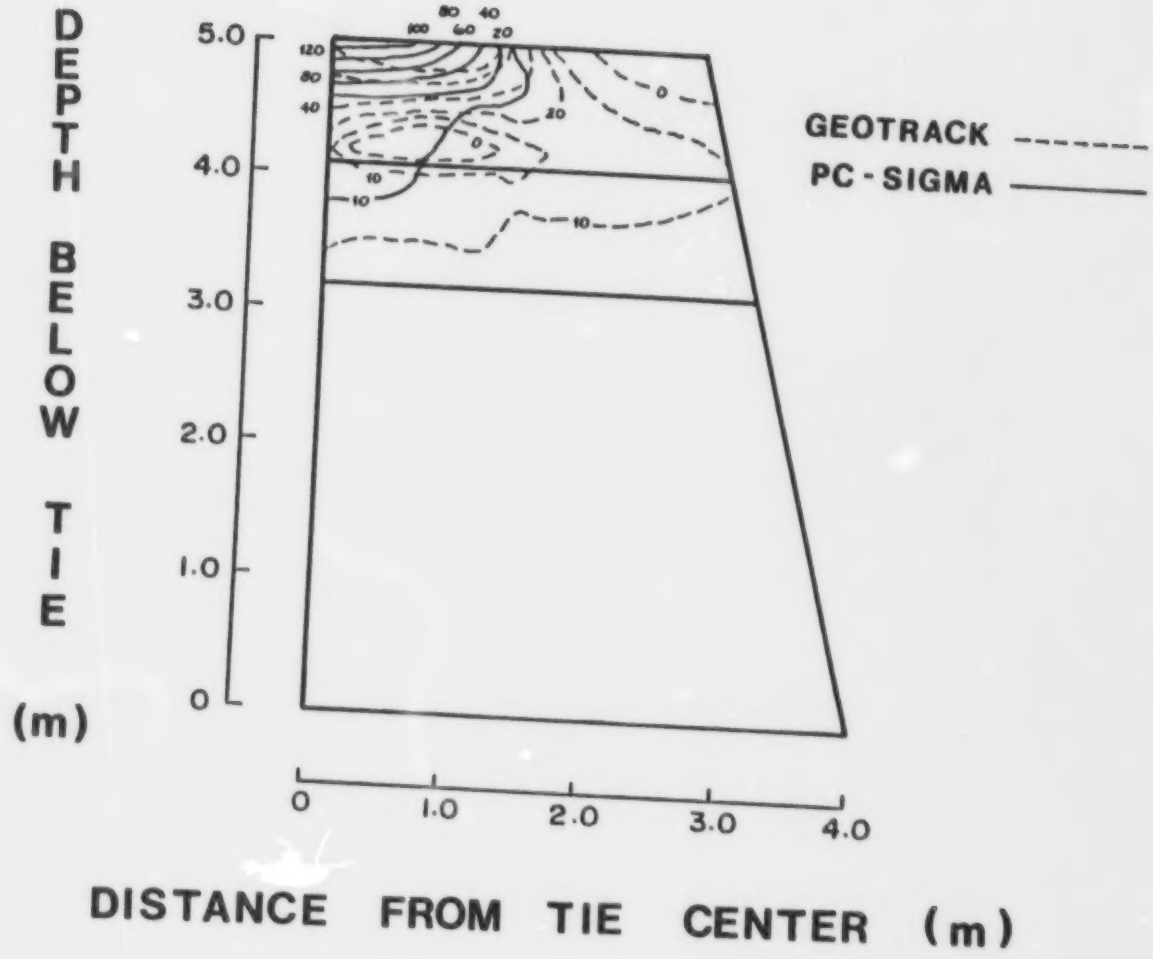

Fig. 4.36 Comparison of GEOTRACK horizontal stress distribution to PC-SIGMA for 0.25:1 embankment slope

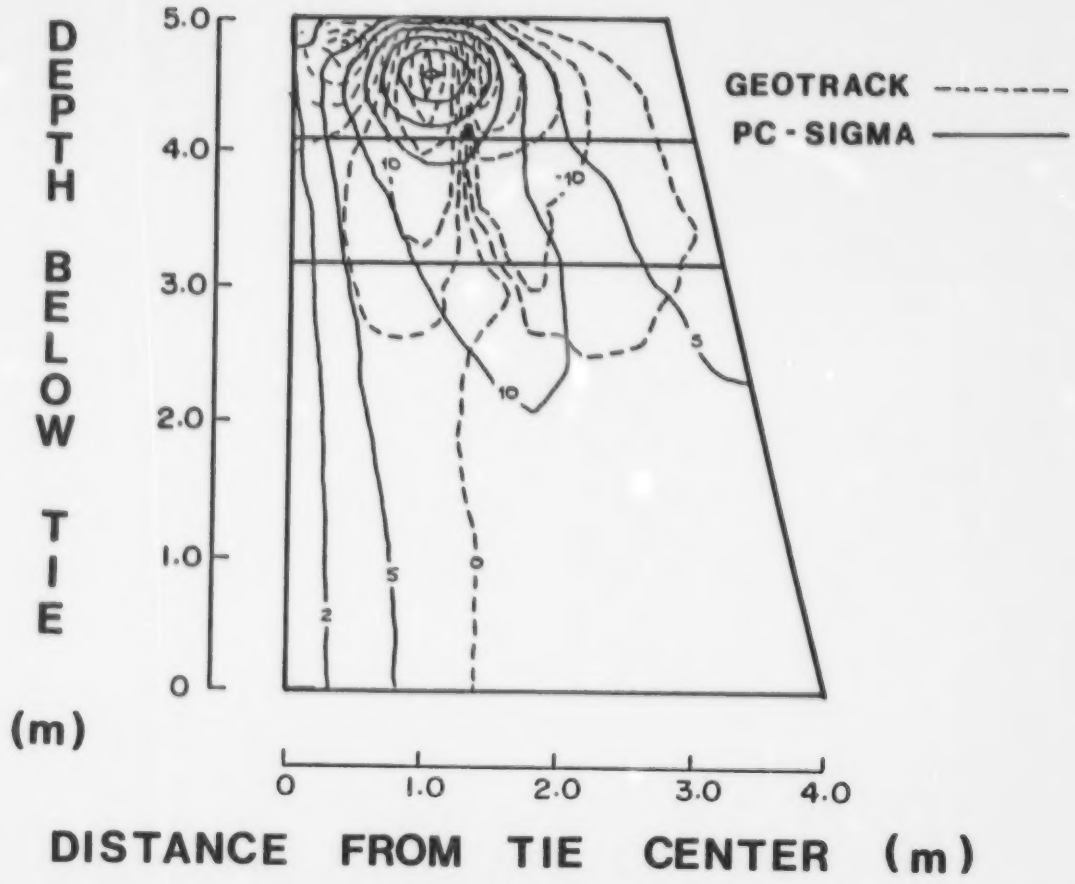

Fig. 4.37 Comparison of GEOTRACK shear stress distribution to PC-SIGMA for 0.25:1 embankment slope

are reasonable and show that the effect of increasing embankment slope is negligible. The comparisons presented in Figures 4.27, 4.30, 4.33, and 4.36 which illustrate the horizontal stress distributions show reasonable agreement between the GEOTRACK stress distribution and the 2-D finitie element analysis only for the zero embankment slope and the 1:1 slope. As expected, the shear stress comparisons do not show agreement because of the different assumptions used to limit tie-ballast separation.

For the comparisons between two-dimensional stress analysis and the GEOTRACK computer results, the loading configurations used with the PC-SIGMA computer program were derived from the tie-soil reaction loads output by the GEOTRACK computer program. The program GEOTRACK distributes the tie-soil reaction loads through the three-dimensional soil plate whereas the program PC-SIGMA assumes the loads are line loads on the two-dimensional soil embankment. Therefore, it is to be expected that the resulting stresses generated will be much higher from the PC-SIGMA computer program than from the GEOTRACK computer program.

4.4 Conclusions of the Stress Analysis Study

The following conclusions were drawn from the preceding stress analysis:

1) Embankment side-slopes have an insignificant effect on vertical stress distribution. Therefore, the use of the vertical stress distribution from the GEOTRACK computer program does not affect the use of the GEOTRACK computer program in the bearing capacity approach to design of railway subgrades developed by Sattler and Fredlund (1988).

2) Embankment side-slopes have an effect on horizontal stresses and shear stresses generated by the calculations. Therefore, the use of horizontal and shear stresses from the GEOTRACK computer program should be limited to applications with zero or small embankment slope. Modifications to the original GEOTRACK computer program have been made to enable the calculation of stresses on the slope and are documented in the updated User's Manual for GEOTRACK (Sattler, Fredlund, and Neis, 1990).

3) The significance of changing embankment side-slopes on horizontal and shear stresses suggests there is a need to investigate the effect of embankment slope on bearing capacity. It is recommended that slope stability analyses be performed in conjunction with bearing capacity analyses for embankment slopes. The following two chapters of this report document the research into the effect of embankment side-slopes on bearing capacity and the use of slope stability analyses for railway subgrades with negative pore-water pressures.

5.0 BEARING CAPACITY ANALYSES

The load carrying capacity of soil beneath a footing has long been expressed as a bearing capacity (Terzaghi, 1943). Ultimate bearing capacity is defined as the maximum load that the ground beneath a footing can sustain (Terzaghi, 1943). Observations of bearing capacity failures have established that failure usually occurs as a shear failure of the soil supporting the footing (Vesic, 1973). Three principal modes of shear failure have been identified: 1) general shear failure (Fig. 5.1), 2) local shear failure (Fig. 5.2), and 3) punching shear failure (Fig. 5.3) (Vesic, 1973).

General shear failure is characterized by a well-defined failure pattern, which consists of a continuous slip surface from one edge of the footing to the ground surface (Figure 5.1). Failure is generally sudden and catastrophic, also accompanied by considerable tilting of the foundation. A tendency toward bulging of the soil can usually be recorded on both sides of the footing, although the final soil collapse usually occurs only on one side (Vesic, 1973).

On the other hand, the punching shear failure mode is characterized by a failure pattern that is not easily observed (Figure 5.3). Vertical movement of the footing is accompanied by compression of the soil immediately underneath. The soil outside the loaded area remains

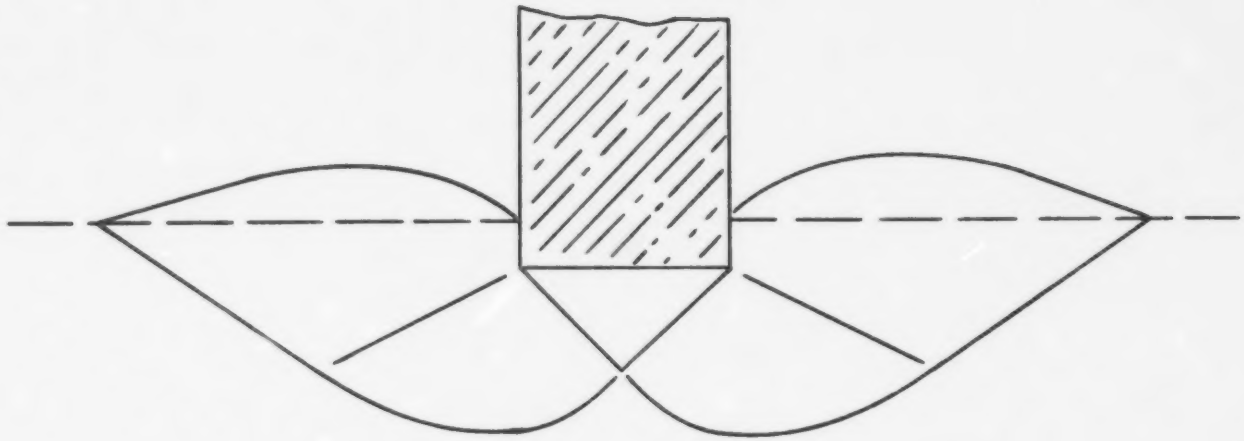

Fig. 5.1 Modes of bearing capacity failure - general shear failure (after Vesic, 1973)

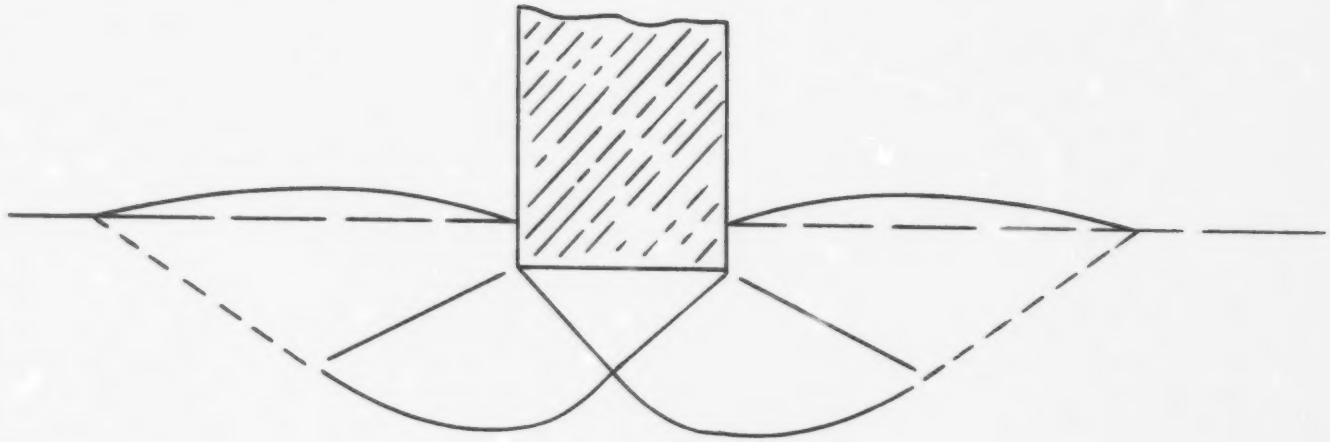

Fig. 5.2 Modes of bearing capacity failure - local shear failure (after Vesic, 1973)

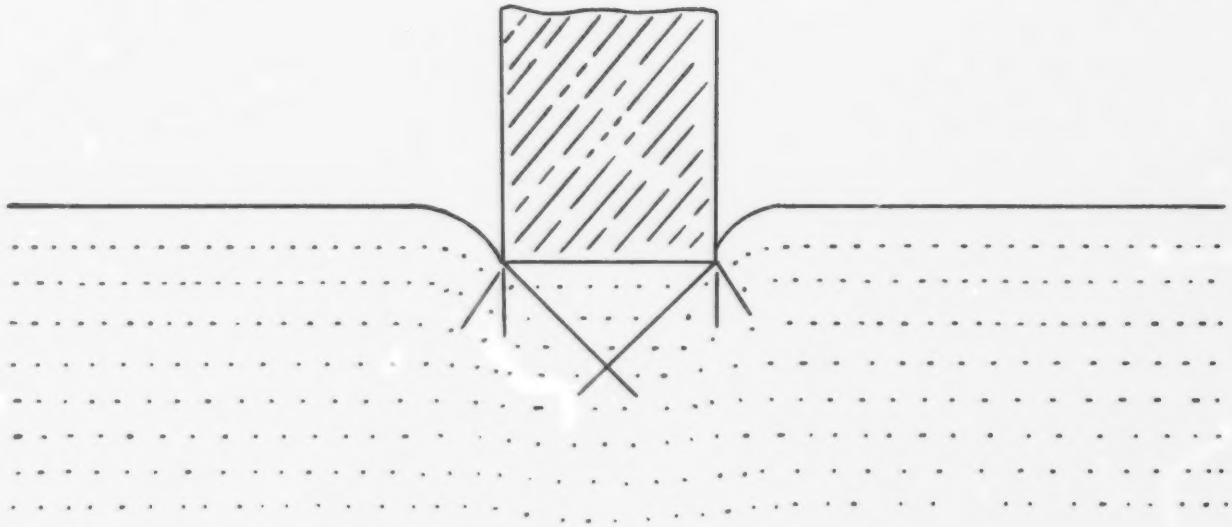

Fig. 5.3 Modes of bearing capacity failure - punching shear failure (after Vesic, 1973)

relatively unaffected and there are practically no movements of the soil on the sides of the footing (Vesic, 1973).

Local shear failure is characterized by a failure pattern somewhere between the extremes of general shear failure and punching shear failure (Figure 5.2). The failure pattern consists of a wedge and slip surfaces just as for the case of general shear failure and there is also significant vertical compression under the footing as for a punching shear failure (Vesic, 1973).

The general shear failure pattern is divided into three zones of failure for the purposes of analysis: 1) Zone I, an active Rankine[2] zone, 2) Zone II, a radial Prandtl[3] zone, and 3) Zone III, a passive Rankine zone (Figure 5.4) (Vesic, 1973). Because of friction between the soil and the base of the footing, Zone I remains in an elastic state (i.e., called the "elastic wedge") and behaves as though it were a part of the footing, penetrating the soil like a wedge (Terzaghi and Peck, 1967). The weight of the soil in Zone I, the active Rankine zone, contributes to the bearing capacity failure whereas the weight of the soil in Zone III,

---

[2] Rankine (1857) investigated the stress conditions developed by gravity acting on a retaining wall. Two states of plastic equilibrium were identified: 1) the active Rankine state, and 2) the passive Rankine state. When the soil behind a retaining wall pushes against the wall causing the wall to move away from the soil, the active earth pressure is mobilized. When the soil behind a retaining wall resists the tilting of the wall into the soil mass, the passive earth pressure is mobilized (Terzaghi and Peck, 1967).

[3] Prandtl (1921) determined an analytical solution to the resistance of metal by a punch. Terzaghi adopted the log-spiral geometry of the Prandtl solution for bearing capacity problems in soils (Spangler and Handy, 1982).

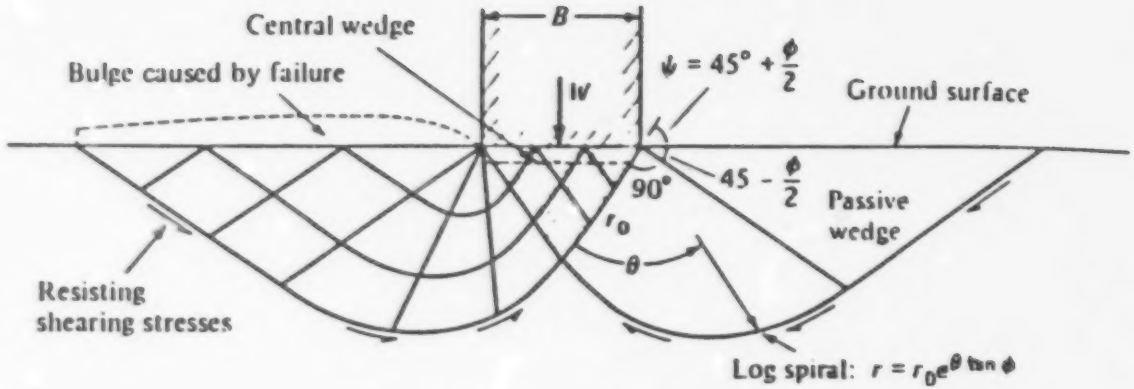

Fig. 5.4 Idealized bearing capacity failure geometry for Prandtl log-spiral (Spangler and Handy, 1982)

the passive Rankine zone, resists the bearing capacity failure. Shear stresses developed along Zones II and III resist the bearing capacity failure.

The solution to the failure geometry illustrated in Figure 5.4, based upon the classical Terzaghi-Prandtl solution, results in the general bearing capacity equation:

$$q_u = c\,N_c + 1/2\,\gamma\,B\,N_\gamma + q_o N_q \qquad [1]$$

where:

N_c, N_γ, N_q = bearing capacity factors

c = total cohesion or undrained shear strength

γ = unit weight of the overlying soil

B = footing width for a strip footing

q_o = surcharge loading

The bearing capacity factors have been described in terms of equations by Brinch-Hansen (1970) and Vesic (1973) as follows:

$$N_q = e^{(\pi \tan \phi)} \frac{1 + \sin \phi}{1 - \sin \phi} \qquad [2]$$

$$N_c = (N_q - 1) \cot \phi \qquad [3]$$

$$N_\gamma = 1.5\,(N_q - 1) \tan \phi \qquad [4]$$

where:

ϕ = the friction angle of the subgrade material

If the bearing area is not assumed to be infinite in length, shape factors are applied to each individual term of the bearing capacity equation in order to correct for the foundation shape (Canadian Foundation Engineering Manual, 1985):

$$s = 1 - 0.4\,(B/L) \qquad [5]$$

$$s_c = s_q = 1 + (B/L)\,(N_q/N_c) \qquad [6]$$

where:

B = the width of the bearing area considered

L = the length of the bearing area considered

Differences in the computation of bearing capacity result from the use of failure geometries other than the classical Terzaghi-Prandtl solution (Spangler and Handy, 1982). Other published equations for the bearing capacity factors could also have been used. Loading eccentricity factors may also be applied to each individual term (Meyerhof, 1953). As well, the influence of base roughness and varying ground-water table conditions have been investigated (Meyerhof, 1955).

For the application of conventional bearing capacity theories to the design of railway subgrade systems, loading

eccentricity and the influence of base roughness have been excluded as insignificant. The extension of bearing capacity theory to layered systems for use in the ballast-subballast-subgrade system are discussed in the following section. The extension of conventional bearing capacity theory to the condition of soils with negative pore-water pressures is presented in section 5.2 and the development of bearing capacity theory for foundations on slopes is presented in section 5.3.

5.1 Modification of Conventional Bearing Capacity for Layered Systems

The conventional bearing capacity equation presented in Equation [1] was modified for layered systems for use in the bearing capacity approach to design of railway subgrades (Sattler and Fredlund, 1988). Two approaches were utilized to extend the conventional bearing capacity equation to layered ground: 1) the Broms' approach (1965) which assumes the transfer of load through the granular material to the surface of the subgrade and the computation of conventional bearing capacity using the reduced load at the subgrade surface, and 2) the Hanna and Meyerhof approach (1980) which treats the upper granular material as a continuation of the footing, which punches into the subgrade material, in many ways like a driven pile.

Two overall configurations were considered for the bearing capacity analysis as it applies to railway subgrades: 1) the geometry perpendicular to the track (Figure 5.5), and 2) the geometry parallel to the track (Figure 5.6). Two potential failure geometries were identified within each overall configuration leading to four possible failure geometries: 1) the failure of the complete tie-track system for the length of the track (Figure 5.7), 2) the failure of a portion of the track beneath the heavily stressed outer 1/3 of the tie and the distance of a double truck loading (Figure 5.8), 3) the local failure of an individual tie punching into the subgrade (Figure 5.9), and 4) the failure of a portion of the track corresponding to the loading arrangement shown in Figure 5.10 (Sattler and Fredlund, 1988).

Field experience suggests that the failures represented by Figures 5.9 and 5.10 occur in the absence of subballast for extremely weak clay subgrades. Generally, the direction of the shear plane depicted for the failure in Figure 5.10 requires additional braking loads such as those which occur on corners. Although all four geometries have again been presented, previous research has indicated that the failure geometry presented in Figure 5.8 is most critical (Sattler and Fredlund, 1988).

The failure geometry depicted in Figure 5.9 is analyzed by the Hanna and Meyerhof approach (1980) to bearing capacity for layered ground whereas the failure geometries

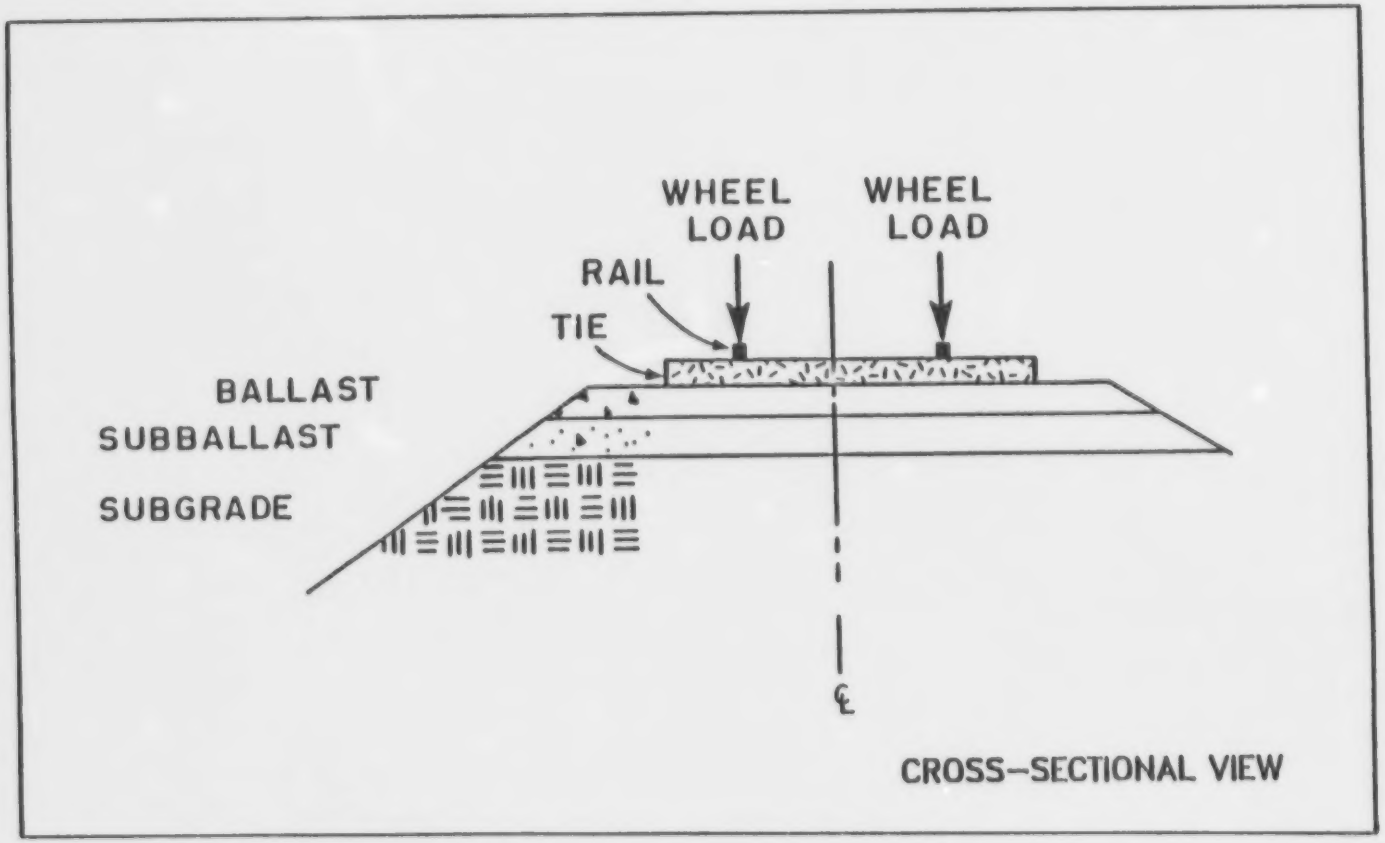

Fig. 5.5 Cross-sectional view of the track system showing the geometry perpendicular to the track

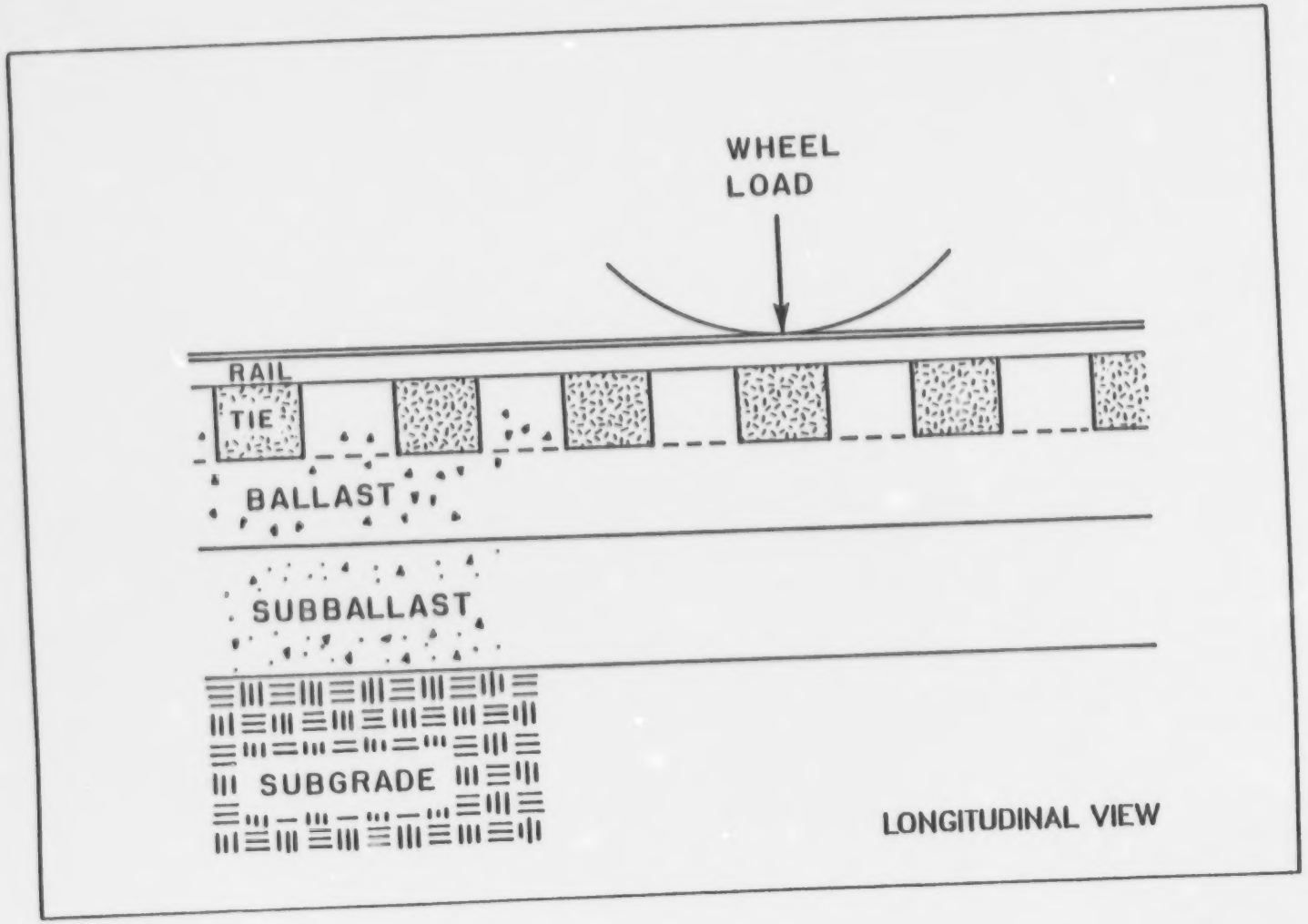

Fig. 5.6 Longitudinal view of the track system showing the geometry parallel to the track

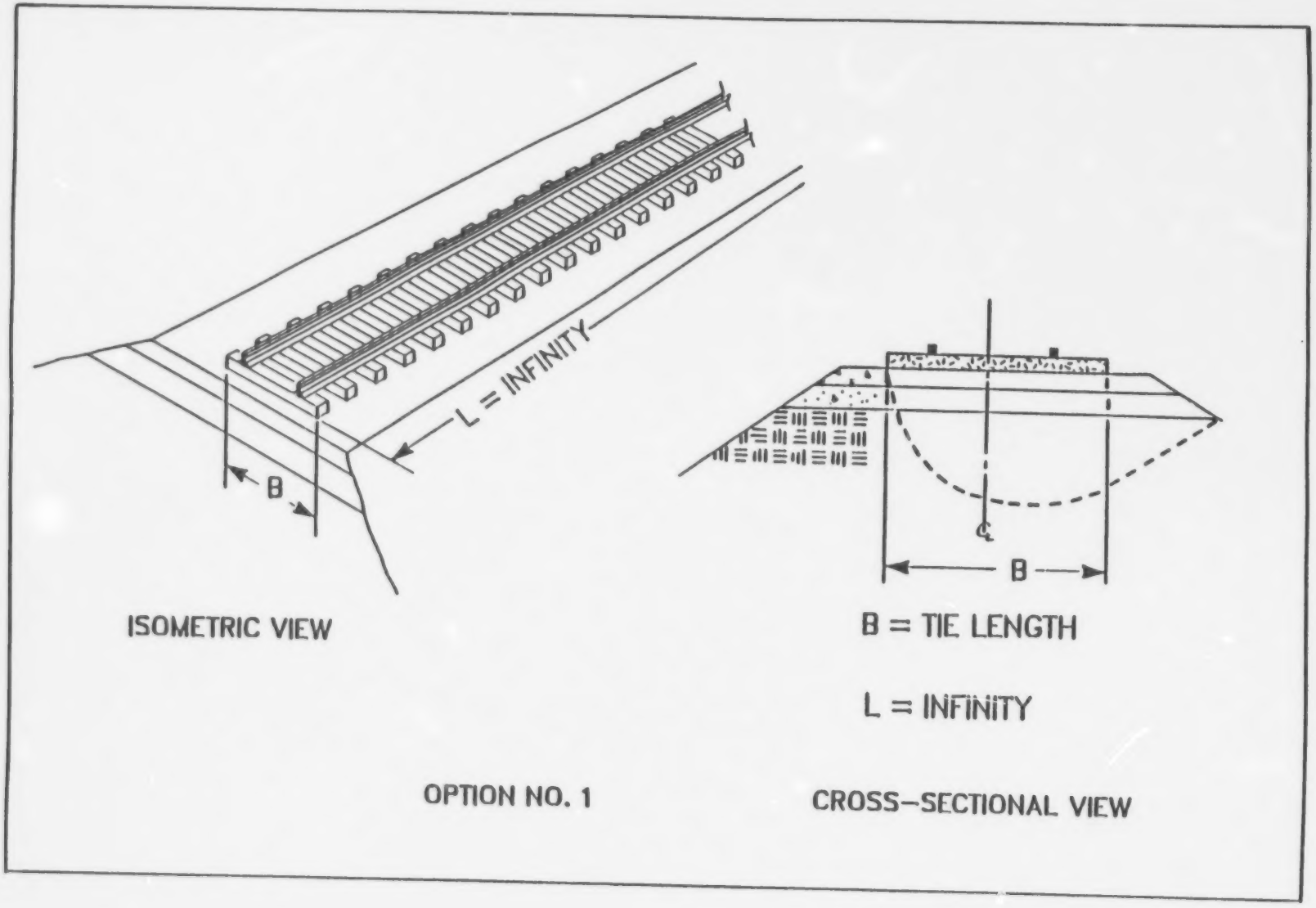

Fig. 5.7 Failure geometry for the complete tie-track system for the length of the track

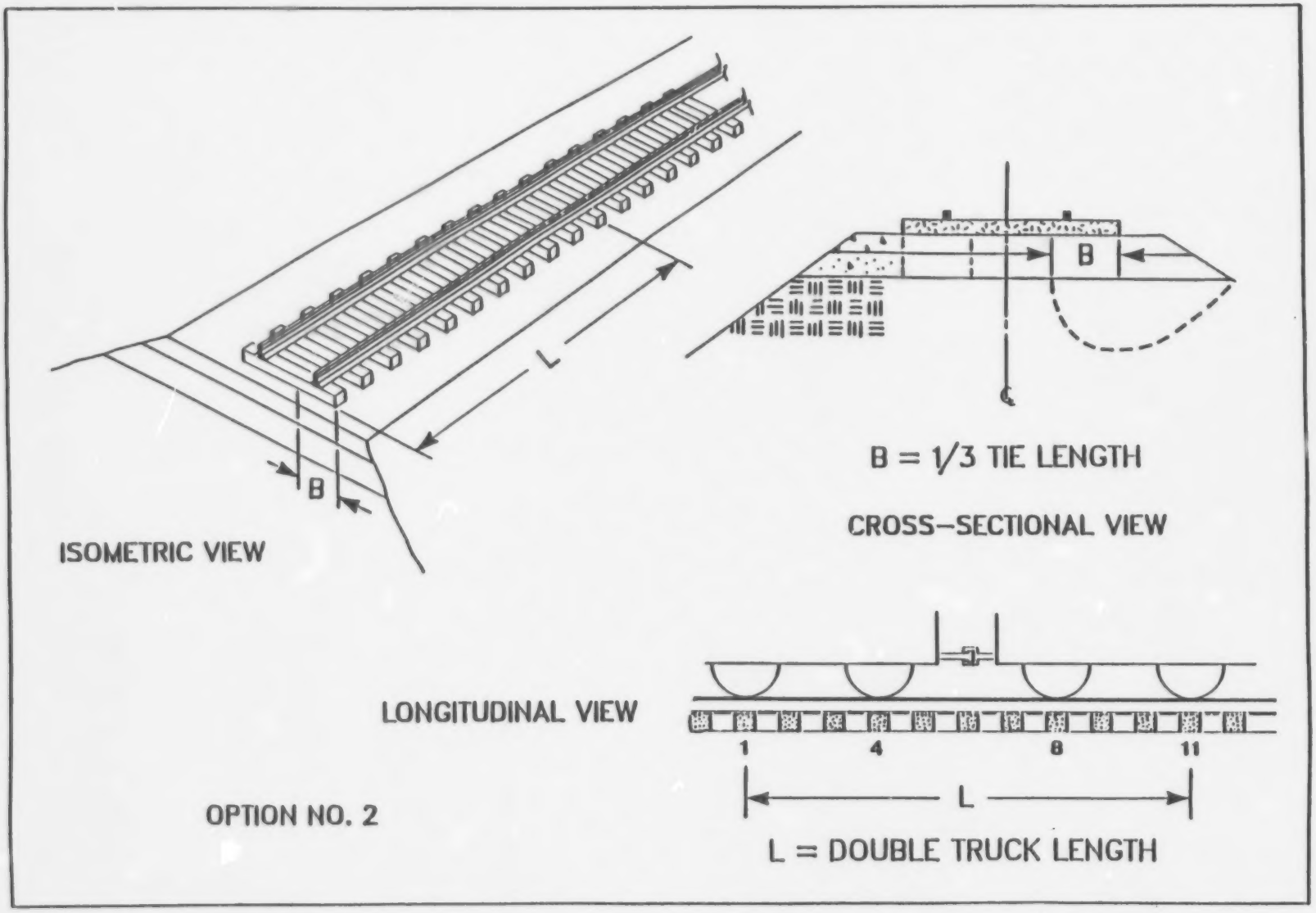

Fig. 5.8 Failure geometry for the heavily stressed outer third of the tie and the distance of a double truck loading

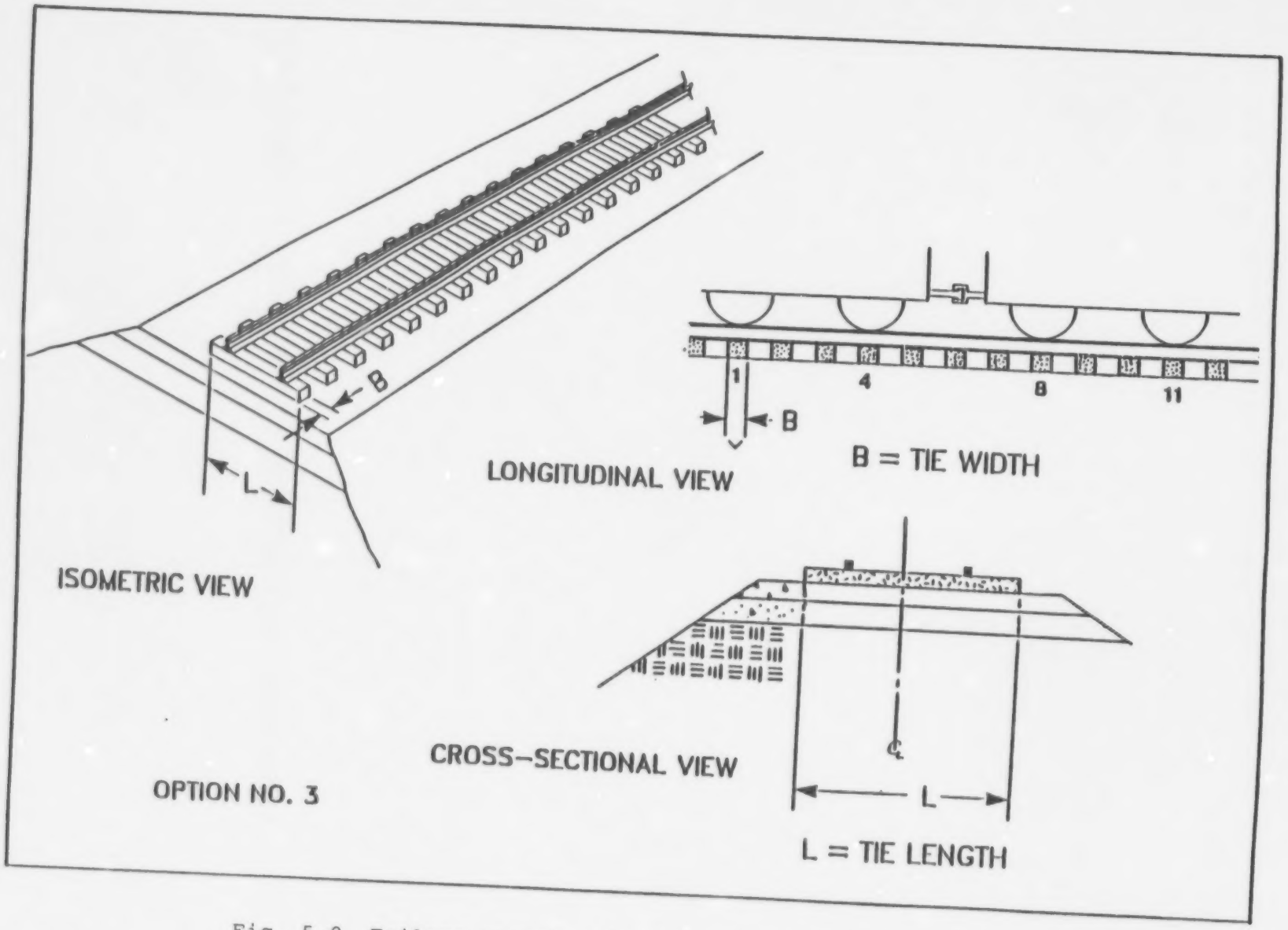

Fig. 5.9 Failure geometry for the local failure of an individual tie punching into a weak subgrade

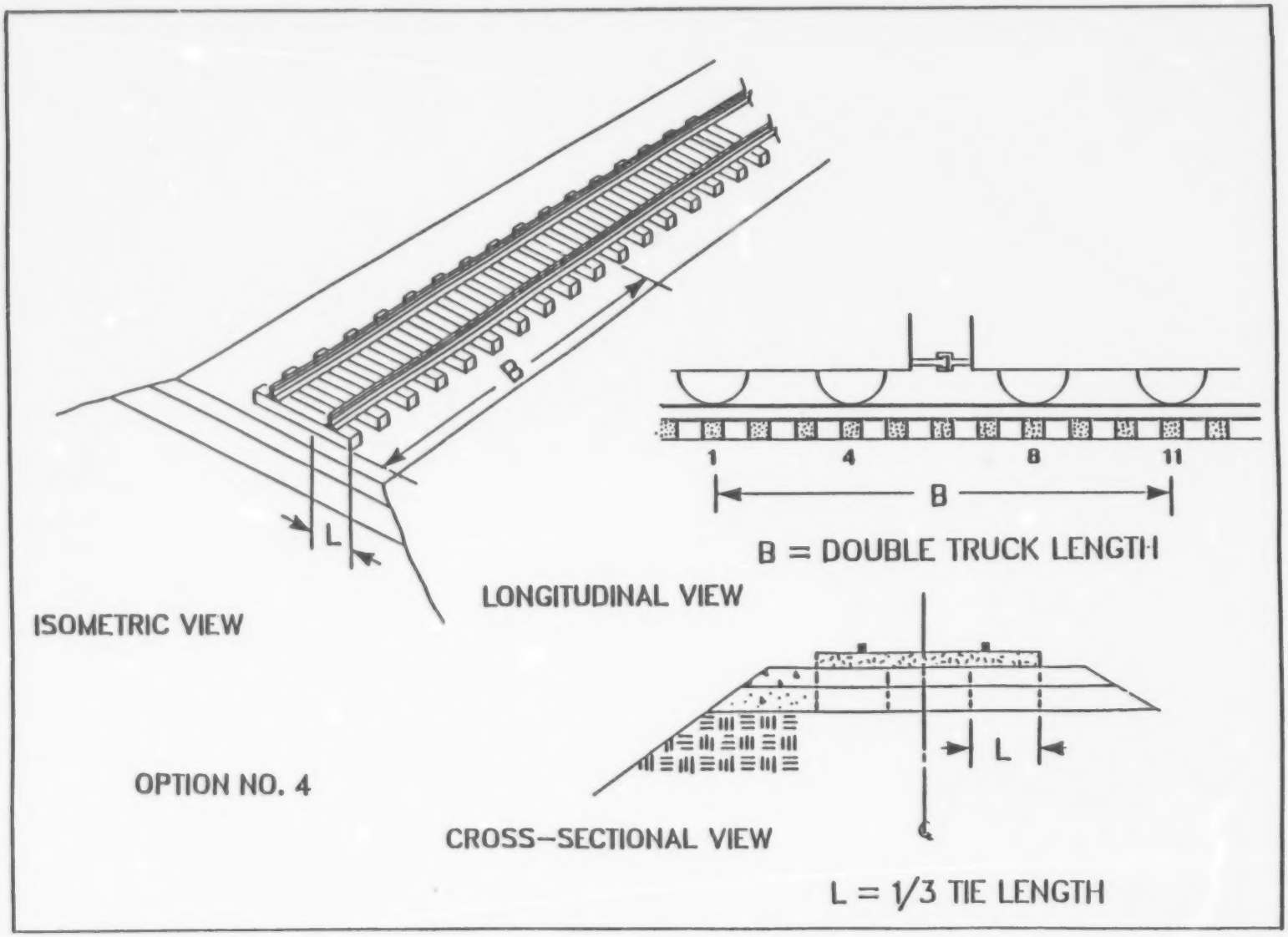

Fig. 5.10 Failure geometry for a portion of the track beneath a double truck arrangement for weak subgrades

shown in Figures 5.7, 5.8, and 5.10 are all analyzed by the Broms' approach (1965).

The Broms' approach to computing bearing capacity for layered ground systems is illustrated in Figure 5.11. The granular material distributes the applied load to an enlarged area such that the stress at the subgrade surface is smaller than the applied stress immediately beneath the footing. The conventional bearing capacity equation may be used taking into account the decreased stress at the subgrade surface (i.e., caused by the distribution of the applied stress through the granular layers).

The conventional bearing capacity equation is used with the actual dimensions of the footing (i.e., or tie-track system). The bearing capacity computed in this manner is then compared to the stress which reaches the subgrade surface through the granular material from the applied load (i.e., the subgrade surface stress modelled by the GEOTRACK computer program) (Sattler and Fredlund, 1988).

Broms (1965) used a somewhat different approach to computing subgrade bearing capacity since a convenient method for the computation of stresses at the subgrade surface was not available. Broms assumed that the load was distributed through the granular material in a 2:1 ratio and therefore, the applied load was distributed over the enlarged area at the subgrade surface (Sattler and Fredlund, 1988).

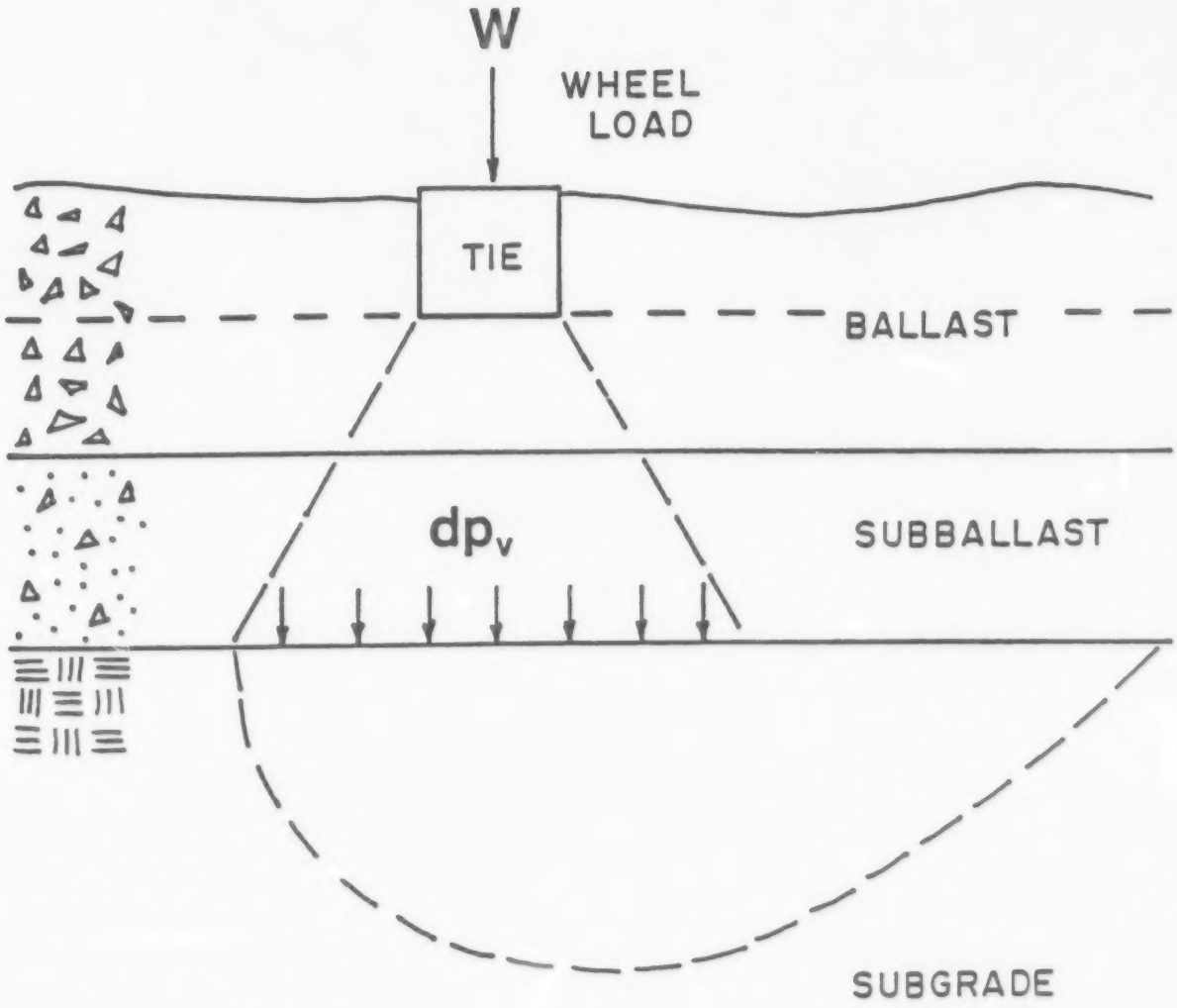

Fig. 5.11 Broms' approach to computing bearing capacity (after Broms, 1965)

The Hanna and Meyerhof approach to computing bearing capacity for layered ground systems (1980) is presented in Figure 5.12. The assumed failure mechanism is one in which the upper granular layer of approximately pyramidal shape is pushed into the lower clay layer. At the point of limiting equilibrium, the sum of forces in the vertical direction yields an equation for the ultimate bearing capacity in the layered system:

$$q_u = c\ N_c + \gamma_1\ H^2\ (1 + 2D/H)\ K_s \tan \phi'/B - \gamma_1\ H \qquad [7]$$

where:

c = undrained shear strength of the soft clay subgrade

N_c = bearing capacity factor

γ_1 = unit weight of overlying granular material

H = thickness of granular material below the bottom of the footing (i.e., railway tie)

D = depth of embedment of the footing (i.e., railway tie)

Ks = coefficient of punching shear resistance (i.e. determined from published charts by Hanna and Meyerhof (1980))

ϕ' = friction angle of the upper granular material

B = width of footing (i.e.,or bearing area equal to width of railway tie)

Kraft and Helfrich (1983) suggest that the Hanna and Meyerhof approach for computing bearing capacity cannot be

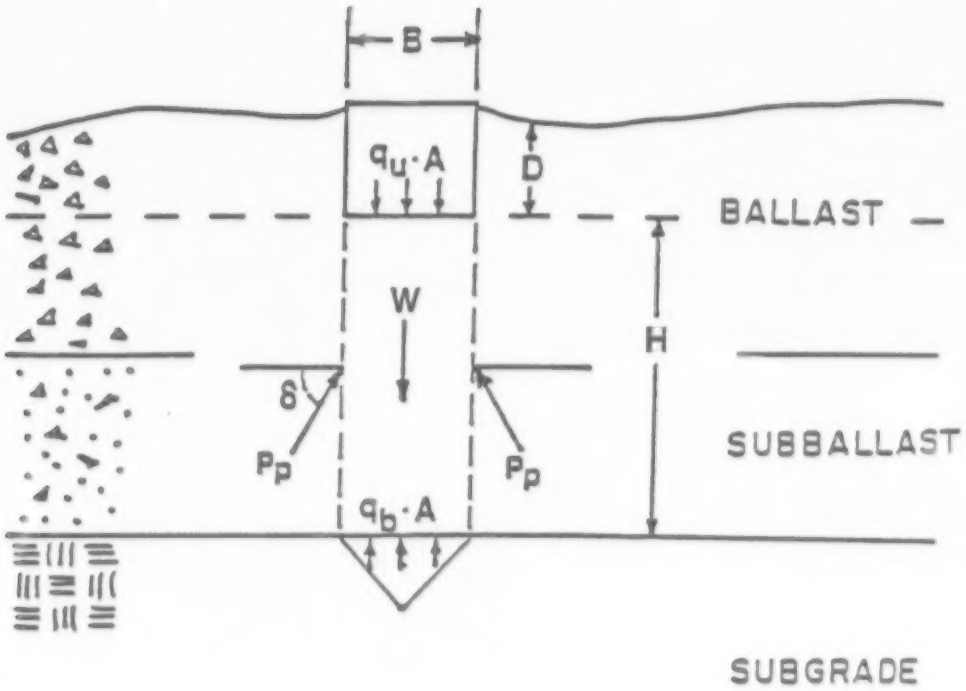

$$\Sigma F_v = 0$$

$$q_u = q_b + (2/B)(P_p \sin \delta) - \gamma H \leq q_t$$

The passive earth force is:

$$P_p = 1/2\, \gamma H^2 (1 + 2D/H) K_p / \cos \delta$$

Assume a coefficient of punching shear resistance on the vertical plane through the footing edge such that:

$$K_s \tan \phi' = K_p \tan \delta$$

$$\therefore \quad q_u = cN_c + \gamma H^2 (1+2D/H) K_s \tan \phi' / B - \gamma H$$

Fig. 5.12 Hanna and Meyerhof approach to computing bearing capacity (Hanna and Meyerhof, 1980)

extended to stronger deposits while still maintaining reliable predictions. Therefore, the Hanna and Meyerhof approach (1980) has been recommended for application only to the multi-layered failure over weak subgrades as depicted in Figure 5.9. The Broms' approach (1965) may be applied to all four layered ground failure geometries, but has been recommended particularly for the geometries shown in Figures 5.7., 5.8, and 5.10 (Sattler and Fredlund, 1988).

5.2 Incorporation of Unsaturated Soil Mechanics in Conventional Bearing Capacity Theory

In 1925, Terzaghi acknowledged the influence of the groundwater table on bearing capacity. For a footing on a completely submerged soil, the unit weight of the material is equal to the submerged unit weight. The bearing capacity is therefore reduced due to the buoyant effects of the ground-water table beneath the footing (Meyerhof, 1955).

Meyerhof (1955) extended the work of Terzaghi by researching the extremes between full submergence and zero submergence (Figure 5.13). Meyerhof (1955) illustrated that the presence of the ground-water table was significant to the computation of bearing capacity when the groundwater table was located within a depth equal to two foundation widths for a strip footing and within one foundation width for a circular or square footing. The conventional bearing

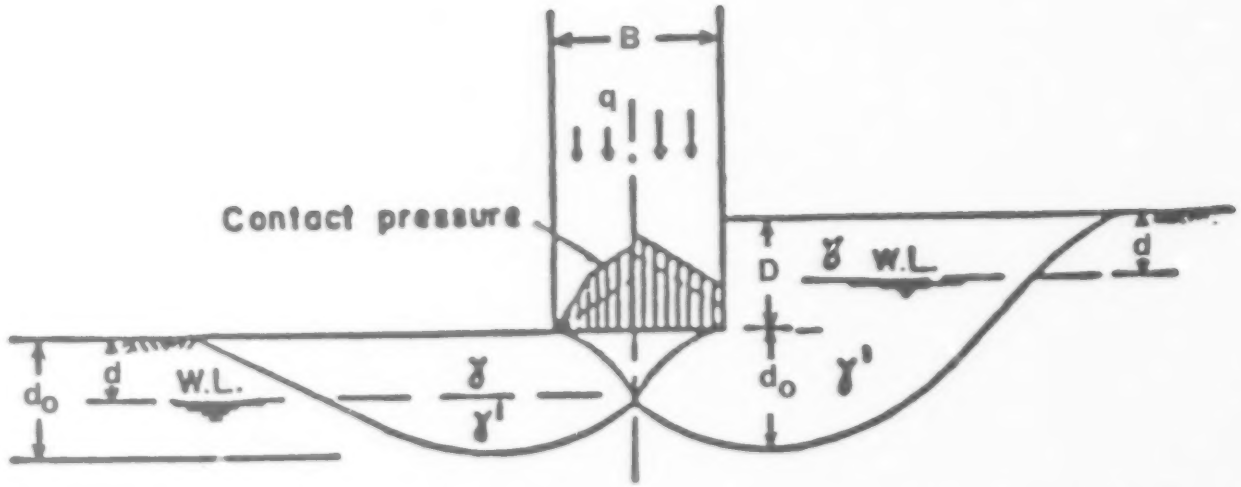

(a) SURFACE FOUNDATION (b) SHALLOW FOUNDATION

$$q = [\gamma' + F(\gamma - \gamma')] \frac{B}{2} N_\gamma$$

F = 0 water table at ground surface
F = 1 water table below failure zone

Fig. 5.13 Effect of partial submergence on bearing capacity (Meyerhof, 1955)

capacity was reduced by a factor varying linearly from zero outside the depth of significance to one hundred percent of the factor value for full submergence.

The work of Terzaghi (1925) and Meyerhof (1955) considered the effects of **positive pore-water pressures** beneath the footing in **reducing** conventional bearing capacity. If the ground-water table is located at considerable depth, **negative pore-water pressures** beneath the footing may conversely result in an **increase** in the conventionally computed bearing capacity (Figure 5.14).

In saturated soil mechanics, one stress state variable (i.e., effective stress, $(\sigma - u_w)$) is sufficient to characterize the shear strength of the soil. Beneath the groundwater table, the pore-water pressure is positive and acts to reduce the shear strength accordingly.

In unsaturated soil mechanics, two stress state variables are required to completely describe the engineering behavior of the soil (Fredlund, 1979). The two most commonly used stress state variables are: 1) net total stress, $(\sigma - u_a)$ and 2) matric suction, $(u_a - u_w)$. Matric suction is the negative pore-water pressure referenced to pore-air pressure. Above the ground-water table, negative pore-water pressures (i.e., or matric suction) contribute to increases in shear strength as illustrated by Figure 5.15.

In extrapolation of conventional bearing capacity to unsaturated soil mechanics, the total cohesion (i.e., or

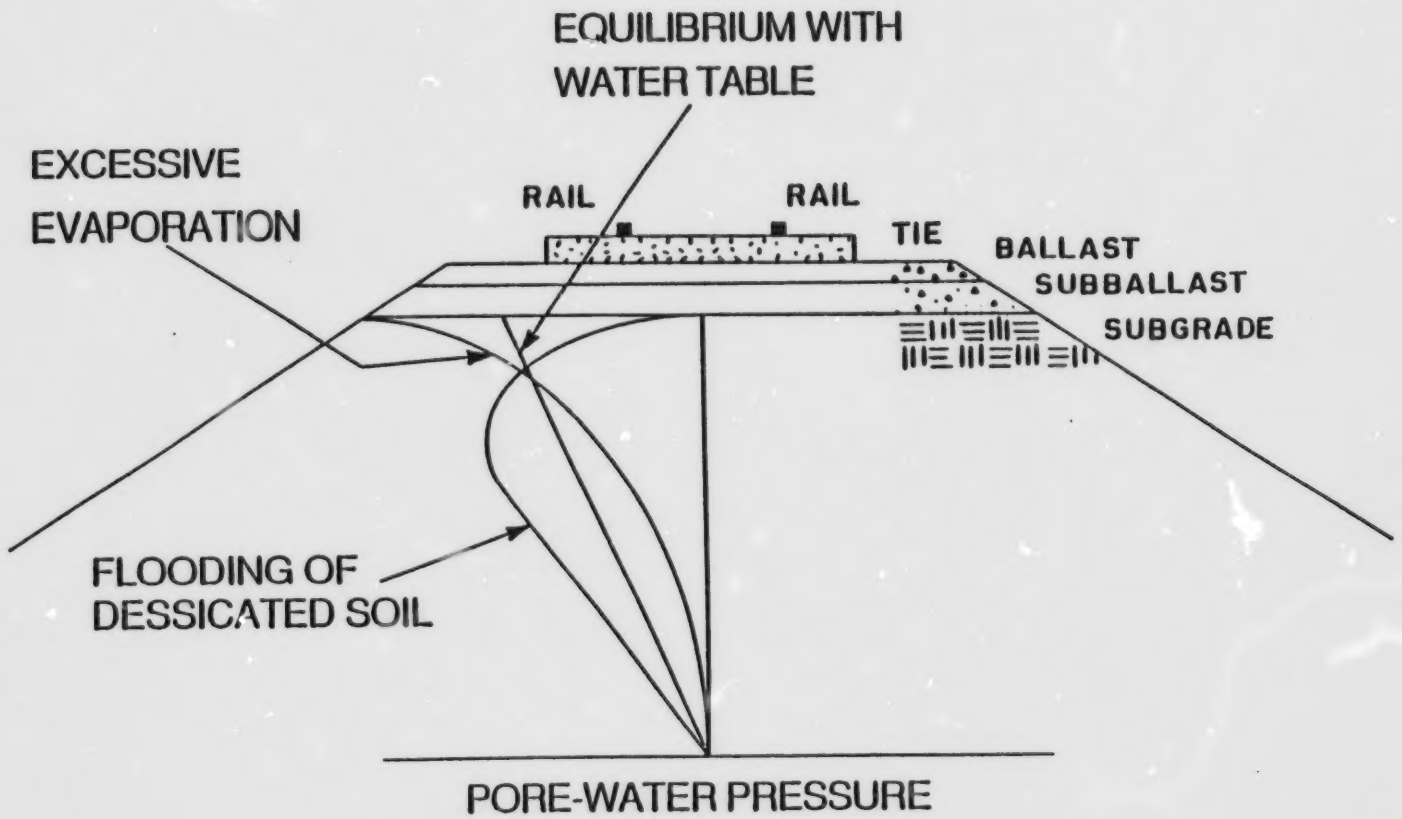

Fig. 5.14 Typical schematic pore-water pressure profiles

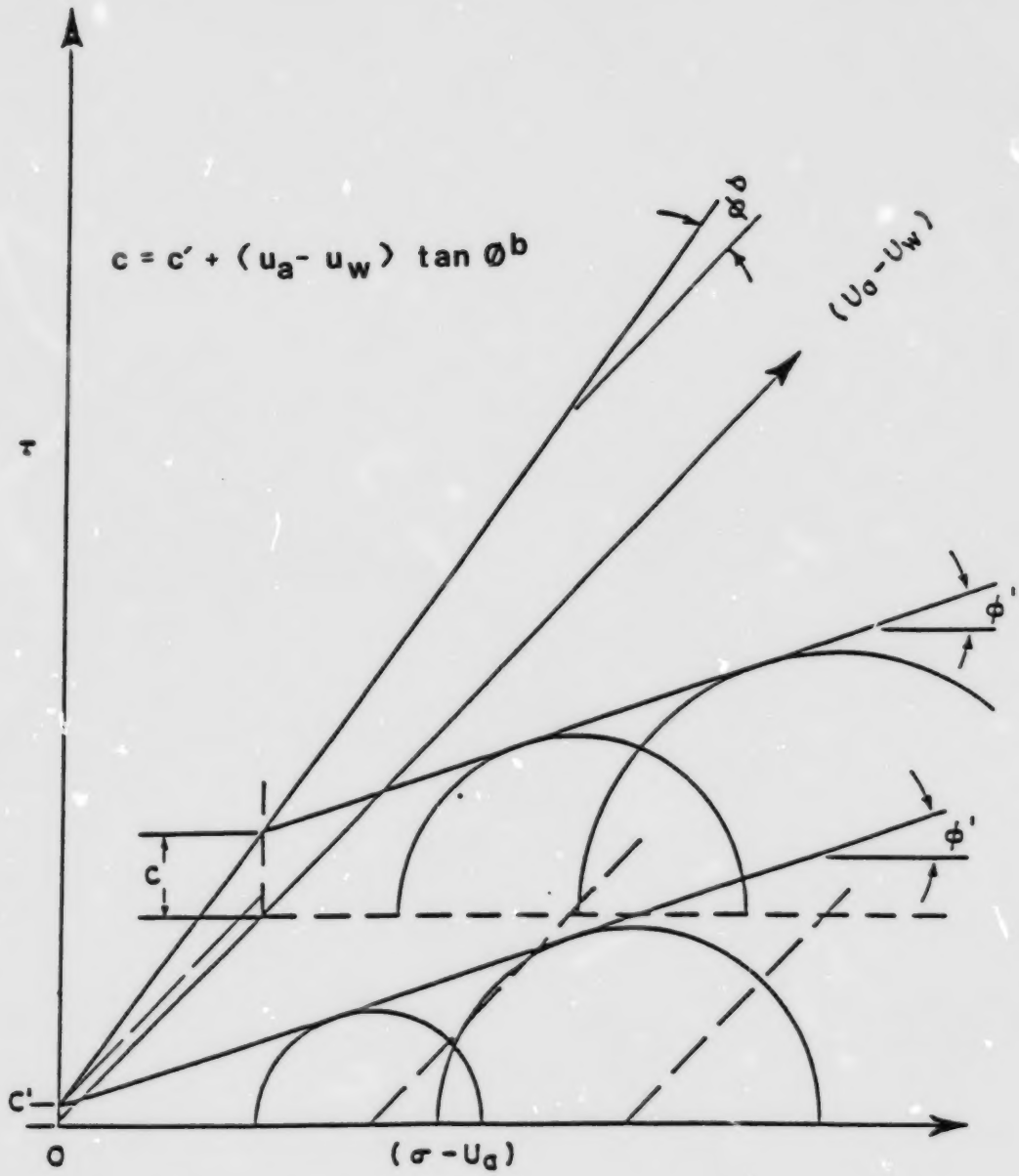

Fig. 5.15 Components of the total cohesion term for unsaturated soils

undrained shear strength) term in equation [1] is replaced with the following equation:

$$c = c' + (u_a - u_w) \tan \phi^b \qquad [8]$$

where:

c' = the effective cohesion of the subgrade

(ua - uw) = matric suction in the subgrade

ϕ^b = rate of change of shear strength with respect to matric suction

Clifton, Lam and Sattler (1988) demonstrated the significance of matric suction to the computation of shear strength for a railway embankment with the groundwater table located at considerable depth. The presence of only 35 kPa of matric suction was responsible for the stability of a 3 meter high embankment slope on the Canadian Pacific Railways Ltd., Emerson Subdivision Floodway Trackage south of Winnipeg, Manitoba.

The influence of embankment side-slopes on the computation of conventional bearing capacity is discussed in the following section.

5.3 Influence of Embankment Side-Slopes on the Computation of Conventional Bearing Capacity

Railway embankments are sometimes constructed with relatively steep embankment side-slopes. Besides the necessity to analyze the embankment slope for slope stability, modifications to conventional bearing capacity are required in order to accommodate the reduction in bearing capacity.

Figure 5.16 illustrates the effect of embankment slope on the failure geometry beneath the footing (i.e., failure geometry corresponding to the rail-tie system is illustrated in Figures 5.7, 5.8, 5.9, and 5.10). Whereas the failure pattern for a footing placed on level ground is symmetrical about the center of the footing (i.e., refer back to Figure 5.4), the failure pattern for a footing placed on an embankment slope is asymmetric (Figure 5.16). The theoretical elastic wedge LMNR is also asymmetric in shape.

On level ground, the contribution of Zone III to bearing capacity is due to both the shear strength and the weight of the Zone III material in preventing outward movement of the soil in Zone II. On the embankment slope, the vertical component of the weight in Zone III may contribute to failure due to slope stability (See Chapter 6 for further explanation of the slope stability mechanism of failure).

Meyerhof (1957) published research work dealing with the subject of bearing capacity on slopes. He identified two

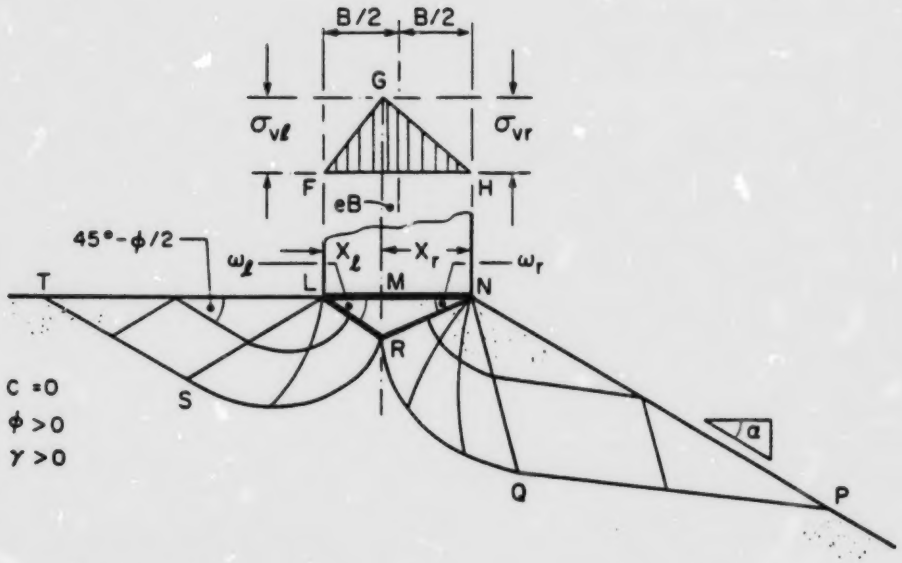

Fig. 5.16 Schematic of the failure zone for a footing at the crest of slope (Graham, Andrews and Shields, 1988)

geometries for bearing capacity of strip footings on slopes: 1) bearing capacity of a foundation on the **face** of a slope, and 2) bearing capacity of a foundation on the **top** of a slope. With respect to railway embankments, the foundation would be considered a "**face of slope**" case for rail-tie track system carved out of the side of a mountain and a "**top of slope**" case for a steep embankment fill.

The geometry of failure for Meyerhof's (1957) "face of slope" case is illustrated in Figure 5.17 and the geometry of failure for the "top of slope" case is illustrated in Figure 5.18. The magnitude of the slope is expressed as a slope angle in degrees, β . For Figure 5.18, the distance H is the overall height of the embankment and the variable b is the distance of the foundation from the edge of the slope. The bearing capacity equation is rewritten with modified bearing capacity factors:

$$q = c\, N_{cq} + \gamma (B/2)\, N_{\gamma q} \qquad [9]$$

where:

c = the total cohesion or undrained shear strength

B = the footing width (i.e., corresponding to track geometry)

N_{cq} = modified bearing capacity factor for purely cohesive soil

$N_{\gamma q}$ = modified bearing capacity factor for purely cohesionless soil

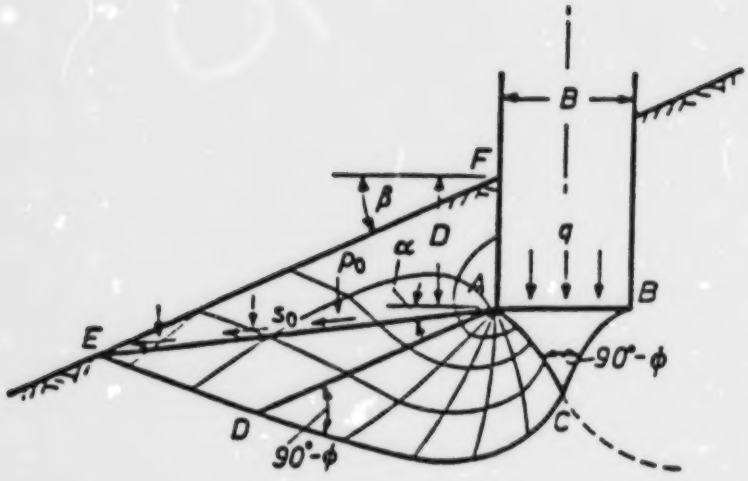

Fig. 5.17 Bearing capacity of a foundation on the face of a slope (Meyerhof, 1957)

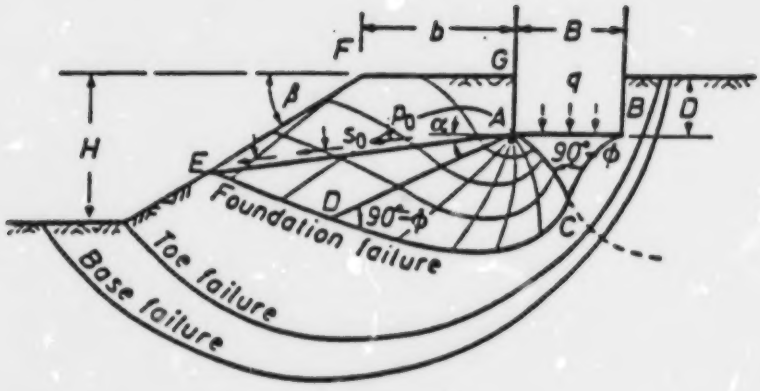

Fig. 5.18 Bearing capacity of a foundation on the top of a slope (Meyerhof, 1957)

The modified bearing capacity factors for the **"face of slope"** case for purely cohesive and purely cohesionless soil are illustrated in Figures 5.19 and 5.20, respectively. The modified bearing capacity factors for the **"top of slope"** case for purely cohesive and purely cohesionless soil are illustrated in Figures 5.21 and 5.22, respectively. The stability factor, N_S, for use with Figures 5.19 and 5.21 is computed from:

$$Ns = \gamma H / c \qquad [10]$$

where:

γ = the unit weight of the embankment material

H = the overall height of the embankment

c = the total cohesion or undrained shear strength

If the embankment height is zero, the stability factor, N_S, equals zero, and the modified bearing capacity factor, N_{Cq}, reverts back to the conventional bearing capacity factor, N_C equal to 5.14.

The modified bearing capacity computed from Meyerhof (1957) may be modified for foundation shape using the shape factors of Equations [5] and [6]. The concepts utilized from the Brom's approach (1965) for layered ground may also be incorporated. Equation [8] may be substituted for the

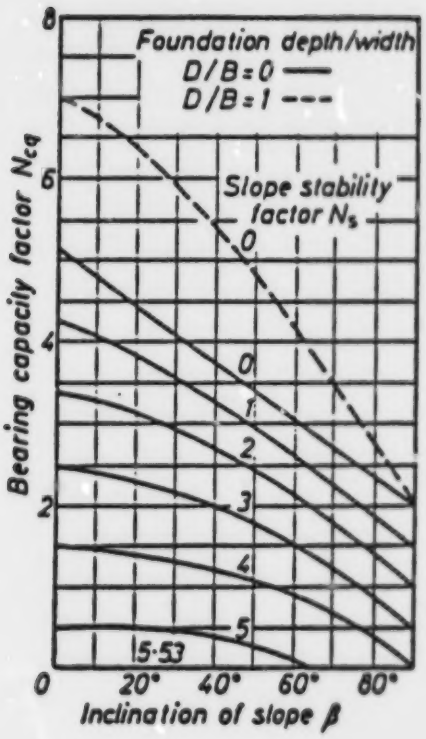

Fig. 5.19 Bearing capacity factor for a strip foundation on the **face** of a slope of purely **cohesive** material (Meyerhof, 1957)

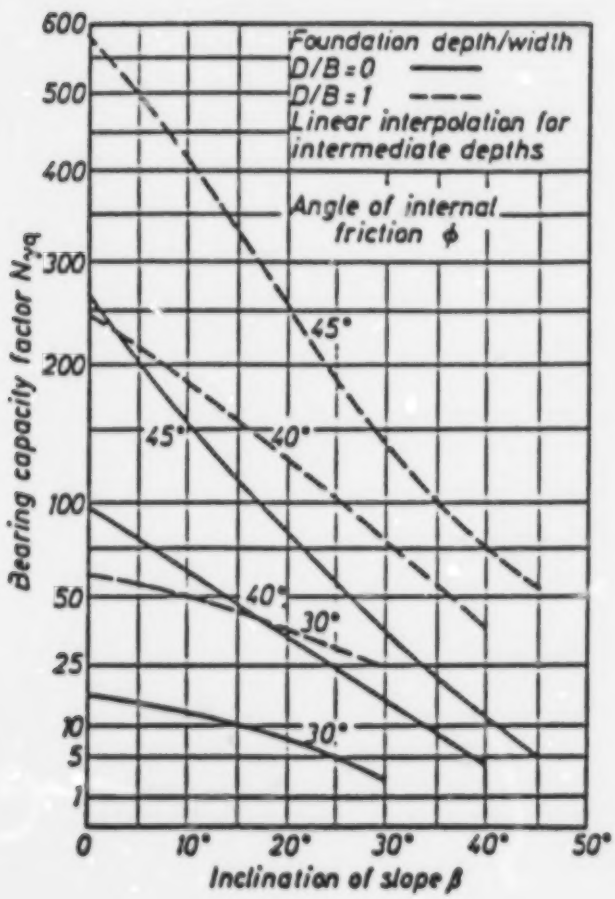

c = 0

Fig. 5.20 Bearing capacity factor for a strip foundation on the face of a slope of purely cohesionless material (Meyerhof, 1957)

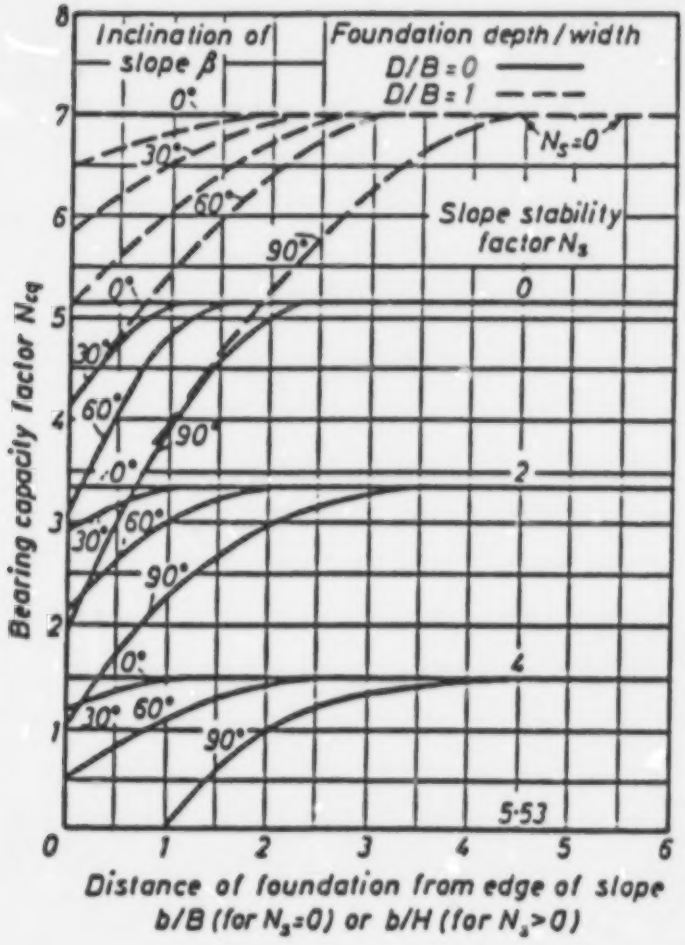

Fig. 5.21 Bearing capacity factor for a strip foundation on the **top** of a slope of purely **cohesive** material (Meyerhof, 1957)

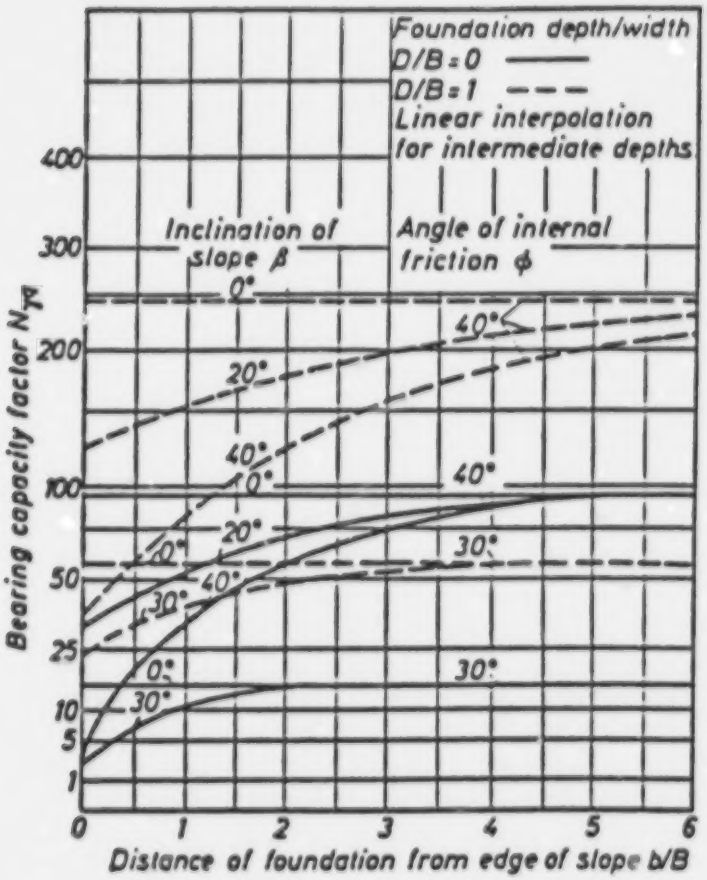

c = 0

Fig. 5.22 Bearing capacity factor for a strip foundation on the **top** of a slope of purely **cohesionless** material (Meyerhof, 1957)

total cohesion, c, in order to accommodate the additional strength due to matric suction in the subgrade.

The following generalizations may be deduced from the theoretical bearing capacity proposed by Meyerhof (1957): 1) bearing capacity decreases with greater inclination of slope, especially for cohesionless soils[4]; 2) bearing capacity decreases with greater overall height of embankment, especially for cohesive soils[5]; and 3) at greater distance from the edge of the slope, bearing capacity becomes independent of the slope angle. Meyerhof (1957) reported that the theoretical mechanisms of failure were based upon previous observations of bearing capacity failures but that sufficient research was not available at the time to validate the theory.

Further research into bearing capacity theories which consider the proximity of a slope were reported in 1960, 1964, and 1971 (Mizuno et al, 1960; Kovalev, 1964; and Giroud et al, 1971). However, only Meyerhof (1957) and Giroud et al (1971) deal with the **"face of slope"** case (Bauer et al, 1981).

Preliminary model tests were conducted in 1977 (Shields et al, 1977) to review the bearing capacity theories proposed by Meyerhof (1957) and Giroud (1971) for purely cohesionless soils. The tests were conducted for dense sand and compact sand and reported in terms of the ultimate

---

4 An example of a cohesionless soil is sand.
5 An example of a cohesive soil is clay.

bearing capacity and the modified bearing capacity factor, $N_{\gamma q}$.

Contours of the theoretical $N_{\gamma q}$ values are presented in Figure 5.23 for: a) ϕ' = 30 degrees, and b) ϕ' = 40 degrees. Contours of the theoretical modified bearing capacity factors indicate that the two theories are relatively similar for the compact sand but significantly different for the dense sand.

Experimental bearing pressures were determined from model tests and converted into modified bearing capacity factors, $N_{\gamma q}$ (Shields et al., 1977). Experimental $N_{\gamma q}$ factors are presented in Figure 5.24 for compact sand and dense sand. Both theories underestimate the ultimate bearing capacity and are therefore conservative. At shallow depths close to the crest of the slope, the theoretical bearing capacities are closer to the experimentally determined bearing capacities.

Subsequent to the preliminary model tests reported by Shields et al (1977), Bauer et al (1981) reported the results of over fifty footing tests located within a granular slope. The modified bearing capacity factors $N_{\gamma q}$ published by Bauer et al (1981) are simply an extension of the results shown in Figure 5.24 for footings located on the face of the slope (Figure 5.25).

The experimental $N_{\gamma q}$ values presented in Figure 5.25 are for a 0.3 meter footing and a 0.6 meter footing. Vesic (1973) has demonstrated that foundation size is significant

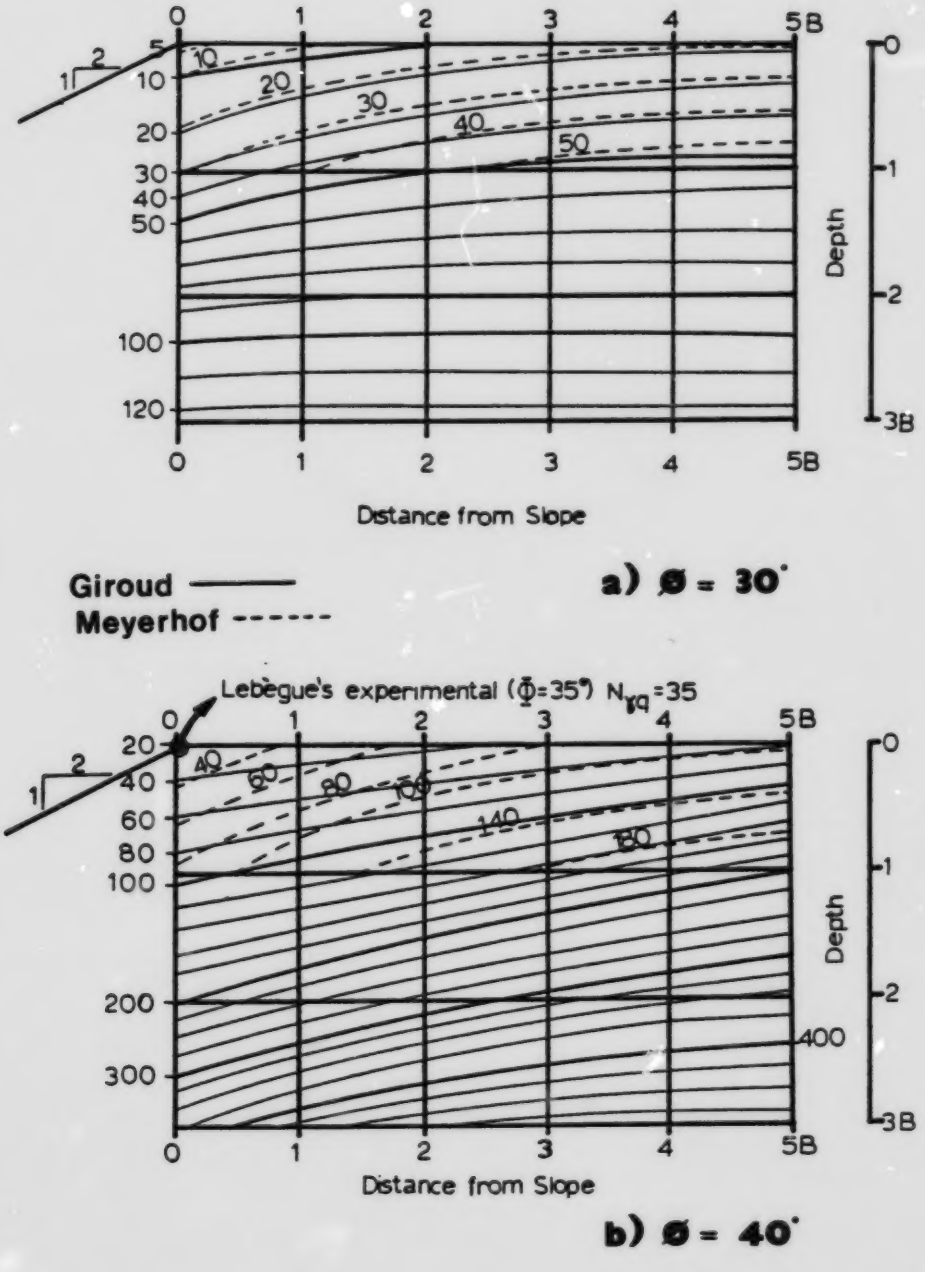

Fig. 5.23 Contours of theoretical $N_{\gamma q}$ values
(Shields et al, 1977)

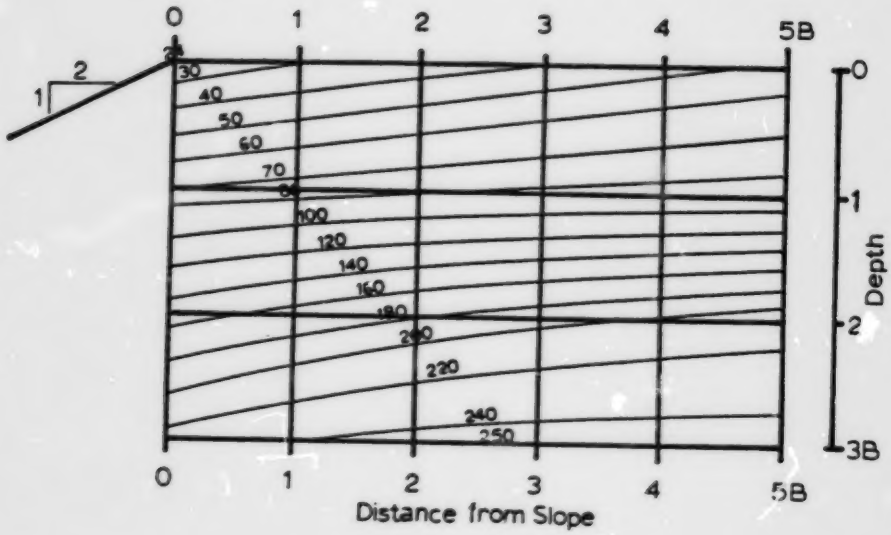

a) compact sand

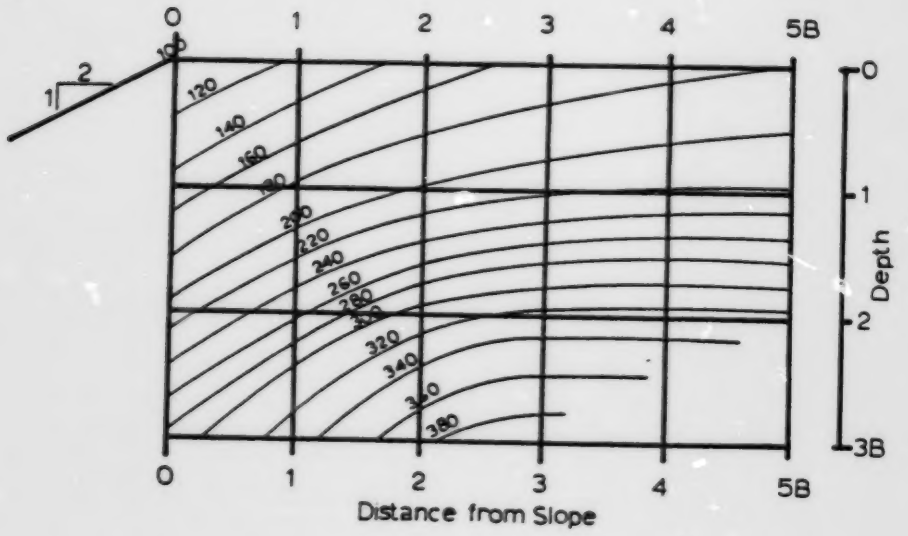

b) dense sand

Fig. 5.24 Contours of experimental $N_{\gamma q}$ values (Shields et al, 1977)

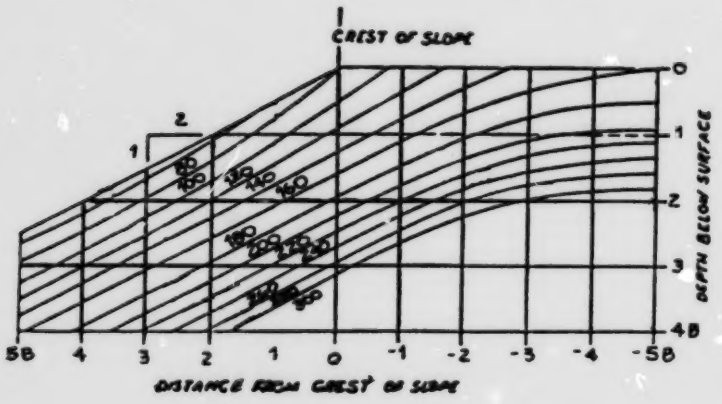

a) .3m footing

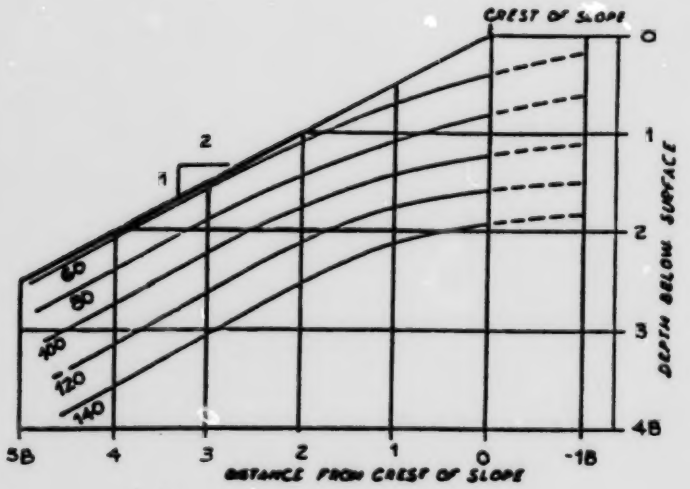

b) .6m footing

Fig. 5.25 Experimental $N_{\gamma q}$ contours for vertical loading (Bauer et al, 1981)

to the determination of the bearing capacity factor, N_γ. However, there do not exist scale factors allowing the extrapolation of model results to full-scale.

A completely new approach to the determination of bearing capacity for footings placed in cohesionless soils was proposed by Graham, Andrews, and Shields (1988). The method is based upon previous studies of boundary conditions for the bearing capacity problem in slopes (Graham, 1974; Graham and Stuart, 1971) and is based upon "critical state" soil mechanics theory (Graham and Hovan, 1986). Instead of adopting an assumed failure pattern, the shape and stress distribution of the failure zones are developed as the analysis proceeds. Schematics of the failure zones for depth of embedment and setback are illustrated in Figure 5.26. The $N_{\gamma q}$ values predicted from the method of stress characteristics are presented in Figure 5.27.

A comparison of the theoretical values for $N_{\gamma q}$ with the experimentally determined values of Shields et al (1977) is presented in Figure 5.28 for the compact sand and the dense sand. The theoretical results appear promising but the authors suggest that validation is incomplete and further testing is required (Graham, Andrews, and Shields, 1988).

Research has shown that: 1) bearing capacity decreases with greater inclination of slope, especially for cohesionless soils; 2) bearing capacity decreases with greater overall height of embankment, especially for cohesive soils; and 3) at greater distance from the edge

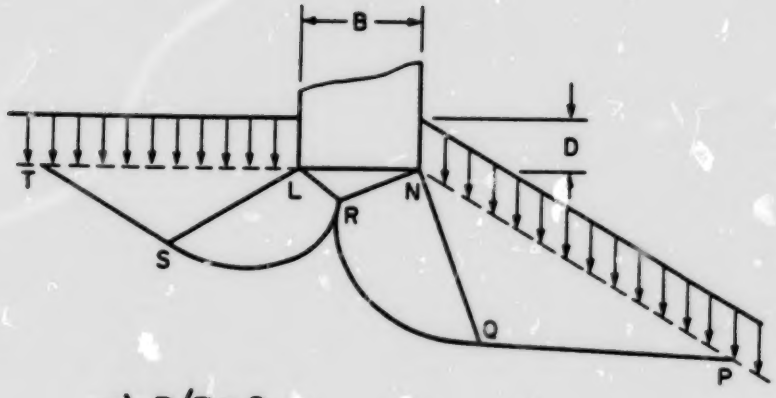

a) D/B > 0

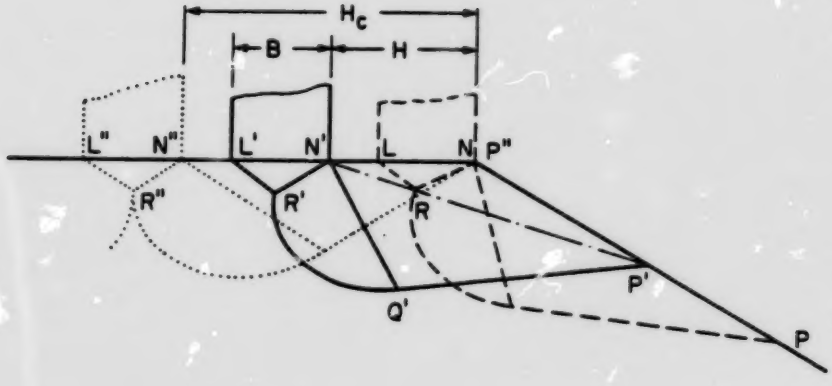

b) H/B > 0

Fig. 5.26 Schematic of failure zone for embedment and set-back (Graham, Andrews and Snields, 1988)

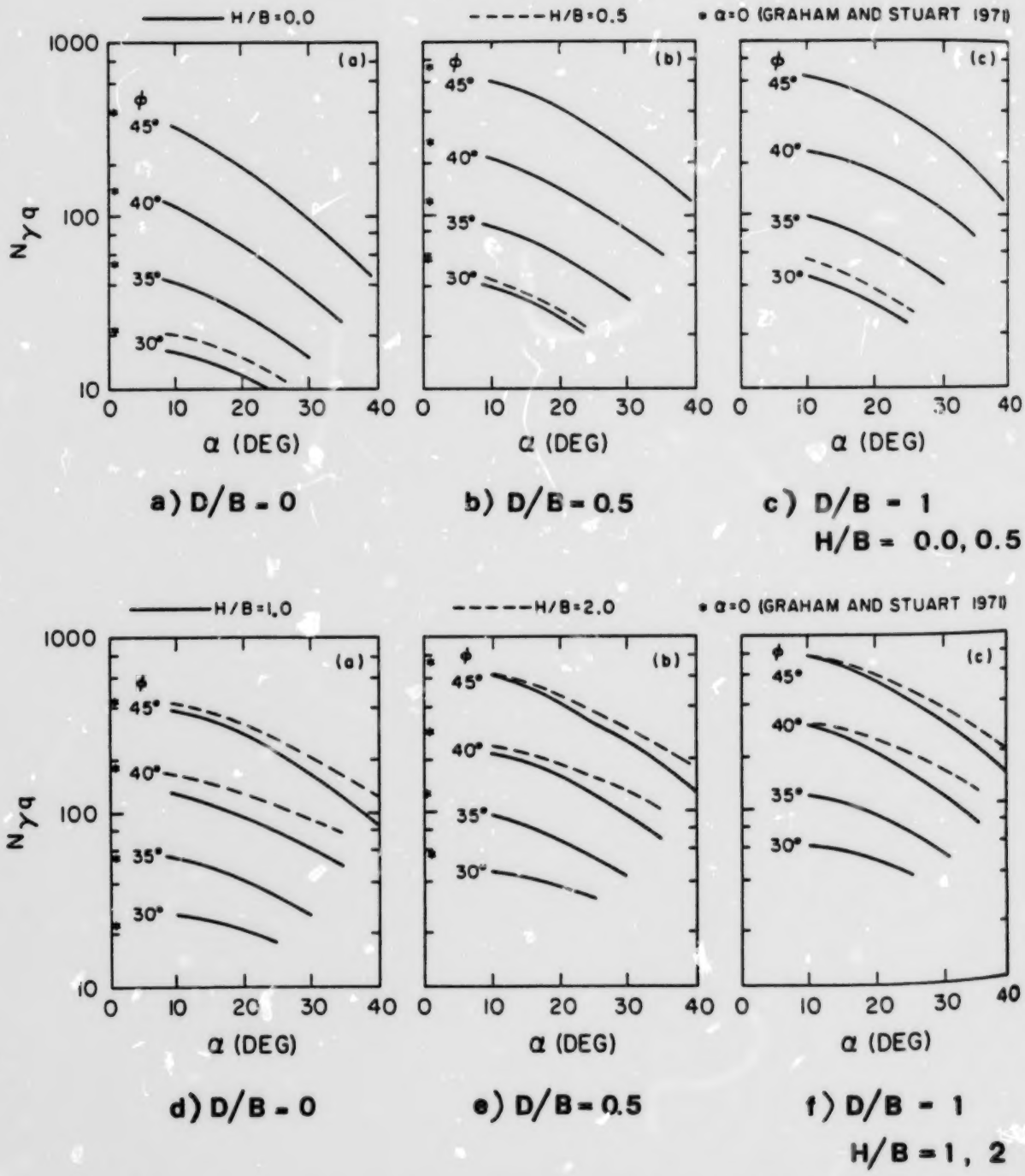

Fig. 5.27 Predicted $N_{\gamma q}$ values (Graham, Andrews and Shields, 1988)

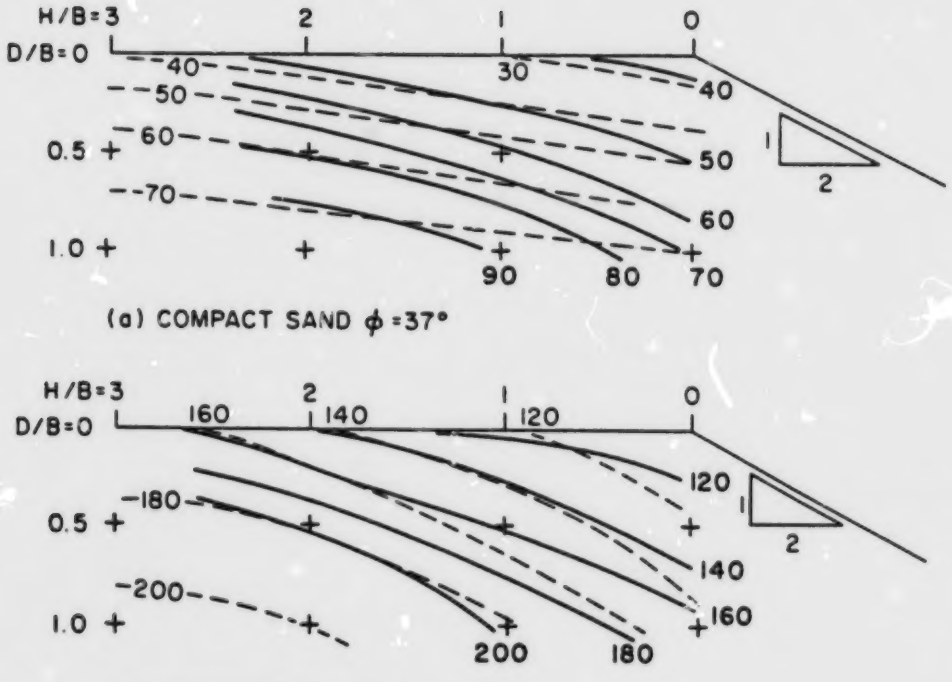

Fig. 5.28 Comparison of predicted and experimental $N_{\gamma q}$ values for B = 300 m (Graham, Andrews and Shields, 1988)

of the slope, bearing capacity becomes independent of the slope angle.

The review of literature which has been presented suggests that new technology is emerging which may prove practical in computing bearing capacity for foundations placed on slopes. However, at present, it is believed conservative to use the theories presented by Meyerhof (1957).

5.4 Conclusions Based on the Bearing Capacity Analysis

Conventional bearing capacity theory may be applied to the rail-tie track system using modifications for: 1) layered systems, 2) unsaturated soil mechanics theory, and 3) embankment slopes.

Modifications for layered systems include the Broms' (1965) approach and the Hanna and Meyerhof (1980) approach. The Broms' approach may be applied to most loading geometries and soil conditions whereas the Hanna and Meyerhof approach is reserved for application to punching failure in weak clay subgrades. The application of the two approaches are made for four loading configuration options (i.e., presented in Figure 5.7 through Figure 5.10) but it is suggested that Option No. 2 presented in Figure 5.8 is the most critical in terms of bearing capacity for railway engineering.

The conventional total cohesion term, c, may be replaced with Equation [8] describing the shear strength in terms of matric suction. Using this substitution allows for the incorporation of the additional strength of the subgrade due to the presence of negative pore-water pressures.

With respect to bearing capacity on embankment slopes, two conditions may be examined: 1) the "face of slope" case and 2) the "top of slope" case. Meyerhof (1957) illustrated that: 1) bearing capacity decreases with greater inclination of slope, especially in granular material; 2) bearing capacity decreases with greater overall height of embankment, especially for clay embankments; and 3) at greater distance from the edge of the slope, bearing capacity becomes independent of the slope angle. The modifications presented by Meyerhof (1957) are considered to be conservative. New techniques are emerging for the computation of bearing capacity of footings placed on slopes, however validation and general acceptance of these theories will require further research.

The development of bearing capacity technology for embankment slopes will never replace the necessity to perform slope stability analyses in conjunction with bearing capacity analyses. The application of slope stability analyses in railway engineering and particularly for soils with negative pore-water pressures is described in Chapter 6.

6.0 SLOPE STABILITY ANALYSES

The concept of slope stability in a frictional material (i.e., a cohesionless material such as sand) is introduced by examining a sliding block as shown in Figure 6.1. The block will slide down the slope if the component of the weight (i.e., the tangential force) in the direction of the slope is large enough to overcome the frictional resistance opposing movement. If the tangential force is less than the frictional resistance, the block will remain stable.

Soil structures with sloping surfaces (i.e., such as railway embankment side-slopes) are subject to internal shear stresses as a result of the gravitational force tending to pull the upper portion of the slope downward (Figure 6.2). If the shear strength of the soil mass is greater than the shear forces tending to pull the soil mass downward, the slope will remain stable. On the other hand, if the shear force is greater than the internal shear strength of the soil mass, then the slope will be unstable.

An analysis of the stability of a slope consists of three parts: 1) the determination of the location of the surface which is subject to the largest shear forces (i.e., the "critical slip surface"), 2) the determination of the magnitude of the forces on that surface acting to pull the soil mass downward (i.e., activating forces), and 3) the

Movement occurs if:

$W \sin \phi > S$

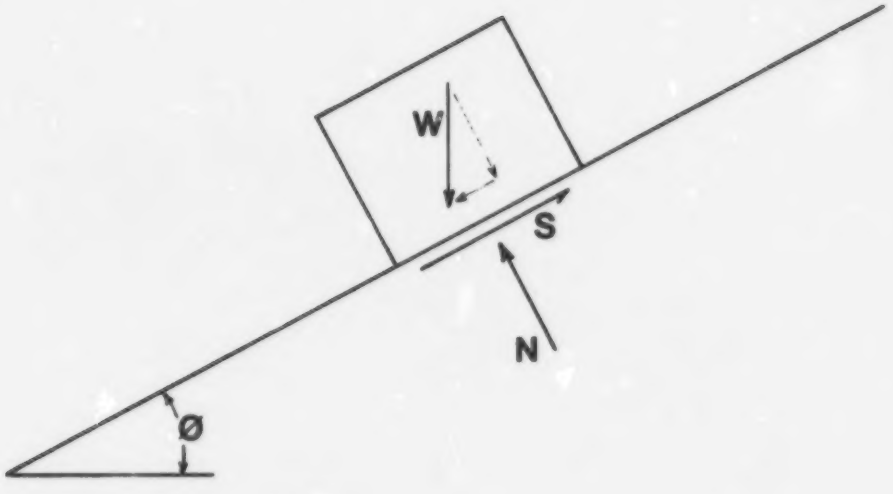

Fig. 6.1 Concept of slope stability in a purely frictional material

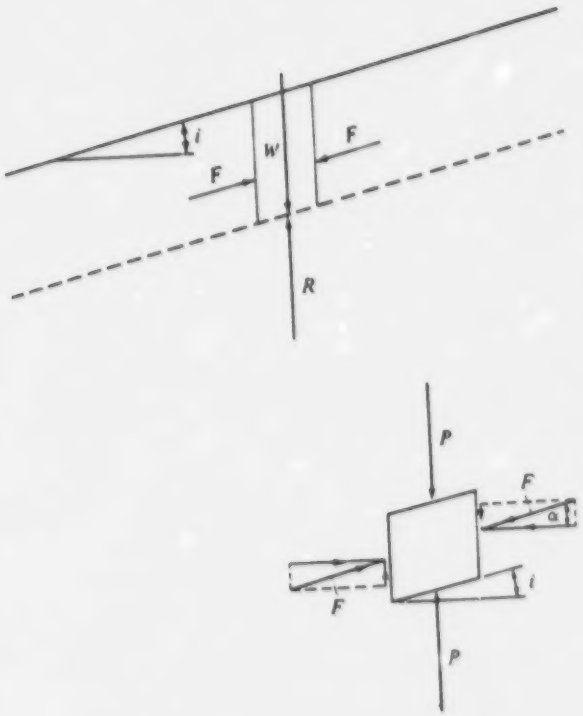

Fig. 6.2 Concept of slope stability in a slope of infinite extent (Spangler and Handy, 1982)

determination of the shear strength (i.e., forces resisting movement) along the same surface.

Slope stability analyses requires the determination of several potential slip surfaces for both activating and resisting forces. The stability of a slope can be expressed as a factor of safety against failure. By definition, the factor of safety with respect to slope stability is "the factor by which the shear strength must be reduced in order to bring the soil mass into a state of limiting equilibrium" (Fredlund, 1987).

A factor of safety greater than 1.0 indicates that a slope is stable and a factor of safety less than 1.0 indicates that a slope is unstable. If the factor of safety is equal to 1.0, the slope is said to be in a state of "limiting equilibrium". Each potential slip surface is characterized by a factor of safety. The surface represented by the lowest factor of safety is referred to as the "critical slip surface". Determination of the factor of safety for several potential slip surfaces is an iterative procedure which is well-adapted to computer solution (Fredlund and Fredlund, 1988).

The forces resisting movement arise from the shear strength of the soil. The primary activating force in a slope stability analysis is the gravitational force. For bearing capacity analyses, the primary force contributing to failure is due to the applied load of the structure on the foundation (See Chapter 5). For foundations located on

slopes (i.e., such as railway embankments), it is difficult to distinguish between failures due to bearing capacity and failures due to slope stability. Therefore, it is important to perform both bearing capacity and slope stability analyses. Alternatively, the bearing capacity problem may be interpreted as a slope stability problem with the application of point or line loads on the slope.

Figure 6.3 illustrates the forces which act upon an individual slice of a sliding mass of soil. The weight of the soil mass is determined from the dimensions (i.e., width, b, and height, h) and the density of the soil. For conventional soil mechanics, the mobilized shear force, S_m, is the portion of the shear strength of the soil which must be mobilized in order to bring the sliding soil mass into a state of limiting equilibrium (i.e., factor of safety equal to 1.0):

$$Sm = \frac{\beta}{F} (c + \sigma_n' \tan \phi') \qquad [11]$$

where:

β = the length across the base of the slice

F = the factor by which the shear strength must be reduced in order to bring the soil mass into a state of limiting equilibrium (i.e., factor of safety)

c = total cohesion

σ_n' = effective normal stress

ϕ' = effective angle of internal friction

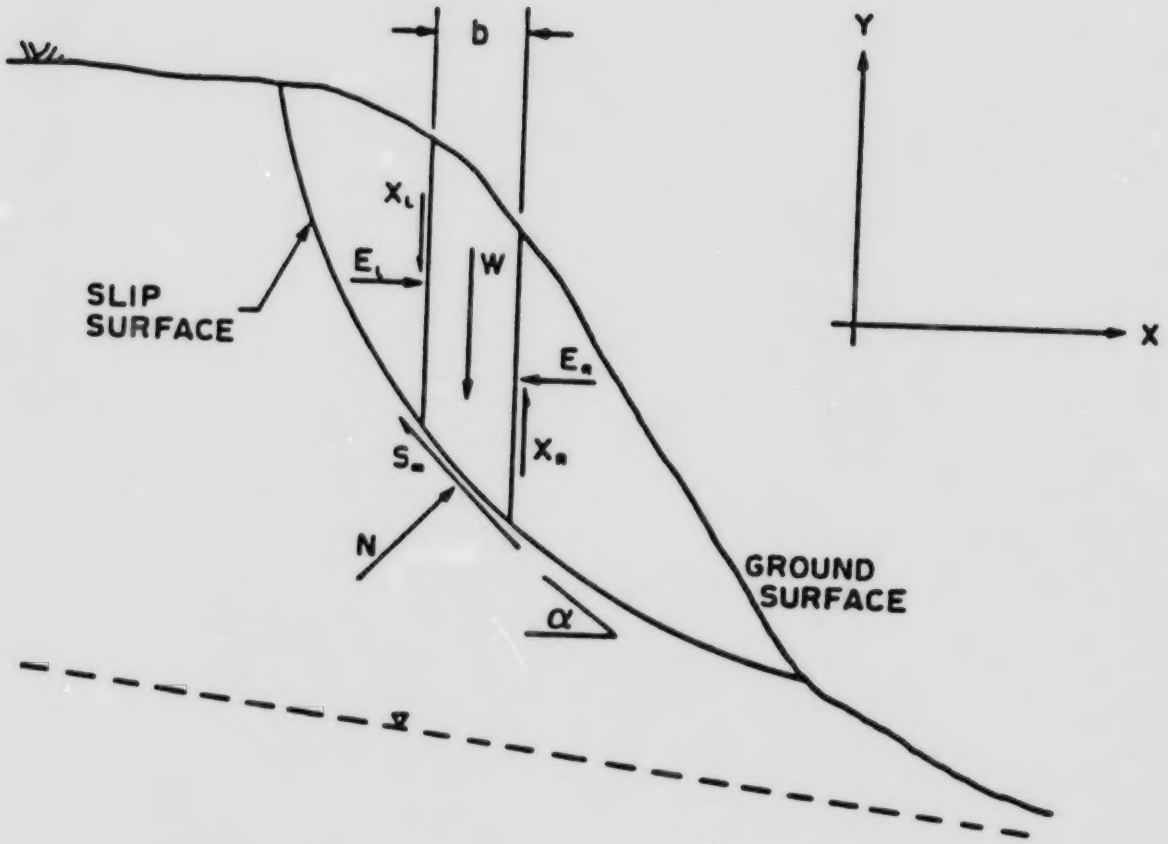

Fig. 6.3 Forces acting upon an individual slice of a sliding mass of soil

The normal force, N, is derived by summing the forces in the vertical direction. The horizontal interslice normal forces, E_L and E_R, and the vertical interslice shear forces, X_L and X_R, are assumed to be various mathematical functions for various methods of analyses (Fan, 1983; Fredlund, Krahn and Pufahl, 1981). The factor of safety with respect to the slope stability analysis, F, is determined from the summation of the horizontal forces, the vertical forces and the moments about the center of rotation and equating each sum to zero. The three equations may then be solved for the factor of safety for the slope stability analysis.

A groundwater table located within the sliding mass of soil in Figure 6.3 reduces the normal effective stress and therefore the shear force mobilized through the introduction of positive pore-water pressures. For slopes with positive pore-water pressures, the effect of the positive pore-water pressures is to reduce the effective normal stress in equation [11] as illustrated below:

$$\sigma_n' = \sigma_n - u_w \qquad [13]$$

where:

σ_n' = effective normal stress

σ_n = total normal stress

u_w = pore-water pressure

Saturated shear strength parameters have conventionally been used in slope stability analyses. The portion of the soil profile above the groundwater table where the pore-water pressures are negative has usually been ignored. This assumption is reasonable for situations in which the major portion of the slip surface passes through saturated soil. In this case, the exclusion of the negative pore-water pressures is conservative from an analysis standpoint (Fredlund, 1987).

However, for situations in which the groundwater table is deep or where there is concern over the possibility of a shallow failure, the effect of excluding negative pore-water pressures may be unrealistically conservative. The effect of negative pore-water pressures on the stability of a slope is to increase the net normal stress and also the shear force mobilized. Slope stability analyses incorporating the effect of negative pore-water pressures are described in the next section.

6.1 Slope Stability Analyses for Soils With Negative Pore-Water Pressures

Conventional slope stability methods of analysis have been extended to incorporate the effects of unsaturated soil mechanics and negative pore-water pressures (Fredlund, 1987). The effective shear strength for a saturated soil is

defined in terms of one stress state variable (i.e., $(\sigma - u_w)$) and a Mohr-Coulomb failure envelope with effective cohesion intercept, c', and a slope, tan ϕ'.

An unsaturated soil requires two stress state variables (i.e., $(\sigma - u_a)$ and $(u_a - u_w)$) and the extension of the two-dimensional failure **line** into a three-dimensional failure **surface** (Figure 6.4).

The unsaturated shear strength can be written as follows:

$$\tau = c' + (\sigma_n - u_a) \tan \phi' + (u_a - u_w) \tan \phi^b \qquad [14]$$

where:

c'	=	effective cohesion intercept
$(\sigma_n - u_a)$	=	net normal stress
ϕ'	=	effective angle of internal friction
$(u_a - u_w)$	=	matric suction
ϕ^b	=	rate of increase in strength due to increasing matric suction

Figure 6.5 presents the Mohr circles at failure for an unsaturated soil. The diagram illustrates the increase in shear strength for an increase in matric suction and/or an increase in net total stress. The total cohesion term is comprised of two components: 1) effective cohesion and 2) the increase in cohesion due to matric suction for various ϕ^b values. The components of the cohesion term have already

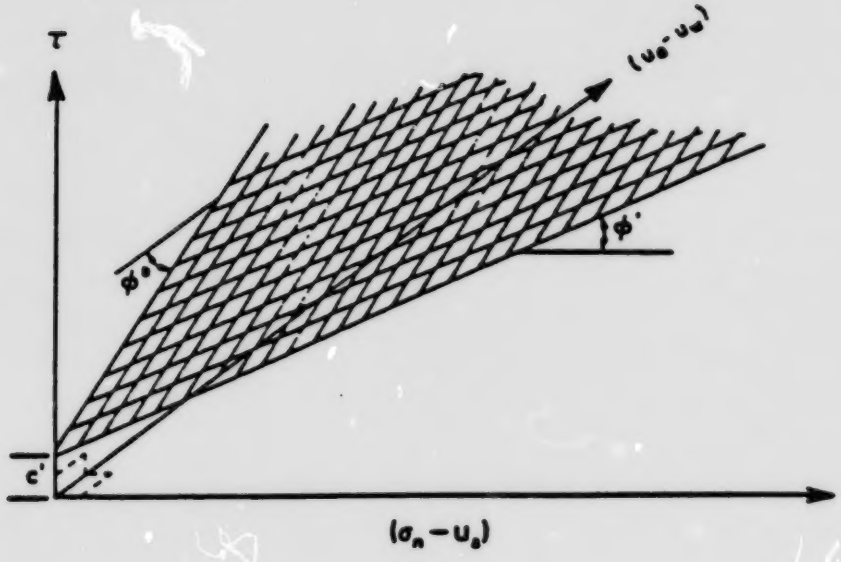

Fig. 6.4 Three-dimensional failure surface for an unsaturated soil

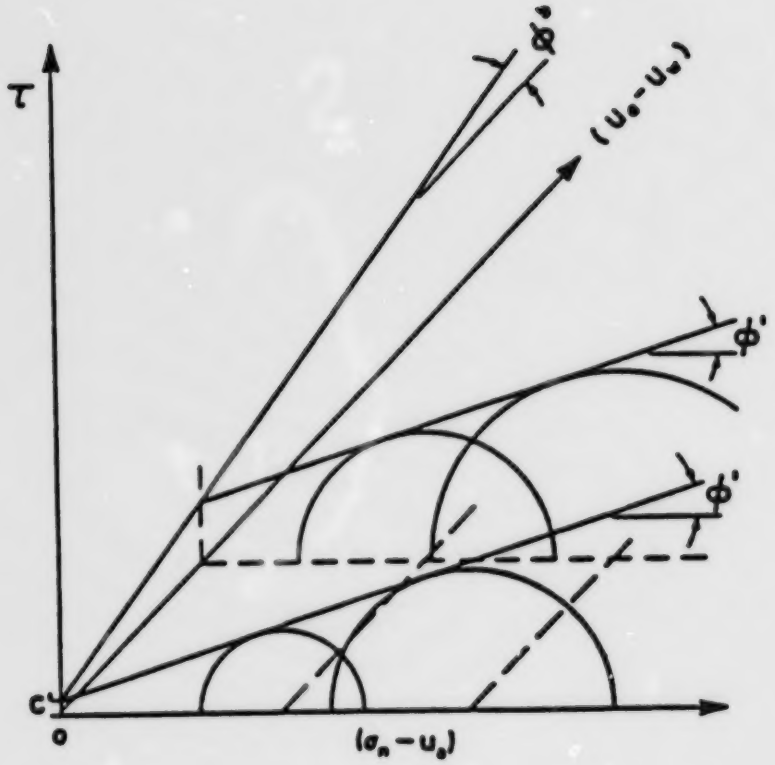

Fig. 6.5 Mohr circles at failure for an unsaturated soil

been presented in Figure 5.15 and Equation [8] as shown below:

$$c = c' + (u_a - u_w) \tan \phi^b \qquad [8]$$

where:

c = total cohesion

c′ = effective cohesion

(ua - uw) = matric suction

ϕ^b = rate of increase in strength with respect to increasing matric suction

Figure 6.6 illustrates the relationship between cohesion, matric suction, and angle, ϕ^b. The maximum theoretical value that ϕ^b can assume for a particular soil is equal to the angle ϕ' for the particular soil. Typical measured values for ϕ^b vary from 13 degrees to 20 degrees with an average value around 16 degrees (Fredlund, 1987). Details of the triaxial apparatus used for testing are documented by Ho and Fredlund (1982).

The increase in factor of safety due to the incorporation of negative pore-water pressures can be significant. Fredlund (1981) demonstrated the effect of increasing cohesion on a selected slip surface for a slope in Hong Kong. The factor of safety doubled for an increase in the total cohesion of 60 kPa (Fredlund, 1981). Clifton, Lam and Sattler (1988) demonstrated that the presence of

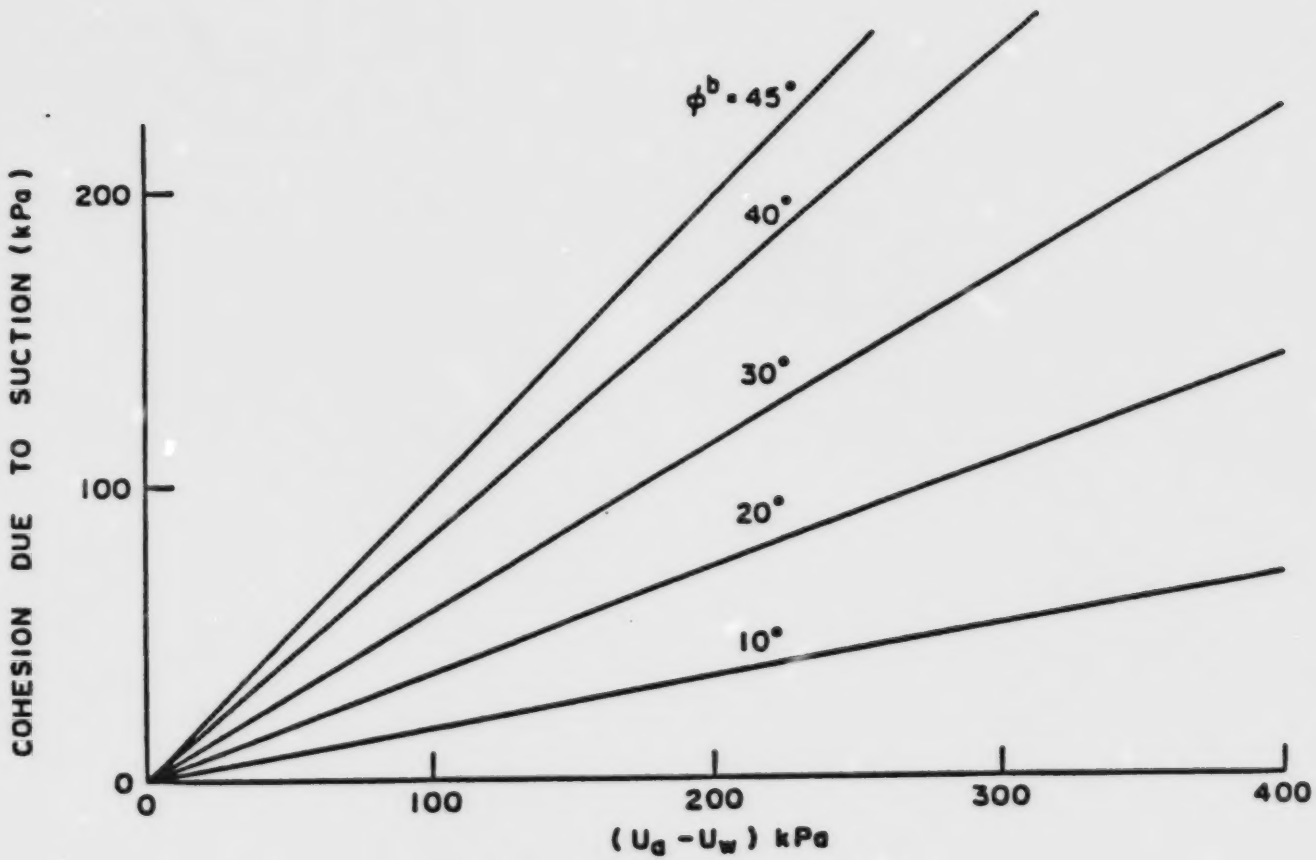

Fig. 6.6 Relationship between cohesion, matric suction and the angle ϕ^b (Fredlund, 1987)

only 35 kPa suction was responsible for the stability of a 3 meter high railway embankment constructed of highly plastic clay south of Winnipeg, Manitoba. Conversely, the factor of safety can decrease significantly when the cohesion due to matric suction is reduced due to prolonged wetting (Fredlund, 1987).

For slope stability analyses with negative pore-water pressures, the forces acting on the slice are written in terms of unsaturated soil parameters. The forces acting on a slice within the sliding soil mass illustrated in Figure 6.3 can be defined as follows:

W = total weight of a slice of width 'b' and height 'h'

N = total normal force acting on the base of a slice. It is equal to $\sigma_n \cdot \beta$ where σ_n is the normal stress acting over the sloping distance,

E_L, E_R = horizontal interslice normal force on the left and right sides of a slice, respectively

X_L, X_R = vertical interslice shear force on the left and right sides of a slice, respectively

R = radius or moment arm associated with the mobilized shear resistance, S_m

α = angle between the base of the slice and the horizontal

The shear force which is mobilized at the base of the slice is rewritten from Equation [11] as follows:

$$S_m = \frac{\beta}{F} (c' + (\sigma_n - u_a)\tan \phi' + (u_a - u_w)\tan \phi^b \quad [15]$$

where:

c' = effective cohesion

$(\sigma_n - u_a)$ = net normal stress

ϕ' = effective friction angle

$(u_a - u_w)$ = matric suction

ϕ^b = rate of increase in strength with respect to matric suction

The weight, W, for a slope containing unsaturated soil is computed in the same manner as for conventional slope stability analyses using the dimensions and the density of the soil. The normal force, N, which is derived by summing forces in the vertical direction, contains additional terms due to the introduction of the tan ϕ^b term for unsaturated soil mechanics. For most analyses the pore-air pressure can be set to zero and the normal force equation becomes:

$$N = \frac{W - (X_R - X_L) - \frac{c'\beta \sin\alpha}{F} + u_w \frac{\beta \sin \tan \phi^b}{F}}{\cos\alpha + \frac{\sin\alpha \tan \phi'}{F}} \quad [16]$$

When the soil becomes saturated, ϕ^b can be set to ϕ' and therefore the same equation can be used for both saturated

and unsaturated soils. The interslice force functions computed for an unsaturated slope stability problem, X_R, X_L, E_R, and E_L also become more complex.

Two independent factor of safety equations can be derived: 1) one with respect to moment equilibrium, and 2) one with respect to horizontal force equilibrium. Assuming that the pore-air pressures can be set equal to zero, the moment equilibrium factor of safety, F_m, can be written as:

$$F_m = \frac{\sum \left\{ c' \beta R + \left[N - u_w \beta \frac{\tan \phi^b}{\tan \phi'} \right] R \tan \phi' \right\}}{\sum W x - \sum N f} \qquad [17]$$

where:

x = horizontal distance from the center of each slice to the center of moments

f = offset distance from the normal force to the center of moments

The factor of safety with respect to force equilibrium, F_f, can be derived by summing the forces in the horizontal direction for all slices:

$$F_f = \frac{\sum \left\{ c' \beta \cos\alpha + \left[N - u_w \beta \frac{\tan \phi^b}{\tan \phi'} \right] \tan \phi' \cos\alpha \right\}}{\sum N \sin\alpha} \qquad [18]$$

The solution to the slope stability problem with negative pore-water pressures is accomplished in the same manner as conventional slope stability analyses. Each potential slip surface is characterized by a factor of safety. The factor of safety with respect to the slope stability analysis, F, is determined by summing the horizontal forces, the vertical forces and the moments about the center of rotation and equating each sum to zero. The three equations may then be solved for the overall factor of safety. The slip surface represented by the lowest factor of safety is referred to as the "critical slip surface". Determination of the factor of safety for several potential slip surfaces is an iterative procedure which is well-adapted to computer solution (Fredlund and Fredlund, 1988).

The PC-SLOPE computer program distributed by GEO-SLOPE Programming Ltd. performs stability analyses for soils with negative pore-water pressures in accordance with the procedure outlined above (Fredlund, 1985). Negative pore-water pressures may be input as a grid of points (i.e., using the POGP keyword), a series of contour lines (i.e., using the PCON keyword), or a grid of hydraulic head values (i.e., using the POGH keyword).

6.2 Slope Stability Analyses for Railway Embankments

The analyses of railway embankments located above a deep groundwater table may utilize procedures for slope stability

analyses with negative pore-water pressures as described in the preceding section. The use of pore-water pressure contours or grids allows the input of both positive and negative pore-water pressures in the same problem. Therefore, there is the capability to model perched water tables (i.e., characterized by positive pore-water pressures) or water pockets within an embankment slope characterized by predominantly negative pore-water pressures.

Negative pore-water pressure data for use in the analysis may be obtained by field measurement (van der Raadt, 1988) or laboratory measurement (Sattler and Fredlund, 1989). Alternatively, computer analyses using the environmental conditions applied at the surface boundary may be utilized for determination of negative pore-water pressures (Fredlund, 1990). The use of seepage modelling in conjunction with slope stability analyses further allows the determination of water movement in reponse to the changing environmental and loading conditions.

The essence of seepage modelling (i.e., saturated-unsaturated flow modelling) is the prediction of pore-water pressures in a slope which occur as a result of the changing surface flux boundary condition (Fredlund, 1989b). The surface flux boundary condition consists of infiltration due to precipitation and exfiltration due to evaporation and evapotranspiration.

Several numerical models have been developed to perform saturated-unsaturated transient flow analyses. These models, generally in the finite element form, can be used to predict pore-water pressures which may exist in a slope as a result of changes in the microclimate. The changing negative and positive pore-water pressures can then be used in a limit equilibrium slope stability analysis to compute the factor of safety with respect to time. An example slope stability problem utilizing negative pore-water pressures determined from saturated-unsaturated flow modelling is included in Appendix B.

The pore-air pressure in a natural slope can generally be assumed to be equal to atmospheric conditions. As a result, only water flow needs to be modelled. Water flow occurs in reponse to variations in hydraulic head and is governed by Darcy's law for both saturated and unsaturated conditions (Childs and Collis-George, 1950). However, there is one difference. The coefficient of permeability for a saturated soil is generally assumed to be constant. For unsaturated soils, the coefficient of permeability must be written as a function of either matric suction, pore-water pressure head, pore-water pressure, or water content.

The seepage equation for an unsaturated soil is derived by substituting the water phase constitutive relationship for an unsaturated soil into the rate of change of water volume in a referential element (Fredlund, 1989b). Assuming

the pore-air pressure is atmospheric and the net normal stress remains constant, the seepage equation becomes:

$$\frac{\partial}{\partial x}\left[k_x \frac{\partial h}{\partial x}\right] + \frac{\partial}{\partial y}\left[k_y \frac{\partial h}{\partial y}\right] = \rho_w \, g \, m_2^w \frac{\partial h}{\partial t} \quad [19]$$

where:

k_x = the coefficient of permeability in the x-direction

k_y = the coefficient of permeability in the y-direction

h = the hydraulic head

ρ_w = the density of water

g = the acceleration due to gravity

m_2^w = the rate of change of water volume with respect to change in matric suction

Equation [19] has been programmed in the PC-SEEP computer software marketed by GEO-SLOPE Programming Ltd., Calgary, Alberta and was used for the solution to the problem presented in Appendix B.

Slope stability analyses may also be conducted for shallow slip surfaces to emulate bearing capacity failures. A conventional slope stability analysis is conducted in two-dimensional space. Therefore, the emulation of bearing capacity is limited to the modelling of the track loading configuration as a strip footing. However, the use of slope stability analyses in conjunction with bearing capacity analyses is strongly recommended due to the complementary nature of the two analyses. The use of slope stability

analyses to complement bearing capacity analyses for steep railway embankments is especially critical.

A conventional slope stability analysis is conducted in two-dimensional space. The analysis of a railway embankment in two-dimensional space requires the input of the train loading configuration as a surcharge load applied to the slope (Clifton, Lam and Sattler, 1988). This places some restrictions on the loading used for a slope stability analysis. Further research is presently underway that will allow the modelling of three-dimensional slope stability problems (Lam, in progress). This research work may prove valuable with repect to the analysis of complex railway loading configurations on steep embankments.

6.3 Conclusions of Slope Stability Analyses

Slope stability analyses may be conducted for slopes with negative pore-water pressures with the introduction of unsaturated soil theory into the development of slope stability analyses. The use of negative pore-water pressures in the analysis of slopes is especially important for situations in which the groundwater table is located at considerable depth and the exclusion of negative pore-water pressure renders the analysis overly conservative and uneconomic.

It is recommended that any analysis of bearing capacity for embankment side-slopes also incorporate complementary slope stability analyses. Used together, bearing capacity and slope stability analyses provide a valuable tool for the analysis of loaded railway embankments. Seepage analyses may also be utilized for the determination of the effects of water movement (i.e., due to rainfall) on overall stability of the embankment.

7.0 CONCLUSIONS

The objective of this research was to extend the bearing capacity design procedure for railway subgrades to incorporate the effects of embankment side-slopes. Three types of analyses were utilized: 1) stress analyses, 2) bearing capacity analyses, and 3) slope stability analyses.

The investigation revealed that the magnitude of embankment side-slope was insignificant to the computation of the vertical stress distribution beneath the loaded track system. The observation that horizontal and shear stress distributions were affected by the presence of embankment side-slopes indicated a necessity to research bearing capacity and slope stability methods of analysis.

Two bearing capacity geometries were identified as being relevant to the investigation of railway embankment side-

slopes: 1) bearing capacity of a foundation on the "face" of a slope, and 2) bearing capacity of a foundation on the "top" of a slope. Three observations were noted from the literature: 1) bearing capacity decreases with greater inclination of slope, especially in granular materials; 2) bearing capacity decreases with overall height of slope, especially in cohesive materials; and 3) bearing capacity becomes independent of slope height at greater distances from the edge of the slope.

The approach which has been adopted to account for embankment slopes in a bearing capacity analysis has been to modify the bearing capacity factors for the individual terms of the conventional bearing capacity equation. Recent research has suggested that the modified bearing capacity factors may be unduly conservative for many cases.

New techniques are emerging for the analysis of bearing capacity of footings placed on slopes. The literature pertaining to these new techniques have been summarized in the report. Validation and acceptance of these theories will require further research. In the meantime, the application of slope stability analyses to complement bearing capacity analyses is essential.

Slope stability analyses for soils with negative pore-water pressures may be conducted for railway embankments in which the groundwater table is located at considerable depth. The use of conservative negative pore-water pressures is significant to slope stability analyses for

unsaturated soils. Slope stability analyses used in conjunction with and as a complement to bearing capacity analyses for railway embankments with steep side-slopes provide the engineer with a valuable set of tools. Seepage analyses may also be used to characterize the movement of water within the embankment due to changing environmental and loading conditions.

REFERENCES

Bauer, G.E., Shields, D.H., Scott, J.D. and Gruspier, J.E. (1981) Bearing capacity of footings in granular slopes. Proceedings of the Tenth International Conference on Soil Mechanics and Foundation Engineering, Stockholm, Volume 2, pp. 33 to 36.

Brinch-Hansen, J. (1970) A revised and extended formula for bearing capacity. Danish Geotechnical Institute, Bulletin No. 28, Copenhagen, Denmark. pp. 5 to 11.

Broms, Bengt B. (1965) Effect of degree of saturation on bearing capacity of flexible pavements. Presented at the 43rd Annual Meeting of the Committee on Flexible Pavement Design, Ithaca, New York.

Burmister, D.M. (1943) The theory of stresses and displacements in layered systems and applications to design of airport runways. Highway Research Board Proceedings, pp. 126 to 148.

Canadian Foundation Engineering Manual, Second Edition (1985) Canadian Geotechnical Society, Technical Committee on Foundations, Part 2: Shallow Foundations, pp. 155.

Chang, C.S., Adegoke, C.W. and Selig, E.T. (1980) GEOTRACK model for railroad track performance. Journal of the Geotechnical Engineering Division, ASCE, Vol. 106, pp. 1201 to 1218.

Childs, E.C. and Collis-George, N. (1950) The permeability of porous material. Proceedings of the Royal Society, 201A, pp. 392 to 405.

Clifton, A.W., Lam, L. and Sattler, P.J. (1988) Embankment Instability, Investigation and Analysis, Emerson Subdivision, Winnipeg, Manitoba. A report to Canadian Pacific Railways. Prepared by Clifton Associates Ltd., Regina, Saskatchewan and the University of Saskatchewan, Geotechnical Group, Saskatoon, Saskatchewan, July, 29 pps.

Fan, K. (1983) Evaluation of Interslice Side Forces for Lateral Earth Force and Slope Stability Problems. M.Sc. Thesis. Department of Civil Engineering, University of Saskatchewan, Saskatoon, Saskatchewan.

Fredlund, D.G. (1979) Appropriate concepts and technology for unsaturated soils. Second Canadian Geotechnical Colloquium, Canadian Geotechnical Journal, Vol. 16, No. 1, pp. 121 to 139.

Fredlund, D.G. (1981) The shear strength of unsaturated soil and its relationship to slope stability problems in Hong Kong. Hong Kong Engineer, Journal of the Hong Kong Institute of Engineers, April, pp. 37 to 45.

Fredlund, D.G. (1985) PC-SLOPE User's Manual, A Comprehensive Program for Slope Stabilty Analysis. Geo-Slope Programing Ltd., Calgary, Alberta.

Fredlund, D.G. (1990) PC-SEEP User's Manual. Geo-Slope Programming Ltd., Calgary, Alberta.

Fredlund, D.G. (1987) "Slope Stability Analysis Incorporating the Effect of Soil Suction", Chapter 4, pp. 113 to 144 of **Slope Stability**, Edited by M.G. Anderson and K.S. Richards. Published by John Wiley and Sons Ltd.

Fredlund, D.G. (1989a) PC-SIGMA User's Manual, Finite Element Software for Stress and Deformation Analysis. Geo-Slope Programming Ltd., Calgary, Alberta, Canada.

Fredlund, D.G. (1989b) Negative pore-water pressures in slope stability. Session II - Invited Main Lecture. South American Symposium on Soil Mechanics, August 7 to 10, 1989. Paipa, Columbia.

Fredlund, D.G. and Fredlund, L.D. (1988) The PC-SLOPE family of software for slope stability analysis. Proceedings of the Symposium on Microcomputer Applications in Geotechnical Engineering, Regina, Saskatchewan, pp. 173 to 181.

Fredlund, D.G., Krahn, J. and Pufahl, D.E. (1981) The relationship between limit equilibrium slope stability methods. Proceedings of the Tenth International Conference on Soil Mechanics and Foundation Engineering, Stockholm, Sweden, Volume 3, pp. 409 to 416.

Fredlund, D.G. and Wong, D.K.H. (1989) Calibration of thermal conductivity sensors for measuring soil suction. ASTM Geotechnical Testing Journal.

Giroud, J.P. and Tran-Vo-Nhiem (1971) Force portante d'une fondation sur une pente. A.I.T.B.T.P. No. 283 to 284, July-August issue. Serie: theorie et methodes de calcul, No. 142, Paris.

Graham, J. (1974) Plasticity solutions to stability problems in sand. Canadian Geotechnical Journal, Volume 11, pp. 238 to 247.

Graham, J. and Stuart, J.G. (1971) Scale and boundary effects in foundation analysis. ASCE Journal of the Soil Mechanics and Foundations Division, Volume 97, pp. 1533 to 1548.

Graham, J. and Hovan, J.M. (1986) Stress characteristics for bearing capacity in sand using a critical state model. Canadian Geotechnical Journal, Volume 23, pp. 195 to 202.

Graham, J., Andrews, M. and Shields, D.H. (1988) Stress characteristics for shallow footings in cohesionless slopes. Canadian Geotechnical Journal, Volume 25, pp. 238 to 249.

Hanna, A.M. and Meyerhof, G.G. (1980) Design charts for ultimate bearing capacity of foundations on sand overlying soft clay. Canadian Geotechnical Journal, Vol. 17, pp. 300 to 303.

Ho, D.Y.F. and Fredlund, D.G. (1982) Strain rates for unsaturated soil shear strength testing. Proceedings of the Seventh Southeast Asian Geotechnical Conference. pp. 787 to 803.

Kovalev, I.U. (1964) De la resistance ultime de fondations limitees par un talus. Translated from Russian by L.C.P.C., Paris, 1973.

Kraft, Leland M. and Helfrich, Steven C. (1983) Bearing capacity of shallow footing, sand over clay. Canadian Geotechnical Journal, Vol. 20, pp. 182 to 185.

Lam, L. (in progress) Three-Dimensional Slope Stability. Ph.D. Thesis, Department of Civil Engineering, University of Saskatchewan, Saskatoon, Saskatchewan.

McClarty, D.V.B. and Fredlund, D.G. (1990) Spline interpolation: A means of interfacing finite element analysis and limit equilibrium analysis. Presented to the CSCE Annual Conference on "Engineering in Our Environment", Hamilton, Ontario, May 15 to 18, 1990.

Meyerhof, G.G. (1953) The bearing capacity of foundations under eccentric and inclined loads. Proceedings of the Third International Conference on Soil Mechanics, Vol. 1, pp. 440.

Meyerhof, G.G. (1955) Influence of roughness of base and groundwater conditions on the ultimate bearing capacity of foundations. Geotechnique, Volume 5, pp. 227.

Meyerhof, G.G. (1957) The ultimate bearing capacity of foundations on slopes. Proceedings of the Fourth

International Conference on Soil Mechanics and Foundation Engineering, London, Volume 1, pp. 384 to 386.

Mizuno, T., Takumitsu, Y., Kavakami, H. (1960) On the bearing capacity of a slope of cohesionless soil. Soil and Foundations, Tokyo, Japan, Volume 1, Number 2, pp. 30 to 37.

Ng, Tony (1988) The Effect of Negative Pore-Water Pressures on Slope Stability Analysis. M.Sc. Thesis, Department of Civil Engineering, University of Saskatchewan, Saskatoon, Saskatchewan.

Prandtl, L. (1921) On the penetrating strengths (hardness) of plastic construction materials and the strength of cutting edges. Zeit. angew. Math. Mech., Volume 1, No. 1, pp. 15 to 20.

Rankine, W.J.M. (1857) On the stability of loose earth. Phil. Trans. Roy. Soc., London, Volume 147, Part 1, pp. 9 to 27.

Sattler, P.J. and Fredlund, D.G. (1988) The Development of Bearing Capacity Design Charts for Track Systems, Final Report. Transport Canada Publication Number TP 9521E, Transportation Development Centre, 200 Rene-Levesque Blvd. West, Suite 601, West Tower, Montreal, Quebec, H2Z 1X4, 262 pps.

Sattler, P.J. and Fredlund, D.G. (1989a) Use of thermal conductivity sensors to measure matric suction in the laboratory. Canadian Geotechnical Journal, Volume 26, No. 3, pp. 491 to 498.

Sattler, P.J. and Fredlund, D.G. (1989b) The Installation of Thermal Conductivity Sensors in Canadian Pacific Railways Ltd. Emerson Subdivision Trackage. A report prepared by Geo-Slope Ltd. for Canadian Pacific Railways Ltd.

Sattler, P.J., Fredlund, D.G. and Neis, V.V. (1990) GEOTRACK and GEOPLOT, STRESS, BEARING and COMPARE User's Manual, Second Edition. (Subgrade Stress Analysis and Bearing Capacity). Transport Canada Publication, Transportation Development Centre, 200 Rene Levesque Blvd. West, Suite 601, West Tower, Montreal, Quebec, H2Z 1X4.

Shields, D.H., Scott, J.D., Bauer, G.E., Deschenes, J.H. and Barsvary, A.K. (1977) Bearing capacity of foundations near slopes. Proceedings of the Ninth International Conference on Soil Mechanics and Foundation Engineering, Tokyo, Japan, Volume 2, pp. 715 to 720.

Spangler, M.G. and Handy, R.L. (1982) Soil Engineering, Fourth Edition. Harper & Row Publishers, New York.

Terzaghi, K. (1925) Erdbaumechanik auf bodenphysikalischer Grundlage (Soil Mechanics on Soil Physics Basis) F. Deuticke, Vienna.

Terzaghi, K. (1943) Theoretical Soil Mechanics. John Wiley and Sons, Inc., New York.

Terzaghi, K. and Peck, R.B. (1967) Soil Mechanics in Engineering Practice. John Wiley and Sons, Inc., New York.

van der Raadt, P. (1988) Field Measurement of Soil Suction Using Thermal Conductivity Matric Potential Sensors. M.Sc. Thesis, Department of Civil Engineering, University of Saskatchewan, Saskatoon, Saskatchewan.

van der Raadt, P. and Clifton, A.W. (1985) Soil Suction Measurement Final Report. A report prepared for CP Rail, CN Rail and the Transportation Development Centre by Clifton Associates Ltd., Regina, Saskatchewan.

Vesic, A.S. (1973) Analysis of ultimate loads of shallow foundations. Proceedings, ASCE, Journal of the Geotechnical Engineering Division, Vol. 99, pp. 45 to 73.

Wong, D.K.H. and Ho, A. (1987) An Evaluation of a Thermal Conductivity Sensor for the Measurement of Soil Matric Suction. A report by The Geotechnical Group, Department of Civil Engineering, University of Saskatchewan, Saskatoon, Saskatchewan, S7N 0W0.

Wong, D.K.H., Fredlund, D.G., Imre, E. and Putz, G. (1990) Difficulties associated with the use of AGWA-II thermal conductivity sensors to measure soil suction. Submitted to the Transportation Research Board, Washington, D.C., January, 1989. In press.

Appendix A: Comparison of GEOTRACK Stress Distribution at Various Embankment Side-Slopes, Computer Output

COMPUTATION OF STRESSES AT VARIOUS OFFSETS

FILENAME E1035T36 OFFSET 1 = 52 in.

TIE LENGTH ..... 102.0 IN.
NUMBER OF SEGMENTS PER TIE 10
NUMBER OF SEGMENTS BETWEEN RAILS .. 6
TIE SPACING ..... 20.0 IN.
TIE WIDTH ..... 9.0 IN.
TIE AREA ..... 63.0 SQ.IN.
TIE WEIGHT ..... 250.0 LBS
TIE EI ..... .63296E+09 LB-SQ.IN.
RAIL SPACING ..... 59.25 IN.
RAIL AREA ..... 13.35 SQ.IN.
RAIL WEIGHT ..... 115.0 LBS PER YARD
RAIL EI ..... .28470E+10 LB-SQ.IN.
RAIL FASTENER STIFFNESS ..... 7000000.0 LBS PER IN.
NUMBER OF AXLE LOADS 4
AXLE LOADS ARE ON TIE NUMBER(S) ... 1 4 8 11
WHEEL LOAD PER AXLE (KIPS) 49.40 49.40 49.40 49.40
NUMBER OF SOIL LAYERS 5
SOLVE FOR FULL TRACK RESPONSE 1
NUMBER OF ITERATIONS 0
CALCULATE AT OTHER DEPTH POINTS ... 1
CALCULATE AT OFFSET LOCATIONS 1
LIMIT TIE/BALLAST TENSION 0
FIRST TIE OUTPUT 1
LAST TIE OUTPUT 16
FIRST TIE SEGMENT OUTPUT 1
LAST TIE SEGMENT OUTPUT 5
PRINT STANDARD SOIL OUTPUT 1
PRINT PRINCIPAL STRESSES 0
PRINT EQUIVALENT TRIAXIAL DATA 0

LAYER	MODULUS (PSI)	VRAT	DEPTH (IN.)	GAMMA (PCF)	KNOT
1	35000.	.30	12.00	125.0	1.00
2	35000.	.30	12.00	125.0	1.00
3	35000.	.30	12.00	125.0	1.00
4	10000.	.40	36.00	125.0	.75
5	10000.	.40	.00	125.0	.75

LAYER	KTYPE	MODULUS DESCRIPTION				
1	1	LOG E - LOG BULK STRESS	K1 =	1058.00	K2 =	.593
2	1	LOG E - LOG BULK STRESS	K1 =	941.00	K2 =	.687
3	1	LOG E - LOG BULK STRESS	K1 =	941.00	K2 =	.687
4	1	LOG E - LOG BULK STRESS	K1 =	877.00	K2 =	1.100
5	1	LOG E - LOG BULK STRESS	K1 =	877.00	K2 =	1.100

DIFFERENT DEPTHS AT WHICH MODULI ARE COMPUTED

Z(1) = 6.00 IN.

Z(2) = 18.00 IN.

Z(3) = 30.00 IN.

Z(4) = 54.00 IN.

Z(5) = 120.00 IN.

CALC. STEP NO. 1

DEFLECTIONS AND REACTIONS
NEGATIVE DEFLECTION IS DOWNWARD
NEGATIVE REACTION IS TENSION

---- SINGLE AXLE ----

TIE NO.	DEFLECTION RAIL IN.	REACTION RAIL SEAT LBS	DEFLECTION TIE IN.
1	-.091398	20344.5	-.088492
2	-.077485	12016.1	-.075769
3	-.057334	3486.7	-.056836
4	-.041996	124.7	-.041979
5	-.030307	-880.5	-.030433
6	-.019646	-219.3	-.019677

TIE NO.	TIE CENTER BENDING MOMENT (IN.-LBS)	TIE RAIL-SEAT BENDING MOMENT (IN.-LBS)
1	-.27364E+05	.94323E+05
2	-.14080E+05	.57626E+05
3	-.10234E+04	.18929E+05
4	.31582E+04	.27332E+04
5	.35304E+04	-.26352E+04
6	.14311E+04	-.39672E+03

TIE NO.	TIE/SOIL REACTIONS, LBS DIV 1	DIV 2	DIV 3	DIV 4	DIV 5
1	3750.6	5478.5	5668.5	3459.0	1988.0
2	2354.7	3177.4	3271.8	2016.8	1195.5
3	936.7	974.4	981.5	550.2	343.9
4	168.9	-2.7	-21.5	-15.5	-4.7
5	-65.6	-258.1	-279.7	-175.2	-102.1
6	-.4	-64.2	-71.8	-49.1	-33.8

TIE NO.	TIE SEGMENT DEFLECTION ,IN. DIV 1	DIV 2	DIV 3	DIV 4	DIV 5
1	-.072807	-.084460	-.088670	-.084529	-.080587
2	-.064547	-.072715	-.076268	-.074542	-.072561
3	-.051049	-.055069	-.057508	-.057998	-.057925
4	-.039272	-.041041	-.042530	-.043555	-.044072
5	-.029312	-.029976	-.030806	-.031719	-.032270
6	-.019021	-.019429	-.019853	-.020243	-.020469

PEAK RAIL BENDING MOMENT= .29490E+06 IN.-LBS

TRACK MODULUS U = 7.766 KIPS/IN./IN. = 53.539 MN/M/M

SUPERIMPOSED RESULTS FROM CALC. STEP NO. 1

----- DEFLECTIONS AND REACTIONS ----

TIE NO.	DEFLECTION RAIL IN.	REACTION RAIL SEAT LBS	DEFLECTION TIE IN.
1	-.133394	20469.2	-.130471
2	-.134819	15302.9	-.132605
3	-.154465	15283.6	-.152282
4	-.163701	19588.7	-.160903
5	-.149788	11260.2	-.148180
6	-.153959	6535.0	-.153026
7	-.149788	11260.2	-.148180
8	-.163701	19588.7	-.160903
9	-.154465	15283.6	-.152282
10	-.134819	15302.9	-.132605
11	-.133394	20469.2	-.130471
12	-.107792	11135.6	-.106201
13	-.076979	3267.5	-.076513
14	-.041996	124.7	-.041979
15	-.030307	-880.5	-.030433
16	-.019646	-219.3	-.019677

TIE NO.	TIE CENTER BENDING MOMENT (IN.-LBS)	TIE RAIL-SEAT BENDING MOMENT (IN.-LBS)	RAIL BENDING MOMENT (IN.-LBS)
1	-.24206E+05	.97057E+05	.26852E+06
2	-.15103E+05	.76555E+05	-.41535E+05
3	-.13672E+05	.76158E+05	-.41536E+05
4	-.20676E+05	.94421E+05	.26414E+06
5	-.73913E+04	.57724E+05	-.26419E+05
6	.81548E+03	.37065E+05	-.91768E+05
7	-.73913E+04	.57724E+05	-.26418E+05
8	-.20676E+05	.94421E+05	.26414E+06
9	-.13672E+05	.76158E+05	-.41536E+05
10	-.15103E+05	.76555E+05	-.41536E+05
11	-.24206E+05	.97057E+05	.26852E+06
12	-.10549E+05	.54990E+05	-.37082E+02
13	.40774E+03	.18533E+05	-.45884E+05
14	.31582E+04	.27332E+04	-.26381E+05
15	.35304E+04	-.26352E+04	-.43851E+04
16	.14311E+04	-.39672E+03	.00000E+00

TIE NO.	TIE/SOIL REACTIONS, LBS DIV 1	DIV 2	DIV 3	DIV 4	DIV 5
1	3919.6	5475.8	5647.0	3443.5	1983.3
2	3191.4	4051.8	4153.3	2567.0	1539.4
3	3191.0	3987.6	4081.5	2518.0	1505.6
4	3854.0	5217.7	5367.4	3268.4	1881.2
5	2458.1	2916.6	2970.6	1826.2	1088.7
6	1672.6	1620.5	1619.4	1002.3	620.3
7	2458.1	2916.6	2970.6	1826.2	1088.7
8	3854.0	5217.7	5367.4	3268.4	1881.2
9	3191.0	3987.6	4081.5	2518.0	1505.6
10	3191.4	4051.8	4153.3	2567.0	1539.4
11	3919.6	5475.8	5647.0	3443.5	1983.3
12	2289.1	2919.3	2992.1	1841.6	1093.4
13	836.3	810.2	809.7	501.2	310.1
14	158.9	-2.7	-21.5	-15.5	-4.7
15	-65.6	-258.1	-279.7	-175.2	-102.1
16	-.4	-64.2	-71.8	-49.1	-33.8

TIE NO.	TIE SEGMENT DEFLECTION ,IN. DIV 1	DIV 2	DIV 3	DIV 4	DIV 5
1	-.112079	-.125501	-.131200	-.128084	-.124659
2	-.115596	-.127784	-.133776	-.132539	-.130487
3	-.134617	-.147214	-.153629	-.152783	-.150956
4	-.141391	-.155477	-.162006	-.159802	-.156929
5	-.133131	-.143732	-.149605	-.149815	-.148904
6	-.140139	-.148998	-.154720	-.156482	-.156789
7	-.133131	-.143732	-.149605	-.149815	-.148904
8	-.141391	-.155477	-.162006	-.159802	-.156929

9	-.134617	-.147214	-.153629	-.152783	-.150956
10	-.115596	-.127784	-.133776	-.132539	-.130487
11	-.112079	-.123501	-.131200	-.128084	-.124659
12	-.093859	-.102691	-.107075	-.106260	-.104832
13	-.070070	-.074499	-.077360	-.078241	-.078395
14	-.039272	-.041041	-.042530	-.043555	-.044072
15	-.029312	-.029976	-.030806	-.031719	-.032270
16	-.019021	-.019429	-.019853	-.020243	-.020469

SOIL VERTICAL DISPLACEMENTS AND INCREMENTAL STRESSES

T = TIE NUMBER (1=CENTER TIE)
SEG = SEGMENT NUMBER
Z = DEPTH POINT NUMBER
XX = DIRECTION PARALLEL TO TIES
YY = DIRECTION PARALLEL TO RAILS
ZZ = VERTICAL DIRECTION
UNITS ARE INCHES AND PSI
COMPRESSION IS NEGATIVE FOR STRESSES
DOWNWARD IS POSITIVE FOR DEFLECTIONS

Z(1) = 6.00 IN.

Z(2) = 18.00 IN.

Z(3) = 30.00 IN.

Z(4) = 54.00 IN.

Z(5) = 120.00 IN.

T	SEG	Z	W	THETA	S-XX	S-YY	S-ZZ	S-XY	S-XZ	S-YZ
1	1	1	.10828	-52.0	-13.2	-9.7	-29.2	-1.1	-6.8	-.7
1	1	2	.10337	-20.5	-4.1	-3.7	-12.8	.3	-7.3	-1.9
1	1	3	.09998	-5.5	1.4	1.9	-8.8	1.4	-4.9	-1.7
1	1	4	.08846	-9.5	-1.7	-1.4	-6.3	.4	-2.2	-1.2
1	1	5	.06181	-4.0	-.4	-.3	-3.4	.2	-.9	-.6
1	2	1	.12005	-72.5	-18.7	-11.9	-41.9	-1.0	-2.9	-.9
1	2	2	.11264	-26.2	-4.0	-4.3	-17.9	.2	-4.1	-2.3
1	2	3	.10799	-5.4	3.1	2.5	-11.0	1.1	-3.2	-2.1
1	2	4	.09387	-10.5	-1.6	-1.6	-7.3	.4	-1.7	-1.4
1	2	5	.06375	-4.2	-.3	-.3	-3.6	.1	-.7	-.6

1	3	1	.12563	-74.8	-19.5	-12.6	-42.6	-.7	1.4	-1.0
1	3	2	.11826	-27.6	-4.7	-4.5	-18.3	.0	-.0	-2.5
1	3	3	.11342	-5.6	3.4	2.7	-11.8	.7	-1.0	-2.3
1	3	4	.09800	-11.3	-1.6	-1.7	-7.9	.3	-1.2	-1.5
1	3	5	.06521	-4.4	-.2	-.3	-3.8	.0	-.6	-.7
1	4	1	.12506	-57.5	-18.2	-11.7	-27.6	-.5	3.4	-1.0
1	4	2	.12037	-25.3	-6.1	-4.4	-14.8	-.0	2.0	-2.5
1	4	3	.11623	-5.9	2.6	2.8	-11.2	.4	.4	-2.3
1	4	4	.10064	-11.7	-1.5	-1.8	-8.3	.2	-.7	-1.5
1	4	5	.06616	-4.4	-.2	-.3	-4.0	.0	-.3	-.7
1	5	1	.12331	-43.6	-16.0	-10.8	-16.8	-.2	1.5	-.9
1	5	2	.12070	-22.8	-7.0	-4.2	-11.6	-.0	1.1	-2.4
1	5	3	.11726	-6.2	1.6	2.8	-10.6	.1	.3	-2.3
1	5	4	.10192	-11.9	-1.7	-1.8	-8.4	.0	-.2	-1.6
1	5	5	.06663	-4.5	-.2	-.3	-4.0	.0	-.1	-.7

T	SEG	Z	W	THETA	S-XX	S-YY	S-ZZ	S-XY	S-XZ	S-YZ
2	1	1	.11274	-46.5	-12.2	-10.7	-23.6	-1.8	-5.7	.0
2	1	2	.10898	-20.6	-4.1	-5.0	-11.6	1.5	-7.2	-.0
2	1	3	.10575	-5.8	1.6	1.8	-9.2	3.1	-5.2	-.3
2	1	4	.09317	-10.3	-1.8	-1.5	-7.0	.8	-2.4	-.4
2	1	5	.06371	-4.2	-.4	-.2	-3.6	.2	-1.0	-.2
2	2	1	.12410	-61.6	-17.1	-13.0	-31.4	-1.6	-2.3	.0
2	2	2	.11873	-25.9	-4.0	-6.1	-15.8	.9	-4.1	.0
2	2	3	.11439	-5.7	3.4	2.2	-11.3	2.3	-3.4	-.2
2	2	4	.09904	-11.4	-1.7	-1.6	-8.0	.6	-1.9	-.5
2	2	5	.06573	-4.4	-.3	-.2	-3.9	.2	-.8	-.2
2	3	1	.13006	-63.4	-17.9	-13.8	-31.7	-1.3	.9	.0
2	3	2	.12483	-27.2	-4.7	-6.4	-16.1	.0	-.4	.0
2	3	3	.12032	-5.9	3.8	2.5	-12.1	1.3	-1.1	-.3
2	3	4	.10354	-12.2	-1.7	-1.8	-8.8	.4	-1.3	-.5
2	3	5	.06728	-4.6	-.2	-.2	-4.1	.1	-.6	-.2
2	4	1	.13065	-50.8	-17.0	-12.9	-20.8	-.9	2.5	-.0
2	4	2	.12741	-25.4	-6.1	-6.0	-13.3	-.5	1.6	-.0
2	4	3	.12347	-6.2	2.9	2.6	-11.7	.5	.2	-.3
2	4	4	.10645	-12.8	-1.8	-1.8	-9.2	.3	-.7	-.5
2	4	5	.06831	-4.7	-.2	-.2	-4.2	.0	-.4	-.2

2	5	1	.12976	-40.6	-15.4	-12.1	-13.2	-.3	1.1	-.0
2	5	2	.12804	-23.3	-7.0	-5.6	-10.7	-.3	.9	-.2
2	5	3	.12468	-6.5	1.9	2.6	-11.1	.1	.3	-.4
2	5	4	.10785	-13.0	-1.8	-1.9	-9.3	.0	-.2	-.3
2	5	5	.06882	-4.7	-.2	-.2	-4.3	.0	-.1	-.2

T	SEG	Z	M	THETA	S-XX	S-YY	S-ZZ	S-XY	S-XZ	S-YZ
3	1	1	.13172	-46.1	-12.5	-10.0	-23.6	-2.3	-5.6	-.0
3	1	2	.12798	-21.2	-4.3	-5.3	-11.6	1.5	-7.1	-.1
3	1	3	.12483	-7.4	1.4	.5	-9.3	3.5	-5.2	-.0
3	1	4	.11237	-11.5	-2.0	-2.1	-7.4	1.0	-2.5	-.0
3	1	5	.08081	-5.1	-.5	-.4	-4.2	.3	-1.1	-.2
3	2	1	.14357	-60.6	-17.5	-12.1	-31.0	-2.0	-2.2	-.0
3	2	2	.13830	-26.4	-4.3	-6.4	-15.7	.8	-4.0	-.2
3	2	3	.13406	-7.4	3.3	.8	-11.5	2.7	-3.4	-.0
3	2	4	.11885	-12.7	-1.9	-2.3	-8.5	.8	-2.1	-.0
3	2	5	.08321	-5.3	-.4	-.5	-4.5	.2	-.9	-.2
3	3	1	.14997	-62.3	-18.4	-12.8	-31.1	-1.6	.9	-.0
3	3	2	.14485	-27.7	-5.1	-6.7	-15.9	-.0	-.4	-.2
3	3	3	.14046	-7.7	3.6	.9	-12.2	1.6	-1.2	-.0
3	3	4	.12383	-13.6	-1.9	-2.5	-9.2	.6	-1.4	-.0
3	3	5	.08506	-5.5	-.3	-.5	-4.8	.2	-.7	-.2
3	4	1	.15093	-49.9	-17.5	-11.9	-20.5	-1.1	2.4	-.0
3	4	2	.14777	-28.0	-6.4	-6.4	-13.2	-.5	1.5	-.0
3	4	3	.14396	-8.1	2.8	1.0	-11.9	.7	.2	.0
3	4	4	.12707	-14.1	-1.9	-2.6	-9.6	.3	-.8	-.0
3	4	5	.08630	-5.7	-.2	-.5	-4.9	.1	-.4	-.2
3	5	1	.15026	-39.9	-15.9	-11.0	-12.9	-.4	1.1	.0
3	5	2	.14859	-23.9	-7.3	-5.9	-10.7	-.3	.9	.0
3	5	3	.14534	-8.4	1.9	1.0	-11.3	.2	.3	.0
3	5	4	.12865	-14.4	-2.0	-2.6	-9.8	.1	-.3	-.0
3	5	5	.08691	-5.7	-.2	-.5	-5.0	.0	-.1	-.2

T	SEG	Z	M	THETA	S-XX	S-YY	S-ZZ	S-XY	S-XZ	S-YZ
4	1	1	.13768	-51.4	-13.8	-9.1	-28.6	-2.0	-6.6	.5
4	1	2	.13293	-21.8	-4.5	-4.5	-12.8	.4	-7.3	1.1
4	1	3	.12963	-8.1	1.2	.0	-9.3	2.3	-5.1	.9
4	1	4	.11776	-11.6	-2.1	-2.4	-7.2	.8	-2.5	.3
4	1	5	.08646	-5.4	-.5	-.5	-4.4	.3	-1.2	.0

4	2	1	.15035	-70.5	-19.4	-11.1	-40.0	-1.7	-2.7	.6
4	2	2	.14334	-27.4	-4.5	-5.2	-17.7	.2	-4.1	1.5
4	2	3	.13862	-8.2	3.0	.3	-11.5	1.8	-3.3	1.1
4	2	4	.12430	-12.8	-1.9	-2.6	-8.3	.7	-2.0	.4
4	2	5	.08900	-5.7	-.4	-.6	-4.7	.2	-1.0	.0
4	3	1	.15681	-72.5	-20.3	-11.7	-40.6	-1.3	1.4	.6
4	3	2	.14988	-28.8	-5.3	-5.5	-18.0	.0	-.2	1.6
4	3	3	.14520	-8.5	3.4	.4	-12.3	1.2	-1.1	1.2
4	3	4	.12932	-13.7	-1.9	-2.8	-9.0	.5	-1.4	.4
4	3	5	.09094	-5.9	-.3	-.6	-4.9	.2	-.7	.0
4	4	1	.15704	-56.1	-19.1	-10.7	-26.3	-.8	3.2	.6
4	4	2	.15267	-26.6	-6.6	-5.3	-14.6	-.0	1.8	1.5
4	4	3	.14867	-8.9	2.5	.4	-11.8	.7	.3	1.2
4	4	4	.13258	-14.3	-1.9	-2.9	-9.4	.3	-.8	.4
4	4	5	.09222	-6.0	-.2	-.6	-5.1	.1	-.5	.0
4	5	1	.15576	-42.9	-17.0	-9.8	-16.0	-.3	1.4	.6
4	5	2	.15338	-24.3	-7.6	-5.1	-11.6	-.0	1.0	1.4
4	5	3	.15004	-9.2	1.7	.3	-11.1	.2	.3	1.2
4	5	4	.13417	-14.5	-2.0	-3.0	-9.5	.0	-.3	.5
4	5	5	.09286	-6.0	-.2	-.6	-5.2	.0	-.2	.0

T	SEG	Z	W	THETA	S-XX	S-YY	S-ZZ	S-XY	S-XZ	S-YZ
5	1	1	.13095	-35.8	-10.4	-7.2	-18.1	-2.7	-4.2	.8
5	1	2	.12815	-17.9	-3.8	-4.9	-9.1	1.2	-5.5	2.0
5	1	3	.12577	-8.4	.9	-1.5	-7.8	3.6	-4.2	1.5
5	1	4	.11560	-11.2	-2.0	-2.5	-6.7	1.1	-2.4	.6
5	1	5	.08592	-5.3	-.5	-.6	-4.3	.4	-1.2	.2
5	2	1	.14117	-45.9	-14.5	-8.7	-22.8	-2.3	-1.6	1.1
5	2	2	.13737	-21.9	-3.9	-5.9	-12.1	.7	-3.1	2.7
5	2	3	.13419	-8.6	2.4	-1.5	-9.5	2.8	-2.8	1.9
5	2	4	.12181	-12.3	-1.8	-2.8	-7.6	.9	-1.9	.6
5	2	5	.08840	-5.6	-.4	-.6	-4.6	.3	-1.0	.3
5	3	1	.14707	-47.0	-15.2	-9.1	-22.7	-1.8	.6	1.2
5	3	2	.14344	-22.9	-4.5	-6.2	-12.2	.0	-.4	2.8
5	3	3	.14015	-8.9	2.8	-1.6	-10.1	1.8	-1.0	2.0
5	3	4	.12661	-13.1	-1.8	-3.0	-8.3	.7	-1.3	.7
5	3	5	.09031	-5.8	-.3	-.6	-4.9	.2	-.7	.3
5	4	1	.14862	-37.9	-14.7	-8.4	-14.9	-1.2	1.8	1.0
5	4	2	.14643	-21.7	-5.5	-5.9	-10.2	-.4	1.1	2.6
5	4	3	.14357	-9.4	2.2	-1.7	-9.9	.9	.0	1.9
5	4	4	.12977	-13.7	-1.8	-3.2	-8.7	.4	-.8	.7
5	4	5	.09160	-5.9	-.2	-.7	-5.0	.1	-.4	.3

5	5	1	.14855	-30.6	-13.6	-7.7	-9.4	-.4	.8	.9
5	5	2	.14746	-20.2	-6.3	-5.6	-8.3	-.2	.6	2.3
5	5	3	.14501	-9.7	1.5	-1.7	-9.5	.2	.2	1.8
5	5	4	.13133	-13.9	-1.9	-3.2	-8.8	.1	-.2	.7
5	5	5	.09224	-6.0	-.2	-.7	-5.1	.0	-.2	.3

T	SEG	Z	W	THETA	S-XX	S-YY	S-ZZ	S-XY	S-XZ	S-YZ
6	1	1	.13875	-26.4	-8.7	-5.5	-12.3	-3.3	-2.8	.0
6	1	2	.13706	-15.7	-3.6	-5.3	-6.9	1.3	-4.4	.0
6	1	3	.13530	-9.5	.6	-3.2	-6.9	4.3	-3.7	.0
6	1	4	.12634	-11.6	-2.0	-3.0	-6.6	1.3	-2.3	.0
6	1	5	.09661	-5.8	-.5	-.8	-4.6	.5	-1.3	.0
6	2	1	.14782	-31.3	-11.9	-6.4	-13.0	-2.8	-.9	.0
6	2	2	.14585	-18.7	-3.7	-6.3	-8.7	.7	-2.5	.0
6	2	3	.14356	-9.8	2.0	-3.6	-8.2	3.3	-2.5	.0
6	2	4	.13269	-12.7	-1.9	-3.3	-7.5	1.1	-1.9	.0
6	2	5	.09928	-6.1	-.4	-.8	-4.9	.4	-1.0	.0
6	3	1	.15363	-31.8	-12.5	-6.6	-12.6	-2.2	.3	.0
6	3	2	.15188	-19.5	-4.3	-6.6	-8.6	.0	-.5	.0
6	3	3	.14953	-10.3	2.3	-3.8	-8.8	2.1	-1.0	.0
6	3	4	.13763	-13.5	-1.8	-3.6	-8.1	.8	-1.4	.0
6	3	5	.10135	-6.3	-.3	-.9	-5.1	.3	-.8	.0
6	4	1	.15612	-26.9	-12.4	-6.1	-8.4	-1.4	.9	.0
6	4	2	.15519	-18.8	-5.0	-6.4	-7.4	-.4	.6	.0
6	4	3	.15311	-10.8	1.9	-3.9	-8.7	1.0	-.1	.0
6	4	4	.14091	-14.1	-1.9	-3.7	-8.5	.5	-.8	.0
6	4	5	.10276	-6.5	-.2	-.9	-5.3	.2	-.5	.0
6	5	1	.15685	-22.9	-11.8	-5.7	-5.5	-.5	.4	.0
6	5	2	.15652	-18.0	-5.6	-6.1	-6.3	-.2	.4	.0
6	5	3	.15470	-11.1	1.3	-4.0	-8.4	.3	.0	.0
6	5	4	.14254	-14.3	-1.9	-3.8	-8.6	.2	-.3	.0
6	5	5	.10348	-6.5	-.2	-.9	-5.4	.0	-.2	.0

T	SEG	Z	W	THETA	S-XX	S-YY	S-ZZ	S-XY	S-XZ	S-YZ
7	1	1	.13095	-35.8	-10.4	-7.2	-18.1	-2.7	-4.2	-.8
7	1	2	.12815	-17.9	-3.8	-4.9	-9.1	1.2	-5.5	-2.0
7	1	3	.12577	-8.4	.9	-1.5	-7.8	3.6	-4.2	-1.5
7	1	4	.11560	-11.2	-2.0	-2.5	-6.7	1.1	-2.4	-.6
7	1	5	.08592	-5.3	-.5	-.6	-4.3	.4	-1.2	-.2

7	2	1	.14117	-45.9	-14.5	-8.7	-22.8	-2.3	-1.6	-1.1
7	2	2	.13737	-21.9	-3.9	-5.9	-12.1	.7	-3.1	-2.7
7	2	3	.13419	-8.6	2.4	-1.5	-9.5	2.8	-2.8	-1.9
7	2	4	.12181	-12.3	-1.8	-2.8	-7.6	.9	-1.9	-.6
7	2	5	.08840	-5.6	-.4	-.6	-4.6	.3	-1.0	-.3
7	3	1	.14707	-47.0	-15.2	-9.1	-22.7	-1.8	.6	-1.2
7	3	2	.14344	-22.9	-4.5	-6.2	-12.2	.0	-.4	-2.8
7	3	3	.14015	-8.9	2.8	-1.6	-10.1	1.8	-1.0	-2.0
7	3	4	.12661	-13.1	-1.8	-3.0	-8.3	.7	-1.3	-.7
7	3	5	.09031	-5.8	-.3	-.6	-4.8	.2	-.7	-.3
7	4	1	.14862	-37.9	-14.7	-8.4	-14.9	-1.2	1.8	-1.0
7	4	2	.14643	-21.7	-5.5	-5.9	-10.2	-.4	1.1	-2.6
7	4	3	.14357	-9.4	2.2	-1.7	-9.9	.9	.0	-1.9
7	4	4	.12977	-13.7	-1.8	-3.2	-8.7	.4	-.8	-.7
7	4	5	.09160	-5.9	-.2	-.7	-5.0	.1	-.4	-.3
7	5	1	.14855	-30.6	-13.6	-7.7	-9.4	-.4	.8	-.9
7	5	2	.14746	-20.2	-6.3	-5.6	-8.3	-.2	.6	-2.3
7	5	3	.14501	-9.7	1.5	-1.7	-9.5	.2	.2	-1.8
7	5	4	.13133	-13.9	-1.9	-3.2	-8.8	.1	-.2	-.7
7	5	5	.09224	-6.0	-.2	-.7	-5.1	.0	-.2	-.3

T	SEG	Z	W	THETA	S-XX	S-YY	S-ZZ	S-XY	S-XZ	S-YZ
8	1	1	.13768	-31.4	-13.8	-9.1	-28.6	-2.0	-6.6	-.5
8	1	2	.13293	-21.8	-4.5	-4.5	-12.8	.4	-7.3	-1.1
8	1	3	.12963	-8.1	1.2	.0	-9.3	2.3	-5.1	-.9
8	1	4	.11776	-11.6	-2.1	-2.4	-7.2	.8	-2.5	-.3
8	1	5	.08646	-5.4	-.5	-.5	-4.4	.3	-1.2	-.0
8	2	1	.15035	-70.3	-19.4	-11.1	-40.0	-1.7	-2.7	-.6
8	2	2	.14334	-27.4	-4.5	-5.2	-17.7	.2	-4.1	-1.5
8	2	3	.13882	-8.2	3.0	.3	-11.5	1.8	-3.3	-1.1
8	2	4	.12430	-12.8	-1.9	-2.6	-8.3	.7	-2.0	-.4
8	2	5	.08900	-5.7	-.4	-.6	-4.7	.2	-1.0	-.0
8	3	1	.15681	-72.5	-20.3	-11.7	-40.6	-1.3	1.4	-.6
8	3	2	.14988	-28.8	-5.3	-5.5	-18.0	.0	-.2	-1.6
8	3	3	.14520	-8.5	3.4	.4	-12.3	1.2	-1.1	-1.2
8	3	4	.12932	-13.7	-1.9	-2.8	-9.0	.5	-1.4	-.4
8	3	5	.09094	-5.9	-.3	-.6	-4.9	.2	-.7	-.0

8	4	1	.15704	-56.1	-19.1	-10.7	-26.3	-.8	3.2	-.6
8	4	2	.15267	-26.6	-6.6	-5.3	-14.6	-.0	1.8	-1.5
8	4	3	.14867	-8.9	2.5	.4	-11.8	.7	.3	-1.2
8	4	4	.13258	-14.3	-1.9	-2.9	-9.4	.3	-.8	-.4
8	4	5	.09222	-6.0	-.2	-.6	-5.1	.1	-.5	-.0
8	5	1	.15576	-42.9	-17.0	-9.8	-16.0	-.3	1.4	-.6
8	5	2	.15338	-24.3	-7.6	-3.1	-11.6	-.0	1.0	-1.4
8	5	3	.15004	-9.2	1.7	.3	-11.1	.2	.3	-1.2
8	5	4	.13417	-14.5	-2.0	-3.0	-9.5	.0	-.3	-.5
8	5	5	.09286	-6.0	-.2	-.6	-5.2	.0	-.2	-.0

T	SEG	Z	W	THETA	S-XX	S-YY	S-ZZ	S-XY	S-XZ	S-YZ
9	1	1	.13172	-46.1	-12.5	-10.0	-23.6	-2.3	-5.6	.0
9	1	2	.12798	-21.2	-4.3	-5.3	-11.6	1.5	-7.1	.1
9	1	3	.12483	-7.4	1.4	.5	-9.3	3.5	-5.2	.0
9	1	4	.11237	-11.5	-2.0	-2.1	-7.4	1.0	-2.5	.0
9	1	5	.08081	-5.1	-.5	-.4	-4.2	.3	-1.1	.2
9	2	1	.14357	-60.6	-17.5	-12.1	-31.0	-2.0	-2.2	.0
9	2	2	.13830	-26.4	-4.3	-6.4	-15.7	.8	-4.0	.2
9	2	3	.13406	-7.4	3.3	.8	-11.5	2.7	-3.4	.0
9	2	4	.11885	-12.7	-1.9	-2.3	-8.5	.8	-2.1	.0
9	2	5	.08321	-5.3	-.4	-.5	-4.5	.2	-.9	.2
9	3	1	.14997	-62.3	-18.4	-12.9	-31.1	-1.6	.9	.0
9	3	2	.14485	-27.7	-5.1	-6.7	-15.9	-.0	-.4	.2
9	3	3	.14046	-7.7	3.6	.9	-12.2	1.6	-1.2	.0
9	3	4	.12383	-13.6	-1.9	-2.5	-9.2	.6	-1.4	.0
9	3	5	.08506	-5.5	-.3	-.5	-4.8	.2	-.7	.2
9	4	1	.15093	-49.9	-17.5	-11.9	-20.5	-1.1	2.4	.0
9	4	2	.14777	-26.0	-6.4	-6.4	-13.2	-.5	1.5	.0
9	4	3	.14396	-8.1	2.8	1.0	-11.9	.7	.2	.0
9	4	4	.12707	-14.1	-1.9	-2.6	-9.6	.3	-.8	.0
9	4	5	.08630	-5.7	-.2	-.5	-4.9	.1	-.4	.2
9	5	1	.15026	-39.9	-15.9	-11.0	-12.9	-.4	1.1	-.0
9	5	2	.14859	-23.9	-7.3	-5.9	-10.7	-.3	.9	.0
9	5	3	.14534	-8.4	1.9	1.0	-11.3	.2	.3	-.0
9	5	4	.12865	-14.4	-2.0	-2.6	-9.8	.1	-.3	.0
9	5	5	.08691	-5.7	-.2	-.5	-5.0	.0	-.1	.2

T	SEG	Z	W	THETA	S-XX	S-YY	S-ZZ	S-XY	S-XZ	S-YZ
10	1	1	.11274	-46.5	-12.2	-10.7	-23.6	-1.8	-5.7	.0
10	1	2	.10898	-20.6	-4.1	-5.0	-11.6	1.5	-7.2	.0
10	1	3	.10575	-5.8	1.6	1.8	-9.2	3.1	-5.2	.3
10	1	4	.09317	-10.3	-1.8	-1.5	-7.0	.8	-2.4	.4
10	1	5	.06371	-4.2	-.4	-.2	-3.6	.2	-1.0	.2
10	2	1	.12410	-61.6	-17.1	-13.0	-31.4	-1.6	-2.3	-.0
10	2	2	.11873	-25.9	-4.0	-6.1	-15.8	.9	-4.1	-.0
10	2	3	.11439	-5.7	3.4	2.2	-11.3	2.3	-3.4	.2
10	2	4	.09904	-11.4	-1.7	-1.6	-8.0	.6	-1.9	.5
10	2	5	.06573	-4.4	-.3	-.2	-3.9	.2	-.8	.2
10	3	1	.13006	-63.4	-17.9	-13.8	-31.7	-1.3	.9	-.0
10	3	2	.12483	-27.2	-4.7	-6.4	-16.1	.0	-.4	-.0
10	3	3	.12032	-5.9	3.8	2.5	-12.1	1.3	-1.1	.3
10	3	4	.10354	-12.2	-1.7	-1.8	-8.8	.4	-1.3	.5
10	3	5	.06728	-4.6	-.2	-.2	-4.1	.1	-.6	.2
10	4	1	.13065	-50.8	-17.0	-12.9	-20.8	-.9	2.5	.0
10	4	2	.12741	-25.4	-6.1	-6.0	-13.3	-.5	1.6	.0
10	4	3	.12347	-6.2	2.9	2.6	-11.7	.5	.2	.3
10	4	4	.10645	-12.8	-1.8	-1.8	-9.2	.3	-.7	.5
10	4	5	.06831	-4.7	-.2	-.2	-4.2	.0	-.4	.2
10	5	1	.12976	-40.6	-15.4	-12.1	-13.2	-.3	1.1	.0
10	5	2	.12804	-23.3	-7.0	-5.6	-10.7	-.3	.9	.2
10	5	3	.12468	-6.5	1.9	2.6	-11.1	.1	.3	.4
10	5	4	.10785	-13.0	-1.8	-1.9	-9.3	.0	-.2	.5
10	5	5	.06882	-4.7	-.2	-.2	-4.3	.0	-.1	.2

T	SEG	Z	W	THETA	S-XX	S-YY	S-ZZ	S-XY	S-XZ	S-YZ
11	1	1	.10828	-52.0	-13.2	-9.7	-29.2	-1.1	-6.8	.7
11	1	2	.10337	-20.5	-4.1	-3.7	-12.8	.3	-7.3	1.9
11	1	3	.09998	-5.5	1.4	1.9	-8.8	1.4	-4.9	1.7
11	1	4	.08846	-9.5	-1.7	-1.4	-6.3	.4	-2.2	1.2
11	1	5	.06181	-4.0	-.4	-.3	-3.4	.2	-.9	.6
11	2	1	.12005	-72.5	-18.7	-11.9	-41.9	-1.0	-2.9	.9
11	2	2	.11264	-26.2	-4.0	-4.3	-17.9	.2	-4.1	2.3
11	2	3	.10799	-5.4	3.1	2.5	-11.0	1.1	-3.2	2.1
11	2	4	.09287	-10.5	-1.6	-1.6	-7.3	.4	-1.7	1.4
11	2	5	.06375	-4.2	-.3	-.3	-3.6	.1	-.7	.6

11	3	1	.12563	-74.8	-19.5	-12.6	-42.6	-.7	1.4	1.0
11	3	2	.11826	-27.6	-4.7	-4.5	-18.3	.0	-.0	2.5
11	3	3	.11342	-5.6	3.4	2.7	-11.8	.7	-1.0	2.3
11	3	4	.09800	-11.3	-1.6	-1.7	-7.9	.3	-1.2	1.5
11	3	5	.06521	-4.4	-.2	-.3	-3.8	.0	-.6	.7
11	4	1	.12506	-57.5	-18.2	-11.7	-27.6	-.5	3.4	1.0
11	4	2	.12037	-25.3	-6.1	-4.4	-14.8	-.0	2.0	2.5
11	4	3	.11623	-5.9	2.6	2.8	-11.2	.4	.4	2.3
11	4	4	.10064	-11.7	-1.6	-1.8	-8.3	.2	-.7	1.5
11	4	5	.06616	-4.4	-.2	-.3	-4.0	.0	-.3	.7
11	5	1	.12331	-43.6	-16.0	-10.8	-16.8	-.2	1.5	.9
11	5	2	.12070	-22.8	-7.0	-4.2	-11.6	-.0	1.1	2.4
11	5	3	.11726	-6.2	1.6	2.8	-10.6	.1	.3	2.3
11	5	4	.10192	-11.9	-1.7	-1.8	-8.4	.0	-.2	1.6
11	5	5	.06663	-4.5	-.2	-.3	-4.0	.0	-.1	.7

T	SEG	Z	W	THETA	S-XX	S-YY	S-ZZ	S-XY	S-XZ	S-YZ
12	1	1	.09174	-32.3	-8.8	-6.6	-17.0	-1.5	-4.0	1.5
12	1	2	.08901	-14.6	-3.0	-3.4	-8.2	.9	-4.9	3.9
12	1	3	.08683	-5.2	.9	.2	-6.4	2.2	-3.5	3.2
12	1	4	.07851	-7.9	-1.4	-1.5	-5.0	.6	-1.7	1.8
12	1	5	.05714	-3.6	-.3	-.3	-2.9	.2	-.8	.8
12	2	1	.09997	-42.9	-12.3	-8.1	-22.6	-1.3	-1.6	2.0
12	2	2	.09607	-18.3	-3.0	-4.2	-11.1	.5	-2.7	5.0
12	2	3	.09312	-5.2	2.2	.4	-7.8	1.7	-2.3	4.0
12	2	4	.08293	-8.7	-1.3	-1.7	-5.7	.5	-1.4	2.0
12	2	5	.05882	-3.7	-.3	-.4	-3.1	.2	-.7	.9
12	3	1	.10433	-44.1	-12.8	-8.5	-22.8	-1.1	.7	2.1
12	3	2	.10053	-19.2	-3.5	-4.4	-11.3	-.0	-.2	5.3
12	3	3	.09747	-5.4	2.4	.5	-8.4	1.0	-.8	4.3
12	3	4	.08634	-9.3	-1.3	-1.8	-6.2	.4	-1.0	2.2
12	3	5	.06012	-3.9	-.2	-.4	-3.3	.1	-.5	.9
12	4	1	.10485	-35.0	-12.2	-7.9	-14.9	-.7	1.8	2.0
12	4	2	.10248	-17.9	-4.4	-4.1	-9.3	-.3	1.1	5.1
12	4	3	.09984	-5.7	1.8	.5	-8.1	.5	.2	4.3
12	4	4	.08855	-9.7	-1.3	-1.9	-6.5	.2	-.5	2.3
12	4	5	.06098	-4.0	-.2	-.4	-3.4	.0	-.3	1.0

12	5	1	.10428	-27.6	-11.1	-7.2	-9.3	-.3	.8	1.8
12	5	2	.10301	-16.4	-5.1	-3.9	-7.5	-.2	.6	4.7
12	5	3	.10077	-5.9	1.2	.5	-7.7	.1	.2	4.1
12	5	4	.08963	-9.9	-1.4	-1.9	-6.6	.0	-.2	2.3
12	5	5	.06140	-4.0	-.1	-.4	-3.5	.0	-.1	1.0

T	SEG	Z	W	THETA	S-XX	S-YY	S-ZZ	S-XY	S-XZ	S-YZ
13	1	1	.06937	-13.2	-4.4	-2.7	-6.1	-1.6	-1.4	1.3
13	1	2	.06853	-7.9	-1.8	-2.6	-3.4	.7	-2.2	3.3
13	1	3	.06765	-4.8	.3	-1.6	-3.5	2.1	-1.8	2.9
13	1	4	.06317	-5.8	-1.0	-1.5	-3.3	.7	-1.2	1.8
13	1	5	.04831	-2.9	-.2	-.4	-2.3	.2	-.6	.9
13	2	1	.07201	-15.7	-5.9	-3.2	-6.5	-1.4	-.4	1.6
13	2	2	.07293	-9.3	-1.9	-3.1	-4.3	.4	-1.2	4.1
13	2	3	.07178	-4.9	1.0	-1.8	-4.1	1.7	-1.2	3.5
13	2	4	.06635	-6.3	-.9	-1.7	-3.7	.5	-1.0	2.0
13	2	5	.04964	-3.0	-.2	-.4	-2.4	.2	-.5	.9
13	3	1	.07681	-15.9	-6.3	-3.3	-6.3	-1.1	.1	1.8
13	3	2	.07594	-9.8	-2.1	-3.3	-4.3	.0	-.2	4.5
13	3	3	.07477	-5.1	1.2	-1.9	-4.4	1.1	-.5	3.8
13	3	4	.06881	-6.8	-.9	-1.8	-4.1	.4	-.7	2.2
13	3	5	.05068	-3.2	-.2	-.4	-2.6	.1	-.4	1.0
13	4	1	.07806	-13.4	-6.2	-3.1	-4.2	-.7	.5	1.7
13	4	2	.07760	-9.4	-2.5	-3.2	-3.7	-.2	.3	4.3
13	4	3	.07655	-5.4	.9	-2.0	-4.3	.5	-.0	3.8
13	4	4	.07046	-7.0	-.9	-1.9	-4.2	.2	-.4	2.3
13	4	5	.05138	-3.2	-.1	-.4	-2.7	.0	-.2	1.0
13	5	1	.07843	-11.5	-5.9	-2.8	-2.7	-.2	.2	1.6
13	5	2	.07826	-9.0	-2.8	-3.0	-3.2	-.1	.2	4.1
13	5	3	.07735	-5.5	.7	-2.0	-4.2	.1	.0	3.8
13	5	4	.07127	-7.2	-1.0	-1.9	-4.3	.0	-.1	2.3
13	5	5	.05174	-3.3	-.1	-.4	-2.7	.0	-.0	1.0

T	SEG	Z	W	THETA	S-XX	S-YY	S-ZZ	S-XY	S-XZ	S-YZ
14	1	1	.03920	-3.5	-1.7	-.6	-1.2	-1.1	-.2	.7
14	1	2	.03914	-3.3	-.8	-1.5	-1.0	.3	-.6	1.9
14	1	3	.03893	-3.2	.0	-1.7	-1.4	1.4	-.7	1.7
14	1	4	.03709	-3.3	-.6	-1.0	-1.7	.4	-.6	1.2
14	1	5	.02878	-1.7	-.1	-.2	-1.4	.2	-.4	.6

14	2	1	.04121	-3.0	-2.2	-.6	-.2	-1.0	.0	.9
14	2	2	.04131	-3.6	-.9	-1.7	-1.0	.2	-.4	2.3
14	2	3	.04107	-3.3	.3	-2.0	-1.6	1.1	-.5	2.1
14	2	4	.03889	-3.6	-.5	-1.1	-1.9	.4	-.5	1.4
14	2	5	.02957	-1.8	-.1	-.3	-1.5	.1	-.3	.6
14	3	1	.04274	-2.8	-2.3	-.6	.0	-.7	-.0	1.0
14	3	2	.04291	-3.7	-1.0	-1.8	-.9	.0	-.2	2.3
14	3	3	.04268	-3.5	.4	-2.1	-1.7	.7	-.3	2.3
14	3	4	.04028	-3.8	-.5	-1.2	-2.1	.3	-.4	1.5
14	3	5	.03019	-1.9	-.0	-.3	-1.5	.0	-.2	.7
14	4	1	.04377	-2.9	-2.5	-.5	.0	-.5	-.0	1.0
14	4	2	.04395	-3.8	-1.1	-1.8	-.9	-.0	-.0	2.5
14	4	3	.04373	-3.6	.4	-2.2	-1.8	.4	-.1	2.3
14	4	4	.04122	-4.0	-.5	-1.3	-2.2	.2	-.2	1.5
14	4	5	.03062	-1.9	-.0	-.3	-1.6	.0	-.1	.7
14	5	1	.04427	-3.0	-2.5	-.5	-.0	-.2	-.0	.9
14	5	2	.04445	-3.8	-1.2	-1.8	-.9	-.0	.0	2.4
14	5	3	.04423	-3.7	.3	-2.2	-1.8	.1	-.0	2.3
14	5	4	.04170	-4.1	-.5	-1.3	-2.3	.0	-.0	1.6
14	5	5	.03084	-1.9	-.0	-.3	-1.6	.0	-.0	.7

T	SEG	Z	W	THETA	S-XX	S-YY	S-ZZ	S-XY	S-XZ	S-YZ
15	1	1	.02940	.6	-.6	.6	.5	-.9	.2	.3
15	1	2	.02956	-1.3	-.5	-.8	.0	.0	.0	.7
15	1	3	.02965	-2.6	-.2	-1.9	-.5	.9	-.2	.8
15	1	4	.02930	-2.2	-.4	-.9	-.9	.2	-.3	.9
15	1	5	.02464	-1.4	-.1	-.3	-1.0	.1	-.3	.6
15	2	1	.03030	2.0	-.7	.8	1.8	-.7	.2	.3
15	2	2	.03070	-1.2	-.5	-.9	.3	.0	.0	.8
15	2	3	.03084	-2.8	-.1	-2.1	-.5	.7	-.1	1.0
15	2	4	.03043	-2.3	-.3	-1.0	-1.0	.3	-.3	1.0
15	2	5	.02525	-1.5	-.0	-.3	-1.1	.1	-.2	.6
15	3	1	.03118	2.3	-.7	1.0	2.1	-.5	-.0	.3
15	3	2	.03162	-1.2	-.6	-1.0	.3	.0	-.0	.9
15	3	3	.03178	-2.9	-.0	-2.3	-.5	.5	-.1	1.0
15	3	4	.03132	-2.5	-.3	-1.1	-1.1	.2	-.2	1.0
15	3	5	.02573	-1.5	-.0	-.3	-1.1	.0	-.2	.6
15	4	1	.03198	1.5	-.9	1.0	1.4	-.3	-.2	.4
15	4	2	.03230	-1.3	-.6	-1.0	.2	-.0	-.1	.9
15	4	3	.03244	-3.0	-.0	-2.4	-.6	.3	-.0	1.1
15	4	4	.03194	-2.6	-.3	-1.1	-1.1	.1	-.1	1.1
15	4	5	.02606	-1.5	-.0	-.3	-1.1	.0	-.1	.6

15	5	1	.03245	.8	-1.0	1.0	.8	-.1	-.0	.4
15	5	2	.03268	-1.5	-.5	-1.0	.0	.0	-.0	1.0
15	5	3	.03278	-3.1	.0	-2.5	-.6	.0	-.0	1.1
15	5	4	.03225	-2.6	-.3	-1.2	-1.1	.0	-.0	1.1
15	5	5	.02623	-1.6	-.0	-.3	-1.2	.0	-.0	.7

T	SEG	Z	W	THETA	S-XX	S-YY	S-ZZ	S-XY	S-XZ	S-YZ
16	1	1	.01898	.4	-.3	.7	.0	-.5	.0	.0
16	1	2	.01900	-.6	-.3	-.3	.0	-.0	.0	.1
16	1	3	.01908	-1.6	-.2	-1.3	-.1	.4	-.0	.3
16	1	4	.01921	-1.2	-.2	-.6	-.4	.2	-.2	.5
16	1	5	.01710	-.9	-.0	-.2	-.6	.1	-.2	.4
16	2	1	.01947	.9	-.4	.9	.4	-.4	.0	.0
16	2	2	.01956	-.5	-.3	-.3	.0	-.0	.0	.1
16	2	3	.01967	-1.7	-.2	-1.4	-.1	.3	-.0	.3
16	2	4	.01981	-1.3	-.2	-.7	-.4	.2	-.1	.5
16	2	5	.01748	-1.0	-.0	-.3	-.6	.0	-.1	.4
16	3	1	.01991	1.1	-.4	1.0	.5	-.3	.0	.0
16	3	2	.02002	-.5	-.3	-.3	.1	-.0	.0	.1
16	3	3	.02014	-1.8	-.1	-1.5	-.1	.3	-.0	.3
16	3	4	.02029	-1.3	-.2	-.7	-.4	.1	-.1	.6
16	3	5	.01776	-1.0	-.0	-.3	-.7	.0	-.1	.5
16	4	1	.02026	.9	-.5	1.0	.4	-.2	-.0	.0
16	4	2	.02037	-.6	-.3	-.3	.0	.0	-.0	.1
16	4	3	.02048	-1.9	-.1	-1.6	-.1	.2	-.0	.3
16	4	4	.02062	-1.4	-.2	-.8	-.5	.0	-.0	.6
16	4	5	.01799	-1.0	-.0	-.3	-.7	.0	-.0	.5
16	5	1	.02050	.8	-.5	1.0	.3	-.0	-.0	.0
16	5	2	.02056	-.6	-.3	-.4	.0	.0	-.0	.2
16	5	3	.02066	-1.9	-.0	-1.6	-.2	.0	-.0	.4
16	5	4	.02079	-1.4	-.2	-.8	-.5	.0	-.0	.6
16	5	5	.01810	-1.0	-.0	-.3	-.7	.0	-.0	.5

SUPERIMPOSED RESULTS FROM CALC. STEP NO. 2

----- DEFLECTIONS AND REACTIONS ----

TIE NO.	DEFLECTION RAIL IN.	REACTION RAIL SEAT LBS	DEFLECTION TIE IN.
1	-.076979	3267.5	-.076513
2	-.072303	-755.9	-.072411
3	-.163701	19588.7	-.160903
4	-.154463	15283.6	-.152282
5	-.165126	14622.3	-.163038
6	-.266789	40938.4	-.260941
7	-.165126	14622.3	-.163038
8	-.154463	15283.6	-.152282
9	-.163701	19588.7	-.160903
10	-.072303	-755.9	-.072411
11	-.076979	3267.5	-.076513
12	-.107792	11135.6	-.106201
13	-.133394	20469.2	-.130471
14	-.057334	3486.7	-.056836
15	-.077485	12016.1	-.075769
16	-.091398	20344.5	-.088492

TIE NO.	TIE CENTER BENDING MOMENT (IN.-LBS)	TIE RAIL-SEAT BENDING MOMENT (IN.-LBS)	RAIL BENDING MOMENT (IN.-LBS)
1	.48539E+06	.97057E+05	.12472E+08
2	.46656E+06	.76555E+05	.11253E+08
3	-.14121E+06	.76158E+05	.10019E+08
4	.10686E+06	.94421E+05	.91774E+07
5	-.10699E+06	.57724E+05	.76530E+07
6	-.10184E+07	.37065E+05	.64210E+07
7	-.10699E+06	.57724E+05	.60079E+07
8	.10686E+06	.94421E+05	.58871E+07
9	-.14121E+06	.76158E+05	.50841E+07
10	.46656E+06	.76555E+05	.46728E+07
11	.48539E+06	.97057E+05	.42464E+07
12	-.10549E+05	.54990E+05	.28974E+07
13	-.50919E+06	.18533E+05	.17711E+07
14	-.96444E+05	.27332E+04	.10541E+07
15	-.37853E+06	-.26352E+04	.40689E+06
16	-.60777E+06	-.39572E+03	.00000E+00

TIE NO.	TIE/SOIL REACTIONS, LBS DIV 1	DIV 2	DIV 3	DIV 4	DIV 5
1	3919.6	5475.8	5647.0	3443.5	1983.3
2	3191.4	4051.8	4153.3	2567.0	1539.4
3	3191.0	3987.6	4081.5	2518.0	1505.6
4	3854.0	5217.7	5367.4	3268.4	1881.2
5	2438.1	2916.6	2970.6	1826.2	1088.7
6	1672.6	1620.5	1619.4	1002.3	620.3
7	2438.1	2916.6	2970.6	1826.2	1088.7
8	3854.0	5217.7	5367.4	3268.4	1881.2
9	3191.0	3987.6	4081.5	2518.0	1505.6
10	3191.4	4051.8	4153.3	2567.0	1539.4
11	3919.6	5475.8	5647.0	3443.5	1983.3
12	2289.1	2919.3	2992.1	1841.6	1093.4
13	836.3	810.2	809.7	501.2	310.1
14	168.9	-2.7	-21.5	-15.5	-4.7
15	-65.6	-258.1	-279.7	-175.2	-102.1
16	-.4	-64.2	-71.8	-49.1	-33.8

TIE NO.	TIE SEGMENT DEFLECTION ,IN. DIV 1	DIV 2	DIV 3	DIV 4	DIV 5
1	-.058122	-.071544	-.077242	-.074126	-.070702
2	-.055403	-.067591	-.073582	-.072346	-.070293
3	-.143238	-.155835	-.162250	-.161404	-.159577
4	-.132770	-.146856	-.153385	-.151181	-.148308
5	-.147989	-.158590	-.164462	-.164672	-.163762
6	-.248054	-.256913	-.262635	-.264396	-.264704
7	-.147989	-.158590	-.164462	-.164672	-.163762
8	-.132770	-.146856	-.153385	-.151181	-.148308
9	-.143238	-.155835	-.162250	-.161404	-.159577
10	-.055403	-.067591	-.073582	-.072346	-.070293
11	-.058122	-.071544	-.077242	-.074126	-.070702
12	-.093859	-.102691	-.107075	-.106260	-.104832
13	-.124027	-.128456	-.131318	-.132198	-.132352
14	-.054129	-.055899	-.057387	-.058412	-.058930
15	-.074648	-.075312	-.076143	-.077055	-.077607
16	-.087836	-.088244	-.088667	-.089058	-.089284

SOIL VERTICAL DISPLACEMENTS AND INCREMENTAL STRESSES

T = TIE NUMBER (1=CENTER TIE)
SEG = SEGMENT NUMBER
Z = DEPTH POINT NUMBER
XX = DIRECTION PARALLEL TO TIES
YY = DIRECTION PARALLEL TO RAILS
ZZ = VERTICAL DIRECTION
UNITS ARE INCHES AND PSI
COMPRESSION IS NEGATIVE FOR STRESSES
DOWNWARD IS POSITIVE FOR DEFLECTIONS

Z(1) = 1.00 IN.

Z(2) = 37.00 IN.

T	SEG	Z	W	THETA	S-XX	S-YY	S-ZZ	S-XY	S-XZ	S-YZ
1	1	1	.11170	-97.1	-29.4	-32.8	-34.9	-2.0	-.5	-.1
1	1	2	.09766	-12.6	-2.5	-2.3	-7.7	.5	-2.7	-1.3
1	2	1	.12495	-135.0	-41.5	-44.4	-49.1	-1.6	-.3	-.1
1	2	2	.10503	-14.4	-2.4	-2.7	-9.3	.4	-2.0	-1.5
1	3	1	.13064	-140.2	-43.3	-46.1	-50.8	-1.0	-.0	-.2
1	3	2	.11023	-15.5	-2.6	-2.9	-10.0	.3	-1.1	-1.6
1	4	1	.12779	-94.1	-29.3	-33.5	-31.3	-.5	.0	-.2
1	4	2	.11313	-16.1	-3.0	-3.0	-10.1	.2	-.4	-1.7
1	5	1	.12433	-62.5	-19.6	-24.6	-18.3	-.1	.0	-.2
1	5	2	.11432	-16.2	-3.3	-3.0	-10.0	.0	-.0	-1.7

T	SEG	I	W	THETA	S-XX	S-YY	S-ZZ	S-XY	S-XZ	S-YZ
2	1	1	.11533	-82.3	-26.2	-28.0	-28.1	-4.4	-.4	-.0
2	1	2	.10329	-13.8	-2.8	-2.6	-8.4	1.1	-3.0	-.3
2	2	1	.12743	-105.5	-34.5	-34.9	-36.0	-3.2	-.2	-.0
2	2	2	.11128	-15.7	-2.7	-3.0	-10.0	.9	-2.2	-.4
2	3	1	.13342	-109.5	-36.1	-36.3	-37.1	-1.6	-.1	-.0
2	3	2	.11695	-16.9	-2.9	-3.3	-10.8	.5	-1.2	-.4
2	4	1	.13238	-76.8	-25.8	-27.7	-23.3	-.5	.0	-.0
2	4	2	.12018	-17.6	-3.3	-3.3	-11.0	.2	-.5	-.4
2	5	1	.13045	-54.7	-18.6	-21.8	-14.3	-.0	.0	-.0
2	5	2	.12153	-17.8	-3.6	-3.4	-10.8	.0	-.0	-.5

T	SEG	Z	W	THETA	S-XX	S-YY	S-ZZ	S-XY	S-XZ	S-YZ
3	1	1	.13434	-81.7	-26.8	-26.8	-28.2	-5.1	-.4	.0
3	1	2	.12243	-14.9	-3.0	-3.3	-8.6	1.3	-3.1	-.0
3	2	1	.14687	-103.3	-34.7	-33.2	-35.4	-3.8	-.2	.0
3	2	2	.13103	-16.8	-2.9	-3.7	-10.2	1.0	-2.3	-.0
3	3	1	.15328	-106.9	-36.2	-34.4	-36.3	-2.1	-.0	.0
3	3	2	.13718	-18.2	-3.1	-4.0	-11.1	.6	-1.3	-.0
3	4	1	.15263	-74.6	-26.1	-25.8	-22.6	-.7	.0	.0
3	4	2	.14075	-18.8	-3.5	-4.2	-11.2	.3	-.5	-.0
3	5	1	.15093	-52.8	-19.1	-20.0	-13.7	-.1	.0	.0
3	5	2	.14228	-19.1	-3.8	-4.2	-11.1	.0	-.1	.0

T	SEG	Z	W	THETA	S-XX	S-YY	S-ZZ	S-XY	S-XZ	S-YZ
4	1	1	.14103	-94.9	-30.1	-30.9	-34.0	-3.3	-.5	.0
4	1	2	.12733	-14.8	-3.0	-3.4	-8.4	.9	-3.0	.5
4	2	1	.15497	-128.5	-41.1	-41.0	-46.3	-2.6	-.2	.1
4	2	2	.13589	-16.7	-2.9	-3.9	-10.0	.7	-2.2	.5
4	3	1	.16149	-133.0	-43.0	-42.5	-47.6	-1.8	-.0	.1
4	3	2	.14203	-18.0	-3.1	-4.2	-10.8	.5	-1.3	.6
4	4	1	.15955	-89.0	-29.7	-30.4	-28.9	-1.0	.0	.1
4	4	2	.14559	-18.7	-3.4	-4.3	-10.9	.3	-.5	.7
4	5	1	.15685	-58.8	-20.5	-21.8	-16.5	-.3	.0	.1
4	5	2	.14712	-18.9	-3.7	-4.4	-10.8	.0	-.1	.7

T	SEG	Z	W	THETA	S-XX	S-YY	S-ZZ	S-XY	S-XZ	S-YZ
5	1	1	.13293	-62.1	-21.6	-19.4	-21.1	-5.3	-.3	.0
5	1	2	.12390	-13.8	-2.8	-3.7	-7.4	1.4	-2.7	.8
5	2	1	.14350	-75.2	-27.0	-23.1	-25.1	-4.0	-.2	.0
5	2	2	.13183	-15.6	-2.7	-4.1	-8.7	1.1	-2.0	.9

5	3	1	.14939	-77.4	-28.3	-23.7	-25.4	-2.4	-.0	.0
5	3	2	.13761	-16.8	-2.9	-4.5	-9.4	.7	-1.2	1.0
5	4	1	.14974	-53.6	-21.0	-17.4	-15.2	-1.1	.0	.0
5	4	2	.14107	-17.4	-3.2	-4.7	-9.6	.4	-.5	1.0
5	5	1	.14892	-37.6	-15.9	-13.1	-8.6	-.3	.0	.0
5	5	2	.14261	-17.7	-3.4	-4.7	-9.5	.1	-.1	1.0

T	SEG	Z	W	THETA	S-XX	S-YY	S-ZZ	S-XY	S-XZ	S-YZ
6	1	1	.14002	-43.7	-17.3	-12.2	-14.3	-6.3	-.2	.0
6	1	2	.13376	-13.9	-2.8	-4.2	-6.9	1.6	-2.5	.0
6	2	1	.14891	-45.2	-19.4	-12.3	-13.5	-4.8	-.1	.0
6	2	2	.14163	-15.5	-2.7	-4.7	-8.0	1.3	-1.9	.0
6	3	1	.15465	-45.9	-20.4	-12.2	-13.3	-2.9	-.0	.0
6	3	2	.14745	-16.7	-2.8	-5.1	-8.7	.8	-1.2	.0
6	4	1	.15649	-33.2	-16.5	-9.0	-7.8	-1.3	-.0	.0
6	4	2	.15104	-17.3	-3.1	-5.3	-8.9	.4	-.5	.0
6	5	1	.15685	-25.1	-13.7	-6.9	-4.5	-.3	.0	.0
6	5	2	.15270	-17.6	-3.3	-5.4	-8.9	.1	-.1	.0

T	SEG	Z	W	THETA	S-XX	S-YY	S-ZZ	S-XY	S-XZ	S-YZ
7	1	1	.13293	-62.1	-21.6	-19.4	-21.1	-5.3	-.3	-.0
7	1	2	.12390	-13.8	-2.8	-3.7	-7.4	1.4	-2.7	-.8
7	2	1	.14350	-75.2	-27.0	-23.1	-25.1	-4.0	-.2	-.0
7	2	2	.13183	-15.6	-2.7	-4.1	-8.7	1.1	-2.0	-.9
7	3	1	.14939	-77.4	-28.3	-23.7	-25.4	-2.4	-.0	-.0
7	3	2	.13761	-16.8	-2.9	-4.5	-9.4	.7	-1.2	-1.0
7	4	1	.14974	-53.6	-21.0	-17.4	-15.2	-1.1	.0	-.0
7	4	2	.14107	-17.4	-3.2	-4.7	-9.6	.4	-.5	-1.0

7	5	1	.14892	-37.6	-15.9	-13.1	-8.6	-.3	.0	-.0
7	5	2	.14261	-17.7	-3.4	-4.7	-9.5	.1	-.1	-1.0

T	SEG	Z	W	THETA	S-XX	S-YY	S-ZZ	S-XY	S-XZ	S-YZ
8	1	1	.14103	-94.9	-30.1	-30.9	-34.0	-3.3	-.5	-.0
8	1	2	.12733	-14.8	-3.0	-3.4	-8.4	.9	-3.0	-.5
8	2	1	.15497	-128.5	-41.1	-41.0	-46.3	-2.6	-.2	-.1
8	2	2	.13589	-16.7	-2.9	-3.9	-10.0	.7	-2.2	-.6
8	3	1	.16149	-133.0	-43.0	-42.5	-47.6	-1.8	-.0	-.1
8	3	2	.14203	-18.0	-3.1	-4.2	-10.9	.5	-1.3	-.6
8	4	1	.15955	-89.0	-29.7	-30.4	-28.9	-1.0	.0	-.1
8	4	2	.14559	-18.7	-3.4	-4.3	-10.9	.3	-.5	-.7
8	5	1	.15685	-58.8	-20.5	-21.8	-16.5	-.3	.0	-.1
8	5	2	.14712	-18.9	-3.7	-4.4	-10.8	.0	-.1	-.7

T	SEG	Z	W	THETA	S-XX	S-YY	S-ZZ	S-XY	S-XZ	S-YZ
9	1	1	.13434	-81.7	-26.8	-26.8	-28.2	-5.1	-.4	-.0
9	1	2	.12243	-14.9	-3.0	-3.3	-8.6	1.3	-3.1	.0
9	2	1	.14687	-103.3	-34.7	-33.2	-35.4	-3.8	-.2	-.0
9	2	2	.13103	-16.8	-2.9	-3.7	-10.2	1.0	-2.3	.0
9	3	1	.15328	-106.9	-36.2	-34.4	-36.3	-2.1	-.0	-.0
9	3	2	.13718	-18.2	-3.1	-4.0	-11.1	.6	-1.3	.0
9	4	1	.15263	-74.6	-26.1	-25.8	-22.6	-.7	.0	-.0
9	4	2	.14075	-18.8	-3.5	-4.2	-11.2	.3	-.5	.0
9	5	1	.15093	-52.8	-19.1	-20.0	-13.7	-.1	.0	-.0
9	5	2	.14228	-19.1	-3.8	-4.2	-11.1	.0	-.1	.0

T	SEG	Z	W	THETA	S-XX	S-YY	S-ZZ	S-XY	S-XZ	S-YZ
10	1	1	.11533	-82.3	-16.2	-28.0	-28.1	-4.4	-.4	.3
10	1	2	.10329	-13.8	-2.3	-3.6	-8.4	1.1	-3.3	.3
10	2	1	.12743	-105.5	-34.5	-34.9	-36.0	-3.2	-.2	.0
10	2	2	.11129	-15.7	-2.7	-3.9	-10.1	.3	-2.2	.4
10	3	1	.12342	-109.5	-36.1	-36.3	-37.1	-1.6	-.1	.0
10	3	2	.11695	-16.9	-2.9	-3.8	-10.3	.5	-1.2	.4
10	4	1	.13209	-76.9	-25.6	-27.7	-23.3	-.5	.0	.1
10	4	2	.12018	-17.5	-3.3	-3.8	-11.0	.2	-.5	.4
10	5	1	.13045	-54.7	-19.6	-21.9	-14.3	-.0	.0	.0
10	5	2	.12153	-17.5	-3.6	-3.4	-11.6	.0	-.3	.5

T	SEG	Z	W	THETA	S-XX	S-YY	S-ZZ	S-XY	S-XZ	S-YZ
11	1	1	.11170	-97.1	-29.4	-32.8	-34.9	-2.0	-.5	.1
11	1	2	.09765	-12.6	-2.5	-2.8	-7.7	.5	-2.7	1.2
11	2	1	.12495	-105.8	-41.5	-44.4	-49.1	-1.5	-.3	.1
11	2	2	.10503	-14.4	-2.4	-2.7	-9.3	.4	-2.3	1.5
11	3	1	.12064	-140.2	-43.3	-46.1	-50.8	-1.3	-.0	.2
11	3	2	.11023	-15.5	-2.6	-2.9	-10.3	.3	-1.1	1.6
11	4	1	.12779	-94.1	-29.3	-33.5	-31.3	-.5	.0	.2
11	4	2	.11513	-16.1	-3.0	-3.0	-10.1	.2	-.4	1.7
11	5	1	.12455	-62.5	-19.6	-24.6	-18.3	-.1	.0	.1
11	5	2	.11482	-16.2	-3.3	-3.3	-10.3	.0	-.3	1.7

T	SEG	Z	W	THETA	S-XX	S-YY	S-ZZ	S-XY	S-XZ	S-YZ
12	1	1	.09366	-57.7	-16.8	-18.9	-19.1	-3.3	-.3	.2
12	1	2	.08522	-10.1	-2.0	-2.3	-5.8	.3	-2.1	2.3

12	2	1	.10243	-74.2	-24.7	-23.8	-25.6	-2.5	-.2	.2
12	2	2	.09107	-11.4	-2.0	-2.6	-6.9	.6	-1.5	2.4
12	3	1	.10681	-76.8	-25.7	-24.6	-26.5	-1.4	-.0	.2
12	3	2	.09526	-12.3	-2.1	-2.9	-7.5	.4	-.3	2.6
12	4	1	.10614	-52.8	-18.3	-18.2	-16.3	-.5	.0	.3
12	4	2	.09768	-12.8	-2.3	-2.9	-7.6	.2	-.3	2.7
12	5	1	.10481	-36.6	-13.2	-13.8	-9.6	-.1	.0	.3
12	5	2	.09872	-12.9	-2.6	-2.9	-7.5	.0	-.0	2.7

T	SEG	Z	W	THETA	S-XX	S-YY	S-ZZ	S-XY	S-XZ	S-YZ
13	1	1	.07001	-21.9	-8.6	-6.1	-7.1	-3.1	-.1	.1
13	1	2	.06688	-6.9	-1.4	-2.1	-3.4	.8	-1.3	2.0
13	2	1	.07446	-22.6	-9.7	-6.1	-6.8	-2.4	-.0	.2
13	2	2	.07082	-7.8	-1.4	-2.4	-4.0	.5	-1.0	2.3
13	3	1	.07733	-23.0	-10.2	-6.1	-6.6	-1.5	-.0	.2
13	3	2	.07372	-8.3	-1.4	-2.6	-4.2	.4	-.5	2.5
13	4	1	.07825	-16.6	-8.2	-4.5	-3.9	-.7	.0	.2
13	4	2	.07552	-8.7	-1.6	-2.7	-4.4	.2	-.3	2.6
13	5	1	.07842	-12.6	-6.9	-3.4	-2.3	-.2	.0	.2
13	5	2	.07635	-8.8	-1.7	-2.7	-4.4	.0	-.0	2.6

T	SEG	Z	W	THETA	S-XX	S-YY	S-ZZ	S-XY	S-XZ	S-YZ
14	1	1	.03928	-4.3	-2.9	-.5	-1.0	-2.0	-.0	.1
14	1	2	.03868	-3.7	-.8	-1.4	-1.6	.5	-.6	1.3
14	2	1	.04108	-1.0	-2.4	.6	.7	-1.6	-.0	.1
14	2	2	.04076	-4.2	-.7	-1.6	-1.8	.4	-.5	1.5
14	3	1	.04257	-.6	-2.5	.9	1.1	-1.0	-.0	.2
14	3	2	.04235	-4.4	-.8	-1.7	-2.0	.3	-.3	1.6
14	4	1	.04360	-.8	-2.7	.8	1.1	-.5	.0	.2
14	4	2	.04339	-4.6	-.8	-1.8	-2.0	.2	-.2	1.7

14	5	1	.04412	-1.1	-2.7	.7	1.0	-.1	.0	.2
14	5	2	.04390	-4.7	-.8	-1.8	-2.1	.0	-.0	1.7

T	SEG	Z	W	THETA	S-XX	S-YY	S-ZZ	S-XY	S-XZ	S-YZ
15	1	1	.02933	2.1	-.6	1.9	.9	-1.3	.0	.0
15	1	2	.02967	-2.2	-.4	-1.1	-.7	.3	-.3	.8
15	2	1	.03002	6.5	.3	3.3	2.8	-1.1	.0	.0
15	2	2	.03086	-2.4	-.4	-1.2	-.7	.3	-.2	.9
15	3	1	.03086	7.2	.3	3.7	3.2	-.8	.0	.0
15	3	2	.03180	-2.5	-.4	-1.3	-.8	.2	-.2	1.0
15	4	1	.03176	5.2	-.4	3.2	2.4	-.5	.0	.0
15	4	2	.03246	-2.6	-.4	-1.4	-.8	.1	-.1	1.0
15	5	1	.03230	3.6	-.9	2.8	1.8	-.1	.0	.0
15	5	2	.03279	-2.7	-.4	-1.4	-.8	.0	-.0	1.0

T	SEG	Z	W	THETA	S-XX	S-YY	S-ZZ	S-XY	S-XZ	S-YZ
16	1	1	.01901	.5	-.5	1.1	-.0	-.7	.0	-.0
16	1	2	.01915	-1.1	-.2	-.6	-.2	.2	-.0	.4
16	2	1	.01943	2.1	-.2	1.7	.6	-.6	.0	.0
16	2	2	.01975	-1.2	-.2	-.7	-.2	.1	-.0	.4
16	3	1	.01986	2.5	-.2	1.9	.8	-.5	.0	-.0
16	3	2	.02023	-1.2	-.2	-.8	-.2	.1	-.0	.4
16	4	1	.02025	2.2	-.4	1.9	.7	-.3	.0	-.0
16	4	2	.02057	-1.3	-.2	-.8	-.3	.0	-.0	.5
16	5	1	.02047	1.9	-.5	1.9	.6	-.1	.0	-.0
16	5	2	.02074	-1.3	-.2	-.8	-.3	.0	-.0	.5

LATERAL OFFSET FROM TRACK CENTERLINE = 52.0 IN. = 4.33 FT
INCREMENTAL SOIL DEFLECTIONS AND STRESSES

DEPTH IN.	W IN.	S-XX PSI	S-YY PSI	S-ZZ PSI	S-XY PSI	S-XZ PSI	S-YZ PSI
6.0	.06116	-9.2	-6.9	-11.2	.0	9.3	.0
18.0	.05910	-3.6	-1.8	-7.6	.0	6.9	.0
30.0	.05692	.2	3.1	-3.8	.0	4.5	.0
54.0	.04890	-1.2	-.4	-4.1	.0	1.6	.0
120.0	.03227	-.2	-.0	-1.9	.0	.6	.0

LATERAL OFFSET FROM TRACK CENTERLINE = 78.0 IN. = 6.50 FT
INCREMENTAL SOIL DEFLECTIONS AND STRESSES

DEPTH IN.	W IN.	S-XX PSI	S-YY PSI	S-ZZ PSI	S-XY PSI	S-XZ PSI	S-YZ PSI
6.0	.04039	-.0	-2.8	-.0	.0	.8	.0
18.0	.04057	-1.8	-.9	-.8	.0	2.2	.0
30.0	.04036	-2.5	1.1	-1.7	.0	2.1	.0
54.0	.03794	-1.3	-.3	-2.0	.0	1.4	.0
120.0	.02854	-.3	.0	-1.4	.0	.7	.0

LATERAL OFFSET FROM TRACK CENTERLINE = 104.0 IN. = 8.67 FT
INCREMENTAL SOIL DEFLECTIONS AND STRESSES

DEPTH IN.	W IN.	S-XX PSI	S-YY PSI	S-ZZ PSI	S-XY PSI	S-XZ PSI	S-YZ PSI
6.0	.02939	1.1	-1.4	-.1	.0	.2	.0
18.0	.02942	-.7	-.5	-.3	.0	.6	.0
30.0	.02944	-2.1	.2	-.6	.0	.7	.0
54.0	.02903	-1.1	-.2	-.9	.0	.9	.0
120.0	.02466	-.4	.0	-.9	.0	.6	.0

LATERAL OFFSET FROM TRACK CENTERLINE = 130.0 IN. = 10.83 FT
INCREMENTAL SOIL DEFLECTIONS AND STRESSES

DEPTH IN.	W IN.	S-XX PSI	S-YY PSI	S-ZZ PSI	S-XY PSI	S-XZ PSI	S-YZ PSI
6.0	.02257	1.1	-.7	-.2	.0	.0	.0
18.0	.02256	-.2	-.4	-.0	.0	.1	.0
30.0	.02262	-1.4	-.0	-.2	.0	.3	.0
54.0	.02275	-.7	-.0	-.4	.0	.5	.0
120.0	.02107	-.4	.0	-.6	.0	.5	.0

LATERAL OFFSET FROM TRACK CENTERLINE = 156.0 IN. = 13.00 FT
INCREMENTAL SOIL DEFLECTIONS AND STRESSES

DEPTH IN.	W IN.	S-XX PSI	S-YY PSI	S-ZZ PSI	S-XY PSI	S-XZ PSI	S-YZ PSI
6.0	.01819	.9	-.5	-.4	.0	-.0	.0
18.0	.01815	-.0	-.3	-.0	.0	.0	.0
30.0	.01821	-.8	-.1	-.0	.0	.0	.0
54.0	.01845	-.5	-.0	-.1	.0	.3	.0
120.0	.01802	-.4	.0	-.4	.0	.4	.0

LATERAL OFFSET FROM TRACK CENTERLINE = 208.0 IN. = 17.33 FT
INCREMENTAL SOIL DEFLECTIONS AND STRESSES

DEPTH IN.	W IN.	S-XX PSI	S-YY PSI	S-ZZ PSI	S-XY PSI	S-XZ PSI	S-YZ PSI
6.0	.01316	.5	-.2	-.5	.0	-.0	.0
18.0	.01309	.0	-.2	-.0	.0	-.0	.0
30.0	.01312	-.3	-.1	.0	.0	.0	.0
54.0	.01328	-.2	-.0	-.0	.0	.0	.0
120.0	.01355	-.3	.0	-.1	.0	.2	.0

FILENAME E103ST36 OFFSET 0.

TIE LENGTH ..... 102.0 IN.
NUMBER OF SEGMENTS PER TIE 10
NUMBER OF SEGMENTS BETWEEN RAILS .. 6
TIE SPACING ..... 20.0 IN.
TIE WIDTH ..... 9.0 IN.
TIE AREA ..... 83.0 SQ.IN.
TIE WEIGHT ..... 250.0 LBS
TIE EI ..... .832965E+09 LB-SQ.IN.
RAIL SPACING ..... 59.25 IN.
RAIL AREA ..... 13.35 SQ.IN.
RAIL WEIGHT ..... 115.0 LBS PER YARD
RAIL EI ..... .23470E+10 LB-SQ.IN.
RAIL FASTENER STIFFNESS ..... 7000000.0 LBS PER IN.
NUMBER OF AXLE LOADS 4
AXLE LOADS ARE ON TIE NUMBER(S) ... 1 4 8 11
WHEEL LOAD PER AXLE (KIPS) 49.40 49.40 49.40 49.40
NUMBER OF SOIL LAYERS 5
SOLVE FOR FULL TRACK RESPONSE 1
NUMBER OF ITERATIONS 0
CALCULATE AT OTHER DEPTH POINTS ... 1
CALCULATE AT OFFSET LOCATIONS 1
LIMIT TIE/BALLAST TENSION 0
FIRST TIE OUTPUT 1
LAST TIE OUTPUT 16
[illegible] TIE SEGMENT OUTPUT 1
[illegible] TIE SEGMENT OUTPUT 5
PRINT STANDARD SOIL OUTPUT 1
PRINT PRINCIPAL STRESSES 0
PRINT EQUIVALENT TRIAXIAL DATA 0

LAYER	MODULUS (PSI)	VRAT	DEPTH (IN.)	GAMMA (PCF)	KNOT
1	35000.	.30	12.00	125.0	1.00
2	35000.	.30	12.00	125.0	1.00
3	35000.	.30	12.00	125.0	1.00
4	10000.	.40	36.00	125.0	.75
5	10000.	.40	.00	125.0	.75

LAYER	KTYPE	MODULUS DESCRIPTION
1	1	LOG E - LOG BULK STRESS K1 = 1058.00 K2 = .593
2	1	LOG E - LOG BULK STRESS K1 = 941.00 K2 = .687
3	1	LOG E - LOG BULK STRESS K1 = 941.00 K2 = .687
4	1	LOG E - LOG BULK STRESS K1 = 877.00 K2 = 1.100
5	1	LOG E - LOG BULK STRESS K1 = 877.00 K2 = 1.100

DIFFERENT DEPTHS AT WHICH MODULI ARE COMPUTED

Z(1) = 6.00 IN.

Z(2) = 18.00 IN.

Z(3) = 30.00 IN.

Z(4) = 54.00 IN.

Z(5) = 120.00 IN.

CALC. STEP NO. 1

DEFLECTIONS AND REACTIONS
NEGATIVE DEFLECTION IS DOWNWARD
NEGATIVE REACTION IS TENSION

---- SINGLE AXLE ----

TIE NO.	DEFLECTION RAIL IN.	REACTION RAIL SEAT LBS	DEFLECTION TIE IN.
1	-.091398	20344.5	-.088492
2	-.077485	12015.1	-.075759
3	-.057334	3486.7	-.056836
4	-.041996	124.7	-.041979
5	-.030307	-860.5	-.030433
6	-.019646	-219.3	-.019677

TIE NO.	TIE CENTER BENDING MOMENT (IN.-LBS)	TIE RAIL-SEAT BENDING MOMENT (IN.-LBS)
1	-.27364E+05	.94323E+05
2	-.14080E+05	.57626E+05
3	-.10234E+04	.18929E+05
4	.31582E+04	.27332E+04
5	.35304E+04	-.26352E+04
6	.14311E+04	-.39672E+03

TIE NO.	TIE/SOIL REACTIONS, LBS DIV 1	DIV 2	DIV 3	DIV 4	DIV 5
1	3750.6	5478.5	5669.5	3459.0	1989.0
2	2354.7	3177.4	3271.8	2016.8	1135.5
3	836.7	874.4	861.5	550.2	343.9
4	168.9	-2.7	-21.5	-15.5	-4.7
5	-65.6	-258.1	-279.7	-175.2	-102.1
6	-.4	-64.2	-71.6	-49.1	-33.8

TIE NO.	TIE SEGMENT DEFLECTION ,IN. DIV 1	DIV 2	DIV 3	DIV 4	DIV 5
1	-.072807	-.084460	-.088570	-.084529	-.080587
2	-.064547	-.072715	-.076266	-.074542	-.072561
3	-.051049	-.055069	-.057505	-.057998	-.057925
4	-.039272	-.041041	-.042530	-.043555	-.044072
5	-.029312	-.029976	-.030806	-.031719	-.032270
6	-.019021	-.019429	-.019853	-.020243	-.020469

PEAK RAIL BENDING MOMENT= .29490E+06 IN.-LBS

TRACK MODULUS U = 7.756 KIPS/IN./IN. = 53.539 MN/M/M

SUPERIMPOSED RESULTS FROM CALC. STEP NO. 1

----- DEFLECTIONS AND REACTIONS ----

TIE NO.	DEFLECTION RAIL IN.	REACTION RAIL SEAT LBS	DEFLECTION IN.
1	-.133394	20469.2	-.130471
2	-.134819	15502.9	-.132605
3	-.154465	15283.6	-.152282
4	-.163701	19588.7	-.160903
5	-.149788	11260.2	-.148180
6	-.153959	6535.0	-.153026
7	-.149786	11260.2	-.148180
8	-.163701	19588.7	-.160903
9	-.154465	15283.6	-.152282
10	-.134819	15502.9	-.132605
11	-.133394	20469.2	-.130471
12	-.107792	11135.9	-.106201
13	-.076979	3267.5	-.076513
14	-.041996	124.7	-.041979
15	-.030307	-880.5	-.030433
16	-.019546	-219.2	-.019677

TIE NO.	TIE CENTER BENDING MOMENT (IN.-LBS)	TIE RAIL-SEAT BENDING MOMENT (IN.-LBS)	RAIL BENDING MOMENT (IN.-LBS)
1	-.24206E+05	.97057E+05	.26852E+06
2	-.15103E+05	.76555E+05	-.41535E+05
3	-.13672E+05	.76159E+05	-.41536E+05
4	-.20676E+05	.94421E+05	.25414E+06
5	-.73913E+04	.57724E+05	-.26419E+05
6	.81548E+03	.37065E+05	-.91768E+05
7	-.73913E+04	.57724E+05	-.26418E+05
8	-.20676E+05	.94421E+05	.26414E+06

9	-.13672E+05	.75158E+05	-.41536E+05
10	-.15103E+05	.76555E+05	-.41536E+05
11	-.24205E+05	.97057E+05	.26852E+06
12	-.10549E+05	.54990E+05	-.37082E+02
13	.40774E+03	.18533E+05	-.45884E+05
14	.31582E+04	.27832E+04	-.26381E+05
15	.35304E+04	-.26352E+04	-.43851E+04
16	.14311E+04	-.39672E+03	.00000E+00

TIE	TIE/SOIL REACTIONS, LBS				
NO.	DIV 1	DIV 2	DIV 3	DIV 4	DIV 5
1	3919.6	5475.8	5647.0	3443.5	1983.3
2	3191.4	4051.9	4153.3	2567.0	1539.4
3	3191.0	3987.6	4081.5	2518.0	1505.6
4	3854.0	5217.7	5367.4	3268.4	1881.2
5	2458.1	2916.6	2970.6	1826.2	1088.7
6	1672.6	1620.5	1619.4	1002.3	620.3
7	2458.1	2916.6	2970.6	1826.2	1088.7
8	3854.0	5217.7	5367.4	3268.4	1881.2
9	3191.0	3987.6	4081.5	2518.0	1505.6
10	3191.4	4051.9	4153.3	2567.0	1539.4
11	3919.6	5475.8	5647.0	3443.5	1983.3
12	2285.1	2919.3	2992.1	1841.6	1058.4
13	836.3	810.2	809.7	501.2	310.1
14	168.9	-2.7	-21.5	-15.5	-4.7
15	-55.6	-258.1	-273.7	-175.2	-102.1
16	-.4	-64.2	-71.8	-49.1	-33.8

TIE	TIE SEGMENT DEFLECTION ,IN.				
NO.	DIV 1	DIV 2	DIV 3	DIV 4	DIV 5
1	-.112079	-.125501	-.131200	-.126084	-.124659
2	-.115596	-.127784	-.133776	-.132539	-.130487
3	-.134617	-.147214	-.153629	-.152783	-.150956
4	-.141391	-.155477	-.162006	-.159802	-.156929
5	-.133131	-.143732	-.149605	-.149815	-.148904
6	-.140139	-.148998	-.154720	-.156482	-.156789
7	-.133131	-.143732	-.149605	-.149815	-.148904
8	-.141391	-.155477	-.162006	-.159802	-.156929
9	-.134617	-.147214	-.153629	-.152783	-.150956
10	-.115596	-.127784	-.133776	-.132539	-.130487
11	-.112079	-.125501	-.131200	-.126084	-.124659
12	-.092859	-.102591	-.107075	-.106260	-.104832
13	-.070070	-.074499	-.077360	-.078241	-.078395
14	-.039272	-.041041	-.042530	-.043555	-.044072
15	-.029312	-.029976	-.030806	-.031719	-.032270
16	-.019021	-.019429	-.019653	-.020243	-.020469

SOIL VERTICAL DISPLACEMENTS AND INCREMENTAL STRESSES

T = TIE NUMBER (1=CENTER TIE)
SEG = SEGMENT NUMBER
Z = DEPTH POINT NUMBER
XX = DIRECTION PARALLEL TO TIES
YY = DIRECTION PARALLEL TO RAILS
ZZ = VERTICAL DIRECTION
UNITS ARE INCHES AND PSI
COMPRESSION IS NEGATIVE FOR STRESSES
DOWNWARD IS POSITIVE FOR DEFLECTIONS

Z(1) = 6.00 IN.

Z(2) = 18.00 IN.

Z(3) = 30.00 IN.

Z(4) = 54.00 IN.

Z(5) = 120.00 IN.

T	SEG	Z	W	THETA	S-XX	S-YY	S-ZZ	S-XY	S-XZ	S-YZ
1	1	1	.10829	-80.0	-13.2	-9.7	-29.2	-1.1	-6.9	-.7
1	1	2	.10337	-20.5	-4.1	-3.7	-12.8	.3	-7.3	-1.9
1	1	3	.09998	-5.5	1.4	1.9	-6.8	1.4	-4.9	-1.7
1	1	4	.08846	-9.5	-1.7	-1.4	-6.3	.4	-2.2	-1.2
1	1	5	.06181	-4.0	-.4	-.3	-3.4	.2	-.9	-.6
1	2	1	.12005	-72.5	-18.7	-11.9	-41.9	-1.0	-2.9	-.9
1	2	2	.11264	-25.2	-4.0	-4.3	-17.9	.2	-4.1	-2.3
1	2	3	.10799	-5.4	3.1	2.5	-11.0	1.1	-3.2	-2.1
1	2	4	.09387	-10.5	-1.6	-1.6	-7.3	.4	-1.7	-1.4
1	2	5	.06375	-4.2	-.3	-.3	-3.6	.1	-.7	-.6
1	3	1	.12563	-74.8	-19.5	-12.6	-42.6	-.7	1.4	-1.0
1	3	2	.11826	-27.6	-4.7	-4.5	-18.3	.0	-.0	-2.5
1	3	3	.11342	-5.6	3.4	2.7	-11.6	.7	-1.0	-2.3
1	3	4	.09800	-11.3	-1.6	-1.7	-7.9	.3	-1.2	-1.5
1	3	5	.06521	-4.4	-.2	-.3	-3.8	.0	-.5	-.7
1	4	1	.12506	-57.5	-18.2	-11.7	-27.6	-.5	3.4	-1.0
1	4	2	.12037	-25.3	-6.1	-4.4	-14.9	-.0	2.0	-2.5
1	4	3	.11523	-5.9	2.6	2.8	-11.2	.4	.4	-2.3
1	4	4	.10064	-11.7	-1.6	-1.8	-8.3	.2	-.7	-1.5
1	4	5	.06616	-4.4	-.2	-.3	-4.0	.0	-.3	-.7

1	5	1	.12331	-43.6	-15.0	-10.8	-16.8	-.2	1.5	-.9
1	5	2	.12070	-22.8	-7.0	-4.2	-11.6	-.0	1.1	-2.4
1	5	3	.11726	-6.2	1.6	2.9	-10.6	.1	.3	-2.3
1	5	4	.10192	-11.9	-1.7	-1.8	-8.4	.0	-.2	-1.6
1	5	5	.06663	-4.5	-.2	-.3	-4.0	.3	-.1	-.7

T	SEG	I	A	THETA	S-XX	S-YY	S-ZZ	S-XY	S-XZ	S-YZ
2	1	1	.11874	-46.5	-12.2	-10.7	-23.6	-1.8	-5.7	.0
2	1	2	.10898	-20.6	-4.1	-5.0	-11.5	1.5	-7.2	-.0
2	1	3	.10575	-5.8	1.6	1.8	-9.2	3.1	-5.2	-.3
2	1	4	.09317	-10.3	-1.5	-1.5	-7.0	.8	-2.4	-.4
2	1	5	.06371	-4.2	-.4	-.2	-3.6	.2	-1.0	-.2
2	2	1	.12410	-61.6	-17.1	-13.0	-31.4	-1.5	-2.3	.0
2	2	2	.11873	-25.9	-4.0	-5.1	-15.8	.5	-4.1	.0
2	2	3	.11439	-5.7	3.4	2.2	-11.3	2.3	-3.4	-.2
2	2	4	.09904	-11.4	-1.7	-1.6	-9.0	.6	-1.9	-.5
2	2	5	.06573	-4.4	-.3	-.2	-3.9	.2	-.8	-.2
2	3	1	.13006	-63.4	-17.9	-13.8	-31.7	-1.3	.9	.0
2	3	2	.12463	-27.2	-4.7	-5.4	-16.1	.0	-.4	.0
2	3	3	.12032	-5.9	3.8	2.5	-12.1	1.3	-1.1	-.3
2	3	4	.10354	-12.2	-1.7	-1.8	-8.8	.4	-1.3	-.5
2	3	5	.06728	-4.6	-.2	-.2	-4.1	.1	-.6	-.2
2	4	1	.13065	-50.8	-17.3	-12.9	-20.3	-.9	2.5	-.0
2	4	2	.12741	-25.4	-5.1	-6.0	-13.3	-.5	1.6	-.0
2	4	3	.12347	-6.2	2.9	2.5	-11.7	.5	.2	-.3
2	4	4	.10645	-12.8	-1.8	-1.8	-9.2	.3	-.7	-.5
2	4	5	.06831	-4.7	-.2	-.2	-4.2	.0	-.4	-.2
2	5	1	.12978	-40.6	-15.4	-12.1	-13.2	-.3	1.1	-.0
2	5	2	.12804	-23.3	-7.0	-5.6	-10.7	-.3	.9	-.2
2	5	3	.12483	-6.5	1.9	2.6	-11.1	.1	.3	-.4
2	5	4	.10785	-13.0	-1.9	-1.9	-9.3	.0	-.2	-.5
2	5	5	.06882	-4.7	-.2	-.2	-4.3	.0	-.1	-.2

T	SEG	I	A	THETA	S-XX	S-YY	S-ZZ	S-XY	S-XZ	S-YZ
3	1	1	.13172	-46.1	-12.5	-10.0	-23.6	-2.2	-5.6	-.0
3	1	2	.12796	-21.2	-4.3	-5.2	-11.5	1.5	-7.1	-.1
3	1	3	.12483	-7.4	1.4	.5	-9.3	3.5	-5.2	-.0
3	1	4	.11237	-11.5	-2.0	-2.1	-7.4	1.0	-2.5	-.0
3	1	5	.08081	-5.1	-.5	-.4	-4.2	.3	-1.1	-.2

3	2	1	.14357	-60.6	-17.5	-12.1	-31.0	-2.0	-2.2	-.0
3	2	2	.13830	-25.4	-4.3	-6.4	-15.7	.8	-4.0	-.2
3	2	3	.13406	-7.4	3.3	.8	-11.5	2.7	-3.4	-.0
3	2	4	.11985	-12.7	-1.9	-2.3	-8.5	.2	-2.1	-.0
3	2	5	.08221	-5.3	-.4	-.5	-4.5	.2	-.9	-.2
3	3	1	.14997	-62.3	-18.4	-12.8	-31.1	-1.5	.9	-.0
3	3	2	.14485	-27.7	-5.1	-6.7	-15.9	-.0	-.4	-.2
3	3	3	.14046	-7.7	3.6	.9	-12.2	1.6	-1.2	-.0
3	3	4	.12383	-13.6	-1.9	-2.5	-9.2	.6	-1.4	-.0
3	3	5	.08506	-5.5	-.3	-.5	-4.8	.2	-.7	-.2
3	4	1	.15093	-49.9	-17.5	-11.9	-20.5	-1.1	2.4	-.0
3	4	2	.14777	-26.0	-6.4	-8.4	-13.2	-.5	1.5	-.0
3	4	3	.14396	-8.1	2.8	1.0	-11.9	.7	.2	.0
3	4	4	.12707	-14.1	-1.9	-2.6	-9.6	.3	-.8	-.0
3	4	5	.08530	-5.7	-.2	-.5	-4.9	.1	-.4	-.2
3	5	1	.15026	-39.9	-15.9	-11.0	-12.9	-.4	1.1	.0
3	5	2	.14859	-23.9	-7.3	-5.9	-10.7	-.3	.9	.0
3	5	3	.14534	-8.4	1.9	1.0	-11.3	.2	.3	.0
3	5	4	.12865	-14.4	-2.0	-2.6	-9.8	.1	-.3	-.0
3	5	5	.08691	-5.7	-.2	-.5	-5.0	.0	-.1	-.2

T	SEG	Z	W	THETA	S-XX	S-YY	S-ZZ	S-XY	S-XZ	S-YZ
4	1	1	.13768	-51.4	-13.6	-9.1	-28.6	-2.0	-6.6	.5
4	1	2	.13293	-21.8	-4.5	-4.5	-12.8	.4	-7.3	1.1
4	1	3	.12963	-8.1	1.2	.0	-9.3	2.3	-5.1	.9
4	1	4	.11776	-11.5	-2.1	-2.4	-7.2	.8	-2.5	.3
4	1	5	.08646	-5.4	-.5	-.5	-4.4	.3	-1.2	.0
4	2	1	.15025	-70.5	-19.4	-11.1	-40.0	-1.7	-2.7	.6
4	2	2	.14334	-27.4	-4.5	-5.2	-17.7	.2	-4.1	1.5
4	2	3	.13882	-8.2	3.0	.3	-11.5	1.8	-3.3	1.1
4	2	4	.12430	-12.8	-1.9	-2.6	-8.3	.7	-2.0	.4
4	2	5	.08900	-5.7	-.4	-.6	-4.7	.2	-1.0	.0
4	3	1	.15681	-72.5	-20.3	-11.7	-40.6	-1.3	1.4	.6
4	3	2	.14988	-29.8	-5.3	-5.5	-18.0	.0	-.2	1.6
4	3	3	.14520	-8.5	3.4	.4	-12.3	1.2	-1.1	1.2
4	3	4	.12932	-13.7	-1.9	-2.8	-9.0	.5	-1.4	.4
4	3	5	.09094	-5.9	-.3	-.6	-4.9	.2	-.7	.0
4	4	1	.15704	-56.1	-19.1	-10.7	-26.3	-.8	3.2	.6
4	4	2	.15267	-26.6	-6.6	-5.3	-14.6	-.0	1.8	1.5
4	4	3	.14867	-8.9	2.5	.4	-11.8	.7	.3	1.2
4	4	4	.13258	-14.3	-1.9	-2.9	-9.4	.3	-.8	.4
4	4	5	.09222	-6.0	-.2	-.6	-5.1	.1	-.5	.0

4	5	1	.15575	-42.9	-17.0	-9.5	-16.0	-.3	1.4	.6
4	5	2	.15038	-24.3	-7.6	-5.1	-11.6	-.0	1.0	1.4
4	5	3	.15004	-9.2	1.7	.3	-11.1	.2	-.3	1.2
4	5	4	.13417	-14.5	-2.0	-3.0	-9.5	.0	-.3	.5
4	5	5	.09286	-6.0	-.2	-.5	-5.2	.0	-.2	.0

T	SEG	Z	W	THETA	S-XX	S-YY	S-ZZ	S-XY	S-XZ	S-YZ
5	1	1	.13095	-35.9	-10.4	-7.2	-18.1	-2.7	-4.2	.9
5	1	2	.12815	-17.9	-3.8	-4.9	-9.1	1.2	-5.5	2.0
5	1	3	.12577	-8.4	.9	-1.5	-7.8	3.6	-4.2	1.5
5	1	4	.11580	-11.2	-2.0	-2.5	-6.7	1.1	-2.4	.6
5	1	5	.08592	-5.3	-.5	-.5	-4.3	.4	-1.2	.2
5	2	1	.14117	-45.9	-14.5	-8.7	-22.8	-2.3	-1.6	1.1
5	2	2	.13737	-21.9	-3.9	-5.9	-12.1	.7	-3.1	2.7
5	2	3	.13419	-8.6	2.4	-1.5	-9.5	2.8	-2.6	1.9
5	2	4	.12181	-12.3	-1.8	-2.8	-7.6	.9	-1.9	.6
5	2	5	.08840	-5.6	-.4	-.6	-4.6	.3	-1.0	.3
5	3	1	.14707	-47.0	-15.2	-9.1	-22.7	-1.8	.5	1.2
5	3	2	.14344	-22.9	-4.5	-6.2	-12.2	.0	-.4	2.6
5	3	3	.14015	-8.9	2.8	-1.5	-10.1	1.8	-1.0	2.0
5	3	4	.12551	-13.1	-1.8	-3.0	-8.3	.7	-1.0	.7
5	3	5	.09031	-5.8	-.3	-.6	-4.8	.2	-.7	.3
5	4	1	.14862	-37.9	-14.7	-8.4	-14.9	-1.2	1.8	1.0
5	4	2	.14643	-21.7	-5.5	-5.9	-10.2	-.4	1.1	2.6
5	4	3	.14357	-9.4	2.2	-1.7	-9.9	.9	.0	1.9
5	4	4	.12977	-13.7	-1.8	-3.2	-8.7	.4	-.8	.7
5	4	5	.09160	-5.9	-.2	-.7	-5.0	.1	-.4	.3
5	5	1	.14855	-30.6	-13.6	-7.7	-9.4	-.4	.9	.9
5	5	2	.14746	-20.2	-6.3	-5.6	-8.3	-.2	.6	2.3
5	5	3	.14501	-9.7	1.5	-1.7	-9.5	.2	.2	1.8
5	5	4	.13133	-13.9	-1.9	-3.2	-8.8	.1	-.2	.7
5	5	5	.09224	-6.0	-.2	-.7	-5.1	.0	-.2	.3

T	SEG	Z	W	THETA	S-XX	S-YY	S-ZZ	S-XY	S-XZ	S-YZ
6	1	1	.13875	-26.4	-8.7	-5.5	-12.3	-3.3	-2.8	.9
6	1	2	.13796	-15.7	-3.6	-5.3	-6.9	1.3	-4.4	.0
6	1	3	.13530	-9.5	.6	-3.2	-6.9	4.3	-3.7	.9
6	1	4	.12671	-11.3	-2.0	-3.0	-5.6	1.3	-2.3	.0
6	1	5	.09661	-5.8	-.5	-.8	-4.6	.5	-1.3	.0

6	2	1	.14782	-31.3	-11.9	-6.4	-13.0	-2.8	-.9	.0
6	2	2	.14585	-19.7	-8.7	-6.3	-8.7	.7	-2.5	.0
6	2	3	.14356	-9.8	2.0	-3.6	-8.2	3.3	-2.5	.0
6	2	4	.13269	-12.7	-1.9	-3.2	-7.5	1.1	-1.9	.0
6	2	5	.09923	-5.1	-.4	-.8	-4.9	.4	-1.0	.0
6	3	1	.15363	-31.8	-12.5	-6.6	-12.6	-2.2	.3	.0
6	3	2	.15188	-19.5	-4.3	-5.5	-8.6	.0	-.5	.0
6	3	3	.14953	-10.3	2.3	-3.6	-8.9	2.1	-1.0	.0
6	3	4	.13763	-13.5	-1.6	-3.5	-8.1	.6	-1.4	.0
6	3	5	.10125	-5.3	-.3	-.9	-5.1	.3	-.9	.0
6	4	1	.15612	-25.9	-12.4	-6.1	-6.4	-1.4	.9	.0
6	4	2	.15519	-18.8	-5.0	-6.4	-7.4	-.4	.6	.0
6	4	3	.15311	-10.3	1.9	-3.9	-8.7	1.0	-.1	.0
6	4	4	.14091	-14.1	-1.9	-3.7	-8.5	.5	-.8	.0
6	4	5	.10276	-6.5	-.2	-.9	-5.3	.2	-.5	.0
6	5	1	.15685	-22.9	-11.8	-5.7	-5.5	-.5	.4	.0
6	5	2	.15652	-16.0	-5.5	-6.1	-6.3	-.2	.4	.0
6	5	3	.15470	-11.1	1.3	-4.0	-8.4	.3	.0	.0
6	5	4	.14254	-14.3	-1.9	-3.8	-8.6	.2	-.3	.0
6	5	5	.10348	-5.5	-.2	-.5	-5.4	.0	-.2	.0

T	SEG	Z	M	THETA	S-XX	S-YY	S-ZZ	S-XY	S-XZ	S-YZ
7	1	1	.13095	-35.8	-10.4	-7.2	-18.1	-2.7	-4.2	-.8
7	1	2	.12815	-17.6	-3.8	-4.9	-9.1	1.2	-5.5	-2.0
7	1	3	.12577	-9.4	.9	-1.5	-7.8	3.6	-4.2	-1.5
7	1	4	.11560	-11.2	-2.0	-2.5	-6.7	1.1	-2.4	-.6
7	1	5	.08592	-5.3	-.5	-.6	-4.3	.4	-1.2	-.2
7	2	1	.14117	-45.6	-14.5	-8.7	-22.8	-2.3	-1.6	-1.1
7	2	2	.13737	-21.9	-3.9	-5.9	-12.1	.7	-3.1	-2.7
7	2	3	.13419	-8.5	2.4	-1.5	-9.5	2.8	-2.8	-1.9
7	2	4	.12181	-12.3	-1.8	-2.8	-7.6	.9	-1.9	-.6
7	2	5	.08840	-5.6	-.4	-.6	-4.6	.3	-1.0	-.3
7	3	1	.14707	-47.0	-15.2	-9.1	-22.7	-1.8	.6	-1.2
7	3	2	.14344	-22.3	-4.5	-6.2	-12.2	.0	-.4	-2.3
7	3	3	.14015	-8.9	2.8	-1.6	-10.1	1.8	-1.0	-2.9
7	3	4	.12661	-12.1	-1.8	-3.0	-8.3	.7	-1.3	-.7
7	3	5	.09031	-5.8	-.3	-.6	-4.8	.2	-.7	-.3
7	4	1	.14862	-37.9	-14.7	-8.4	-14.9	-1.2	1.8	-.0
7	4	2	.14642	-21.7	-5.8	-5.9	-10.2	-.4	1.1	-2.6
7	4	3	.14357	-9.4	2.2	-1.7	-9.9	.9	.0	-1.9
7	4	4	.12977	-13.7	-1.8	-3.2	-8.7	.4	-.8	-.7
7	4	5	.09160	-5.9	-.2	-.7	-5.0	.1	-.4	-.3

7	5	1	.14855	-30.6	-13.6	-7.7	-9.4	-.4	.8	-.3
7	5	2	.14746	-20.2	-6.2	-5.6	-8.3	-.2	.6	-2.3
7	5	3	.14501	-9.7	1.5	-1.7	-9.5	.2	.2	-1.8
7	5	4	.13133	-13.9	-1.9	-3.2	-8.9	.1	-.2	-.7
7	5	5	.09224	-6.0	-.2	-.7	-5.1	.0	-.2	-.3

T	SEG	Z	W	THETA	S-XX	S-YY	S-ZZ	S-XY	S-XZ	S-YZ
8	1	1	.13768	-51.4	-13.8	-9.1	-28.6	-2.0	-6.6	-.5
8	1	2	.13293	-21.1	-4.6	-5.5	-10.3	.4	-7.3	-1.1
8	1	3	.12963	-8.1	1.2	.0	-9.3	2.3	-5.1	-.3
8	1	4	.11776	-11.5	-2.1	-2.4	-7.2	.6	-2.5	-.3
8	1	5	.08648	-5.4	-.5	-.5	-4.4	.3	-1.2	-.0
8	2	1	.15035	-70.3	-19.4	-11.1	-40.0	-1.7	-2.7	-.6
8	2	2	.14334	-27.4	-4.5	-5.2	-17.7	.2	-4.1	-1.5
8	2	3	.13882	-8.2	3.0	.3	-11.5	1.8	-3.3	-1.1
8	2	4	.12430	-12.8	-1.9	-2.6	-9.3	.7	-2.0	-.4
8	2	5	.08900	-5.7	-.4	-.5	-4.7	.2	-1.0	-.0
8	3	1	.15681	-72.5	-20.3	-11.7	-40.6	-1.3	1.4	-.6
8	3	2	.14988	-28.8	-5.2	-5.5	-18.0	.3	-.2	-1.6
8	3	3	.14520	-8.5	2.4	.4	-12.3	1.2	-1.1	-1.2
8	3	4	.12932	-13.7	-1.9	-2.8	-9.0	.5	-1.4	-.4
8	3	5	.09094	-5.9	-.3	-.6	-4.9	.2	-.7	-.0
8	4	1	.15704	-56.1	-13.1	-10.7	-25.3	-.8	3.2	-.5
8	4	2	.15267	-26.6	-6.6	-5.3	-14.6	-.0	1.8	-1.5
8	4	3	.14867	-8.9	2.5	.4	-11.8	.7	.3	-1.2
8	4	4	.13258	-14.3	-1.9	-2.9	-9.4	.3	-.8	-.4
8	4	5	.09222	-6.0	-.2	-.6	-5.1	.1	-.5	-.0
8	5	1	.15576	-42.9	-17.0	-9.8	-16.0	-.3	1.4	-.6
8	5	2	.15338	-24.3	-7.6	-5.1	-11.6	-.0	1.0	-1.4
8	5	3	.15004	-9.2	1.7	.3	-11.1	.2	.3	-1.2
8	5	4	.13417	-14.5	-2.0	-3.0	-9.5	.0	-.3	-.5
8	5	5	.09286	-6.0	-.2	-.6	-5.2	.0	-.2	-.0

T	SEG	Z	W	THETA	S-XX	S-YY	S-ZZ	S-XY	S-XZ	S-YZ
9	1	1	.13172	-46.1	-12.5	-10.0	-23.6	-2.3	-5.5	.0
9	1	2	.12798	-21.2	-4.3	-5.3	-11.6	1.5	-7.1	.1
9	1	3	.12483	-7.4	1.4	.5	-9.3	3.5	-5.2	.0
9	1	4	.11237	-11.5	-2.0	-2.1	-7.4	1.0	-2.5	.0
9	1	5	.08081	-5.1	-.5	-.4	-4.2	.5	-1.1	.2

9	2	1	.14357	-60.6	-17.5	-12.1	-31.0	-2.0	-2.2	.0
9	2	2	.13830	-26.4	-4.3	-6.4	-15.7	.9	-4.0	.2
9	2	3	.13406	-7.4	3.2	.8	-11.5	2.7	-3.4	.0
9	2	4	.11885	-12.7	-1.9	-2.3	-8.5	.8	-2.1	.0
9	2	5	.08321	-5.3	-.4	-.5	-4.5	.2	-.9	.2
9	3	1	.14997	-62.3	-18.4	-12.8	-31.1	-1.6	.9	.0
9	3	2	.14485	-27.7	-5.1	-6.7	-15.9	-.0	-.4	.2
9	3	3	.14046	-7.7	3.6	.9	-12.2	1.6	-1.2	.0
9	3	4	.12383	-13.6	-1.9	-2.5	-9.2	.6	-1.4	.0
9	3	5	.08506	-5.5	-.3	-.5	-4.8	.2	-.7	.2
9	4	1	.15093	-49.9	-17.5	-11.9	-20.5	-1.1	2.4	.0
9	4	2	.14777	-26.0	-6.4	-6.4	-13.2	-.5	1.5	.0
9	4	3	.14396	-8.1	2.8	1.0	-11.9	.7	.2	.0
9	4	4	.12707	-14.1	-1.9	-2.6	-9.6	.3	-.8	.0
9	4	5	.08630	-5.7	-.2	-.5	-4.9	.1	-.4	.2
9	5	1	.15026	-39.9	-15.9	-11.0	-12.9	-.4	1.1	-.0
9	5	2	.14859	-23.9	-7.2	-8.9	-10.7	-.3	.9	.0
9	5	3	.14596	-8.4	1.9	1.0	-11.0	.2	.3	-.0
9	5	4	.12865	-14.4	-2.0	-3.6	-9.8	.1	-.8	.0
9	5	5	.08691	-5.7	-.2	-.5	-5.0	.0	-.1	.2

T	SEG	Z	W	THETA	S-XX	S-YY	S-ZZ	S-XY	S-XZ	S-YZ
10	1	1	.11274	-46.5	-12.2	-10.7	-23.6	-1.8	-5.7	.0
10	1	2	.10898	-20.6	-4.1	-5.0	-11.6	1.5	-7.2	.0
10	1	3	.10575	-5.8	1.6	1.8	-9.2	3.1	-5.2	.3
10	1	4	.09317	-10.3	-1.3	-1.5	-7.0	.8	-2.4	.4
10	1	5	.06371	-4.2	-.4	-.2	-3.6	.2	-1.0	.2
10	2	1	.12410	-61.6	-17.1	-13.0	-31.4	-1.6	-2.3	-.0
10	2	2	.11873	-25.9	-4.0	-6.1	-15.8	.9	-4.1	-.0
10	2	3	.11439	-5.7	3.4	2.2	-11.3	2.3	-3.4	.2
10	2	4	.09904	-11.4	-1.7	-1.6	-8.0	.6	-1.9	.5
10	2	5	.06573	-4.4	-.3	-.2	-3.5	.2	-.8	.2
10	3	1	.13006	-63.4	-17.9	-13.8	-31.7	-1.3	.9	-.0
10	3	2	.12483	-27.2	-4.7	-6.4	-16.1	.0	-.4	-.0
10	3	3	.12033	-6.9	3.8	2.5	-12.1	1.3	-1.1	.3
10	3	4	.10354	-12.2	-1.7	-1.8	-8.8	.4	-1.3	.5
10	3	5	.06728	-4.6	-.2	-.2	-4.1	.1	-.6	.2
10	4	1	.13065	-50.8	-17.0	-12.9	-20.8	-.9	2.5	.0
10	4	2	.12741	-25.4	-6.1	-6.0	-13.3	-.5	1.6	.0
10	4	3	.12347	-6.2	2.9	2.6	-11.7	.5	.2	.3
10	4	4	.10645	-12.9	-1.8	-1.8	-9.2	.3	-.7	.5
10	4	5	.06831	-4.7	-.2	-.2	-4.2	.0	-.4	.2

10	5	1	.12976	-40.6	-15.4	-12.1	-13.2	-.3	1.1	.0
10	5	2	.12804	-23.3	-7.0	-5.6	-10.7	-.3	.9	.2
10	5	3	.12468	-6.5	1.9	2.6	-11.1	.1	.3	.4
10	5	4	.10785	-13.0	-1.8	-1.9	-9.3	.0	-.2	.5
10	5	5	.06882	-4.7	-.2	-.2	-4.3	.0	-.1	.2

T	SEG	I	W	THETA	S-XX	S-YY	S-ZZ	S-XY	S-XZ	S-YZ
11	1	1	.10828	-52.0	-13.2	-9.7	-29.2	-1.1	-6.8	.7
11	1	2	.10337	-20.5	-4.1	-3.7	-12.6	.3	-7.3	1.9
11	1	3	.09998	-5.5	1.4	1.9	-8.8	1.4	-4.9	1.7
11	1	4	.08846	-9.5	-1.7	-1.4	-6.3	.4	-2.2	1.2
11	1	5	.06181	-4.0	-.4	-.2	-3.4	.2	-.9	.6
11	2	1	.12005	-72.5	-18.7	-11.9	-41.9	-1.0	-2.9	.9
11	2	2	.11264	-25.2	-4.0	-4.3	-17.9	.2	-4.1	2.3
11	2	3	.10799	-5.4	3.1	2.5	-11.0	1.1	-3.2	2.1
11	2	4	.09387	-10.5	-1.5	-1.9	-7.3	.4	-1.7	1.4
11	2	5	.06375	-4.2	-.3	-.3	-3.6	.1	-.7	.6
11	3	1	.12563	-74.5	-19.5	-12.5	-42.6	-.7	1.4	1.0
11	3	2	.11626	-27.6	-4.7	-4.5	-18.3	.0	-.0	2.5
11	3	3	.11342	-5.5	3.4	2.7	-11.8	.7	-1.0	2.3
11	3	4	.09900	-11.3	-1.6	-1.7	-7.9	.3	-1.2	1.5
11	3	5	.06521	-4.4	-.2	-.3	-3.8	.0	-.6	.7
11	4	1	.12506	-57.5	-18.2	-11.7	-27.6	-.5	3.4	1.0
11	4	2	.12037	-25.3	-8.1	-4.4	-14.8	-.0	2.0	2.5
11	4	3	.11622	-5.9	2.6	2.6	-11.2	.4	.4	2.3
11	4	4	.10054	-11.7	-1.6	-1.8	-8.3	.2	-.7	1.5
11	4	5	.06616	-4.4	-.2	-.3	-4.0	.0	-.3	.7
11	5	1	.12331	-43.5	-16.0	-10.5	-15.9	-.2	1.5	.9
11	5	2	.12070	-22.8	-7.0	-4.2	-11.5	-.0	1.1	2.4
11	5	3	.11725	-5.2	1.6	2.8	-10.5	.1	.3	2.3
11	5	4	.10192	-11.9	-1.7	-1.8	-8.4	.0	-.2	1.6
11	5	5	.06663	-4.5	-.2	-.3	-4.0	.0	-.1	.7

T	SEG	I	W	THETA	S-XX	S-YY	S-ZZ	S-XY	S-XZ	S-YZ
12	1	1	.09174	-32.3	-8.8	-6.6	-17.0	-1.5	-4.0	1.5
12	1	2	.08901	-14.6	-3.0	-3.4	-8.2	.9	-4.9	3.3
12	1	3	.08683	-5.2	.9	.2	-6.4	2.2	-3.5	3.2
12	1	4	.07651	-7.9	-1.4	-1.5	-5.0	.6	-1.7	1.3
12	1	5	.05714	-3.6	-.3	-.3	-2.9	.2	-.8	.8

12	2	1	.09997	-42.9	-12.3	-8.1	-22.6	-1.3	-1.6	2.0
12	2	2	.09607	-18.3	-3.0	-4.2	-11.1	.5	-2.7	5.0
12	2	3	.09312	-5.2	2.2	.4	-7.8	1.7	-2.3	4.0
12	2	4	.08293	-8.7	-1.3	-1.7	-5.7	.5	-1.4	2.0
12	2	5	.05982	-3.7	-.3	-.4	-3.1	.2	-.7	.9
12	3	1	.10433	-44.1	-12.8	-8.5	-22.9	-1.1	.7	2.1
12	3	2	.10053	-19.2	-3.5	-4.4	-11.3	-.0	-.2	5.3
12	3	3	.09747	-5.4	2.4	.5	-8.4	1.0	-.8	4.3
12	3	4	.08634	-9.3	-1.3	-1.8	-5.2	.4	-1.0	2.2
12	3	5	.06012	-3.9	-.2	-.4	-3.3	.1	-.5	.9
12	4	1	.10485	-35.0	-12.2	-7.9	-14.9	-.7	1.8	2.0
12	4	2	.10248	-17.9	-4.4	-4.1	-9.3	-.3	1.1	5.1
12	4	3	.09984	-5.7	1.8	.5	-8.1	.5	.2	4.3
12	4	4	.08855	-9.7	-1.3	-1.9	-6.5	.2	-.5	2.3
12	4	5	.06098	-4.0	-.2	-.4	-3.4	.0	-.3	1.0
12	5	1	.10428	-27.6	-11.1	-7.2	-9.3	-.3	.8	1.8
12	5	2	.10301	-16.4	-5.1	-3.9	-7.5	-.2	.6	4.7
12	5	3	.10077	-5.9	1.2	.5	-7.7	.1	.2	4.1
12	5	4	.08963	-9.9	-1.4	-1.9	-6.6	.0	-.2	2.3
12	5	5	.06140	-4.0	-.1	-.4	-3.5	.0	-.1	1.0

T	SEG	Z	W	THETA	S-XX	S-YY	S-ZZ	S-XY	S-XZ	S-YZ
13	1	1	.06937	-13.2	-4.4	-2.7	-6.1	-1.6	-1.4	1.3
13	1	2	.06853	-7.9	-1.8	-2.6	-3.4	.7	-2.2	3.3
13	1	3	.06765	-4.8	.3	-1.5	-3.5	2.1	-1.3	2.9
13	1	4	.06317	-5.5	-1.0	-1.5	-3.3	.7	-1.2	1.8
13	1	5	.04831	-2.9	-.2	-.4	-2.3	.2	-.5	.9
13	2	1	.07691	-15.7	-5.5	-3.2	-6.5	-1.4	-.4	1.8
13	2	2	.07293	-9.3	-1.9	-3.1	-4.3	.4	-1.2	4.1
13	2	3	.07178	-4.9	1.0	-1.8	-4.1	1.7	-1.2	3.5
13	2	4	.06635	-6.3	-.9	-1.7	-3.7	.5	-1.0	2.0
13	2	5	.04964	-3.0	-.2	-.4	-2.4	.2	-.5	.9
13	3	1	.07681	-15.9	-6.3	-3.3	-5.3	-1.1	.1	1.8
13	3	2	.07594	-9.8	-2.1	-3.3	-4.3	.0	-.2	4.5
13	3	3	.07477	-5.1	1.2	-1.9	-4.4	1.1	-.5	3.8
13	3	4	.06881	-6.8	-.9	-1.8	-4.1	.4	-.7	2.2
13	3	5	.05066	-3.2	-.2	-.4	-2.5	.1	-.4	1.0

13	4	1	.07806	-13.4	-6.2	-3.1	-4.2	-.7	.5	1.7
13	4	2	.07760	-9.4	-2.5	-3.2	-2.7	-.2	.2	4.3
13	4	3	.07655	-5.4	.9	-2.0	-4.3	.5	-.0	3.9
13	4	4	.07046	-7.0	-.9	-1.9	-4.2	.2	-.4	2.3
13	4	5	.05138	-3.2	-.1	-.4	-2.7	.0	-.2	1.0
13	5	1	.07843	-11.5	-5.3	-2.8	-2.7	-.2	.2	1.5
13	5	2	.07626	-9.0	-2.6	-3.0	-3.2	-.1	.2	4.1
13	5	3	.07735	-5.5	.7	-2.0	-4.2	.1	.0	3.8
13	5	4	.07127	-7.2	-1.0	-1.9	-4.3	.0	-.1	2.2
13	5	5	.05174	-3.2	-.1	-.4	-2.7	.0	-.0	1.0

T	SEG	Z	W	THETA	S-XX	S-YY	S-ZZ	S-XY	S-XZ	S-YZ
14	1	1	.03920	-3.5	-1.7	-.6	-1.2	-1.1	-.2	.7
14	1	2	.03914	-3.3	-.8	-1.5	-1.0	.3	-.6	1.9
14	1	3	.03893	-3.2	.0	-1.7	-1.4	1.4	-.7	1.7
14	1	4	.03709	-3.3	-.5	-1.0	-1.7	.4	-.5	1.2
14	1	5	.02876	-1.7	-.1	-.2	-1.4	.2	-.4	.6
14	2	1	.04121	-3.0	-2.2	-.5	-.2	-1.0	.0	.9
14	2	2	.04131	-3.6	-.9	-1.7	-1.0	.2	-.4	2.3
14	2	3	.04107	-3.3	.3	-2.0	-1.6	1.1	-.5	2.1
14	2	4	.03888	-3.6	-.5	-1.1	-1.9	.4	-.5	1.4
14	2	5	.02957	-1.8	-.1	-.3	-1.5	.1	-.3	.8
14	3	1	.04274	-2.8	-2.3	-.6	.0	-.7	-.0	1.0
14	3	2	.04291	-3.7	-1.0	-1.8	-.9	.0	-.2	2.5
14	3	3	.04268	-3.5	.4	-2.1	-1.7	.7	-.3	2.3
14	3	4	.04026	-3.8	-.5	-1.2	-2.1	.3	-.4	1.5
14	3	5	.03019	-1.9	-.0	-.3	-1.5	.0	-.2	.7
14	4	1	.04277	-2.9	-2.5	-.5	.0	-.5	-.0	1.0
14	4	2	.04395	-3.9	-1.1	-1.8	-.9	-.0	-.0	2.5
14	4	3	.04373	-3.5	.4	-2.2	-1.8	.4	-.1	2.3
14	4	4	.04122	-4.0	-.5	-1.3	-2.2	.2	-.2	1.5
14	4	5	.03062	-1.9	-.0	-.3	-1.5	.0	-.1	.7
14	5	1	.04427	-3.0	-2.5	-.5	-.0	-.2	-.0	.9
14	5	2	.04445	-3.8	-1.2	-1.8	-.9	-.0	.0	2.4
14	5	3	.04423	-2.7	.3	-2.2	-1.8	.1	-.0	2.0
14	5	4	.04170	-4.1	-.5	-1.3	-2.3	.3	-.0	1.6
14	5	5	.03084	-1.9	-.0	-.3	-1.5	.0	-.0	.7

T	SEG	Z	K	THETA	S-XX	S-YY	S-ZZ	S-XY	S-XZ	S-YZ
15	1	1	.02940	.6	-.6	.6	.5	-.3	.2	.3
15	1	2	.02955	-1.3	-.5	-.6	.0	.0	.0	.7
15	1	3	.02965	-2.6	-.2	-1.9	-.5	.3	-.2	.8
15	1	4	.02930	-2.2	-.4	-.9	-.9	.3	-.3	.9
15	1	5	.02464	-1.4	-.1	-.3	-1.0	.1	-.2	.6
15	2	1	.03030	2.0	-.7	.8	1.8	-.7	.2	.3
15	2	2	.03070	-1.2	-.3	-.9	.3	.0	.0	.8
15	2	3	.03084	-2.8	-.1	-2.1	-.5	.7	-.1	1.0
15	2	4	.03042	-2.3	-.3	-1.0	-1.0	.3	-.3	1.0
15	2	5	.02525	-1.5	-.0	-.3	-1.1	.1	-.2	.8
15	3	1	.03118	2.3	-.7	1.0	2.1	-.6	-.0	.3
15	3	2	.03162	-1.2	-.6	-1.1	.2	.0	-.0	.9
15	3	3	.03179	-2.9	-.0	-2.3	-.5	.5	-.1	1.0
15	3	4	.03132	-2.5	-.3	-1.1	-1.1	.2	-.2	1.0
15	3	5	.02573	-1.6	-.0	-.3	-1.1	.0	-.2	.8
15	4	1	.03198	1.5	-.9	1.0	1.4	-.3	-.2	.4
15	4	2	.03230	-1.3	-.6	-1.0	.2	-.0	-.1	.9
15	4	3	.03244	-3.0	-.0	-2.4	-.6	.3	-.0	1.1
15	4	4	.03194	-2.6	-.3	-1.1	-1.1	.1	-.1	1.1
15	4	5	.02626	-1.5	-.0	-.3	-1.1	.0	-.1	.8
15	5	1	.03245	.8	-1.0	1.0	.8	-.1	-.0	.4
15	5	2	.03269	-1.5	-.5	-1.0	.0	.0	-.0	1.0
15	5	3	.03278	-3.1	.0	-2.5	-.6	.0	-.0	1.1
15	5	4	.03225	-2.6	-.3	-1.2	-1.1	.0	-.0	1.1
15	5	5	.02623	-1.6	-.0	-.3	-1.2	.0	-.0	.7

T	SEG	Z	K	THETA	S-XX	S-YY	S-ZZ	S-XY	S-XZ	S-YZ
16	1	1	.01998	.4	-.3	.7	.0	-.5	.0	.0
16	1	2	.01900	-.5	-.3	-.3	.0	-.0	.0	.1
16	1	3	.01909	-1.6	-.2	-1.3	-.1	.4	-.0	.3
16	1	4	.01921	-1.2	-.2	-.6	-.4	.2	-.2	.5
16	1	5	.01710	-.9	-.0	-.2	-.6	.1	-.2	.4
16	2	1	.01947	.9	-.4	.9	.4	-.4	.0	.0
16	2	2	.01956	-.5	-.3	-.3	.0	-.0	.0	.1
16	2	3	.01967	-1.7	-.2	-1.4	-.1	.3	-.0	.3
16	2	4	.01981	-1.3	-.2	-.7	-.4	.2	-.1	.5
16	2	5	.01748	-1.0	-.0	-.3	-.6	.0	-.1	.4

16	3	1	.01991	1.1	-.4	1.0	.5	-.2	.0	.0
16	3	2	.02002	-.5	-.3	-.3	.1	-.0	.0	.1
16	3	3	.02014	-1.8	-.1	-1.5	-.1	.2	-.0	.3
16	3	4	.02029	-1.3	-.2	-.7	-.4	.1	-.1	.5
16	3	5	.01776	-1.0	-.0	-.3	-.7	.0	-.1	.5
16	4	1	.02028	.9	-.5	1.0	.4	-.2	-.0	.0
16	4	2	.02037	-.5	-.3	-.3	.0	.0	-.0	.1
16	4	3	.02048	-1.9	-.1	-1.6	-.1	.2	-.0	.3
16	4	4	.02062	-1.4	-.2	-.8	-.5	.0	-.0	.5
16	4	5	.01799	-1.0	-.0	-.3	-.7	.0	-.0	.5
16	5	1	.02050	.8	-.5	1.0	.3	-.0	-.0	.0
16	5	2	.02059	-.6	-.3	-.4	.0	.0	-.0	.2
16	5	3	.02068	-1.9	-.0	-1.6	-.2	.0	-.0	.4
16	5	4	.02079	-1.4	-.2	-.8	-.5	.0	-.0	.5
16	5	5	.01810	-1.0	-.0	-.3	-.7	.0	-.0	.5

SUPERIMPOSED RESULTS FROM CALC. STEP NO. 2

----- DEFLECTIONS AND REACTIONS ----

TIE NO.	DEFLECTION RAIL IN.	REACTION RAIL SEAT LBS	DEFLECTION TIE IN.
1	-.076979	3267.5	-.076513
2	-.072303	-755.9	-.072411
3	-.163701	19586.7	-.160903
4	-.154465	15283.6	-.152282
5	-.165126	14622.3	-.163038
6	-.266789	40938.4	-.260541
7	-.165126	14622.3	-.163036
8	-.154465	15283.6	-.152282
9	-.163701	19588.7	-.160903
10	-.072303	-755.9	-.072411
11	-.076979	3267.5	-.076512
12	-.107792	11135.6	-.106201
13	-.133394	20469.2	-.130471
14	-.057034	3486.7	-.056836
15	-.077485	12016.1	-.075769
16	-.091398	20344.5	-.088492

TIE NO.	TIE CENTER BENDING MOMENT (IN.-LBS)	TIE RAIL-SEAT BENDING MOMENT (IN.-LBS)	RAIL BENDING MOMENT (IN.-LBS)
1	.48539E+06	.97057E+05	.12472E+08
2	.40351E+06	.75555E+05	.11253E+08
3	-.14121E+06	.76158E+05	.10019E+08
4	.10686E+06	.94421E+05	.91774E+07
5	-.10699E+06	.57724E+05	.78530E+07
6	-.10184E+07	.37065E+05	.54210E+07
7	-.10699E+06	.57724E+05	.60079E+07
8	.10685E+06	.94421E+05	.58871E+07
9	-.14121E+06	.76158E+05	.50841E+07
10	.46656E+06	.76555E+05	.46728E+07
11	.48539E+06	.97057E+05	.42464E+07
12	-.10549E+05	.54990E+05	.28274E+07
13	-.50919E+06	.18533E+05	.17711E+07
14	-.96444E+05	.27332E+04	.10541E+07
15	-.37953E+06	-.26352E+04	.40689E+06
16	-.50777E+06	-.39672E+03	.00000E+00

TIE NO.	TIE/SOIL REACTIONS, LBS DIV 1	DIV 2	DIV 3	DIV 4	DIV 5
1	3919.6	5475.8	5647.0	3443.5	1983.3
2	3191.4	4051.8	4153.3	2567.0	1539.4
3	3191.0	3987.5	4091.5	2518.0	1505.6
4	3854.0	5217.7	5367.4	3268.4	1881.2
5	2458.1	2916.6	2970.6	1826.2	1098.7
6	1572.6	1820.5	1819.4	1002.3	620.3
7	2458.1	2916.6	2970.6	1826.2	1088.7
8	3854.0	5217.7	5367.4	3268.4	1981.2
9	3191.0	3987.6	4091.5	2518.0	1505.6
10	3191.4	4051.8	4153.3	2567.0	1539.4
11	3919.6	5475.8	5647.0	3443.5	1983.3
12	2289.1	2919.3	2992.1	1841.6	1093.4
13	836.3	810.2	809.7	501.2	310.1
14	158.9	-2.7	-21.5	-15.5	-4.7
15	-65.6	-258.1	-279.7	-175.2	-102.1
16	-.4	-64.2	-71.8	-49.1	-33.2

TIE NO.	TIE SEGMENT DEFLECTION ,IN. DIV 1	DIV 2	DIV 3	DIV 4	DIV 5
1	-.058122	-.071544	-.077242	-.074125	-.070702
2	-.055403	-.067591	-.073582	-.072346	-.070293
3	-.143238	-.155835	-.162250	-.161404	-.159577
4	-.132770	-.146655	-.153385	-.151181	-.148308
5	-.147989	-.158590	-.164462	-.164672	-.163762
6	-.248054	-.256913	-.262635	-.264396	-.264704
7	-.147989	-.158590	-.164462	-.164672	-.163762
8	-.132770	-.146856	-.153385	-.151181	-.148308

9	-.143238	-.155835	-.162250	-.161404	-.159577
10	-.055403	-.067591	-.072582	-.072346	-.070293
11	-.058122	-.071544	-.077242	-.074126	-.070702
12	-.093859	-.102591	-.107075	-.105250	-.104832
13	-.124027	-.128456	-.131318	-.132198	-.132252
14	-.054129	-.055899	-.057387	-.058412	-.058930
15	-.074648	-.075312	-.076143	-.077055	-.077607
16	-.087836	-.088244	-.088667	-.089058	-.089284

SOIL VERTICAL DISPLACEMENTS AND INCREMENTAL STRESSES

T = TIE NUMBER (1=CENTER TIE)
SEG = SEGMENT NUMBER
Z = DEPTH POINT NUMBER
XX = DIRECTION PARALLEL TO TIES
YY = DIRECTION PARALLEL TO RAILS
ZZ = VERTICAL DIRECTION
UNITS ARE INCHES AND PSI
COMPRESSION IS NEGATIVE FOR STRESSES
DOWNWARD IS POSITIVE FOR DEFLECTIONS

Z(1) = 1.00 IN.

Z(2) = 37.00 IN.

T	SEG	Z	W	THETA	S-XX	S-YY	S-ZZ	S-XY	S-XZ	S-YZ
1	1	1	.11170	-97.1	-29.4	-32.8	-34.9	-2.0	-.5	-.1
1	1	2	.09765	-12.6	-2.5	-2.3	-7.7	.5	-2.7	-1.3
1	2	1	.12495	-135.0	-41.5	-44.4	-49.1	-1.5	-.3	-.1
1	2	2	.10503	-14.4	-2.4	-2.7	-9.3	.4	-3.0	-1.5
1	3	1	.13064	-140.2	-43.3	-46.1	-50.8	-1.0	-.0	-.2
1	3	2	.11023	-15.5	-2.6	-2.9	-10.0	.3	-3.1	-1.6
1	4	1	.12779	-94.1	-29.3	-33.5	-31.3	-.5	.0	-.2
1	4	2	.11313	-16.1	-3.0	-3.0	-10.1	.2	-.4	-1.7
1	5	1	.12455	-62.5	-19.6	-24.5	-18.3	-.1	.0	-.2
1	5	2	.11452	-16.2	-3.3	-3.0	-10.0	.0	-.0	-1.7

T	SEG	Z	W	THETA	S-XX	S-YY	S-ZZ	S-XY	S-XZ	S-YZ
2	1	1	.11533	-82.3	-26.2	-28.0	-26.1	-4.4	-.4	-.0
2	1	2	.10329	-13.8	-2.6	-2.6	-8.4	1.1	-3.0	-.3
2	2	1	.12743	-105.5	-34.5	-34.9	-36.0	-3.2	-.2	-.0
2	2	2	.11128	-15.7	-2.7	-3.0	-10.0	.9	-2.2	-.4
2	3	1	.13342	-109.5	-36.1	-36.3	-37.1	-1.6	-.1	-.0
2	3	2	.11695	-16.9	-2.9	-3.3	-10.8	.5	-1.2	-.4
2	4	1	.13238	-76.8	-25.8	-27.7	-23.3	-.5	.0	-.0
2	4	2	.12018	-17.5	-3.3	-3.3	-11.0	.2	-.5	-.4
2	5	1	.13045	-54.7	-18.5	-21.8	-14.3	-.0	.0	-.0
2	5	2	.12153	-17.9	-3.5	-3.4	-10.8	.0	-.0	-.5

T	SEG	Z	W	THETA	S-XX	S-YY	S-ZZ	S-XY	S-XZ	S-YZ
3	1	1	.13434	-81.7	-26.6	-25.8	-28.2	-5.1	-.4	.0
3	1	2	.12243	-14.9	-3.0	-3.3	-8.6	1.3	-3.1	-.0
3	2	1	.14687	-103.3	-34.7	-33.2	-35.4	-3.6	-.2	.0
3	2	2	.13102	-15.8	-2.9	-3.7	-10.2	1.0	-2.3	-.0
3	3	1	.15328	-106.9	-36.2	-34.4	-36.2	-2.1	-.0	.0
3	3	2	.13718	-18.2	-3.1	-4.0	-11.1	.6	-1.3	-.0
3	4	1	.15253	-74.6	-26.1	-25.8	-22.6	-.7	.0	.0
3	4	2	.14075	-16.8	-3.5	-4.2	-11.2	.3	-.5	-.0
3	5	1	.15093	-52.8	-19.1	-20.0	-13.7	-.1	.0	.0
3	5	2	.14229	-19.1	-3.8	-4.2	-11.1	.0	-.1	.0

T	SEG	Z	W	THETA	S-XX	S-YY	S-ZZ	S-XY	S-XZ	S-YZ
4	1	1	.14103	-94.9	-30.1	-30.9	-34.0	-3.3	-.5	.1
4	1	2	.12733	-14.5	-3.0	-3.4	-8.4	.9	-3.0	.5
4	2	1	.15497	-128.5	-41.1	-41.0	-46.3	-2.6	-.2	.1
4	2	2	.13589	-16.7	-2.9	-3.9	-10.0	.7	-2.2	.6
4	3	1	.16149	-133.0	-43.0	-42.5	-47.6	-1.8	-.0	.1
4	3	2	.14203	-18.0	-3.1	-4.2	-10.3	.5	-1.3	.6
4	4	1	.15955	-89.0	-29.7	-30.4	-28.9	-1.0	.0	.1
4	4	2	.14559	-18.7	-3.4	-4.3	-10.9	.2	-.5	.7
4	5	1	.15695	-58.8	-20.5	-21.8	-16.5	-.3	.0	.1
4	5	2	.14712	-18.9	-3.7	-4.4	-10.8	.0	-.1	.7

T	SEG	Z	W	THETA	S-XX	S-YY	S-ZZ	S-XY	S-XZ	S-YZ
5	1	1	.13293	-62.1	-21.6	-19.4	-21.1	-5.3	-.3	.0
5	1	2	.12390	-13.5	-2.8	-3.7	-7.4	1.4	-2.7	.8
5	2	1	.14350	-75.2	-27.0	-23.1	-25.1	-4.0	-.2	.0
5	2	2	.13183	-15.6	-2.7	-4.1	-9.2	1.1	-2.0	.9
5	3	1	.14939	-77.4	-28.2	-23.7	-25.4	-2.4	-.0	.0
5	3	2	.13751	-16.6	-2.9	-4.5	-9.4	.7	-1.2	1.0
5	4	1	.14974	-52.6	-21.0	-17.4	-15.2	-1.1	.0	.0
5	4	2	.14107	-17.4	-3.2	-4.7	-9.6	.4	-.5	1.0
5	5	1	.14892	-37.6	-15.9	-13.1	-8.6	-.3	.0	.0
5	5	2	.14261	-17.7	-3.4	-4.7	-9.5	.1	-.1	1.0

T	SEG	Z	W	THETA	S-XX	S-YY	S-ZZ	S-XY	S-XZ	S-YZ
6	1	1	.14002	-43.7	-17.3	-12.2	-14.3	-5.3	-.2	.0
6	1	2	.12376	-13.9	-2.8	-4.2	-6.9	1.6	-2.5	.0

5	2	1	.14891	-45.2	-19.4	-12.8	-13.5	-4.8	-.1	.0
6	2	2	.14163	-15.5	-2.7	-4.7	-8.0	1.2	-1.9	.0
5	3	1	.15465	-45.9	-20.4	-12.2	-13.3	-2.9	-.0	.0
6	3	2	.14745	-16.7	-2.6	-5.1	-8.7	.8	-1.2	.0
6	4	1	.15649	-33.2	-16.5	-9.0	-7.8	-1.3	-.0	.0
6	4	2	.15104	-17.3	-3.1	-5.3	-8.9	.4	-.6	.0
6	5	1	.15685	-25.1	-13.7	-6.6	-4.5	-.3	.0	.0
6	5	2	.15170	-17.5	-3.8	-5.4	-8.9	..	-..	.0

T	SEG	Z	W	THETA	S-XX	S-YY	S-ZZ	S-XY	S-XZ	S-YZ
7	1	1	.12293	-62.1	-21.5	-19.4	-21.1	-5.3	-.3	-.0
7	1	2	.12390	-13.8	-2.8	-3.7	-7.4	1.4	-2.7	-.8
7	2	1	.14350	-75.2	-27.0	-23.1	-25.1	-4.0	-.2	-.0
7	2	2	.13193	-15.5	-2.7	-4.1	-8.7	1.1	-2.0	-.9
7	3	1	.14939	-77.4	-28.3	-23.7	-25.4	-2.4	-.0	-.0
7	3	2	.13761	-16.8	-2.9	-4.5	-9.4	.7	-1.2	-1.0
7	4	1	.14974	-53.6	-21.0	-17.4	-15.2	-1.1	.0	-.0
7	4	2	.14107	-17.4	-3.2	-4.7	-9.6	.4	-.5	-1.0
7	5	1	.14892	-37.6	-15.9	-13.1	-8.6	-.3	.0	-.0
7	5	2	.14261	-17.7	-3.4	-4.7	-9.5	.1	-.1	-1.0

T	SEG	Z	W	THETA	S-XX	S-YY	S-ZZ	S-XY	S-XZ	S-YZ
8	1	1	.14103	-94.9	-30.1	-30.9	-34.0	-3.3	-.5	-.0
8	1	2	.12783	-14.8	-3.0	-3.4	-8.4	.9	-3.0	-.5
8	2	1	.15497	-128.5	-41.1	-41.0	-46.3	-2.6	-.2	-.1
8	2	2	.13589	-16.7	-2.9	-3.9	-10.0	.7	-2.2	-.6
8	3	1	.16149	-133.0	-43.0	-42.5	-47.6	-1.9	-.0	-.1
8	3	2	.14203	-19.0	-3.1	-4.2	-10.9	.5	-1.9	-.6

8	4	1	.15955	-89.0	-29.7	-30.4	-28.9	-1.0	.0	-.1
8	4	2	.14559	-18.7	-3.4	-4.3	-10.9	.3	-.5	-.7
8	5	1	.15685	-58.8	-20.5	-21.8	-16.5	-.3	.0	-.1
8	5	2	.14712	-18.9	-3.7	-4.4	-10.8	.0	-.1	-.7

T	SEG	Z	W	THETA	S-XX	S-YY	S-ZZ	S-XY	S-XZ	S-YZ
9	1	1	.13434	-81.7	-26.8	-26.9	-28.2	-5.1	-.4	-.0
9	1	2	.12243	-14.9	-3.0	-3.3	-8.6	1.3	-3.1	.0
9	2	1	.14687	-103.3	-34.7	-33.2	-35.4	-3.8	-.2	-.0
9	2	2	.13103	-15.8	-2.9	-3.7	-10.2	1.0	-2.3	.0
9	3	1	.15328	-106.9	-35.2	-34.4	-36.3	-2.1	-.0	-.0
9	3	2	.13716	-16.2	-3.1	-4.0	-11.1	.6	-1.3	.0
9	4	1	.15263	-74.6	-26.1	-25.8	-22.8	-.7	.0	-.0
9	4	2	.14075	-16.8	-3.6	-4.2	[illegible]	[illegible]	[illegible]	[illegible]
9	5	1	.15093	-52.8	-19.1	-20.0	-13.7	-.1	.0	-.0
9	5	2	.14228	-19.1	-3.8	-4.2	-11.1	.0	-.1	.0

T	SEG	Z	W	THETA	S-XX	S-YY	S-ZZ	S-XY	S-XZ	S-YZ
10	1	1	.11553	-62.3	-26.2	-26.0	-28.1	-4.4	-.4	.0
10	1	2	.10329	-13.8	-2.8	-2.6	-8.4	1.1	-3.0	.3
10	2	1	.12743	-105.5	-34.5	-34.9	-36.0	-3.2	-.2	.0
10	2	2	.11128	-15.7	-2.7	-3.0	-10.0	.9	-2.2	.4
10	3	1	.13342	-109.5	-35.1	-36.3	-37.1	-1.6	-.1	.0
10	3	2	.11695	-16.9	-2.9	-3.3	-10.8	.5	-1.2	.4
10	4	1	.13236	-76.8	-25.8	-27.7	-23.3	-.5	.0	.0
10	4	2	.12018	-17.6	-3.3	-3.3	-11.0	.2	-.5	.4
10	5	1	.13045	-54.7	-18.6	-21.8	-14.3	-.0	.0	.0
10	5	2	.12153	-17.8	-3.6	-3.4	-10.3	.0	-.0	.5

T	SEG	Z	W	THETA	S-XX	S-YY	S-ZZ	S-XY	S-XZ	S-YZ
11	1	1	.11170	-97.1	-29.4	-32.8	-34.9	-2.0	-.5	.1
11	1	2	.09766	-12.6	-2.5	-2.3	-7.7	.5	-2.7	1.3
11	2	1	.12495	-135.0	-41.5	-44.4	-49.1	-1.6	-.3	.1
11	2	2	.10503	-14.4	-2.4	-2.7	-9.3	.4	-2.0	1.5
11	3	1	.13064	-140.2	-43.3	-46.1	-50.8	-1.0	-.0	.2
11	3	2	.11023	-15.5	-2.6	-2.9	-10.0	.3	-1.1	1.6
11	4	1	.12779	-94.1	-29.3	-33.5	-31.3	-.5	.0	.2
11	4	2	.11213	-15.1	-3.0	-3.0	-10.1	.2	-.4	1.7
11	5	1	.12455	-62.5	-19.6	-24.5	-18.3	-.1	.0	.2
11	5	2	.11432	-16.2	-3.3	-3.0	-10.0	.0	-.0	1.7

T	SEG	Z	W	THETA	S-XX	S-YY	S-ZZ	S-XY	S-XZ	S-YZ
12	1	1	.09366	-57.7	-18.8	-18.9	-20.1	-3.3	-.3	.2
12	1	2	.08522	-10.1	-2.0	-2.3	-5.8	.8	-2.1	2.0
12	2	1	.10243	-74.2	-24.7	-23.8	-25.8	-2.5	-.2	.2
12	2	2	.09167	-11.4	-2.0	-2.6	-6.7	.6	-1.6	2.4
12	3	1	.10681	-76.8	-25.7	-24.6	-26.5	-1.4	-.0	.2
12	3	2	.09525	-12.3	-2.1	-2.8	-7.5	.4	-.9	2.6
12	4	1	.10614	-52.8	-18.3	-19.2	-16.3	-.5	.0	.3
12	4	2	.09758	-12.9	-2.3	-2.9	-7.6	.2	-.3	2.7
12	5	1	.10481	-35.6	-13.2	-13.8	-9.6	-.1	.0	.3
12	5	2	.09872	-12.9	-2.6	-2.9	-7.5	.0	-.0	2.7

T	SEG	Z	W	THETA	S-XX	S-YY	S-ZZ	S-XY	S-XZ	S-YZ
13	1	1	.07001	-21.9	-8.6	-6.1	-7.1	-3.1	-.1	.1
13	1	2	.05688	-6.9	-1.4	-2.1	-3.4	.8	-1.2	2.0

13	2	1	.07446	-22.6	-9.7	-6.1	-6.8	-2.4	-.0	.2
13	2	2	.07082	-7.8	-1.4	-2.4	-4.0	.5	-1.0	2.2
13	3	1	.07733	-22.0	-10.2	-6.1	-6.6	-1.5	-.0	.2
13	3	2	.07372	-8.3	-1.4	-2.6	-4.3	.4	-.5	2.5
13	4	1	.07825	-15.6	-8.2	-4.5	-3.9	-.7	.0	.2
13	4	2	.07552	-8.7	-1.6	-2.7	-4.4	.2	-.3	2.6
13	5	1	.07842	-12.6	-6.9	-3.4	-2.3	-.2	.0	.2
13	5	2	.07635	-8.8	-1.7	-2.7	-4.4	.0	-.0	2.6

T	SEG	Z	W	THETA	S-XX	S-YY	S-ZZ	S-XY	S-XZ	S-YZ
14	1	1	.03928	-4.3	-2.9	-.5	-1.0	-2.0	-.0	.1
14	1	2	.03868	-3.7	-.8	-1.4	-1.6	.5	-.6	1.3
14	2	1	.04108	-1.0	-2.4	.6	.7	-1.6	-.0	.1
14	2	2	.04078	-4.2	-.7	-1.6	-1.8	.4	-.5	1.5
14	3	1	.04257	-.6	-2.5	.9	1.1	-1.0	-.0	.2
14	3	2	.04235	-4.4	-.8	-1.7	-2.0	.3	-.3	1.6
14	4	1	.04360	-.8	-2.7	.8	1.1	-.5	.0	.2
14	4	2	.04339	-4.6	-.8	-1.8	-2.0	.2	-.2	1.7
14	5	1	.04412	-1.1	-2.7	.7	1.0	-.1	.0	.2
14	5	2	.04390	-4.7	-.8	-1.8	-2.1	.0	-.0	1.7

T	SEG	Z	W	THETA	S-XX	S-YY	S-ZZ	S-XY	S-XZ	S-YZ
15	1	1	.02933	2.1	-.6	1.9	.9	-1.3	.0	.0
15	1	2	.02957	-2.2	-.4	-1.1	-.7	.3	-.2	.8
15	2	1	.03002	6.5	.3	3.8	2.8	-1.1	.0	.0
15	2	2	.03086	-2.4	-.4	-1.2	-.7	.3	-.2	.9
15	3	1	.03098	7.2	.3	3.7	3.2	-.8	.0	.0
15	3	2	.03180	-2.5	-.4	-1.3	-.8	.2	-.2	1.0

15	4	1	.03176	5.2	-.4	3.2	2.4	-.5	.0	.0
15	4	2	.03246	-2.6	-.4	-1.4	-.8	.1	-.1	1.0
15	5	1	.03230	3.6	-.9	2.8	1.3	-.1	.0	.0
15	5	2	.03279	-2.7	-.4	-1.4	-.8	.0	-.0	1.0

T	SEG	Z	W	THETA	S-XX	S-YY	S-ZZ	S-XY	S-XZ	S-YZ
16	1	1	.01901	.5	-.5	1.1	-.0	-.7	.0	-.0
16	1	2	.01915	-1.1	-.2	-.6	-.2	.2	-.0	.4
16	2	1	.01943	2.1	-.2	1.7	.6	-.6	.0	.0
16	2	2	.01975	-1.2	-.2	-.7	-.2	.1	-.0	.4
16	3	1	.01986	2.5	-.2	1.9	.8	-.5	.0	-.0
16	3	2	.02023	-1.2	-.2	-.5	-.2	.1	-.0	.4
16	4	1	.02025	2.2	-.4	1.9	.7	-.3	.0	-.0
16	4	2	.02057	-1.3	-.2	-.8	-.3	.0	-.0	.5
16	5	1	.02047	1.9	-.5	1.9	.6	-.1	.0	-.0
16	5	2	.02074	-1.3	-.2	-.8	-.3	.0	-.0	.5

LATERAL OFFSET FROM TRACK CENTERLINE = 53.0 IN. = 4.42 FT
INCREMENTAL SOIL DEFLECTIONS AND STRESSES

DEPTH IN.	W IN.	S-XX PSI	S-YY PSI	S-ZZ PSI	S-XY PSI	S-XZ PSI	S-YZ PSI
6.0	.05983	-8.9	-6.5	-9.2	.0	8.4	.0
18.0	.05822	-3.7	-1.8	-7.0	.0	6.3	.0
30.0	.05620	.0	3.0	-5.6	.0	4.5	.0
54.0	.04844	-1.2	-.4	-4.0	.0	1.6	.0
120.0	.03213	-.2	-.0	-1.9	.0	.6	.0

LATERAL OFFSET FROM TRACK CENTERLINE = 53.0 IN. = 4.42 FT
INCREMENTAL SOIL DEFLECTIONS AND STRESSES

DEPTH IN.	W IN.	S-XX PSI	S-YY PSI	S-ZZ PSI	S-XY PSI	S-XZ PSI	S-YZ PSI
3.0	.06031	-10.6	-8.7	-8.8	.0	6.0	.0
9.0	.05948	-7.2	-5.2	-8.2	.0	8.0	.0
15.0	.05866	-4.8	-2.9	-7.3	.0	7.2	.0
21.0	.05775	-2.7	-.6	-6.1	.0	6.0	.0
42.0	.05271	-1.7	-.7	-4.7	.0	2.1	.0

LATERAL OFFSET FROM TRACK CENTERLINE = 54.0 IN. = 4.50 FT
INCREMENTAL SOIL DEFLECTIONS AND STRESSES

DEPTH IN.	W IN.	S-XX PSI	S-YY PSI	S-ZZ PSI	S-XY PSI	S-XZ PSI	S-YZ PSI
6.0	.05857	-8.5	-6.3	-5.8	.0	7.3	.0
18.0	.05736	-3.7	-1.7	-6.3	.0	5.7	.0
30.0	.05549	-.2	2.9	-5.3	.0	4.4	.0
54.0	.04800	-1.2	-.4	-3.9	.0	1.7	.0
120.0	.03198	-.2	-.0	-1.9	.0	.6	.0

LATERAL OFFSET FROM TRACK CENTERLINE = 54.0 IN. = 4.50 FT
INCREMENTAL SOIL DEFLECTIONS AND STRESSES

DEPTH IN.	W IN.	S-XX PSI	S-YY PSI	S-ZZ PSI	S-XY PSI	S-XZ PSI	S-YZ PSI
3.0	.05854	-9.0	-8.0	-2.6	.0	5.5	.0
9.0	.05838	-7.1	-5.0	-6.6	.0	7.4	.0
15.0	.05775	-4.7	-2.8	-6.5	.0	7.0	.0
21.0	.05694	-2.8	-.6	-6.1	.0	6.3	.0
42.0	.05215	-1.7	-.5	-4.6	.0	2.1	.0

LATERAL OFFSET FROM TRACK CENTERLINE = 55.0 IN. = 4.58 FT
INCREMENTAL SOIL DEFLECTIONS AND STRESSES

DEPTH IN.	W IN.	S-XX PSI	S-YY PSI	S-ZZ PSI	S-XY PSI	S-XZ PSI	S-YZ PSI
6.0	.05739	-7.8	-6.0	-4.0	.0	6.2	.0
18.0	.05552	-3.7	-1.6	-5.7	.0	6.5	.0
30.0	.05480	-.4	2.8	-5.1	.0	4.4	.0
54.0	.04757	-1.2	-.4	-2.8	.0	1.7	.0
120.0	.03183	-.2	-.0	-1.8	.0	.6	.0

LATERAL OFFSET FROM TRACK CENTERLINE = 55.0 IN. = 4.58 FT
INCREMENTAL SOIL DEFLECTIONS AND STRESSES

DEPTH IN.	W IN.	S-XX PSI	S-YY PSI	S-ZZ PSI	S-XY PSI	S-XZ PSI	S-YZ PSI
3.0	.05725	-7.2	-7.5	-1.3	.0	3.7	.0
9.0	.05732	-6.9	-4.9	-5.2	.0	5.8	.0
15.0	.05685	-4.7	-2.7	-5.8	.0	5.7	.0
21.0	.05614	-2.8	-.6	-3.6	.0	6.2	.0
42.0	.05153	-1.7	-.6	-4.4	.0	2.1	.0

LATERAL OFFSET FROM TRACK CENTERLINE = 56.0 IN. = 4.67 FT
INCREMENTAL SOIL DEFLECTIONS AND STRESSES

DEPTH IN.	W IN.	S-XX PSI	S-YY PSI	S-ZZ PSI	S-XY PSI	S-XZ PSI	S-YZ PSI
6.0	.05629	-7.1	-5.8	-2.8	.0	5.2	.0
18.0	.05589	-3.7	-1.5	-5.2	.0	6.3	.0
30.0	.05410	-.5	2.7	-4.9	.0	4.3	.0
54.0	.04715	-1.2	-.4	-3.7	.0	1.7	.0
120.0	.02168	-.3	.0	-1.8	.0	.6	.0

LATERAL OFFSET FROM TRACK CENTERLINE = 56.0 IN. = 4.67 FT
INCREMENTAL SOIL DEFLECTIONS AND STRESSES

DEPTH IN.	W IN.	S-XX PSI	S-YY PSI	S-ZZ PSI	S-XY PSI	S-XZ PSI	S-YZ PSI
3.0	.05610	-5.7	-7.2	-.8	.0	2.7	.0
9.0	.05630	-6.5	-4.7	-4.1	.0	6.2	.0
15.0	.05597	-4.7	-2.6	-5.1	.0	6.5	.0
21.0	.05535	-2.9	-.5	-5.2	.0	6.0	.0
42.0	.05104	-1.7	-.6	-4.3	.0	2.1	.0

LATERAL OFFSET FROM TRACK CENTERLINE = 57.0 IN. = 4.75 FT
INCREMENTAL SOIL DEFLECTIONS AND STRESSES

DEPTH IN.	W IN.	S-XX PSI	S-YY PSI	S-ZZ PSI	S-XY PSI	S-XZ PSI	S-YZ PSI
6.0	.05525	-6.3	-5.6	-2.0	.0	4.4	.0
18.0	.05486	-3.7	-1.5	-4.7	.0	6.1	.0
30.0	.05341	-.7	2.6	-4.6	.0	4.3	.0
54.0	.04673	-1.2	-.4	-3.7	.0	1.7	.0
120.0	.03154	-.3	.0	-1.8	.0	.6	.0

LATERAL OFFSET FROM TRACK CENTERLINE = 57.0 IN. = 4.75 FT
INCREMENTAL SOIL DEFLECTIONS AND STRESSES

DEPTH IN.	W IN.	S-XX PSI	S-YY PSI	S-ZZ PSI	S-XY PSI	S-XZ PSI	S-YZ PSI
3.0	.05504	-4.5	-6.8	-.4	.0	2.1	.0
9.0	.05531	-6.1	-4.5	-3.2	.0	5.6	.0
15.0	.05510	-4.6	-2.5	-4.4	.0	6.2	.0
21.0	.05457	-2.9	-.5	-4.9	.0	5.9	.0
42.0	.05049	-1.7	-.6	-4.2	.0	2.1	.0

LATERAL OFFSET FROM TRACK CENTERLINE = 58.0 IN. = 4.83 FT
INCREMENTAL SOIL DEFLECTIONS AND STRESSES

DEPTH IN.	W IN.	S-XX PSI	S-YY PSI	S-ZZ PSI	S-XY PSI	S-XZ PSI	S-YZ PSI
6.0	.05427	-5.6	-5.4	-1.4	.0	3.7	.0
18.0	.05405	-3.7	-1.5	-4.2	.0	5.9	.0
30.0	.05272	-.9	2.5	-4.4	.0	4.2	.0
54.0	.04630	-1.2	-.4	-3.6	.0	1.7	.0
120.0	.03140	-.3	.0	-1.8	.0	.6	.0

LATERAL OFFSET FROM TRACK CENTERLINE = 58.0 IN. = 4.83 FT
INCREMENTAL SOIL DEFLECTIONS AND STRESSES

DEPTH IN.	W IN.	S-XX PSI	S-YY PSI	S-ZZ PSI	S-XY PSI	S-XZ PSI	S-YZ PSI
3.0	.05405	-3.3	-5.5	-.0	.0	1.7	.0
9.0	.05437	-5.7	-4.4	-2.5	.0	5.0	.0
15.0	.05424	-4.5	-2.5	-3.9	.0	5.9	.0
21.0	.05380	-2.9	-.5	-4.4	.0	5.7	.0
42.0	.04994	-1.7	-.6	-4.0	.0	2.1	.0

LATERAL OFFSET FROM TRACK CENTERLINE = 60.0 IN. = 5.00 FT
INCREMENTAL SOIL DEFLECTIONS AND STRESSES

DEPTH IN.	W IN.	S-XX PSI	S-YY PSI	S-ZZ PSI	S-XY PSI	S-XZ PSI	S-YZ PSI
6.0	.05245	-4.4	-5.0	-.7	.0	2.8	.0
18.0	.05246	-3.5	-1.4	-3.4	.0	5.4	.0
30.0	.05135	-1.2	2.4	-4.0	.0	4.0	.0
54.0	.04545	-1.3	-.3	-2.-	.0	1.7	.0
120.0	.03112	-.3	.0	-1.7	.0	.6	.0

LATERAL OFFSET FROM TRACK CENTERLINE = 60.0 IN. = 5.00 FT
INCREMENTAL SOIL DEFLECTIONS AND STRESSES

DEPTH IN.	W IN.	S-XX PSI	S-YY PSI	S-ZZ PSI	S-XY PSI	S-XZ PSI	S-YZ PSI
3.0	.05224	-2.6	-5.0	-.0	.0	1.1	.0
9.0	.05258	-4.3	-4.1	-1.6	.0	4.1	.0
15.0	.05259	-4.2	-2.3	-3.0	.0	5.3	.0
21.0	.05227	-2.9	-.5	-3.7	.0	5.3	.0
42.0	.04882	-1.7	-.6	-2.9	.0	2.0	.0

LATERAL OFFSET FROM TRACK CENTERLINE = 65.0 IN. = 5.42 FT
INCREMENTAL SOIL DEFLECTIONS AND STRESSES

DEPTH IN.	W IN.	S-XX PSI	S-YY PSI	S-ZZ PSI	S-XY PSI	S-XZ PSI	S-YZ PSI
6.0	.04848	-2.3	-4.2	-.2	.0	1.7	.0
18.0	.04872	-3.1	-1.2	-2.1	.0	-.2	.0
30.0	.04803	-1.9	1.9	-3.1	.0	3.5	.0
54.0	.04331	-1.3	-.3	-3.0	.0	1.6	.0
120.0	.03043	-.3	.0	-1.6	.0	.6	.0

LATERAL OFFSET FROM TRACK CENTERLINE = 65.0 IN. = 5.42 FT
INCREMENTAL SOIL DEFLECTIONS AND STRESSES

DEPTH IN.	W IN.	S-XX PSI	S-YY PSI	S-ZZ PSI	S-XY PSI	S-XZ PSI	S-YZ PSI
3.0	.04832	-.9	-5.0	.0	.0	.7	.0
9.0	.04862	-3.1	-3.5	-.6	.0	2.6	.0
15.0	.04874	-3.4	-1.9	-1.6	.0	3.9	.0
21.0	.04862	-2.8	-.4	-2.4	.0	4.3	.0
42.0	.04609	-1.9	-.5	-3.2	.0	1.9	.0

LATERAL OFFSET FROM TRACK CENTERLINE = 70.0 IN. = 5.83 FT
INCREMENTAL SOIL DEFLECTIONS AND STRESSES

DEPTH IN.	W IN.	S-XX PSI	S-YY PSI	S-ZZ PSI	S-XY PSI	S-XZ PSI	S-YZ PSI
6.0	.04507	-1.1	-3.6	-.1	.0	1.2	.0
18.0	.04532	-2.6	-1.0	-1.3	.0	3.3	.0
30.0	.04489	-2.2	1.8	-2.4	.0	2.9	.0
54.0	.04120	-1.3	-.3	-2.6	.0	1.6	.0
120.0	.02971	-.3	.0	-1.6	.0	.7	.0

Appendix B: Slope Stability with Negative Pore-Water Pressures, Computer Output

A slope stability analysis was conducted as an example problem with negative pore-water pressures. The results of the analysis are presented in this appendix. The PC-SLOPE computer program (Fredlund, 1985) was used with negative pore-water pressures entered into the analysis as a grid of points superimposed onto the problem geometry. The values used for the negative pore-water pressures were generated through the use of the PC-SEEP computer program (Fredlund, 1990) using typical rainfall data for the example location. Two methods, (i.e., "four-way interpolation" and "kriging - spline interpolation"), can be used as an interface between the finite element PC-SEEP analysis and the limit equilibrium PC-SLOPE analysis (McClarty and Fredlund, 1990). The kriging - spline interpolation method is considered more accurate and has been utilized for the example problem.

The steps which were undertaken to perform the slope stability analysis are illustrated in the flow chart in Figure B-1. The steps taken in the analysis are described below:

1) **Generate Mesh:** The geometry for the PC-SEEP problem was laid out and the finite element mesh was generated for the hypothetical example problem. The example problem simulates a 3.3 meter high railway embankment with 4:1 side-slopes consisting of silty clay till and highly plastic clay. The water table for the hypothetical problem was located 5.4 meters below

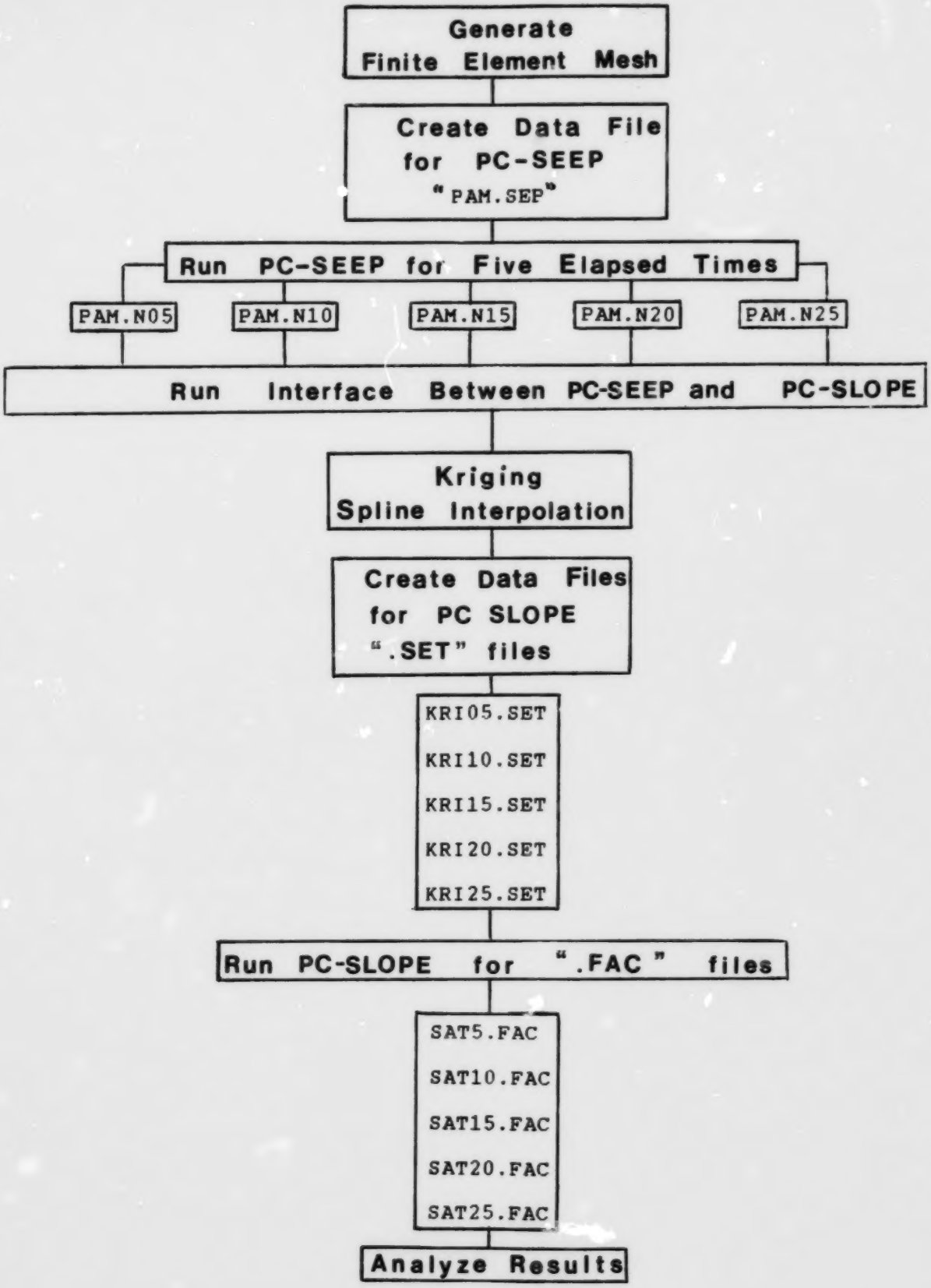

Figure B-1: Flow Chart for Slope Stability Problem with Negative Pore-Water Pressures

the top of the embankment. Node and element numbers were generated for the example problem as illustrated in Figures B-2 and B-3. Details regarding the mesh generation procedure are described in the PC-SEEP User's Manual (Fredlund, 1990).

2) **Create Data File for PC-SEEP:** The next step involved the estimation of the soil permeability and water storage properties, boundary conditions at the surface and at depth, the specification of time step increments, convergence tolerance, and desired number of iterations for the problem under consideration. A "**.SEP**" file was created as the data **input** file for the **PC-SEEP** computer program. The data file **PAM.SEP** was created for the hypothetical example problem using reasonable unsaturated permeability functions based upon experience. (For an actual situation, the soil parameters would likely be measured in the laboratory.) The hypothetical problem was assumed to be subjected to a continuous surface boundary flux of 1.16E-07 m/s which corresponds to approximately 1 centimeter per day of precipitation. During the computational process, review boundaries were added to allow water seepage at the toe of the embankment.

FINITE ELEMENT MESH

SERIAL NO.87011 is licensed to: LEONARD LAM

BEARING CAPACITY REPORT APPENDIX B

MARCH 2, 1990

Demonstration of use of PC-SEEP for -ve pwp beneath track

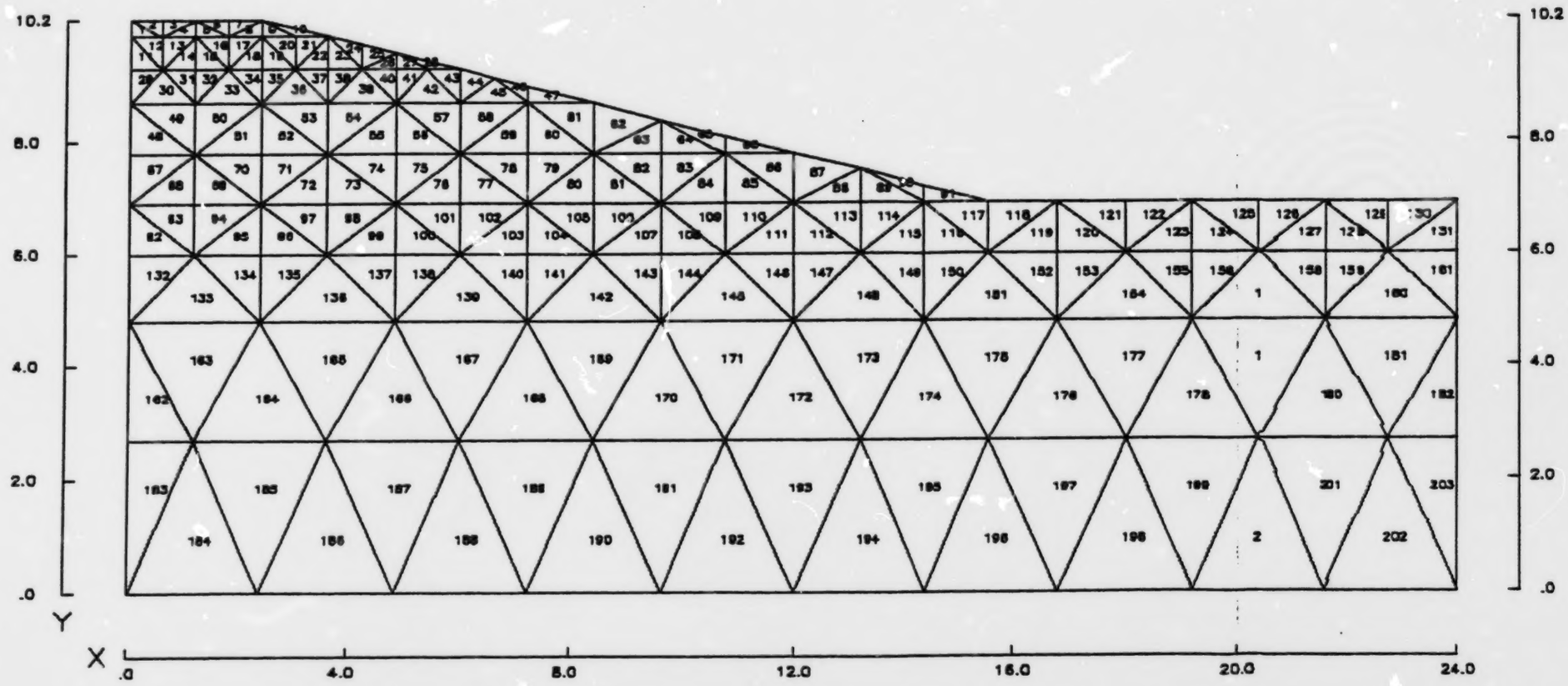

Figure B-2: Finite Element Mesh for PC-SEEP Showing Element Numbers

FINITE ELEMENT MESH

SERIAL NO.87011 is licensed to: LEONARD LAM

BEARING CAPACITY REPORT APPENDIX B

MARCH 2, 1990

Demonstration of use of PC-SEEP for -ve pwp beneath track

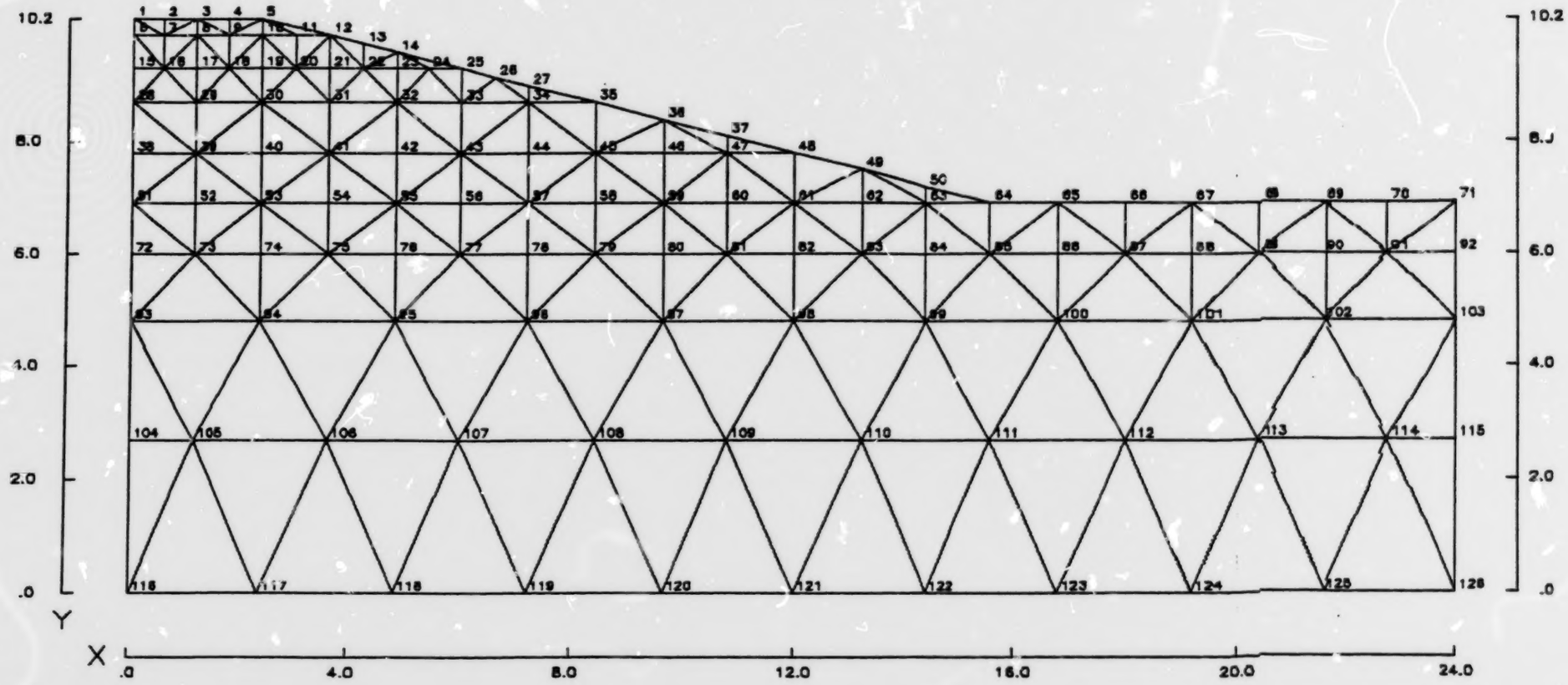

Figure B-3: Finite Element Mesh for PC-SEEP Showing Node Numbers

3) **Run PC-SEEP Computations:** The PC-SEEP computer program was run for the PAM.SEP data file with output generated for five successive elapsed time intervals. Files **PAM.N05**, **PAM.N10**, **PAM.N15**, **PAM.N20**, and **PAM.N25** were generated for elapsed times 8.037E+04 seconds, 2.804E+05 seconds, 6.147E+05 seconds, 9.491E+05 seconds, and 1.283E+06 seconds. The corresponding times in days are: 0.93, 3.25, 7.11, 10.98, and 14.85, respectively. The generated files are included in this Appendix.

4) **Interface Between PC-SEEP and PC-SLOPE:** The total head values generated as PC-SEEP output were reduced to a reasonable number of input values for the PC-SLOPE computer program. The procedures are in accordance with methods currently under investigation by Fredlund and McClarty (1990) at the University of Saskatchewan (See attached technical paper). The "kriging - spline interpolation" method was used to reduce the values to a grid for input into the PC-SLOPE computer program. The data files generated for input into the PC-SLOPE computer program by the kriging method are illustrated in Figure B-1 as the **KRI** series.

5) **Create Data Files for PC-SLOPE:** The cross-section geometry was generated for the PC-

SLOPE computer program according to the details provided in the PS-SLOPE User's Manual (Fredlund, 1985). Then, five data files were generated within the KRI series corresponding to the five output files generated by PC-SEEP for the five elapsed time intervals (i.e., files KRI05.SET, KRI10.SET, KRI15.SET, KRI20.SET, and KRI25.SET were generated corresponding to files PAM.N05, PAM.N10, PAM.N15, PAM.N20, and PAM.N25). Only one file (i.e., file **KRI05.SET** corresponding to the **kriging - spline interpolation** of the total head values from file **PAM.N05**) is included in the Appendix.

6) **Run PC-SLOPE Computations:** Each of the five "**.SET**" files in the KRI series (i.e., five files altogether) were input as data files to the PC-SLOPE computer program. The minimum factor of safety was found for each data file. Five factor of safety (i.e., .FAC files) files were generated. The five factor of safety files generated were: **SAT5.FAC**, **SAT10.FAC**, **SAT15.FAC**, **SAT20.FAC**, and **SAT25.FAC**. The SAT**5**.FAC file has been included in the Appendix. A plot of geometry of the slope failure is illustrated in Figure **B**-4 for SAT**5**.FAC while the contours of the minimum factor of safety from the SAT**5**.FAC file are illustrated in Figure **B**-5.

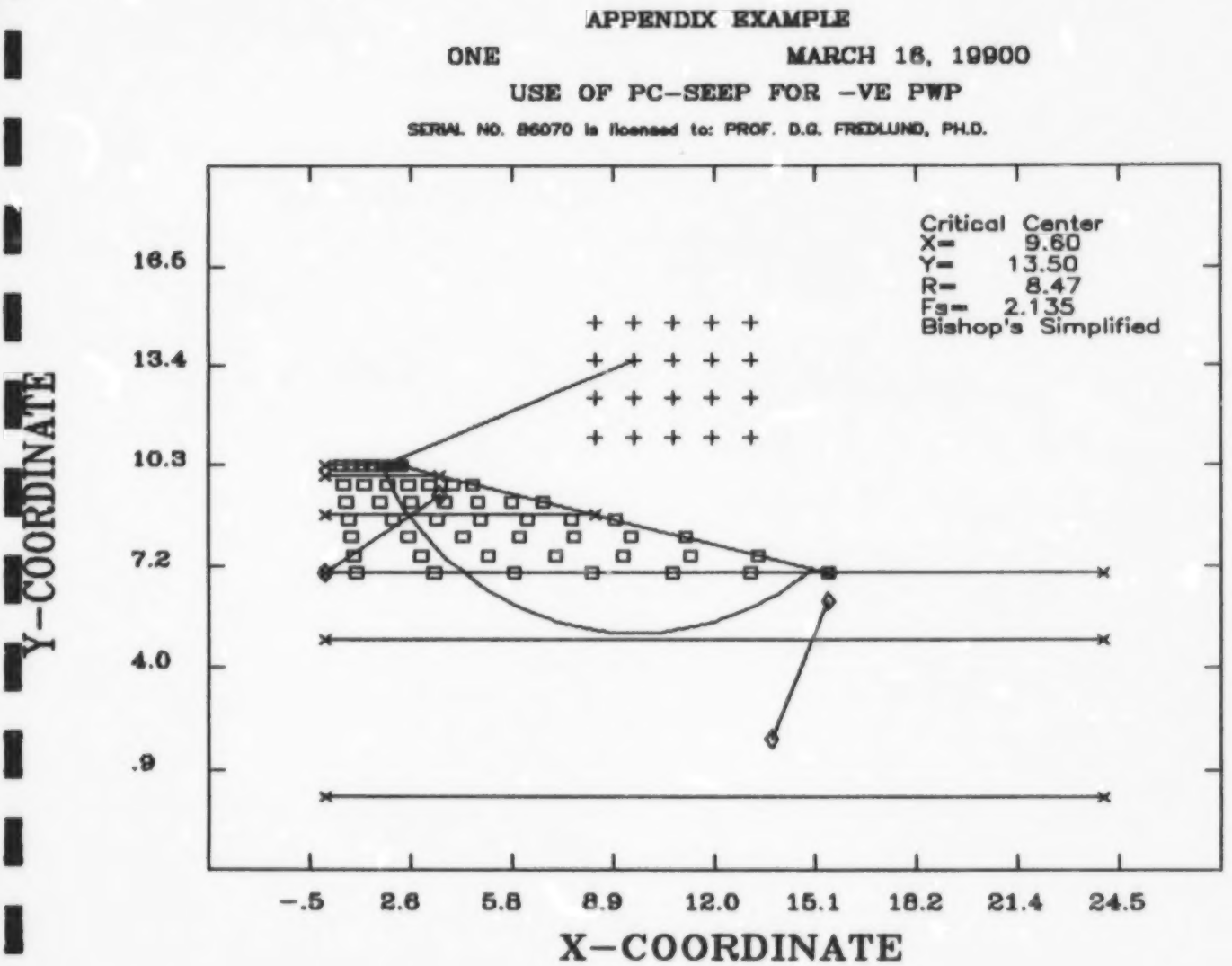

UNIT WEIGHT	COHESION	PHI	DESCRIPTION
18.00	.00	40.00	Ballast
18.00	2.50	25.00	Sandy Silty Subballast
18.00	2.50	10.00	Clay Fill
18.00	5.00	10.00	Clay
18.00	5.00	15.00	Clay
18.00	5.00	20.00	Clay

File name : SAT5.SET

Figure B-4: **CROSS-SECTION OF GEOMETRY**

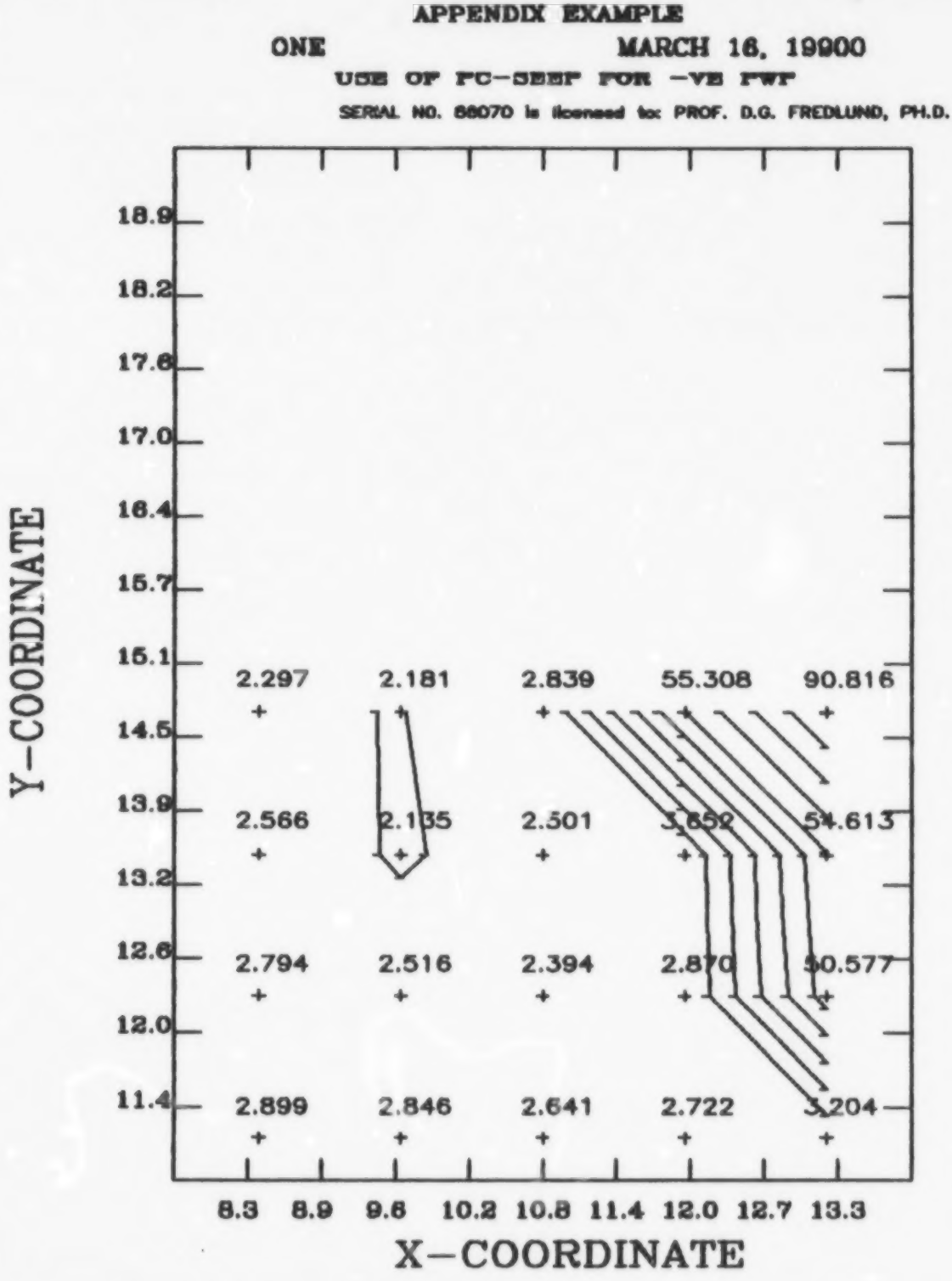

Figure B-5: **GRID OF FACTORS OF SAFETY**

7) **Analyze Slope Stability Results:** The minimum factor of safety by Bishop's Simplified Method was extracted from each generated factor of safety file and plotted against the elapsed time. Table B:1 presents a summary of the minimum factors of safety versus elapsed time. As the 1 cm/day rainfall continues, the factor of safety of the embankment slope decreases. (The increase in factor of safety in the latter elapsed times is due to water ponding to such an extent that the slope is laterally supported by the water. This phenomenon could have been avoided by specifying a lower value for the allowed ponding depth within the PC-SLOPE computer analysis. Therefore, only the first three elapsed time intervals are valid for the kriging - spline interpolation method). A plot of the decrease in factor of safety versus time for the 1 cm/day rainfall is illustrated in Figure B-6 for the kriging - spline interpolation method. Let us assume failure of the embankment slope occurs at a factor of safety equal to 1.0. According to the results generated by the kriging - spline interpolation method, failure of the hypothetical embankment slope would occur between the 2nd and 3rd day of consecutive rainfall at the rate of 1 cm/day. According to Fredlund and

Table B-1: Minimum Factor of Safety Versus Time

KRIGING - SPLINE INTERPOLATION

F.S.	TIME (sec)	TIME (days)
2.135	80370	0.93
0.580	280400	3.25
0.411	614700	7.11
0.617	949100	10.98
1.235	1283000	14.85

Slip Failure Surface Changing

FACTOR OF SAFETY VS TIME
KRIGING – SPLINE INTERPOLATION

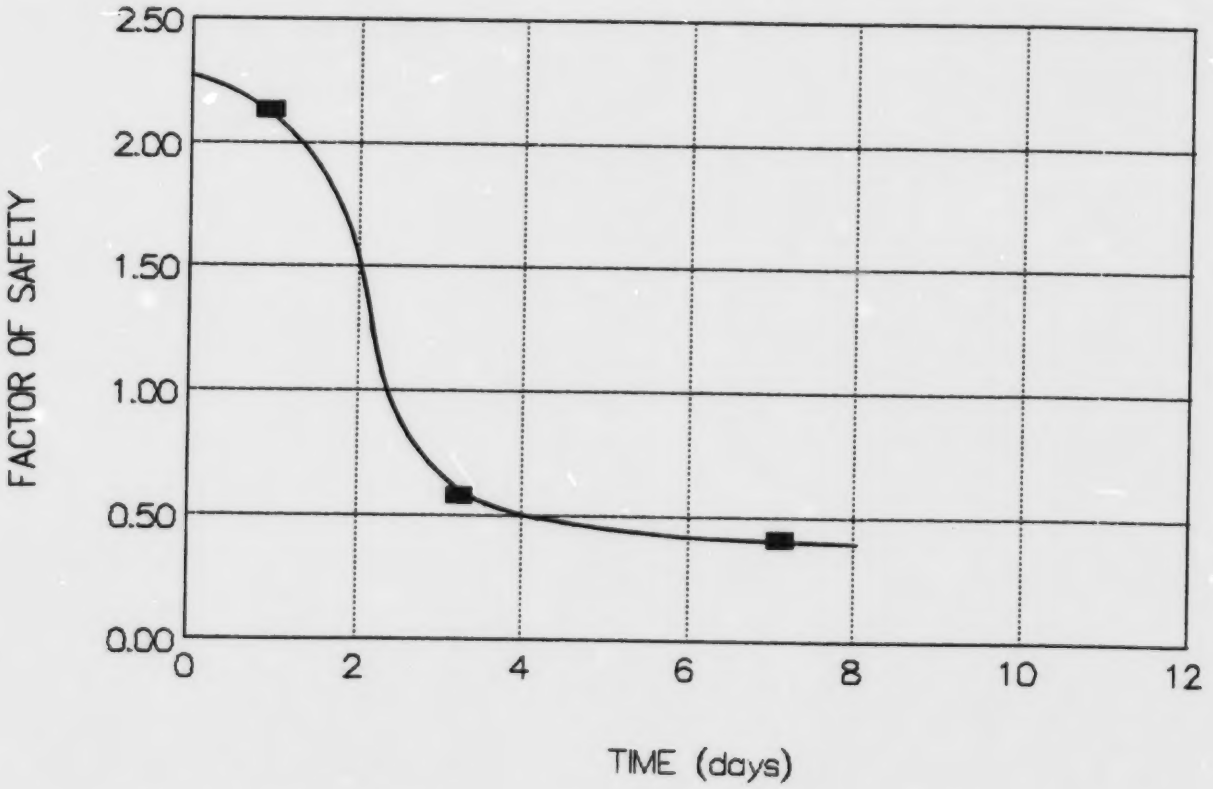

Figure B-6: Factor of Safety with Time for Kriging – Spline Interpolation of Negative Pore-Water Pressures

McClarty (1990) the "kriging - spline interpolation" method is felt to be superior to methods presently utilized for reduction of negative pore-water pressures.

8) **Conclusions and Recommendations**: The preceeding example illustrates the significance of utilizing seepage analyses for performing slope stability analyses for soils with negative pore-water pressures. Further research into the kriging - spline interpolation method is recommended.

DAM.SEP Data File

```
TITLE
     BEARING CAPACITY REPORT APPENDIX B
     ONE              = TRIAL NUMBER
     MARCH 2, 1990    = DATE
     Use of PC-SEEP for -ve pwp beneath track
CONTROL
               2,     = TYPE OF ANALYSIS(1=S-STATE, 2=TRANSIENT)
               1,     = PROBLEM TYPE (1=PLANE 2-D, 2=AXISYMMETRIC, 3=PLAN)
               1,     = ITERATION METHOD (1=R.SUB., 2=SECANT)
               1,     = TIME INTEGRATION SCHEME (1=BD, 2=CD)
UNITS
               1,     = LENGTH UNITS (1=METRES, 2=FEET)
               1,     = TIME UNITS (1=SEC,2=MIN,3=HR,4=DAY,5=YEAR)
CONVERGE
              20,     = MAXIMUM NUMBER OF ITERATIONS
             5.0,     = CONVERG. TOLERANCE BY HEAD (IN %)
            10.0,     = CONVERG. TOLERANCE BY PERM.(IN %)
             2.0,     = CONVERGENCE TOLERANCE (IN %) AT STEADY STATE
TIME
               1,     = NUMBER OF TIME SEGMENTS
       .0000E+00,     = SEGMENT  1 START TIME
       .0000E+00,     = START TIME
        10800.00,     = INITIAL TIME STEP
            1.20,     = TIME STEP EXPAND FACTOR
        66870.78,     = MAXIMUM SIZE OF TIME STEP
              25,     = NUMBER OF TIME STEPS
               5,     = TIME STEP INTERVAL FOR OUTPUT
SOIL      ,  5
    1,      .1000E-02,       1.00,        .00,    1,    0,
    2,      .1000E-04,       1.00,        .00,    2,    2,
       .00,      .1000E-04,      = NEGATIVE PRESSURE, COEF.OF PERMEABILITY
    -60.00,      .1000E-06,      = NEGATIVE PRESSURE, COEF.OF PERMEABILITY
    3,      .1000E-07,       1.00,        .00,    1,    0,
    4,      .1000E-07,       1.00,        .00,    2,    2,
       .00,      .1000E-07,      = NEGATIVE PRESSURE, COEF.OF PERMEABILITY
    -60.00,      .1000E-09,      = NEGATIVE PRESSURE, COEF.OF PERMEABILITY
    5,      .1000E-08,       1.00,        .00,    1,    0,
STORAGE   ,    5
    1,    1,    1,                 = SOIL NUMBER, TYPE
       .000002,          .150000, = SAT. AND  UNSAT. STORAGE COEF.
    2,    1,    1,                 = SOIL NUMBER, TYPE
       .000002,          .015000, = SAT. AND  UNSAT. STORAGE COEF.
    3,    1,    1,                 = SOIL NUMBER, TYPE
       .001500,          .001500, = SAT. AND  UNSAT. STORAGE COEF.
    4,    1,    1,                 = SOIL NUMBER, TYPE
       .001500,          .001500, = SAT. AND  UNSAT. STORAGE COEF.
    5,    1,    1,                 = SOIL NUMBER, TYPE
       .001500,          .001500, = SAT. AND  UNSAT. STORAGE COEF.
BOUNDARY  ,    7
    1,  116,    1,    1,          = START NODE, END NODE, BNDRY TYPE
      .0000E+00,  .0000000E+00, = TIME, BNDRY VALUE
    2,    5,    1,    1,          = START NODE, END NODE, BNDRY TYPE
      .0000E+00,  .1160000E-06, = TIME, BNDRY VALUE
   12,   64,    1,    1,          = START NODE, END NODE, BNDRY TYPE
      .0000E+00,  .1160000E-06, = TIME, BNDRY VALUE
   65,   70,    1,    1,          = START NODE, END NODE, BNDRY TYPE
      .0000E+00,  .1160000E-06, = TIME, BNDRY VALUE
```

```
   71,   92,    1,    1,          = START NODE, END NODE, BNDRY TYPE
     .0000E+00,  .0000000E+00, = TIME, BNDRY VALUE
  103,  126,    2,    1,          = START NODE, END NODE, BNDRY TYPE
     .0000E+00,  .4800000E+01, = TIME, BNDRY VALUE
  117,  125,    1,    1,          = START NODE, END NODE, BNDRY TYPE
     .0000E+00,  .0000000E+00, = TIME, BNDRY VALUE
RBOUNDARY ,    0
FLUX      ,    0
NODE      ,  126
    1,       .000,      10.200,  .4800000E+01,    0,
    2,       .600,      10.200,  .4800000E+01,    1,
    3,      1.200,      10.200,  .4800000E+01,    1,
    4,      1.800,      10.200,  .4800000E+01,    1,
    5,      2.400,      10.200,  .4800000E+01,    0,
    6,       .000,       9.900,  .4800000E+01,    0,
    7,       .600,       9.900,  .4800000E+01,    1,
    8,      1.200,       9.900,  .4800000E+01,    1,
    9,      1.800,       9.900,  .4800000E+01,    1,
   10,      2.400,       9.900,  .4800000E+01,    1,
   11,      3.000,       9.900,  .4800000E+01,    1,
   12,      3.600,       9.900,  .4800000E+01,    0,
   13,      4.200,       9.750,  .4800000E+01,    0,
   14,      4.800,       9.600,  .4800000E+01,    0,
   15,       .000,       9.300,  .4800000E+01,    0,
   16,       .600,       9.300,  .4800000E+01,    1,
   17,      1.200,       9.300,  .4800000E+01,    1,
   18,      1.800,       9.300,  .4800000E+01,    1,
   19,      2.400,       9.300,  .4800000E+01,    1,
   20,      3.000,       9.300,  .4800000E+01,    1,
   21,      3.600,       9.300,  .4800000E+01,    1,
   22,      4.200,       9.300,  .4800000E+01,    1,
   23,      4.800,       9.300,  .4800000E+01,    1,
   24,      5.400,       9.300,  .4800000E+01,    1,
   25,      6.000,       9.300,  .4800000E+01,    0,
   26,      6.600,       9.150,  .4800000E+01,    0,
   27,      7.200,       9.000,  .4800000E+01,    0,
   28,       .000,       8.700,  .4800000E+01,    0,
   29,      1.200,       8.700,  .4800000E+01,    1,
   30,      2.400,       8.700,  .4800000E+01,    1,
   31,      3.600,       8.700,  .4800000E+01,    1,
   32,      4.800,       8.700,  .4800000E+01,    1,
   33,      6.000,       8.700,  .4800000E+01,    1,
   34,      7.200,       8.700,  .4800000E+01,    1,
   35,      8.400,       8.700,  .4800000E+01,    0,
   36,      9.600,       8.400,  .4800000E+01,    0,
   37,     10.800,       8.100,  .4800000E+01,    0,
   38,       .000,       7.800,  .4800000E+01,    0,
   39,      1.200,       7.800,  .4800000E+01,    1,
   40,      2.400,       7.800,  .4800000E+01,    1,
   41,      3.600,       7.800,  .4800000E+01,    1,
   42,      4.800,       7.800,  .4800000E+01,    1,
   43,      6.000,       7.800,  .4800000E+01,    1,
   44,      7.200,       7.800,  .4800000E+01,    1,
   45,      8.400,       7.800,  .4800000E+01,    1,
   46,      9.600,       7.800,  .4800000E+01,    1,
   47,     10.800,       7.800,  .4800000E+01,    1,
```

```
 48,     12.000,      7.800,   .4800000E+01,    0,
 49,     13.200,      7.500,   .4800000E+01,    0,
 50,     14.400,      7.200,   .4800000E+01,    0,
 51,       .000,      6.900,   .4800000E+01,    0,
 52,      1.200,      6.900,   .4800000E+01,    1,
 53,      2.400,      6.900,   .4800000E+01,    1,
 54,      3.600,      6.900,   .4800000E+01,    1,
 55,      4.800,      6.900,   .4800000E+01,    1,
 56,      6.000,      6.900,   .4800000E+01,    1,
 57,      7.200,      6.900,   .4800000E+01,    1,
 58,      8.400,      6.900,   .4800000E+01,    1,
 59,      9.600,      6.900,   .4800000E+01,    1,
 60,     10.800,      6.900,   .4800000E+01,    1,
 61,     12.000,      6.900,   .4800000E+01,    1,
 62,     13.200,      6.900,   .4800000E+01,    1,
 63,     14.400,      6.900,   .4800000E+01,    1,
 64,     15.600,      6.900,   .4800000E+01,    1,
 65,     16.800,      6.900,   .4800000E+01,    1,
 66,     18.000,      6.900,   .4800000E+01,    1,
 67,     19.200,      6.900,   .4800000E+01,    1,
 68,     20.400,      6.900,   .4800000E+01,    1,
 69,     21.600,      6.900,   .4800000E+01,    1,
 70,     22.800,      6.900,   .4800000E+01,    1,
 71,     24.000,      6.900,   .4800000E+01,    0,
 72,       .000,      6.000,   .4800000E+01,    0,
 73,      1.200,      6.000,   .4800000E+01,    1,
 74,      2.400,      6.000,   .4800000E+01,    1,
 75,      3.600,      6.000,   .4800000E+01,    1,
 76,      4.800,      6.000,   .4800000E+01,    1,
 77,      6.000,      6.000,   .4800000E+01,    1,
 78,      7.200,      6.000,   .4800000E+01,    1,
 79,      8.400,      6.000,   .4800000E+01,    1,
 80,      9.600,      6.000,   .4800000E+01,    1,
 81,     10.800,      6.000,   .4800000E+01,    1,
 82,     12.000,      6.000,   .4800000E+01,    1,
 83,     13.200,      6.000,   .4800000E+01,    1,
 84,     14.400,      6.000,   .4800000E+01,    1,
 85,     15.600,      6.000,   .4800000E+01,    1,
 86,     16.800,      6.000,   .4800000E+01,    1,
 87,     18.000,      6.000,   .4800000E+01,    1,
 88,     19.200,      6.000,   .4800000E+01,    1,
 89,     20.400,      6.000,   .4800000E+01,    1,
 90,     21.600,      6.000,   .4800000E+01,    1,
 91,     22.800,      6.000,   .4800000E+01,    1,
 92,     24.000,      6.000,   .4800000E+01,    0,
 93,       .000,      4.800,   .4800000E+01,    0,
 94,      2.400,      4.800,   .4800000E+01,    1,
 95,      4.800,      4.800,   .4800000E+01,    1,
 96,      7.200,      4.800,   .4800000E+01,    1,
 97,      9.600,      4.800,   .4800000E+01,    1,
 98,     12.000,      4.800,   .4800000E+01,    1,
 99,     14.100,      4.800,   .4800000E+01,    1,
100,     16.800,      4.800,   .4800000E+01,    1,
101,     19.200,      4.800,   .4800000E+01,    1,
102,     21.600,      4.800,   .4800000E+01,    1,
```

```
  103,      24.000,        4.800,   .4800000E+01,     0,
  104,        .000,        2.700,   .4800000E+01,     0,
  105,       1.200,        2.700,   .4800000E+01,     0,
  106,       3.600,        2.700,   .4800000E+01,     1,
  107,       6.000,        2.700,   .4800000E+01,     1,
  108,       8.400,        2.700,   .4800000E+01,     1,
  109,      10.800,        2.700,   .4800000E+01,     1,
  110,      13.200,        2.700,   .4800000E+01,     1,
  111,      15.600,        2.700,   .4800000E+01,     1,
  112,      18.000,        2.700,   .4800000E+01,     1,
  113,      20.400,        2.700,   .4800000E+01,     1,
  114,      22.800,        2.700,   .4800000E+01,     0,
  115,      24.000,        2.700,   .4800000E+01,     0,
  116,        .000,         .000,   .4800000E+01,     0,
  117,       2.400,         .000,   .4800000E+01,     1,
  118,       4.800,         .000,   .4800000E+01,     1,
  119,       7.200,         .000,   .4800000E+01,     1,
  120,       9.600,         .000,   .4800000E+01,     1,
  121,      12.000,         .000,   .4800000E+01,     1,
  122,      14.400,         .000,   .4800000E+01,     1,
  123,      16.800,         .000,   .4800000E+01,     1,
  124,      19.200,         .000,   .4800000E+01,     1,
  125,      21.600,         .000,   .4800000E+01,     1,
  126,      24.000,         .000,   .4800000E+01,     0,
ELEMENT     ,  203
    1,    7,    1,    6,    1,    1,    0,     1.000,
    2,    7,    2,    1,    1,    0,    1,     1.000,
    3,    7,    3,    2,    1,    0,    1,     1.000,
    4,    7,    8,    3,    1,    0,    1,     1.000,
    5,    9,    3,    8,    1,    0,    1,     1.000,
    6,    9,    4,    3,    1,    0,    1,     1.000,
    7,    9,    5,    4,    1,    0,    1,     1.000,
    8,    9,   10,    5,    1,    1,    1,     1.000,
    9,   11,    5,   10,    1,    0,    1,     1.000,
   10,   12,    5,   11,    1,    1,    0,     1.000,
   11,   16,    6,   15,    2,    1,    0,     1.000,
   12,   16,    7,    6,    2,    0,    1,     1.000,
   13,   16,    8,    7,    2,    0,    1,     1.000,
   14,   16,   17,    8,    2,    0,    1,     1.000,
   15,   18,    8,   17,    2,    0,    1,     1.000,
   16,   18,    9,    8,    2,    0,    1,     1.000,
   17,   18,   10,    9,    2,    0,    1,     1.000,
   18,   18,   19,   10,    2,    0,    1,     1.000,
   19,   20,   10,   19,    2,    0,    1,     1.000,
   20,   20,   11,   10,    2,    0,    1,     1.000,
   21,   20,   12,   11,    2,    0,    1,     1.000,
   22,   20,   21,   12,    2,    1,    1,     1.000,
   23,   22,   12,   21,    2,    0,    1,     1.000,
   24,   22,   13,   12,    2,    0,    1,     1.000,
   25,   22,   14,   13,    2,    2,    1,     1.000,
   26,   22,   23,   14,    2,    1,    0,     1.000,
   27,   23,   24,   14,    1,    0,    0,     1.000,
   28,   24,   25,   14,    1,    0,    0,     1.000,
   29,   28,   16,   15,    2,    3,    0,     1.000,
   30,   28,   29,   16,    2,    0,    1,     1.000,
   31,   29,   17,   16,    2,    0,    1,     1.000,
```

```
32,   29,   18,   17,   2,   0,   1,   1.000,
33,   29,   30,   18,   2,   0,   1,   1.000,
34,   30,   19,   18,   2,   0,   1,   1.000,
35,   30,   20,   19,   2,   0,   1,   1.000,
36,   30,   31,   20,   2,   0,   1,   1.000,
37,   31,   21,   20,   2,   0,   1,   1.000,
38,   31,   22,   21,   2,   0,   1,   1.000,
39,   31,   32,   22,   2,   0,   1,   1.000,
40,   32,   23,   22,   2,   0,   1,   1.000,
41,   32,   24,   23,   2,   0,   1,   1.000,
42,   32,   33,   24,   2,   0,   1,   1.000,
43,   33,   25,   24,   2,   0,   1,   1.000,
44,   33,   26,   25,   2,   2,   1,   1.000,
45,   33,   34,   26,   2,   0,   1,   1.000,
46,   34,   27,   26,   2,   3,   0,   1.000,
47,   34,   35,   27,   2,   0,   0,   1.000,
48,   39,   28,   38,   3,   1,   0,   1.000,
49,   39,   29,   28,   3,   0,   1,   1.000,
50,   39,   30,   29,   3,   0,   1,   1.000,
51,   39,   40,   30,   3,   0,   1,   1.000,
52,   41,   30,   40,   3,   0,   1,   1.000,
53,   41,   31,   30,   3,   0,   1,   1.000,
54,   41,   32,   31,   3,   0,   1,   1.000,
55,   41,   42,   32,   3,   0,   1,   1.000,
56,   43,   32,   42,   3,   0,   1,   1.000,
57,   43,   33,   32,   3,   0,   1,   1.000,
58,   43,   34,   33,   3,   0,   1,   1.000,
59,   43,   44,   34,   3,   0,   1,   1.000,
60,   45,   34,   44,   3,   0,   1,   1.000,
61,   45,   35,   34,   3,   0,   1,   1.000,
62,   45,   36,   35,   3,   0,   1,   1.000,
63,   45,   46,   36,   3,   2,   1,   1.000,
64,   47,   36,   46,   3,   0,   1,   1.000,
65,   47,   37,   36,   3,   1,   0,   1.000,
66,   47,   48,   37,   3,   0,   0,   1.000,
67,   51,   39,   38,   3,   2,   0,   1.000,
68,   51,   52,   39,   3,   0,   1,   1.000,
69,   53,   39,   52,   3,   0,   1,   1.000,
70,   53,   40,   39,   3,   0,   1,   1.000,
71,   53,   41,   40,   3,   0,   1,   1.000,
72,   53,   54,   41,   3,   0,   1,   1.000,
73,   55,   41,   54,   3,   0,   1,   1.000,
74,   55,   42,   41,   3,   0,   1,   1.000,
75,   55,   43,   42,   3,   0,   1,   1.000,
76,   55,   56,   43,   3,   0,   1,   1.000,
77,   57,   43,   56,   3,   0,   1,   1.000,
78,   57,   44,   43,   3,   2,   1,   1.000,
79,   57,   45,   44,   3,   0,   1,   1.000,
80,   57,   58,   45,   3,   0,   1,   1.000,
81,   59,   45,   58,   3,   0,   1,   1.000,
82,   59,   46,   45,   3,   0,   1,   1.000,
83,   59,   47,   46,   3,   0,   1,   1.000,
84,   59,   60,   47,   3,   0,   1,   1.000,
85,   61,   47,   60,   3,   2,   1,   1.000,
86,   61,   48,   47,   3,   0,   1,   1.000,
```

```
 87,   61,   49,   48,   3,   0,   1,   1.000,
 88,   61,   62,   49,   3,   0,   1,   1.000,
 89,   63,   49,   62,   3,   0,   1,   1.000,
 90,   63,   50,   49,   3,   2,   0,   1.000,
 91,   63,   64,   50,   3,   0,   0,   1.000,
 92,   73,   51,   72,   4,   1,   0,   1.000,
 93,   73,   52,   51,   4,   0,   1,   1.000,
 94,   73,   53,   52,   4,   0,   1,   1.000,
 95,   73,   74,   53,   4,   0,   1,   1.000,
 96,   75,   53,   74,   4,   0,   1,   1.000,
 97,   75,   54,   53,   4,   0,   1,   1.000,
 98,   75,   55,   54,   4,   0,   1,   1.000,
 99,   75,   76,   55,   4,   0,   1,   1.000,
100,   77,   55,   76,   4,   0,   1,   1.000,
101,   77,   56,   55,   4,   0,   1,   1.000,
102,   77,   57,   56,   4,   0,   1,   1.000,
103,   77,   78,   57,   4,   0,   1,   1.000,
104,   79,   57,   78,   4,   0,   1,   1.000,
105,   79,   58,   57,   4,   0,   1,   1.000,
106,   79,   59,   58,   4,   0,   1,   1.000,
107,   79,   80,   59,   4,   0,   1,   1.000,
108,   81,   59,   80,   4,   0,   1,   1.000,
109,   81,   60,   59,   4,   0,   1,   1.000,
110,   81,   61,   60,   4,   0,   1,   1.000,
111,   81,   82,   61,   4,   0,   1,   1.000,
112,   83,   61,   82,   4,   0,   1,   1.000,
113,   83,   62,   61,   4,   0,   1,   1.000,
114,   83,   63,   62,   4,   0,   1,   1.000,
115,   83,   84,   63,   4,   0,   1,   1.000,
116,   85,   63,   84,   4,   0,   1,   1.000,
117,   85,   64,   63,   4,   0,   1,   1.000,
118,   85,   65,   64,   4,   0,   1,   1.000,
119,   85,   86,   65,   4,   0,   1,   1.000,
120,   87,   65,   86,   4,   0,   1,   1.000,
121,   87,   66,   65,   4,   0,   1,   1.000,
122,   87,   67,   66,   4,   0,   1,   1.000,
123,   87,   88,   67,   4,   0,   1,   1.000,
124,   89,   67,   88,   4,   2,   1,   1.000,
125,   89,   68,   67,   4,   3,   1,   1.000,
126,   89,   69,   68,   4,   0,   1,   1.000,
127,   89,   90,   69,   4,   0,   1,   1.000,
128,   91,   69,   90,   4,   0,   1,   1.000,
129,   91,   70,   69,   4,   0,   1,   1.000,
130,   91,   71,   70,   4,   0,   1,   1.000,
131,   91,   92,   71,   4,   1,   0,   1.000,
132,   93,   73,   72,   4,   3,   0,   1.000,
133,   93,   94,   73,   4,   0,   1,   1.000,
134,   94,   74,   73,   4,   0,   1,   1.000,
135,   94,   75,   74,   4,   0,   1,   1.000,
136,   94,   95,   75,   4,   0,   1,   1.000,
137,   95,   76,   75,   4,   0,   1,   1.000,
138,   95,   77,   76,   4,   0,   1,   1.000,
139,   95,   96,   77,   4,   0,   1,   1.000,
```

```
140,   96,   78,   77,   4,   0,   1,   1.000,
141,   96,   79,   78,   4,   0,   1,   1.000,
142,   96,   97,   79,   4,   0,   1,   1.000,
143,   97,   80,   79,   4,   0,   1,   1.000,
144,   97,   81,   80,   4,   0,   1,   1.000,
145,   97,   98,   81,   4,   0,   1,   1.000,
146,   98,   82,   81,   4,   0,   1,   1.000,
147,   98,   83,   82,   4,   0,   1,   1.000,
148,   98,   99,   83,   4,   0,   1,   1.000,
149,   99,   84,   83,   4,   0,   1,   1.000,
150,   99,   85,   84,   4,   0,   1,   1.000,
151,   99,  100,   85,   4,   0,   1,   1.000,
152,  100,   86,   85,   4,   0,   1,   1.000,
153,  100,   87,   86,   4,   0,   1,   1.000,
154,  100,  101,   87,   4,   3,   1,   1.000,
155,  101,   88,   87,   4,   4,   1,   1.000,
156,  101,   89,   88,   4,   0,   1,   1.000,
157,  101,  102,   89,   4,   0,   1,   1.000,
158,  102,   90,   89,   4,   0,   1,   1.000,
159,  102,   91,   90,   4,   0,   1,   1.000,
160,  102,  103,   91,   4,   0,   1,   1.000,
161,  103,   92,   91,   4,   3,   0,   1.000,
162,  105,   93,  104,   5,   4,   0,   1.000,
163,  105,   94,   93,   5,   0,   1,   1.000,
164,  105,  106,   94,   5,   0,   1,   1.000,
165,  106,   95,   94,   5,   0,   1,   1.000,
166,  106,  107,   95,   5,   0,   1,   1.000,
167,  107,   96,   95,   5,   0,   1,   1.000,
168,  107,  108,   96,   5,   0,   1,   1.000,
169,  108,   97,   96,   5,   0,   1,   1.000,
170,  108,  109,   97,   5,   0,   1,   1.000,
171,  109,   98,   97,   5,   0,   1,   1.000,
172,  109,  110,   98,   5,   0,   1,   1.000,
173,  110,   99,   98,   5,   0,   1,   1.000,
174,  110,  111,   99,   5,   0,   1,   1.000,
175,  111,  100,   99,   5,   4,   1,   1.000,
176,  111,  112,  100,   5,   5,   1,   1.000,
177,  112,  101,  100,   5,   0,   1,   1.000,
178,  112,  113,  101,   5,   0,   1,   1.000,
179,  113,  102,  101,   5,   0,   1,   1.000,
180,  113,  114,  102,   5,   0,   1,   1.000,
181,  114,  103,  102,   5,   0,   1,   1.000,
182,  114,  115,  103,   5,   4,   0,   1.000,
183,  116,  105,  104,   5,   5,   0,   1.000,
184,  117,  105,  116,   5,   0,   1,   1.000,
185,  117,  106,  105,   5,   0,   1,   1.000,
186,  118,  106,  117,   5,   0,   1,   1.000,
187,  118,  107,  106,   5,   0,   1,   1.000,
188,  119,  107,  118,   5,   0,   1,   1.000,
189,  119,  108,  107,   5,   0,   1,   1.000,
190,  120,  108,  119,   5,   0,   1,   1.000,
191,  120,  109,  108,   5,   0,   1,   1.000,
192,  121,  109,  120,   5,   0,   1,   1.000,
193,  121,  110,  109,   5,   0,   1,   1.000,
194,  122,  110,  121,   5,   0,   1,   1.000,
195,  122,  111,  110,   5,   0,   1,   1.000,
```

```
   196,   123,   111,   122,     5,     5,     1,      1.000,
   197,   123,   112,   111,     5,     0,     1,      1.000,
   198,   124,   112,   123,     5,     0,     1,      1.000,
   199,   124,   113,   112,     5,     0,     1,      1.000,
   200,   125,   113,   124,     5,     0,     1,      1.000,
   201,   125,   114,   113,     5,     0,     1,      1.000,
   202,   126,   114,   125,     5,     0,     1,      1.000,
   203,   126,   115,   114,     5,     5,     0,      1.000,
END
```

PAM. N05

GEO-SLOPE
Calgary, Alta.

S E E P T R
Finite Element
Seepage Analysis

SERIAL NO. 87011
LEONARD LAM

Project Name .: BEARING CAPACITY REPORT APPENDIX B
Trial Number .: ONE
Date ..: MARCH 2, 1990
Comments ....: Use of PC-SEEP for -ve pwp beneath track

COMPUTED NODAL DATA

TIME STEP : 5, ELAPSED TIME : .8037E+05 (sec), NODES : 126

Nodal Number	Total Head (m)	Major Permeability (m/sec)	X - Direction Velocity (m/sec)	Y - Direction Velocity (m/sec)	X - Direct. Grad.	Y - Direct. Grad.
1	.4820160E+01	.1000E-02	.00000E+00	.00000E+00	-.000	.000
2	.4820255E+01	.1000E-02	-.16282E-06	-.77783E-07	-.000	.000
3	.4820355E+01	.1000E-02	-.19833E-06	-.67148E-07	-.000	.000
4	.4820493E+01	.1000E-02	-.23731E-06	-.78557E-07	-.000	.000
5	.4820640E+01	.1000E-02	-.39495E-06	-.34496E-07	-.000	.000
6	.4820159E+01	.3335E-03	.00000E+00	.00000E+00	.001	-.018
7	.4820231E+01	.6668E-03	-.10396E-06	-.37928E-07	-.000	-.010
8	.4820338E+01	.3335E-03	-.66083E-07	-.23763E-07	-.000	-.019
9	.4820469E+01	.6668E-03	-.16237E-06	-.38968E-07	-.000	-.010
10	.4820638E+01	.3335E-03	-.13304E-06	-.70353E-08	-.001	-.019
11	.4820948E+01	.5001E-03	-.26361E-06	-.17017E-07	-.001	-.014
12	.4821270E+01	.2002E-03	-.12260E-06	-.24947E-07	-.055	-.057
13	.4927474E+01	.2828E-06	-.18760E-07	-.61369E-07	-.073	-.217
14	.4843463E+01	.5002E-03	-.12995E-06	-.60136E-07	.016	-.054
15	.4804127E+01	.3429E-06	.00000E+00	.00000E+00	.002	-.016
16	.4802998E+01	.3334E-06	-.25524E-10	-.50381E-08	.000	-.018
17	.4804187E+01	.3429E-06	-.20027E-10	-.48727E-08	.000	-.016
18	.4803068E+01	.3334E-06	-.58221E-10	-.50840E-08	-.000	-.018
19	.4804413E+01	.3430E-06	-.28143E-09	-.49456E-08	-.001	-.016
20	.4804053E+01	.3338E-06	-.11373E-08	-.47295E-08	-.003	-.017
21	.4809790E+01	.3449E-06	-.74165E-08	-.42561E-08	-.021	-.013
22	.4829814E+01	.3491E-06	-.11604E-07	-.23450E-07	-.038	-.077
23	.4843447E+01	.2503E-03	-.67021E-07	-.22132E-07	-.011	-.023
24	.4843598E+01	.4003E-03	-.10904E-06	-.42994E-07	-.003	-.018
25	.4843770E+01	.3336E-03	-.11695E-06	-.45657E-07	-.050	-.010
26	.4931681E+01	.4811E-06	-.64611E-07	-.32400E-07	-.135	-.065
27	.5001688E+01	.5633E-06	-.14989E-06	-.63498E-07	-.254	-.113
28	.4801240E+01	.2176E-06	.00000E+00	.00000E+00	.000	-.003
29	.4801332E+01	.2868E-06	-.17584E-10	-.10628E-08	.000	-.003
30	.4801394E+01	.2177E-06	-.27958E-09	-.73224E-09	-.001	-.003

31	.4805412E+01	.2886E-06	-.38070E-08	-.35040E-08	-.011	-.010
32	.4816223E+01	.2217E-06	-.26152E-08	-.82441E-08	-.009	-.029
33	.4834918E+01	.3062E-06	-.21716E-07	-.10297E-07	-.067	-.034
34	.4967871E+01	.2403E-06	-.51681E-07	-.24578E-07	-.158	-.190
35	.5402582E+01	.2161E-06	-.79616E-07	-.27907E-07	-.496	-.468
36	.6126976E+01	.1000E-07	-.10317E-07	-.30818E-07	-1.032	-3.082
37	.7491403E+01	.1000E-07	-.19943E-07	-.76895E-07	-1.994	-7.689
38	.4800048E+01	.1000E-07	.00000E+00	.00000E+00	.000	-.001
39	.4800029E+01	.1000E-07	-.17763E-12	-.73566E-11	.000	-.001
40	.4800056E+01	.1000E-07	-.39312E-12	-.77356E-11	.000	-.001
41	.4800124E+01	.1000E-07	-.16842E-10	-.39473E-10	-.002	-.004
42	.4800719E+01	.1000E-07	-.34377E-11	-.90039E-10	-.000	-.009
43	.4800949E+01	.1000E-07	-.17472E-09	-.35228E-09	-.017	-.035
44	.4808669E+01	.1000E-07	-.87093E-10	-.93153E-09	-.009	-.093
45	.4821851E+01	.1000E-07	-.16632E-08	-.45744E-08	-.166	-.457
46	.4929192E+01	.1000E-07	-.15113E-08	-.10682E-07	-.151	-1.068
47	.5184563E+01	.1000E-07	-.76852E-08	-.28489E-07	-.769	-2.849
48	.6299613E+01	.1000E-07	-.70985E-08	-.36395E-07	-.710	-3.639
49	.6140625E+01	.1000E-07	-.90063E-08	-.33309E-07	-.901	-3.331
50	.7492433E+01	.1000E-07	-.20279E-07	-.76854E-07	-2.028	-7.685
51	.4799999E+01	.6453E-08	.00000E+00	.00000E+00	.000	.000
52	.4800000E+01	.6289E-08	-.45160E-14	-.16334E-12	.000	.000
53	.4800001E+01	.6453E-08	-.10017E-12	-.36559E-12	.000	.000
54	.4800002E+01	.6289E-08	-.37683E-13	-.68034E-12	.000	.000
55	.4800015E+01	.6453E-08	-.90756E-12	-.34163E-11	.000	-.000
56	.4800038E+01	.6289E-08	-.47353E-12	-.51158E-11	.000	-.001
57	.4800196E+01	.6453E-08	-.23042E-10	-.54300E-10	-.002	-.006
58	.4801005E+01	.6290E-08	-.76403E-11	-.11725E-09	-.001	-.012
59	.4803111E+01	.6455E-08	-.40128E-09	-.89697E-09	-.042	-.092
60	.4818866E+01	.6304E-08	-.11420E-09	-.20588E-08	-.018	-.214
61	.4846578E+01	.6483E-08	-.16521E-08	-.71573E-08	-.174	-.740
62	.4933512E+01	.6409E-08	-.91275E-09	-.10267E-07	-.142	-1.080
63	.5186801E+01	.6335E-08	-.68035E-08	-.26396E-07	-.785	-2.876
64	.6396230E+01	.6399E-08	-.39374E-08	-.31005E-07	-.499	-3.733
65	.5773925E+01	.4635E-08	-.33222E-09	-.70700E-08	-.055	-1.480
66	.6655007E+01	.5278E-08	-.33822E-11	-.10766E-07	-.001	-2.040
67	.5775867E+01	.4723E-08	-.11324E-13	-.76013E-08	.000	-1.552
68	.6655014E+01	.5279E-08	.30642E-13	-.10769E-07	.000	-2.040
69	.5775846E+01	.4721E-08	.50926E-11	-.75965E-08	.001	-1.552
70	.6652620E+01	.4711E-08	.12397E-08	-.96053E-08	.398	-2.039
71	.4821274E+01	.3706E-08	.00000E+00	.00000E+00	.770	-1.031
72	.4799998E+01	.4354E-08	.00000E+00	.00000E+00	.000	.000
73	.4800000E+01	.4282E-08	-.11063E-14	-.27228E-14	.000	.000
74	.4799999E+01	.4354E-08	.75739E-15	-.46413E-14	.000	.000
75	.4800000E+01	.4282E-08	-.64390E-14	-.11238E-13	.000	.000
76	.4800000E+01	.4354E-08	-.17519E-14	-.27635E-13	.000	.000
77	.4800001E+01	.4282E-08	-.57047E-13	-.13976E-12	.000	.000
78	.4800002E+01	.4354E-08	-.86247E-14	-.35309E-12	.000	-.000
79	.4800005E+01	.4283E-08	-.93062E-12	-.25249E-11	-.000	-.001
80	.4800035E+01	.4355E-08	-.15665E-12	-.56052E-11	.000	-.002
81	.4800092E+01	.4296E-08	-.14095E-10	-.41478E-10	-.005	-.014
82	.4800594E+01	.4374E-08	-.12114E-11	-.84910E-10	-.000	-.026
83	.4800756E+01	.4405E-08	-.12205E-09	-.36318E-09	-.042	-.111
84	.4805688E+01	.4533E-08	-.26743E-10	-.76949E-09	-.006	-.214

85	.4814908E+01	.5055E-08	-.26124E-09	-.31849E-08	-.073	-.719
86	.4817994E+01	.4842E-08	-.85760E-11	-.22516E-08	-.002	-.539
87	.4819159E+01	.5339E-08	-.10635E-11	-.43817E-08	-.000	-.893
88	.4818075E+01	.4846E-08	-.92038E-15	-.22582E-08	.000	-.540
89	.4819160E+01	.5339E-08	.30138E-13	-.43840E-08	.000	-.893
90	.4818058E+01	.4845E-08	.31030E-11	-.22578E-08	.001	-.540
91	.4817623E+01	.5043E-08	.37248E-09	-.34160E-08	.118	-.742
92	.4800634E+01	.4381E-08	.00000E+00	.00000E+00	.014	-.012
93	.4799999E+01	.3719E-08	.00000E+00	.00000E+00	.000	.000
94	.4799999E+01	.4107E-08	-.43477E-15	-.18615E-14	.000	.000
95	.4800000E+01	.4107E-08	-.12469E-14	-.13328E-14	.000	.000
96	.4800000E+01	.4107E-08	-.35835E-14	-.71131E-14	.000	.000
97	.4800001E+01	.4107E-08	-.58032E-13	-.12736E-12	.000	.000
98	.4800004E+01	.4108E-08	-.45844E-12	-.14930E-11	.000	-.000
99	.4800051E+01	.4116E-08	-.93254E-11	-.21124E-10	-.002	-.003
100	.4800137E+01	.4129E-08	-.28417E-11	-.53431E-10	-.001	-.008
101	.4800146E+01	.4131E-08	-.24419E-14	-.57274E-10	.000	-.009
102	.4800141E+01	.4130E-08	.10838E-11	-.55946E-10	.000	-.009
103	.4800000E+01	.3733E-08	.19587E-10	-.27907E-10	.004	-.004
104	.4799998E+01	.1000E-08	.00000E+00	.00000E+00	.000	.000
105	.4800000E+01	.1000E-08	-.49009E-15	.37460E-15	.000	.000
106	.4800000E+01	.1000E-08	.27737E-15	.30007E-15	.000	.000
107	.4799998E+01	.1000E-08	.20725E-15	-.94206E-16	.000	.000
108	.4799998E+01	.1000E-08	-.47524E-16	-.20522E-15	.000	.000
109	.4799997E+01	.1000E-08	-.26995E-15	-.52757E-15	.000	.000
110	.4799999E+01	.1000E-08	-.30767E-14	-.66705E-14	.000	.000
111	.4799997E+01	.1000E-08	-.59261E-14	-.22576E-13	.000	.000
112	.4799998E+01	.1000E-08	-.68706E-15	-.33712E-13	.000	.000
113	.4799998E+01	.1000E-08	.14935E-15	-.34107E-13	.000	.000
114	.4799999E+01	.1000E-08	.93408E-14	-.16731E-13	.000	.000
115	.4800000E+01	.1000E-08	-.12622E-14	-.36325E-16	.000	.000
116	.4799999E+01	.1000E-08	.00000E+00	.00000E+00	.000	.000
117	.4800002E+01	.1000E-08	.00000E+00	.00000E+00	.000	.000
118	.4800000E+01	.1000E-08	.00000E+00	.00000E+00	.000	.000
119	.4800000E+01	.1000E-08	.00000E+00	.00000E+00	.000	.000
120	.4800001E+01	.1000E-08	.00000E+00	.00000E+00	.000	.000
121	.4800001E+01	.1000E-08	.00000E+00	.00000E+00	.000	.000
122	.4799999E+01	.1000E-08	.00000E+00	.00000E+00	.000	.000
123	.4800000E+01	.1000E-08	.00000E+00	.00000E+00	.000	.000
124	.4800000E+01	.1000E-08	.00000E+00	.00000E+00	.000	.000
125	.4800001E+01	.1000E-08	.00000E+00	.00000E+00	.000	.000
126	.4800000E+01	.1000E-08	-.36697E-15	.33710E-15	.000	.000

PAM. N10

GEO-SLOPE
Calgary, Alta.

SEEPTR
Finite Element
Seepage Analysis

SERIAL NO. 87011
LEONARD LAM

Project Name .: BEARING CAPACITY REPORT APPENDIX B
Trial Number .: ONE
Date ..: MARCH 2, 1990
Comments .....: Use of PC-SEEP for -ve pwp beneath track

COMPUTED NODAL DATA

TIME STEP : 10, ELAPSED TIME : .2804E+06 (sec), NODES : 126

Nodal Number	Total Head (m)	Major Permeability (m/sec)	X - Direction Velocity (m/sec)	Y - Direction Velocity (m/sec)	X - Direct. Grad.	Y - Direct. Grad.
1	.4871137E+01	.1000E-02	.00000E+00	.00000E+00	-.000	.000
2	.4871233E+01	.1000E-02	-.16647E-06	-.84883E-07	-.000	.000
3	.4871337E+01	.1000E-02	-.20444E-06	-.72262E-07	-.000	.000
4	.4871479E+01	.1000E-02	-.24732E-06	-.83433E-07	-.000	.000
5	.4871634E+01	.1000E-02	-.41617E-06	-.37381E-07	-.000	.000
6	.4871135E+01	.3335E-03	.00000E+00	.00000E+00	.002	-.047
7	.4871208E+01	.6668E-03	-.10663E-06	-.46130E-07	-.000	-.025
8	.4871319E+01	.3335E-03	-.68337E-07	-.33236E-07	-.000	-.047
9	.4871454E+01	.6668E-03	-.16941E-06	-.45292E-07	-.000	-.024
10	.4871632E+01	.3335E-03	-.14093E-06	-.14495E-07	-.003	-.042
11	.4871958E+01	.5001E-03	-.27726E-06	-.22058E-07	-.001	-.028
12	.4872297E+01	.2002E-03	-.13721E-06	-.27892E-07	-.083	-.062
13	.5011423E+01	.3016E-06	-.37581E-07	-.65681E-07	-.132	-.218
14	.4965623E+01	.5002E-03	-.27873E-06	-.52085E-07	-.017	-.054
15	.4830239E+01	.3501E-06	.00000E+00	.00000E+00	.005	-.043
16	.4826973E+01	.3408E-06	-.14412E-09	-.14200E-07	-.000	-.047
17	.4830732E+01	.3502E-06	-.31610E-09	-.13709E-07	-.001	-.043
18	.4828057E+01	.3411E-06	-.66473E-09	-.13844E-07	-.002	-.046
19	.4833792E+01	.3511E-06	-.29261E-08	-.13267E-07	-.008	-.041
20	.4838060E+01	.3437E-06	-.62140E-08	-.99856E-08	-.016	-.033
21	.4860974E+01	.3588E-06	-.22616E-07	-.63884E-08	-.063	-.018
22	.4913419E+01	.3715E-06	-.33151E-07	-.29692E-07	-.095	-.087
23	.4965620E+01	.2503E-03	-.14630E-06	-.22075E-07	-.044	-.044
24	.4965930E+01	.4003E-03	-.22556E-06	-.32845E-07	-.014	-.011
25	.4966275E+01	.3336E-03	-.26056E-06	-.26366E-07	-.139	.034
26	.5223906E+01	.6063E-06	-.23103E-06	-.28653E-08	-.384	.000
27	.5442375E+01	.8209E-06	-.43968E-06	-.25750E-07	-.511	-.031
28	.4819150E+01	.2210E-06	.00000E+00	.00000E+00	.001	-.018
29	.4820061E+01	.2915E-06	-.33993E-09	-.42677E-08	-.001	-.017
30	.4822481E+01	.2221E-06	-.23708E-08	-.28353E-08	-.009	-.021

31	.4850767E+01	.3002E-06	-.14851E-07	-.69722E-08	-.046	-.032
32	.4913108E+01	.2395E-06	-.12576E-07	-.14504E-07	-.043	-.089
33	.4996974E+01	.3547E-06	-.80531E-07	.36930E-08	-.214	-.055
34	.5432965E+01	.3330E-06	-.16096E-06	-.13108E-07	-.364	-.403
35	.6212145E+01	.3295E-06	-.21976E-06	-.19124E-07	-1.228	-.910
36	.8668886E+01	.1000E-07	-.17400E-07	-.51146E-07	-1.740	-5.115
37	.9578446E+01	.1000E-07	-.26234E-07	-.96058E-07	-2.623	-9.606
38	.4802128E+01	.1000E-07	.00000E+00	.00000E+00	.001	-.011
39	.4801358E+01	.1000E-07	-.44822E-11	-.11277E-09	-.000	-.011
40	.4802599E+01	.1000E-07	-.10596E-10	-.12405E-09	-.001	-.012
41	.4803901E+01	.1000E-07	-.12006E-09	-.32659E-09	-.012	-.033
42	.4814521E+01	.1000E-07	-.59727E-10	-.62318E-09	-.006	-.062
43	.4818235E+01	.1000E-07	-.72197E-09	-.15656E-08	-.072	-.157
44	.4898007E+01	.1000E-07	-.74750E-09	-.34765E-08	-.075	-.348
45	.4997635E+01	.1000E-07	-.57857E-08	-.11955E-07	-.579	-1.195
46	.5817984E+01	.1000E-07	-.70795E-08	-.28965E-07	-.708	-2.896
47	.6696706E+01	.1000E-07	-.13019E-07	-.47071E-07	-1.302	-4.707
48	.9201572E+01	.1000E-07	-.16503E-07	-.61229E-07	-1.650	-6.123
49	.8818389E+01	.1000E-07	-.12851E-07	-.58821E-07	-1.285	-5.882
50	.9657048E+01	.1000E-07	-.25691E-07	-.95406E-07	-2.569	-9.541
51	.4800122E+01	.6453E-08	.00000E+00	.00000E+00	.000	-.001
52	.4800142E+01	.6289E-08	-.79378E-13	-.69595E-11	.000	-.001
53	.4800153E+01	.6453E-08	-.30451E-11	-.13631E-10	-.000	-.001
54	.4800443E+01	.6290E-08	-.20545E-11	-.19838E-10	-.000	-.002
55	.4800937E+01	.6453E-08	-.17385E-10	-.66449E-10	-.002	-.007
56	.4802309E+01	.6291E-08	-.16419E-10	-.91751E-10	-.003	-.010
57	.4807199E+01	.6458E-08	-.22087E-09	-.52691E-09	-.024	-.057
58	.4828108E+01	.6313E-08	-.19357E-09	-.98221E-09	-.031	-.110
59	.4880725E+01	.6511E-08	-.21245E-08	-.52616E-08	-.233	-.572
60	.5092883E+01	.6488E-08	-.10193E-08	-.93861E-08	-.157	-1.051
61	.5258259E+01	.6789E-08	-.47955E-08	-.20352E-07	-.536	-2.234
62	.5936472E+01	.7397E-08	-.47703E-08	-.26961E-07	-.640	-3.016
63	.6794874E+01	.8175E-08	-.12074E-07	-.45111E-07	-1.265	-4.837
64	.9259894E+01	.1000E-07	-.10697E-07	-.62541E-07	-1.070	-6.254
65	.8180918E+01	.9471E-08	-.12546E-08	-.39554E-07	-.127	-4.135
66	.9804791E+01	.1000E-07	-.10246E-09	-.51453E-07	-.010	-5.145
67	.8205507E+01	.9544E-08	-.33180E-11	-.41225E-07	-.000	-4.278
68	.9806187E+01	.1000E-07	-.40226E-11	-.51466E-07	-.000	-5.147
69	.8206470E+01	.9520E-08	.17301E-09	-.41130E-07	.018	-4.277
70	.9756939E+01	.1000E-07	.12547E-07	-.51332E-07	1.255	-5.133
71	.5195077E+01	.6953E-08	.00000E+00	.00000E+00	2.026	-2.766
72	.4800001E+01	.4354E-08	.00000E+00	.00000E+00	.000	.000
73	.4799999E+01	.4282E-08	-.10575E-13	-.25798E-12	.000	.000
74	.4800001E+01	.4354E-08	-.11511E-13	-.27332E-12	.000	.000
75	.4800005E+01	.4282E-08	-.26569E-12	-.92373E-12	.000	-.000
76	.4800025E+01	.4354E-08	-.43990E-13	-.16917E-11	.000	-.001
77	.4800030E+01	.4284E-08	-.21422E-11	-.61068E-11	-.001	-.002
78	.4800232E+01	.4357E-08	-.71263E-12	-.13057E-10	-.000	-.004
79	.4800422E+01	.4307E-08	-.25753E-10	-.69773E-10	-.009	-.023
80	.4802769E+01	.4393E-08	-.84673E-11	-.14924E-09	-.002	-.044
81	.4805048E+01	.4473E-08	-.15115E-09	-.58553E-09	-.049	-.177
82	.4819367E+01	.4593E-08	-.48968E-10	-.93598E-09	-.011	-.252
83	.4830647E+01	.5361E-08	-.10497E-08	-.37063E-08	-.211	-.737
84	.4934514E+01	.5836E-08	-.68588E-09	-.62748E-08	-.116	-1.088

85	.5110168E+01	.7914E-08	-.19386E-08	-.19863E-07	-.212	-2.187
86	.5128633E+01	.7707E-08	-.20584E-09	-.16027E-07	-.027	-1.829
87	.5174051E+01	.8475E-08	-.43641E-10	-.24354E-07	-.005	-2.562
88	.5136435E+01	.7812E-08	-.69969E-12	-.16387E-07	.000	-1.841
89	.5174263E+01	.8487E-08	.38069E-11	-.24426E-07	.001	-2.566
90	.5133848E+01	.7769E-08	.12104E-09	-.16311E-07	.015	-1.842
91	.5137096E+01	.7634E-08	.39375E-08	-.19870E-07	.430	-2.094
92	.4836911E+01	.4957E-08	.00000E+00	.00000E+00	.250	-.214
93	.4799999E+01	.3719E-08	.00000E+00	.00000E+00	.000	.000
94	.4800001E+01	.4107E-08	-.49983E-14	-.41025E-14	.000	.000
95	.4800001E+01	.4107E-08	-.16979E-13	-.59988E-13	.000	.000
96	.4800004E+01	.4107E-08	-.28408E-12	-.67013E-12	.000	-.000
97	.4800057E+01	.4111E-08	-.32134E-11	-.81618E-11	-.001	-.001
98	.4800391E+01	.4132E-08	-.18673E-10	-.54806E-10	-.003	-.009
99	.4803711E+01	.4330E-08	-.20278E-09	-.50077E-09	-.034	-.072
100	.4808481E+01	.4590E-08	-.52312E-10	-.11402E-08	-.008	-.157
101	.4809153E+01	.4629E-08	-.33013E-12	-.12211E-08	.000	-.167
102	.4808780E+01	.4604E-08	.33868E-10	-.11789E-08	.006	-.162
103	.4800000E+01	.4018E-08	.38398E-09	-.60558E-09	.064	-.078
104	.4799999E+01	.1000E-08	.00000E+00	.00000E+00	.000	.000
105	.4799999E+01	.1000E-08	-.88831E-16	.84026E-16	.000	.000
106	.4799999E+01	.1000E-08	.40204E-15	-.56512E-16	.000	.000
107	.4799996E+01	.1000E-08	-.26477E-16	-.48444E-15	.000	.000
108	.4799998E+01	.1000E-08	-.39937E-14	-.70969E-14	.000	.000
109	.4799997E+01	.1000E-08	-.23592E-13	-.53070E-13	.000	.000
110	.4800001E+01	.1000E-08	-.23128E-12	-.48812E-12	-.000	-.000
111	.4800004E+01	.1000E-08	-.33244E-12	-.14511E-11	-.000	-.001
112	.4800009E+01	.1000E-08	-.47052E-13	-.20988E-11	.000	-.002
113	.4800007E+01	.1000E-08	.26190E-13	-.21343E-11	.000	-.002
114	.4800005E+01	.1000E-08	.61146E-12	-.10448E-11	.001	-.001
115	.4800000E+01	.1000E-08	.44059E-14	-.36325E-16	.000	.000
116	.4800000E+01	.1000E-08	.00000E+00	.00000E+00	.000	.000
117	.4800001E+01	.1000E-08	.00000E+00	.00000E+00	.000	.000
118	.4800001E+01	.1000E-08	.00000E+00	.00000E+00	.000	.000
119	.4800001E+01	.1000E-08	.00000E+00	.00000E+00	.000	.000
120	.4800002E+01	.1000E-08	.00000E+00	.00000E+00	.000	.000
121	.4800003E+01	.1000E-08	.00000E+00	.00000E+00	.000	.000
122	.4800000E+01	.1000E-08	.00000E+00	.00000E+00	.000	.000
123	.4800001E+01	.1000E-08	.00000E+00	.00000E+00	.000	.000
124	.4800000E+01	.1000E-08	.00000E+00	.00000E+00	.000	.000
125	.4800002E+01	.1000E-08	.00000E+00	.00000E+00	.000	.000
126	.4800000E+01	.1000E-08	.26133E-14	-.79585E-15	.000	.000

PAH.N15

```
------------------
                  /\     S E E P T R
GEO-SLOPE        /  \    Finite Element          SERIAL NO. 87011
Calgary, Alta.  /    \   Seepage Analysis        LEONARD LAM
               /      \
-------------------------------------------------------------------------

Project Name .: BEARING CAPACITY REPORT APPENDIX B
Trial Number .: ONE                                Date ..: MARCH 2, 1990
Comments .....: Use of PC-SEEP for -ve pwp beneath track

 -------------------------
 :  COMPUTED NODAL DATA  :
 -------------------------

    TIME STEP :  15,   ELAPSED TIME : .6147E+06 (sec),   NODES :  126
```

Nodal Number	Total Head (m)	Major Permeability (m/sec)	X - Direction Velocity (m/sec)	Y - Direction Velocity (m/sec)	X - Direct. Grad.	Y - Direct. Grad.
1	.4951786E+01	.1000E-02	.00000E+00	.00000E+00	-.000	.000
2	.4951887E+01	.1000E-02	-.18355E-06	-.87253E-07	-.000	.000
3	.4952006E+01	.1000E-02	-.23795E-06	-.75819E-07	-.000	.000
4	.4952173E+01	.1000E-02	-.29409E-06	-.84954E-07	-.000	.000
5	.4952359E+01	.1000E-02	-.50611E-06	-.32425E-07	-.001	.000
6	.4951782E+01	.3335E-03	.00000E+00	.00000E+00	.002	-.066
7	.4951861E+01	.6668E-03	-.11802E-06	-.51517E-07	-.000	-.034
8	.4951986E+01	.3335E-03	-.79871E-07	-.40526E-07	-.002	-.063
9	.4952147E+01	.6668E-03	-.20153E-06	-.47657E-07	-.000	-.031
10	.4952359E+01	.3335E-03	-.17288E-06	-.13586E-07	-.009	-.047
11	.4952760E+01	.5001E-03	-.34027E-06	-.17700E-07	-.001	-.022
12	.4953176E+01	.2003E-03	-.17945E-06	-.18544E-07	-.127	-.030
13	.5154706E+01	.3393E-06	-.82088E-07	-.58315E-07	-.251	-.172
14	.5202497E+01	.5002E-03	-.53914E-06	-.33194E-07	-.083	-.043
15	.4894928E+01	.3677E-06	.00000E+00	.00000E+00	.007	-.062
16	.4890699E+01	.3584E-06	-.54663E-09	-.21174E-07	-.001	-.067
17	.4896978E+01	.3683E-06	-.15716E-08	-.20254E-07	-.004	-.060
18	.4895824E+01	.3598E-06	-.27489E-08	-.19239E-07	-.007	-.060
19	.4908554E+01	.3717E-06	-.93113E-08	-.17385E-07	-.025	-.050
20	.4925870E+01	.3674E-06	-.16180E-07	-.74095E-08	-.040	-.023
21	.4973315E+01	.3906E-06	-.49665E-07	.27265E-08	-.126	.010
22	.5077368E+01	.4206E-06	-.81144E-07	-.28912E-07	-.200	-.071
23	.5202512E+01	.2504E-03	-.29057E-06	-.19872E-07	-.105	-.062
24	.5203095E+01	.4003E-03	-.42237E-06	-.99914E-08	-.028	.006
25	.5203728E+01	.3337E-03	-.48094E-06	.16919E-07	-.207	.097
26	.5597672E+01	.8074E-06	-.43224E-06	.33454E-07	-.544	.052
27	.5900346E+01	.1148E-05	-.65054E-06	.12614E-07	-.557	.011
28	.4877572E+01	.2313E-06	.00000E+00	.00000E+00	.001	-.049
29	.4880568E+01	.3057E-06	-.16163E-08	-.69285E-08	-.006	-.041
30	.4892310E+01	.2349E-06	-.72024E-08	-.39905E-08	-.026	-.057

31	.4965736E+01	.3292E-06	-.36955E-07	-.66869E-08	-.107	-.064
32	.5127664E+01	.2800E-06	-.33534E-07	-.20192E-07	-.101	-.182
33	.5291050E+01	.4451E-06	-.15320E-06	.27804E-07	-.319	-.097
34	.5903643E+01	.4571E-06	-.25113E-06	-.15161E-08	-.456	-.500
35	.6637382E+01	.4603E-06	-.29367E-06	-.39932E-08	-1.833	-.894
36	.1136394E+02	.1000E-07	-.25501E-07	-.60145E-07	-2.550	-6.015
37	.1194947E+02	.1000E-07	-.28624E-07	-.98927E-07	-2.862	-9.893
38	.4815521E+01	.1000E-07	.00000E+00	.00000E+00	.004	-.042
39	.4811244E+01	.1000E-07	-.23968E-10	-.44774E-09	-.002	-.045
40	.4819396E+01	.1000E-07	-.60781E-10	-.49980E-09	-.006	-.050
41	.4825831E+01	.1000E-07	-.36526E-09	-.10117E-08	-.037	-.101
42	.4873379E+01	.1000E-07	-.28229E-09	-.17666E-08	-.028	-.177
43	.4893580E+01	.1000E-07	-.13737E-08	-.32041E-08	-.137	-.320
44	.5123676E+01	.1000E-07	-.22154E-08	-.58433E-08	-.222	-.584
45	.5425272E+01	.1000E-07	-.11522E-07	-.17226E-07	-1.152	-1.723
46	.7518376E+01	.1000E-07	-.14818E-07	-.44596E-07	-1.482	-4.460
47	.8981654E+01	.1000E-07	-.16976E-07	-.59862E-07	-1.698	-5.986
48	.1229797E+02	.1000E-07	-.22826E-07	-.76617E-07	-2.283	-7.662
49	.1191882E+02	.1000E-07	-.15449E-07	-.75069E-07	-1.545	-7.507
50	.1207800E+02	.1000E-07	-.25227E-07	-.10002E-06	-2.523	-10.002
51	.4801825E+01	.6454E-08	.00000E+00	.00000E+00	.001	-.007
52	.4802236E+01	.6291E-08	-.13679E-11	-.53176E-10	-.000	-.006
53	.4802347E+01	.6454E-08	-.19516E-10	-.92799E-10	-.002	-.010
54	.4805509E+01	.6293E-08	-.19230E-10	-.12061E-09	-.003	-.014
55	.4809681E+01	.6459E-08	-.92980E-10	-.32197E-09	-.011	-.037
56	.4822456E+01	.6307E-08	-.11085E-09	-.42680E-09	-.018	-.052
57	.4851846E+01	.6490E-08	-.75846E-09	-.15950E-08	-.088	-.188
58	.4975559E+01	.6441E-08	-.10987E-08	-.27697E-08	-.170	-.344
59	.5259415E+01	.6795E-08	-.51692E-08	-.12185E-07	-.587	-1.404
60	.5987875E+01	.7309E-08	-.34504E-08	-.19529E-07	-.478	-2.290
61	.6406383E+01	.8126E-08	-.88505E-08	-.35349E-07	-.933	-3.829
62	.7874853E+01	.9777E-08	-.10857E-07	-.48218E-07	-1.113	-4.890
63	.9077507E+01	.1000E-07	-.14519E-07	-.62735E-07	-1.452	-6.274
64	.1197220E+02	.1000E-07	-.13773E-07	-.77719E-07	-1.377	-7.772
65	.1114120E+02	.1000E-07	-.20634E-08	-.61808E-07	-.206	-6.181
66	.1278490E+02	.1000E-07	-.33460E-09	-.73625E-07	-.033	-7.363
67	.1122150E+02	.1000E-07	-.16313E-10	-.63844E-07	-.002	-6.384
68	.1279089E+02	.1000E-07	.15287E-09	-.73671E-07	.015	-7.367
69	.1118481E+02	.1000E-07	.15385E-08	-.62454E-07	.154	-6.245
70	.1218874E+02	.1000E-07	.20382E-07	-.68495E-07	2.038	-6.850
71	.6293028E+01	.8502E-08	.00000E+00	.00000E+00	2.815	-4.052
72	.4800094E+01	.4355E-08	.00000E+00	.00000E+00	.000	-.001
73	.4800052E+01	.4283E-08	-.19563E-12	-.40071E-11	.000	-.001
74	.4800126E+01	.4355E-08	-.16704E-12	-.42737E-11	.000	-.001
75	.4800144E+01	.4286E-08	-.27079E-11	-.10792E-10	-.001	-.004
76	.4800554E+01	.4359E-08	-.91472E-12	-.17662E-10	-.000	-.005
77	.4800648E+01	.4301E-08	-.16142E-10	-.50994E-10	-.006	-.017
78	.4803380E+01	.4382E-08	-.99093E-11	-.95758E-10	-.002	-.028
79	.4806075E+01	.4449E-08	-.17652E-09	-.45608E-09	-.056	-.134
80	.4833992E+01	.4628E-08	-.10167E-09	-.94743E-09	-.022	-.250
81	.4858819E+01	.5288E-08	-.78717E-09	-.32563E-08	-.170	-.683
82	.4974302E+01	.5667E-08	-.66718E-09	-.46426E-08	-.117	-.865
83	.5139632E+01	.8085E-08	-.44773E-08	-.16091E-07	-.497	-1.789
84	.5713650E+01	.9243E-08	-.31827E-08	-.21742E-07	-.351	-2.229

85	.5980891E+01	.9912E-08	-.39225E-08	-.35979E-07	-.394	-3.604
86	.6324557E+01	.1000E-07	-.74051E-09	-.32687E-07	-.074	-3.269
87	.6158612E+01	.1000E-07	-.17882E-09	-.41314E-07	-.018	-4.131
88	.6357989E+01	.1000E-07	-.76755E-11	-.33061E-07	-.001	-3.306
89	.6160454E+01	.1000E-07	.87404E-10	-.41388E-07	.009	-4.139
90	.6340554E+01	.1000E-07	.56796E-09	-.32897E-07	.057	-3.290
91	.6024144E+01	.9308E-08	.81899E-08	-.31973E-07	.869	-3.259
92	.5164442E+01	.7577E-08	.00000E+00	.00000E+00	.716	-.779
93	.4799999E+01	.3719E-08	.00000E+00	.00000E+00	.000	.000
94	.4800002E+01	.4107E-08	-.67987E-13	-.32765E-12	.000	.000
95	.4800015E+01	.4108E-08	-.38943E-12	-.13386E-11	.000	-.000
96	.4800124E+01	.4112E-08	-.41892E-11	-.95537E-11	-.001	-.002
97	.4801304E+01	.4154E-08	-.38984E-10	-.97014E-10	-.007	-.015
98	.4808086E+01	.4392E-08	-.22894E-09	-.59173E-09	-.039	-.086
99	.4850031E+01	.5449E-08	-.87398E-09	-.33730E-08	-.111	-.385
100	.4901830E+01	.6143E-08	-.24948E-09	-.62146E-08	-.028	-.639
101	.4907915E+01	.6143E-08	-.37428E-11	-.64601E-08	-.001	-.665
102	.4904196E+01	.6143E-08	.23294E-09	-.63263E-08	.029	-.649
103	.4800000E+01	.5038E-08	.15791E-08	-.30667E-08	.201	-.326
104	.4799999E+01	.1000E-08	.00000E+00	.00000E+00	.000	.000
105	.4800001E+01	.1000E-08	-.12777E-15	.26486E-15	.000	.000
106	.4799998E+01	.1000E-08	-.11021E-15	-.18479E-14	.000	.000
107	.4799995E+01	.1000E-08	-.74669E-14	-.16493E-13	.000	.000
108	.4799997E+01	.1000E-08	-.83472E-13	-.16987E-12	.000	-.000
109	.4800005E+01	.1000E-08	-.48065E-12	-.11168E-11	-.000	-.001
110	.4800067E+01	.1000E-08	-.29370E-11	-.69144E-11	-.003	-.007
111	.4800180E+01	.1000E-08	-.36235E-11	-.18069E-10	-.004	-.018
112	.4800256E+01	.1000E-08	-.43324E-12	-.24957E-10	-.000	-.025
113	.4800258E+01	.1000E-08	.27233E-12	-.25238E-10	.000	-.025
114	.4800153E+01	.1000E-08	.72930E-11	-.12398E-10	.007	-.012
115	.4800000E+01	.1000E-08	.12750E-12	-.36325E-16	.000	.000
116	.4800003E+01	.1000E-08	.00000E+00	.00000E+00	.000	.000
117	.4800001E+01	.1000E-08	.00000E+00	.00000E+00	.000	.000
118	.4800002E+01	.1000E-08	.00000E+00	.00000E+00	.000	.000
119	.4800001E+01	.1000E-08	.00000E+00	.00000E+00	.000	.000
120	.4800002E+01	.1000E-08	.00000E+00	.00000E+00	.000	.000
121	.4800003E+01	.1000E-08	.00000E+00	.00000E+00	.000	.000
122	.4800001E+01	.1000E-08	.00000E+00	.00000E+00	.000	.000
123	.4800001E+01	.1000E-08	.00000E+00	.00000E+00	.000	.000
124	.4800000E+01	.1000E-08	.00000E+00	.00000E+00	.000	.000
125	.4800002E+01	.1000E-08	.00000E+00	.00000E+00	.000	.000
126	.4800000E+01	.1000E-08	.64205E-13	-.28191E-13	.000	.000

PAM. N20

```
------------------
                 /\     S E E P T R
GEO-SLOPE       /  \    Finite Element          SERIAL NO. 87011
Calgary, Alta. /    \   Seepage Analysis        LEONARD LAM
              /      \
-------------------------------------------------------------------------
```

Project Name .: BEARING CAPACITY REPORT APPENDIX B
Trial Number .: ONE Date ..: MARCH 2, 1990
Comments .....: Use of PC-SEEP for -ve pwp beneath track

COMPUTED NODAL DATA

TIME STEP : 20, ELAPSED TIME : .9491E+06 (sec), NODES : 126

Nodal Number	Total Head (m)	Major Permeability (m/sec)	X - Direction Velocity (m/sec)	Y - Direction Velocity (m/sec)	X - Direct. Grad.	Y - Direct. Grad.
1	.5036640E+01	.1000E-02	.00000E+00	.00000E+00	-.000	.000
2	.5036751E+01	.1000E-02	-.21218E-06	-.91354E-07	-.000	.000
3	.5036895E+01	.1000E-02	-.29498E-06	-.78348E-07	-.000	.000
4	.5037105E+01	.1000E-02	-.37411E-06	-.87534E-07	-.000	.000
5	.5037344E+01	.1000E-02	-.65725E-06	-.19462E-07	-.001	.000
6	.5036636E+01	.3335E-03	.00000E+00	.00000E+00	.002	-.072
7	.5036724E+01	.6668E-03	-.13711E-06	-.54842E-07	-.000	-.037
8	.5036875E+01	.3335E-03	-.99523E-07	-.43508E-07	-.003	-.067
9	.5037078E+01	.6668E-03	-.25710E-06	-.45518E-07	-.000	-.031
10	.5037351E+01	.3335E-03	-.22622E-06	-.36291E-08	-.015	-.037
11	.5037874E+01	.5001E-03	-.44407E-06	-.48117E-08	-.001	-.003
12	.5038417E+01	.2003E-03	-.24331E-06	-.22856E-09	-.174	.020
13	.5314939E+01	.3860E-06	-.13665E-06	-.45354E-07	-.365	-.118
14	.5441235E+01	.5002E-03	-.71321E-06	-.23394E-07	-.135	-.029
15	.4973898E+01	.3904E-06	.00000E+00	.00000E+00	.007	-.069
16	.4969718E+01	.3808E-06	-.11437E-08	-.24801E-07	-.003	-.073
17	.4978096E+01	.3916E-06	-.35200E-08	-.23435E-07	-.009	-.065
18	.4980513E+01	.3836E-06	-.58144E-08	-.20462E-07	-.014	-.060
19	.5000678E+01	.3985E-06	-.17804E-07	-.16718E-07	-.045	-.044
20	.5034041E+01	.3979E-06	-.28860E-07	.19542E-08	-.065	.005
21	.5106164E+01	.4316E-06	-.82877E-07	.20902E-07	-.190	.057
22	.5262058E+01	.4825E-06	-.13723E-06	-.22833E-07	-.294	-.044
23	.5441253E+01	.2504E-03	-.39624E-06	-.26011E-07	-.150	-.068
24	.5442010E+01	.4004E-03	-.54444E-06	-.21184E-08	-.032	.009
25	.5442817E+01	.3338E-03	-.60433E-06	.41802E-07	-.208	.110
26	.5840908E+01	.9700E-06	-.51298E-06	.50731E-07	-.539	.064
27	.6138719E+01	.1364E-05	-.72942E-06	.27030E-07	-.528	.020
28	.4953845E+01	.2450E-06	.00000E+00	.00000E+00	.001	-.081
29	.4959450E+01	.3247E-06	-.35645E-08	-.82277E-08	-.011	-.064
30	.4984128E+01	.2523E-06	-.13626E-07	-.36463E-08	-.046	-.094

31	.5107076E+01	.3673E-06	-.64150E-07	-.39905E-08	-.168	-.093
32	.5359200E+01	.3298E-06	-.53820E-07	-.25507E-07	-.142	-.256
33	.5542199E+01	.5342E-06	-.18483E-06	.39488E-07	-.322	-.141
34	.6144665E+01	.5439E-06	-.28554E-06	.36630E-08	-.479	-.483
35	.6822885E+01	.5423E-06	-.32320E-06	.36358E-08	-2.236	-.691
36	.1320318E+02	.1000E-07	-.32271E-07	-.62850E-07	-3.227	-6.285
37	.1393980E+02	.1000E-07	-.30268E-07	-.10003E-06	-3.027	-10.003
38	.4840626E+01	.1000E-07	.00000E+00	.00000E+00	.007	-.082
39	.4832037E+01	.1000E-07	-.55966E-10	-.86576E-09	-.006	-.087
40	.4851292E+01	.1000E-07	-.14890E-09	-.97238E-09	-.015	-.097
41	.4867774E+01	.1000E-07	-.64712E-09	-.17746E-08	-.065	-.177
42	.4963190E+01	.1000E-07	-.56917E-09	-.29319E-08	-.057	-.293
43	.5004375E+01	.1000E-07	-.17171E-08	-.42884E-08	-.172	-.429
44	.5343458E+01	.1000E-07	-.36508E-08	-.67264E-08	-.365	-.673
45	.5880577E+01	.1000E-07	-.16193E-07	-.19285E-07	-1.619	-1.929
46	.8976035E+01	.1000E-07	-.21077E-07	-.52638E-07	-2.108	-5.264
47	.1093903E+02	.1000E-07	-.19698E-07	-.66909E-07	-1.970	-6.691
48	.1446592E+02	.1000E-07	-.24999E-07	-.83672E-07	-2.500	-8.367
49	.1414691E+02	.1000E-07	-.16950E-07	-.83224E-07	-1.695	-8.322
50	.1400424E+02	.1000E-07	-.24285E-07	-.10197E-06	-2.429	-10.197
51	.4806988E+01	.6457E-08	.00000E+00	.00000E+00	.001	-.020
52	.4808721E+01	.6295E-08	-.55393E-11	-.14163E-09	-.001	-.018
53	.4809100E+01	.6459E-08	-.51662E-10	-.23387E-09	-.006	-.028
54	.4819607E+01	.6303E-08	-.58736E-10	-.29488E-09	-.009	-.037
55	.4831466E+01	.6473E-08	-.20627E-09	-.67948E-09	-.024	-.082
56	.4867625E+01	.6340E-08	-.27083E-09	-.85592E-09	-.043	-.112
57	.4933906E+01	.6554E-08	-.13993E-08	-.25431E-08	-.168	-.322
58	.5222976E+01	.6683E-08	-.25547E-08	-.43971E-08	-.378	-.586
59	.5841882E+01	.7364E-08	-.82116E-08	-.18117E-07	-.920	-2.090
60	.6999910E+01	.9000E-08	-.66771E-08	-.30572E-07	-.762	-3.274
61	.7671302E+01	.9730E-08	-.11508E-07	-.47585E-07	-1.160	-4.825
62	.9484121E+01	.1000E-07	-.13641E-07	-.59682E-07	-1.364	-5.968
63	.1094503E+02	.1000E-07	-.15359E-07	-.70699E-07	-1.536	-7.070
64	.1385696E+02	.1000E-07	-.15080E-07	-.84968E-07	-1.508	-8.497
65	.1346194E+02	.1000E-07	-.26487E-08	-.72759E-07	-.265	-7.276
66	.1482072E+02	.1000E-07	-.57274E-09	-.83755E-07	-.057	-8.376
67	.1359940E+02	.1000E-07	-.23913E-10	-.74939E-07	-.002	-7.494
68	.1482855E+02	.1000E-07	.44254E-09	-.83802E-07	.044	-8.380
69	.1349318E+02	.1000E-07	.28947E-08	-.72764E-07	.289	-7.276
70	.1378494E+02	.1000E-07	.25924E-07	-.76049E-07	2.592	-7.605
71	.7271445E+01	.1000E-07	.00000E+00	.00000E+00	3.167	-4.590
72	.4800521E+01	.4357E-08	.00000E+00	.00000E+00	.000	-.004
73	.4800313E+01	.4287E-08	-.83483E-12	-.15584E-10	-.000	-.005
74	.4800695E+01	.4359E-08	-.80604E-12	-.16663E-10	-.000	-.005
75	.4800757E+01	.4296E-08	-.89307E-11	-.37522E-10	-.003	-.012
76	.4802576E+01	.4371E-08	-.41127E-11	-.57984E-10	-.001	-.017
77	.4803015E+01	.4338E-08	-.44134E-10	-.14626E-09	-.015	-.046
78	.4813058E+01	.4440E-08	-.41223E-10	-.25423E-09	-.009	-.072
79	.4825294E+01	.4737E-08	-.51765E-09	-.12311E-08	-.136	-.309
80	.4927809E+01	.5172E-08	-.47471E-09	-.25708E-08	-.092	-.558
81	.5045187E+01	.7096E-08	-.24623E-08	-.93434E-08	-.335	-1.232
82	.5412462E+01	.8257E-08	-.23621E-08	-.13092E-07	-.288	-1.492
83	.5735591E+01	.9694E-08	-.68841E-08	-.25727E-07	-.696	-2.593
84	.6664602E+01	.1000E-07	-.51649E-08	-.30773E-07	-.516	-3.077
85	.6975158E+01	.1000E-07	-.52407E-08	-.45204E-07	-.524	-4.520

86	.8788688E+01	.1000E-07	-.18136E-08	-.50505E-07	-.181	-5.050
87	.8430806E+01	.1000E-07	-.53564E-09	-.58148E-07	-.054	-5.815
88	.8910151E+01	.1000E-07	-.13271E-10	-.51278E-07	-.001	-5.128
89	.8433992E+01	.1000E-07	.55738E-09	-.58157E-07	.056	-5.816
90	.8781078E+01	.1000E-07	.24622E-08	-.50502E-07	.246	-5.050
91	.7843062E+01	.1000E-07	.14130E-07	-.45254E-07	1.413	-4.525
92	.6575104E+01	.1000E-07	.00000E+00	.00000E+00	1.057	-1.648
93	.4800076E+01	.3720E-08	.00000E+00	.00000E+00	.000	-.001
94	.4800111E+01	.4110E-08	-.10143E-11	-.53345E-11	-.000	-.001
95	.4800407E+01	.4116E-08	-.52009E-11	-.16857E-10	-.001	-.003
96	.4802574E+01	.4166E-08	-.53844E-10	-.96136E-10	-.010	-.016
97	.4826579E+01	.4659E-08	-.50009E-09	-.10881E-08	-.080	-.149
98	.4933484E+01	.5866E-08	-.13831E-08	-.48038E-08	-.167	-.529
99	.5206542E+01	.6143E-08	-.21844E-08	-.10622E-07	-.245	-1.135
100	.5426525E+01	.6143E-08	-.68184E-09	-.14874E-07	-.082	-1.596
101	.5456422E+01	.6143E-08	-.34421E-11	-.15476E-07	-.000	-1.666
102	.5425990E+01	.6143E-08	.11334E-08	-.14908E-07	.149	-1.587
103	.4800000E+01	.5500E-08	.33593E-08	-.94228E-08	.395	-.976
104	.4799999E+01	.1000E-08	.00000E+00	.00000E+00	.000	.000
105	.4800001E+01	.1000E-08	-.18493E-14	-.21270E-13	.000	.000
106	.4799998E+01	.1000E-08	-.19971E-13	-.61451E-13	.000	.000
107	.4799996E+01	.1000E-08	-.15736E-12	-.35438E-12	-.000	-.000
108	.4800048E+01	.1000E-08	-.17118E-11	-.34659E-11	-.002	-.003
109	.4800318E+01	.1000E-08	-.76000E-11	-.19031E-10	-.008	-.019
110	.4801313E+01	.1000E-08	-.19301E-10	-.64214E-10	-.019	-.064
111	.4802754E+01	.1000E-08	-.15585E-10	-.12284E-09	-.016	-.123
112	.4803529E+01	.1000E-08	-.21848E-11	-.15255E-09	-.002	-.153
113	.4803536E+01	.1000E-08	.23163E-11	-.15249E-09	.002	-.152
114	.4802069E+01	.1000E-08	.44251E-10	-.74435E-10	.044	-.074
115	.4800000E+01	.1000E-08	.17239E-11	-.36325E-16	.002	.000
116	.4800009E+01	.1000E-08	.00000E+00	.00000E+00	.000	.000
117	.4800001E+01	.1000E-08	.00000E+00	.00000E+00	.000	.000
118	.4800002E+01	.1000E-08	.00000E+00	.00000E+00	.000	.000
119	.4800001E+01	.1000E-08	.00000E+00	.00000E+00	.000	.000
120	.4800003E+01	.1000E-08	.00000E+00	.00000E+00	.000	.000
121	.4800008E+01	.1000E-08	.00000E+00	.00000E+00	-.000	-.000
122	.4800011E+01	.1000E-08	.00000E+00	.00000E+00	-.000	-.001
123	.4800019E+01	.1000E-08	.00000E+00	.00000E+00	-.000	-.001
124	.4800019E+01	.1000E-08	.00000E+00	.00000E+00	.000	-.001
125	.4800016E+01	.1000E-08	.00000E+00	.00000E+00	.000	-.001
126	.4800000E+01	.1000E-08	.86529E-12	-.38158E-12	.001	-.000

PAM.N25

```
                    /\      S E E P T R
GEO-SLOPE          /  \     Finite Element          SERIAL NO. 87011
Calgary, Alta.    /    \    Seepage Analysis        LEONARD LAM
                 /      \
```

Project Name .: BEARING CAPACITY REPORT APPENDIX B
Trial Number .: ONE Date ..: MARCH 2, 1990
Comments .....: Use of PC-SEEP for -ve pwp beneath track

COMPUTED NODAL DATA

TIME STEP : 25, ELAPSED TIME : .1283E+07 (sec), NODES : 126

Nodal Number	Total Head (m)	Major Permeability (m/sec)	X - Direction Velocity (m/sec)	Y - Direction Velocity (m/sec)	X - Direct. Grad.	Y - Direct. Grad.
1	.5129871E+01	.1000E-02	.00000E+00	.00000E+00	-.000	.000
2	.5129993E+01	.1000E-02	-.24514E-06	-.95835E-07	-.000	.000
3	.5130165E+01	.1000E-02	-.35778E-06	-.78781E-07	-.000	.000
4	.5130421E+01	.1000E-02	-.46057E-06	-.86672E-07	-.000	.000
5	.5130717E+01	.1000E-02	-.81902E-06	-.24043E-08	-.001	.000
6	.5129867E+01	.3336E-03	.00000E+00	.00000E+00	.002	-.075
7	.5129964E+01	.6668E-03	-.15909E-06	-.57795E-07	-.000	-.039
8	.5130145E+01	.3336E-03	-.12133E-06	-.44680E-07	-.005	-.067
9	.5130394E+01	.6668E-03	-.31705E-06	-.40336E-07	-.000	-.029
10	.5130733E+01	.3336E-03	-.28328E-06	.10085E-07	-.022	-.023
11	.5131386E+01	.5002E-03	-.55429E-06	.11880E-07	-.001	.019
12	.5132063E+01	.2003E-03	-.31085E-06	.21169E-07	-.214	.070
13	.5473300E+01	.4373E-06	-.19181E-06	-.30305E-07	-.452	-.069
14	.5654149E+01	.5003E-03	-.83073E-06	-.16689E-07	-.169	-.017
15	.5064384E+01	.4179E-06	.00000E+00	.00000E+00	.006	-.073
16	.5060586E+01	.4079E-06	-.19016E-08	-.27561E-07	-.004	-.076
17	.5070992E+01	.4201E-06	-.59567E-08	-.25673E-07	-.014	-.066
18	.5077611E+01	.4126E-06	-.95007E-08	-.20243E-07	-.021	-.055
19	.5104957E+01	.4310E-06	-.27380E-07	-.14146E-07	-.063	-.034
20	.5153634E+01	.4343E-06	-.42472E-07	.14016E-07	-.087	.035
21	.5246035E+01	.4792E-06	-.11670E-06	.43061E-07	-.240	.104
22	.5442112E+01	.5508E-06	-.19213E-06	-.14156E-07	-.361	-.016
23	.5654166E+01	.2505E-03	-.47345E-06	-.34266E-07	-.177	-.068
24	.5655035E+01	.4005E-03	-.62048E-06	.10522E-09	-.031	.007
25	.5655948E+01	.3339E-03	-.67634E-06	.57572E-07	-.194	.107
26	.6027704E+01	.1116E-05	-.55003E-06	.60026E-07	-.501	.064
27	.6305731E+01	.1541E-05	-.77408E-06	.33654E-07	-.496	.022
28	.5042766E+01	.2618E-06	.00000E+00	.00000E+00	.001	-.113
29	.5051289E+01	.3482E-06	-.59798E-08	-.91109E-08	-.018	-.086
30	.5089816E+01	.2735E-06	-.20827E-07	-.27228E-08	-.065	-.129

31	.5256873E+01	.4112E-06	-.91922E-07	-.12676E-09	-.214	-.118
32	.5572505E+01	.3834E-06	-.71815E-07	-.29809E-07	-.169	-.310
33	.5752193E+01	.6215E-06	-.20053E-06	.45313E-07	-.302	-.173
34	.6312283E+01	.6171E-06	-.30388E-06	.69165E-08	-.493	-.435
35	.6952774E+01	.6083E-06	-.34471E-06	.84528E-08	-2.538	-.461
36	.1459595E+02	.1000E-07	-.37888E-07	-.63623E-07	-3.789	-6.362
37	.1562411E+02	.1000E-07	-.31710E-07	-.10064E-06	-3.171	-10.064
38	.4876073E+01	.1000E-07	.00000E+00	.00000E+00	.010	-.125
39	.4863675E+01	.1000E-07	-.96660E-10	-.13245E-08	-.010	-.132
40	.4896317E+01	.1000E-07	-.26425E-09	-.14870E-08	-.026	-.149
41	.4927095E+01	.1000E-07	-.90909E-09	-.24953E-08	-.091	-.250
42	.5068660E+01	.1000E-07	-.85174E-09	-.39166E-08	-.085	-.392
43	.5131513E+01	.1000E-07	-.19484E-08	-.50108E-08	-.195	-.501
44	.5545626E+01	.1000E-07	-.49525E-08	-.70445E-08	-.495	-.704
45	.6320102E+01	.1000E-07	-.20056E-07	-.20007E-07	-2.006	-2.001
46	.1019135E+02	.1000E-07	-.26186E-07	-.57147E-07	-2.619	-5.715
47	.1260484E+02	.1000E-07	-.21812E-07	-.71655E-07	-2.181	-7.166
48	.1616778E+02	.1000E-07	-.25903E-07	-.87876E-07	-2.590	-8.788
49	.1592212E+02	.1000E-07	-.18277E-07	-.87702E-07	-1.828	-8.770
50	.1566463E+02	.1000E-07	-.23550E-07	-.10317E-06	-2.355	-10.317
51	.4816904E+01	.6463E-08	.00000E+00	.00000E+00	.001	-.038
52	.4821218E+01	.6303E-08	-.13799E-10	-.26511E-09	-.002	-.035
53	.4822158E+01	.6467E-08	-.97627E-10	-.42005E-09	-.012	-.052
54	.4844887E+01	.6320E-08	-.11943E-09	-.51912E-09	-.019	-.069
55	.4867515E+01	.6496E-08	-.33397E-09	-.10649E-08	-.041	-.135
56	.4934786E+01	.6390E-08	-.47119E-09	-.12882E-08	-.074	-.180
57	.5044277E+01	.6648E-08	-.20787E-08	-.33288E-08	-.254	-.445
58	.5527514E+01	.7047E-08	-.43873E-08	-.59006E-08	-.612	-.806
59	.6511878E+01	.8325E-08	-.11298E-07	-.24020E-07	-1.206	-2.608
60	.7901708E+01	.1000E-07	-.96729E-08	-.39954E-07	-.967	-3.995
61	.8833383E+01	.1000E-07	-.13389E-07	-.54682E-07	-1.339	-5.468
62	.1093782E+02	.1000E-07	-.15567E-07	-.66569E-07	-1.557	-6.657
63	.1256955E+02	.1000E-07	-.15826E-07	-.75958E-07	-1.583	-7.596
64	.1538401E+02	.1000E-07	-.15563E-07	-.89119E-07	-1.556	-8.912
65	.1535788E+02	.1000E-07	-.31607E-08	-.79339E-07	-.316	-7.934
66	.1646585E+02	.1000E-07	-.80025E-09	-.89278E-07	-.080	-8.928
67	.1554994E+02	.1000E-07	-.17304E-10	-.81532E-07	-.002	-8.153
68	.1647097E+02	.1000E-07	.81182E-09	-.89300E-07	.081	-8.930
69	.1535510E+02	.1000E-07	.42007E-08	-.78854E-07	.420	-7.885
70	.1504556E+02	.1000E-07	.29767E-07	-.80028E-07	2.977	-8.003
71	.8210987E+01	.1000E-07	.00000E+00	.00000E+00	3.376	-4.910
72	.4801611E+01	.4364E-08	.00000E+00	.00000E+00	.000	-.009
73	.4801019E+01	.4296E-08	-.22133E-11	-.38073E-10	-.001	-.013
74	.4802157E+01	.4367E-08	-.23675E-11	-.40823E-10	-.001	-.012
75	.4802320E+01	.4315E-08	-.19583E-10	-.85122E-10	-.007	-.028
76	.4807134E+01	.4395E-08	-.11109E-10	-.12602E-09	-.003	-.036
77	.4808389E+01	.4398E-08	-.86666E-10	-.29009E-09	-.027	-.089
78	.4832243E+01	.4538E-08	-.11530E-09	-.48105E-09	-.025	-.130
79	.4869271E+01	.5211E-08	-.11603E-08	-.24660E-08	-.245	-.508
80	.5123076E+01	.6201E-08	-.14117E-08	-.53418E-08	-.227	-.895
81	.5413201E+01	.8758E-08	-.47685E-08	-.15715E-07	-.508	-1.683
82	.6069292E+01	.9770E-08	-.41186E-08	-.19871E-07	-.424	-2.009
83	.6431868E+01	.1000E-07	-.82867E-08	-.32398E-07	-.829	-3.240
84	.7613354E+01	.1000E-07	-.65153E-08	-.37563E-07	-.652	-3.756
85	.7995538E+01	.1000E-07	-.62488E-08	-.51807E-07	-.625	-5.181

86	.7575182E+01	.1000E-07	-.12817E-08	-.42957E-07	-.128	-4.296
87	.7282766E+01	.1000E-07	-.35186E-09	-.51219E-07	-.035	-5.122
88	.7650345E+01	.1000E-07	-.15172E-10	-.43552E-07	-.002	-4.355
89	.7286407E+01	.1000E-07	.28017E-09	-.51276E-07	.028	-5.128
90	.7588949E+01	.1000E-07	.14411E-08	-.43100E-07	.144	-4.310
91	.6940535E+01	.1000E-07	.11727E-07	-.39907E-07	1.173	-3.991
92	.5853640E+01	.1000E-07	.00000E+00	.00000E+00	.906	-1.227
93	.4800016E+01	.3719E-08	.00000E+00	.00000E+00	.000	-.000
94	.4800024E+01	.4108E-08	-.33473E-12	-.17500E-11	.000	-.000
95	.4800107E+01	.4110E-08	-.18359E-11	-.61531E-11	-.000	-.001
96	.4800749E+01	.4128E-08	-.18358E-10	-.37598E-10	-.004	-.006
97	.4807518E+01	.4306E-08	-.17604E-09	-.39757E-09	-.031	-.060
98	.4843069E+01	.5125E-08	-.72496E-09	-.22064E-08	-.103	-.272
99	.4986232E+01	.6130E-08	-.16527E-08	-.72937E-08	-.180	-.764
100	.5114460E+01	.6143E-08	-.46036E-09	-.10782E-07	-.054	-1.132
101	.5130018E+01	.6143E-08	-.62161E-11	-.11214E-07	-.001	-1.181
102	.5117333E+01	.6143E-08	.62787E-09	-.10873E-07	.080	-1.136
103	.4800000E+01	.5500E-08	.26281E-08	-.63428E-08	.293	-.651
104	.4799999E+01	.1000E-08	.00000E+00	.00000E+00	.000	.000
105	.4800001E+01	.1000E-08	-.18807E-15	-.41455E-14	.000	.000
106	.4799998E+01	.1000E-08	-.49893E-14	-.15465E-13	.000	.000
107	.4799995E+01	.1000E-08	-.45463E-13	-.10182E-12	.000	-.000
108	.4800005E+01	.1000E-08	-.48093E-12	-.98313E-12	-.000	-.001
109	.4800072E+01	.1000E-08	-.25245E-11	-.60155E-11	-.003	-.006
110	.4800406E+01	.1000E-08	-.10064E-10	-.27274E-10	-.010	-.027
111	.4800953E+01	.1000E-08	-.90250E-11	-.59557E-10	-.009	-.060
112	.4801270E+01	.1000E-08	-.11254E-11	-.76658E-10	-.001	-.077
113	.4801278E+01	.1000E-08	.95282E-12	-.77002E-10	.001	-.077
114	.4800752E+01	.1000E-08	.22319E-10	-.37746E-10	.022	-.038
115	.4800000E+01	.1000E-08	.62621E-12	-.36325E-16	.001	.000
116	.4800006E+01	.1000E-08	.00000E+00	.00000E+00	.000	.000
117	.4800001E+01	.1000E-08	.00000E+00	.00000E+00	.000	.000
118	.4800002E+01	.1000E-08	.00000E+00	.00000E+00	.000	.000
119	.4800001E+01	.1000E-08	.00000E+00	.00000E+00	.000	.000
120	.4800002E+01	.1000E-08	.00000E+00	.00000E+00	.000	.000
121	.4800004E+01	.1000E-08	.00000E+00	.00000E+00	.000	.000
122	.4800003E+01	.1000E-08	.00000E+00	.00000E+00	.000	-.000
123	.4800005E+01	.1000E-08	.00000E+00	.00000E+00	.000	-.000
124	.4800004E+01	.1000E-08	.00000E+00	.00000E+00	.000	-.000
125	.4800005E+01	.1000E-08	.00000E+00	.00000E+00	.000	-.000
126	.4800000E+01	.1000E-08	.31425E-12	-.13868E-12	.000	-.000

SPLINE INTERPOLATION: A MEANS OF INTERFACING FINITE ELEMENT ANALYSIS AND LIMIT EQUILIBRIUM ANALYSIS

D.V.B. McClarty and D.G. Fredlund
Department of Civil Engineering,
University of Saskatchewan,
Saskatoon, Saskatchewan, Canada, S7N 0W0

ABSTRACT

Geotechnical engineers can perform finite element seepage analyses to augment limit equilibrium slope stability analyses. Typically, a seepage analysis is used to provide pore-water pressure data which in turn is used in the calculation of the factor of safety of a slope. A method of interpolation must be implemented within the slope stability computer program that computes pore-water pressure at any specified location on the cross-section. However, depending on the type of interpolation procedure used, the number of known data points which can be used in the interpolations is limited by the available computer memory.

Spline Interpolation is a spatial interpolation procedure which is widely used to map variables from irregularly spaced data. Recent work has shown that Spline Interpolation is well-suited for interpolating pore-water pressure data for slope stability analyses. The objective of this study is to illustrate how the Spline Interpolation technique can be used as an accurate and cost effective means of interfacing a finite element seepage analysis and a limit equilibrium slope stability analysis. The Spline Interpolation method is compared to the linear least squares method and the inverse distance methods on the basis of estimation accuracy and computing time.

INTRODUCTION

The pore-water pressure conditions in a soil have a significant effect on its strength. As a result, geotechnical engineers perform finite element seepage analyses to augment limit equilibrium slope stability analyses. Typically, a seepage analysis is used to provide pore-water pressure data which in turn is used in the calculation of the factor of safety of a slope. When performing a slope stability analysis, the pore-water pressure values are generally required at positions which fall between the nodes of the finite element mesh. As a result, a method of interpolation is required within the slope stability computer program in order to compute pore-water pressure at any specified location on the cross-section. Factors such as estimation accuracy, computer memory requirements and computational speed must be considered when selecting an appropriate interpolation scheme.

A numerical procedure known as Spline Interpolation was incorporated into the slope stability computer program PC-SLOPE as a means of interpolating pore-water pressure (Fredlund and Fredlund, 1987). Prior to the implementation of this technique, PC-SLOPE relied exclusively on a distance weighting technique known as 4-Way Interpolation for its pore-water pressure estimates. A study conducted by Fredlund et al (1988) showed that, on the basis of estimation accuracy and consistency, the Spline Interpolation technique was superior to the 4-Way Interpolation method. However, because the Spline Interpolation method requires significant computer memory, the number of known data points which can be analyzed (on a microcomputer) within a slope stability computer program is somewhat limited. In the case of PC-SLOPE, Spline Interpolation can be used only when 50 or fewer points are designated. When more than 50 points are specified, the 4-Way Interpolation procedure must be used.

The degree of discretization of the finite element meshes used to analyze seepage problems varies. Typically, these meshes contain from 100 to 1000 or more nodes. Until now, the 4-Way Interpolation method was used within PC-SLOPE when a large number of pore-pressure values were input from a finite element seepage analysis. Fredlund and Barbour (1988) showed that the Spline Interpolation method was a superior alternative to the 4-Way Interpolation method. Therefore, it would be desirable to use the Spline Interpolation method when the number of known data points exceeds 50.

This study presents a procedure for reducing a large amount of finite element data to a smaller data set containing 50 or fewer representative points on a regular grid which can then be used to represent the pore-water pressure data for a slope stability analysis (Figure 1). The primary objective of this paper is to

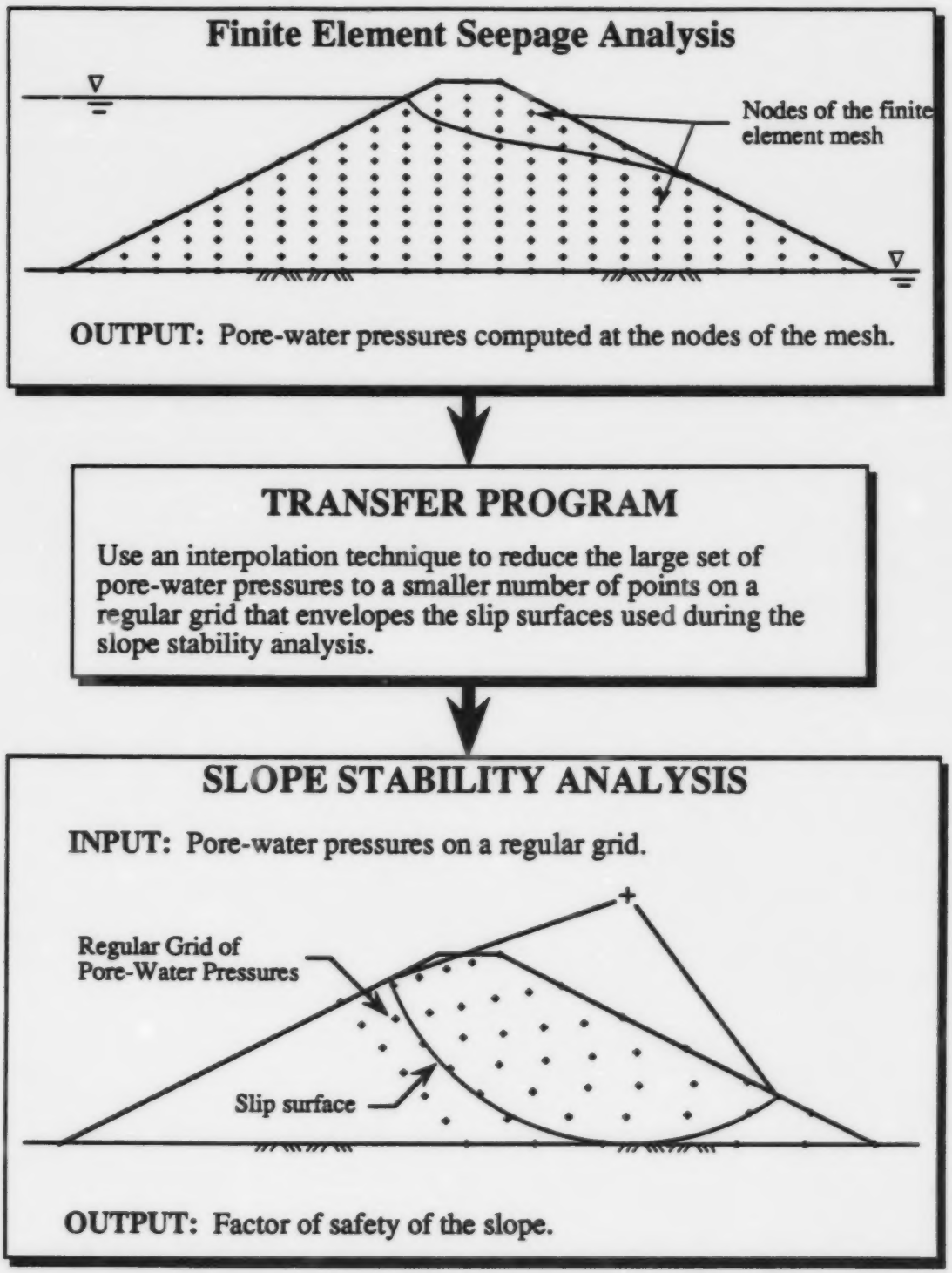
Finite Element Seepage Analysis
Nodes of the finite element mesh
OUTPUT: Pore-water pressures computed at the nodes of the mesh.
TRANSFER PROGRAM
Use an interpolation technique to reduce the large set of pore-water pressures to a smaller number of points on a regular grid that envelopes the slip surfaces used during the slope stability analysis.
SLOPE STABILITY ANALYSIS
INPUT: Pore-water pressures on a regular grid.
Regular Grid of Pore-Water Pressures
Slip surface
OUTPUT: Factor of safety of the slope.

Figure 1 Interfacing Seepage Analysis and Slope Stability Analysis.

present the results of study of the Spline Interpolation technique as an accurate and cost effective means of interfacing finite element data with slope stability analyses. A brief description of the theory associated with Spline Interpolation and comments on its interpolation characteristics are included in this paper. In addition, the results from a comparison of Spline Interpolation with the linear least squares method and the inverse distance methods are presented.

OVERVIEW OF THE SPLINE INTERPOLATION METHOD

Spline Interpolation is numerical procedure that can, given a set of known data points, estimate the value of a parameter at positions where the variable has not been measured or otherwise defined. The objective of this technique is to produce estimates that honor the data points and, at the same time, produce a "smooth" surface or curve. As a result, Spline Interpolation is particularly useful for generating contour maps or wireframe plots from irregularly spaced data .

To illustrate the basic principles of Spline Interpolation it is useful to recall the manual interpolation technique used by draftsmen to draw a smooth curve between a set of one dimensional data points. Thin strips of wood or metal called splines would be used to "fit" a curve to the data points. The draftsman would place weights at various positions along the curve which would fasten the strip. With the strip in place, a smooth continuous line that passed through all data points could then be traced.

For the two dimensional case, one could envision Spline Interpolation as the fitting of a thin plate to a set of two-dimensional coordinates. A function $\sigma(x,y)$ (i.e., an interpolating function) describing the shape of the plate is among all the functions, f, that honor the data points and the one that minimizes a quantity that is analogous to the mechanical energy required to deform a thin strip of infinite extent (Lancaster et al, 1986). The minimized quantity $A(f)$ is equal to (Dubrule, 1983):

$$[1] \quad A(f) = \int\int_{R^2} \left[\left(\frac{\partial^2 f}{\partial x^2} \right)^2 + \left(\frac{\partial^2 f}{\partial y^2} \right)^2 + 2 \left(\frac{\partial^2 f}{\partial x \partial y} \right)^2 \right]$$

where:

x = coordinate in the x direction
y = coordinate in the y direction
f = all functions that honor the data points

The interpolating function $\sigma(x,y)$ relative to N data points is written as (Duchon, 1975):

$$[2] \quad \sigma(x,y) = a + bx + cy + \sum_{i=1}^{N} \lambda_i h_i^2 \log h_i$$

where a, b, c and λ_i are weighting coefficients and h_i is the distance between two points with coordinates x, y and x_i, y_i , that is:

$$h_i = \sqrt{(x - x_i)^2 + (y - y_i)^2}$$

The coefficients of equation [2] are solved by assembling a system of linear equations where:

$$[3] \quad \begin{cases} \sum_{i=1}^{N} \lambda_i = 0 \\ \sum_{i=1}^{N} \lambda_i x_i = \sum_{i=1}^{N} \lambda_i y_i = 0 \\ \sigma(x_i, y_i) = Z(x_i, y_i) \end{cases}$$

The third condition in equation [3] ensures that the estimated values are equal to the known values at the data points. For a complete description of the mathematical details associated with the Spline Interpolation method, see Ahlberg et al (1967) and Lancaster et al (1986).

From equations [2] and [3] one can see that for N data points the solution of a N+3 by N+3 symmetric matrix is required to determine the weighting coefficients (i.e., a, b, c and λ_i). As a result, the computer memory required to store the matrix (and the time required to solve the matrix) increases as N^2. However, the matrix need only be solved once to compute estimates at any number of points within the domain of the known data points. This becomes an important consideration when repeated estimates are needed in a given region (e.g., pore-water pressure estimates along repeated slip surface trials during a slope stability analysis).

RELATIONSHIP BETWEEN SPLINE INTERPOLATION AND UNIVERSAL KRIGING

Under specific criteria, Spline Interpolation is equivalent to another popular interpolation technique known as Universal Kriging (Matheron, 1981); an estimation technique that has been used extensively in the mining industry. Kriging, like Spline Interpolation, determines a set of weighting coefficients (i.e., called kriging coefficients) from a set of known data points and then is able to predict the value of the parameter at any other location. The Kriging technique determines the coefficients subject to a different criterion; that being the variance of the estimated values from the actual values being minimized. The Kriging technique strives to obtain estimates which are, on average, as close as possible to the actual values. Spline Interpolation, on the other hand, uses the shape of the interpolating function to determine the weighting coefficients which results in estimates that are optimized for aesthetics (i.e., "smoothness") rather than accuracy (Dubrule, 1984).

In order to minimize the estimation variance, it is necessary to know the statistical structure of the variable under study. This involves determining the degree of "drift" in the data (i.e., how the variable changes with respect to its position within the region of interest) and the form of the generalized covariance (i.e., how the value of the parameter varies with respect to distance and direction between data points) (Matheron, 1973). Given N known data points $Z(x_i)$, the kriging estimator $Z^*(x)$ is equal to:

$$[4] \quad Z^*(x) = m(x) + \sum_{i=1}^{N} \lambda_i K(x_i - x)$$

where:

x	= one, two or three-dimensional coordinates
$x_i - x$	= distance between two data points x and x_i
$m(x)$	= drift function
$K(x_i - x)$	= generalized covariance

In two dimensions, the Spline Interpolation technique is equivalent to the Kriging technique when kriging with a linear drift (Matheron, 1981):

$$m(x) = a + bx + cy$$

and a generalized covariance of the form:

$$K(h_i) = h_i^2 \log h_i$$

where:

$$h_i = \sqrt{(x - x_i)^2 + (y - y_i)^2}$$

The Kriging technique requires that the drift and the generalized covariance be determined using a structural analysis. This procedure can be computationally intensive and requires a significant knowledge of geostatistics. Since Spline Interpolation does not require a structural analysis, it can be more easily implemented for use with applications such as slope stability. However, without a structural analysis it is impossible to ascertain how well the chosen drift and covariance functions fit the given data.

OTHER INTERPOLATION TECHNIQUES: TREND SURFACE AND INVERSE DISTANCE METHODS

Linear Trend Surface Method

Engineers often use trend surface analyses to fit a surface to data values. The trend surface analysis is useful for showing broad features of the data. In most cases it is used to remove those broad features in order to allow some other estimation technique (such as Kriging) to work with the residuals (Ripley, 1981). The trend surface is usually a low order polynomial function fit to the data by the least squares technique. In two dimensions, these functions are:

a	= a flat function
$a + bx + cy$	= a linear function
$a + bx + cy + dx^2 + exy + fy^2$	= a quadratic function

The linear trend surface function (or drift as we called it in the preceding section) comprises the first portion of the Spline Interpolation estimator (i.e., equation [2]). This is equivalent to passing a sloping two-dimensional plane through the set of data points. Figure 2(a) shows a surface of an aggregate deposit generated from 80 data points using Spline Interpolation while Figure 2(b) shows a linear trend surface generated using the same data. Even though the trend surface is the best least squares fit of the data, this type of plot does not give the analyst a proper feel for local variations of the surface. On the other hand, the plot generated using Spline Interpolation provides a much better perspective for viewing both small and large scale fluctuations.

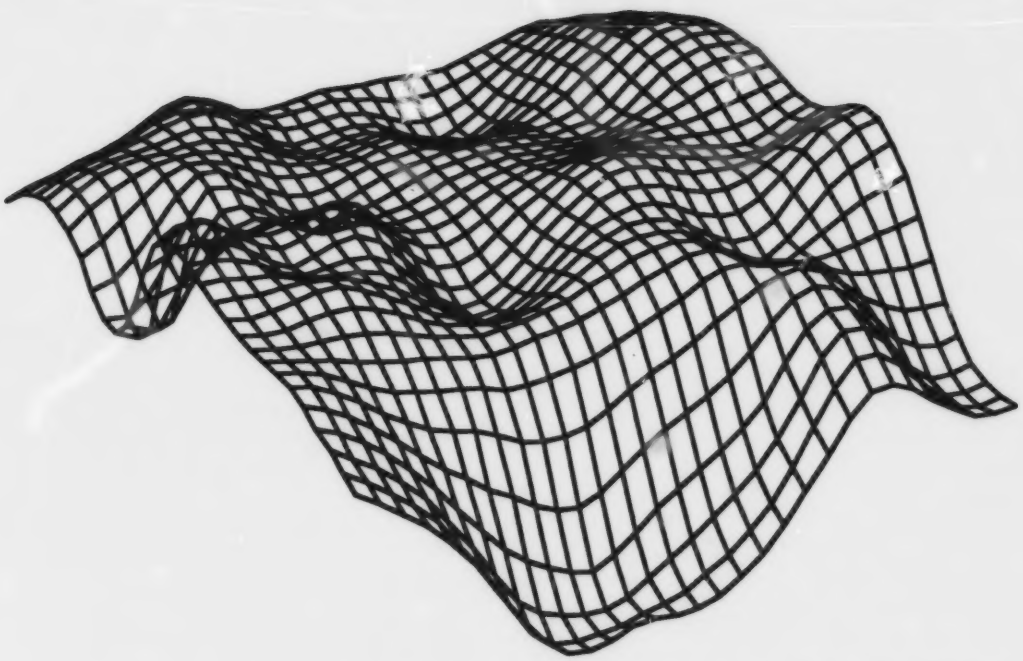

Figure 2(a) Plot of gravel surface generated using the Spline Interpolation technique.

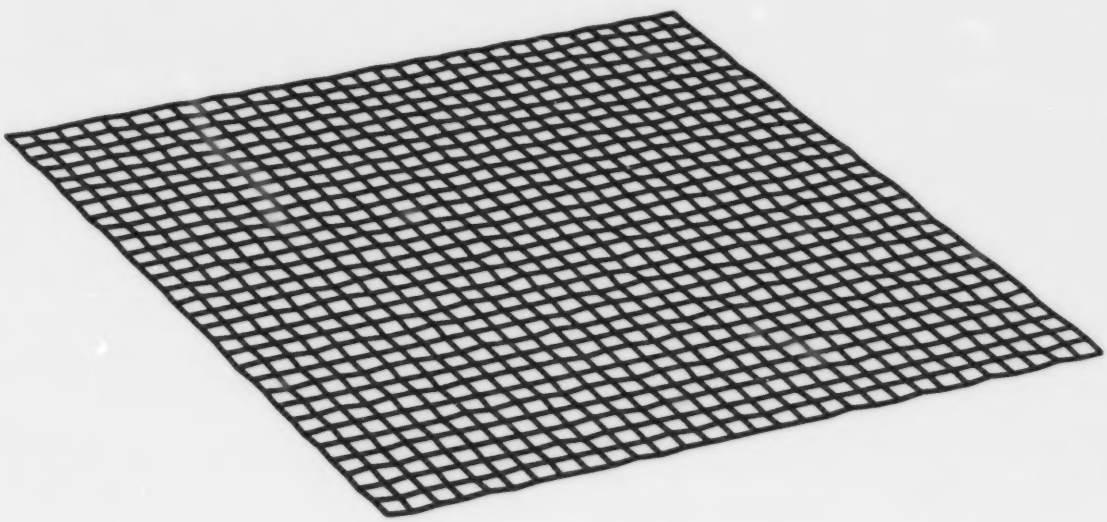

Figure 2(b) Plot of gravel surface generated using the linear least squares method.

Inverse Distance Method

The inverse distance method is a fast and simple interpolation method. Using this technique, the value of the point being estimated is a weighted average of the values at the known data points. The weights are computed as a function of the distances between the point of estimation and the data points:

$$[5] \quad Z^* = \frac{\sum_{i=1}^{n} \frac{Z_i}{d_i^r}}{\sum_{i=1}^{n} \frac{1}{d_i^r}}$$

where:

Z^* = estimated value
Z_i = the value of the neighboring point
d_i = distance to the neighboring point
n = the number of points used in the interpolation
r = the weighting power

The data points are weighted such that the influence of one data point on another declines with distance from the point being estimated. The greater the weighting power, r, the faster the decline in influence and the less effect the data point further away from the point under estimation will have on the computed value. A weighting power of 1 or 2 is used for most applications.

Surfaces produced by the inverse distance method show the major features of the variable but, at the same time, tend to be somewhat irregular. The inverse distance method, unlike the Kriging or the Spline Interpolation methods, is not an exact interpolator (i.e., if the point of estimation coincides with a known data point, the estimated value is not necessarily equal to the measured value). When the point of estimation is "close" to a known data point, the estimate must be forced to equal the measured value. This tends to produce sharp spikes in the surface at the known data points. By comparing the two plots in Figures 3(a) and (b) with those generated from the same data in Figures 2(a) and (b), it can be seen that as the weighting power, r, increases from 1 to 2 the spikes become less pronounced. At the same time, the general shape of the surface becomes more irregular. The inverse distance method is also susceptible to clusters in the data points (Ripley, 1981). For example, a cluster of points near the point of estimation will tend to overshadow any influence of the other points used in the

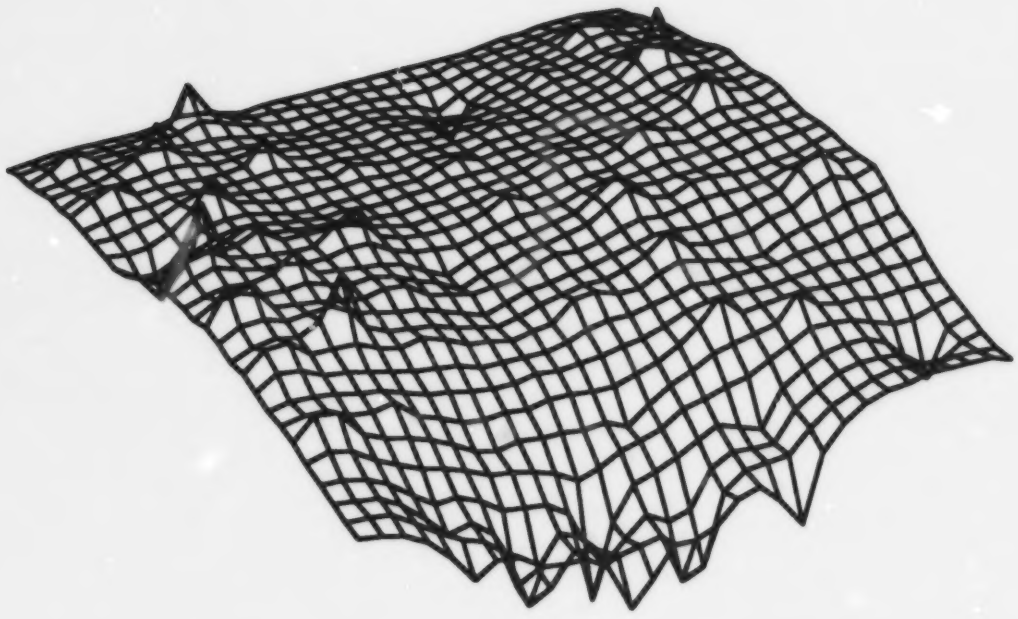

Figure 3(a) Plot of gravel surface generated using the inverse distance method.

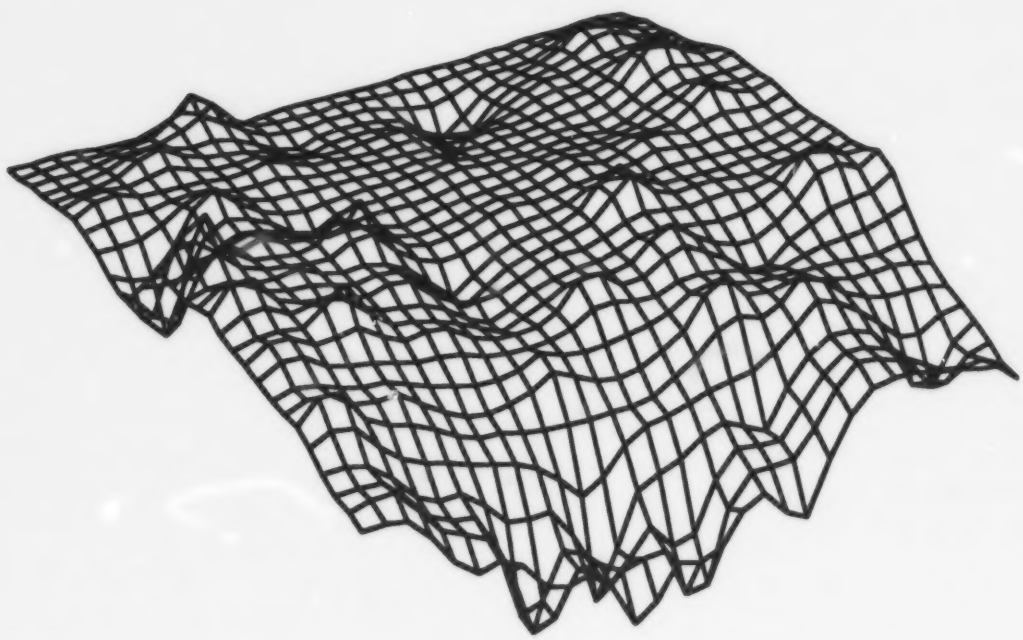

Figure 3(b) Plot of gravel surface generated using the inverse distance squared method.

interpolation. In addition, a surface generated from a set of points that lie on an inclined plane will tend not to look anything like a plane. However, in spite of its drawbacks, the inverse distance method is adequate for many engineering applications.

EVALUATION OF THE INTERPOLATION METHODS

A benchmark example is studied to evaluate the Spline Interpolation, the linear least squares, the inverse distance and the inverse distance squared methods as a means of interfacing finite element seepage analysis data and limit equilibrium slope stability analyses. All interpolation methods are used to generate a rectangular grid of representative pore-water pressure heads over a section of the finite element mesh that envelopes the critical slip surface region. The grid of estimates is then used within the slope stability analysis to compute the factor of safety of the critical slip surface. With these results and the knowledge of an accurate factor of safety for the slope, the interpolation methods are compared on the basis of estimation accuracy. The computational time required to generate the grid of estimates is also used as a basis of comparison.

Description of The Example Problem

An example from the PC-SEEP user's manual (Krahn, 1987) was used to illustrate the transfer of data from a finite element seepage analysis to a slope stability analysis. This example illustrates steady state seepage through a homogeneous earth dam with an impervious lower boundary (Figure 4). The dam cross-section was modelled with a uniform mesh containing 195 nodes and 336 elements. Pore-water pressure heads were computed at each of the nodes.

A preliminary slope stability analysis was performed to determine an accurate value for the factor of safety for the downstream face of the dam. The dam was assumed to have a homogeneous soil profile consisting of a sandy clay till with an unit weight of 19.33 kN/m^3, an angle of internal friction, Ø', of 29 degrees and a cohesion intercept, c', of 24 kPa.

Numerous slip surface positions were analyzed using all pore-water pressure heads and the conventional 4-Way Interpolation method. Once the critical slip surface was identified, the factor of safety was further refined by using a "piezometric line" to represent the pore-water pressures along the critical slip surface. The factor of safety obtained as a result of this analysis was 1.813. This factor of safety value is considered to be the accurate or "true" value since the piezometric line was considered to be the best possible representation of the pore-water pressures. For purposes of comparison, all subsequent slope stability analyses performed during this study used only the critical slip surface.

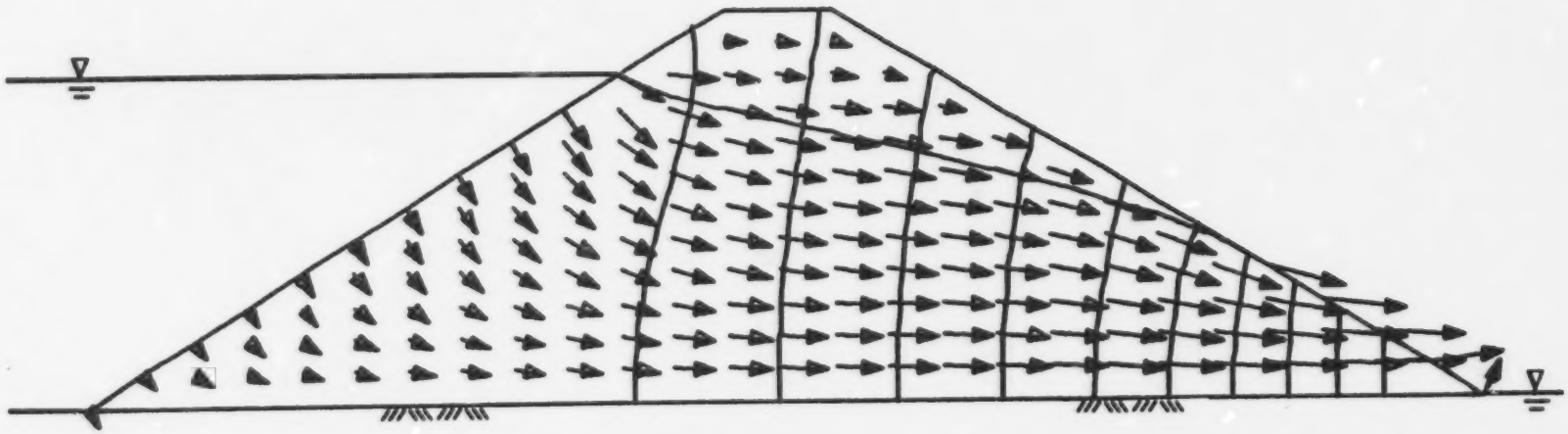

Figure 4 Steady state seepage through a homgenous earth dam.

Computer Programming

A small computer program called T-FER was developed specifically for this study. This program generates a grid of representative pore-water pressure points for any region of the finite element mesh. Spline Interpolation, linear least squares, inverse distance and inverse distance squared methods have been incorporated into the program. Interpolations can be performed using all of the available nodal heads or only those within a specified search radius. Also, by specifying a maximum number of nearest points, n, only the nearest points within the search radius are used in the interpolations. T-FER read nodal head values directly from the PC-SEEP file and wrote the grid of pore-water pressure estimates to a standard ASCII file. These results were then merged into a PC-SLOPE file for subsequent analyses.

Factor of Safety Results

All interpolation methods were used to compute pore-water pressure heads at the nodes of the same grid. In other words, the size and positioning of the grid of estimates were consistent for all analyses. The positioning of the 7 by 7 grid was such that it enveloped the region where the critical surface passed through the cross-section of the dam (Figure 5). The size of the grid chosen maximized the number of data points that can be used (i.e., when using the Spline Interpolation option) within PC-SLOPE.

The interpolation methods were analyzed for their sensitivity to the number of data points used in the interpolations. Each interpolation method was used to generate a grid of estimates using all data points in the finite element mesh (i.e., 195 points) and using the nearest 50, 30, 15, 10 and 5 data points. After each grid of estimates was computed, the generated data was used in two slope stability runs; one run to compute the factor of safety while using the Spline Interpolation method and one run to compute the factor of safety while using the 4-Way Interpolation method. All of the slope stability runs were configured identically to the preliminary slope stability analysis (i.e., single slip surface, same geometry and soil conditions, etc.).

The results of the slope stability runs are shown in Tables 1 and 2. Table 1 presents the factors of safety while using the Spline Interpolation method to interpolate pore-water pressures during the slope stability runs while Table 2 summarizes the factors of safety when the 4-Way Interpolation method is used. These results are presented graphically in Figures 6 and 7. All factors of safety were computed using the Bishop Simplified method.

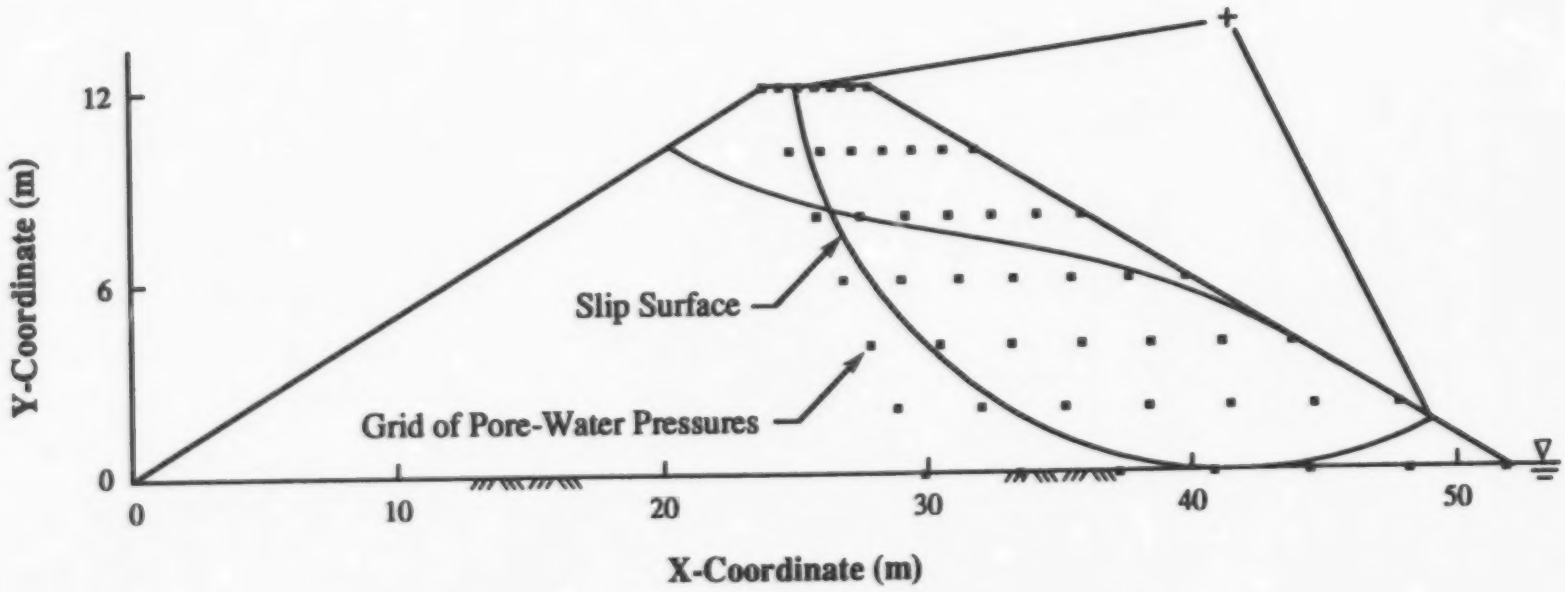

Figure 5 Grid of pore-water pressures superimposed on the cross-section of the dam.

Table 1:
Summary of The Factors of Safety
When Using The Spline Interpolation Option

Interpolation Method Used To Generate Grid	No. of Data Points Used In The Interpolations					
	195	50	30	15	10	5
Spline Interpolation	1.811	1.811	1.810	1.811	1.811	1.811
Linear Least Squares	1.773	1.830	1.819	1.812	1.811	1.811
Inverse Distance	1.834	1.928	1.912	1.890	1.868	1.866
Inverse Distance Squared	1.875	1.876	1.866	1.853	1.841	1.840

Table 2:
Summary of The Factors of Safety
When Using The 4-Way Interpolation Option

Interpolation Method Used To Generate Grid	No. of Data Points Used In The Interpolations					
	195	50	30	15	10	5
Spline Interpolation	1.852	1.851	1.850	1.853	1.853	1.853
Linear Least Squares	1.811	1.857	1.858	1.855	1.855	1.854
Inverse Distance	1.856	1.937	1.924	1.908	1.893	1.893
Inverse Distance Squared	1.897	1.896	1.889	1.882	1.874	1.875

The results shown in Table 1 and Figure 6 indicate that when the Spline Interpolation method was used to generate the grid of estimates, the computed factor of safety remained unchanged over the range of interpolation points tested. This consistent value of the factor of safety is, for all practical purposes, equal to the "true" factor of safety. These results illustrate the consistency of the Spline Interpolation method. The results show that for this example there is no significant benefit to using more than 5 data points for interpolation purposes. This can be attributed in a large part to the simple nature of the flow system studied. It is probable that had there been a more complex flow system involved, there would have been significant deviations in the factor of safety with a changing number of interpolation points.

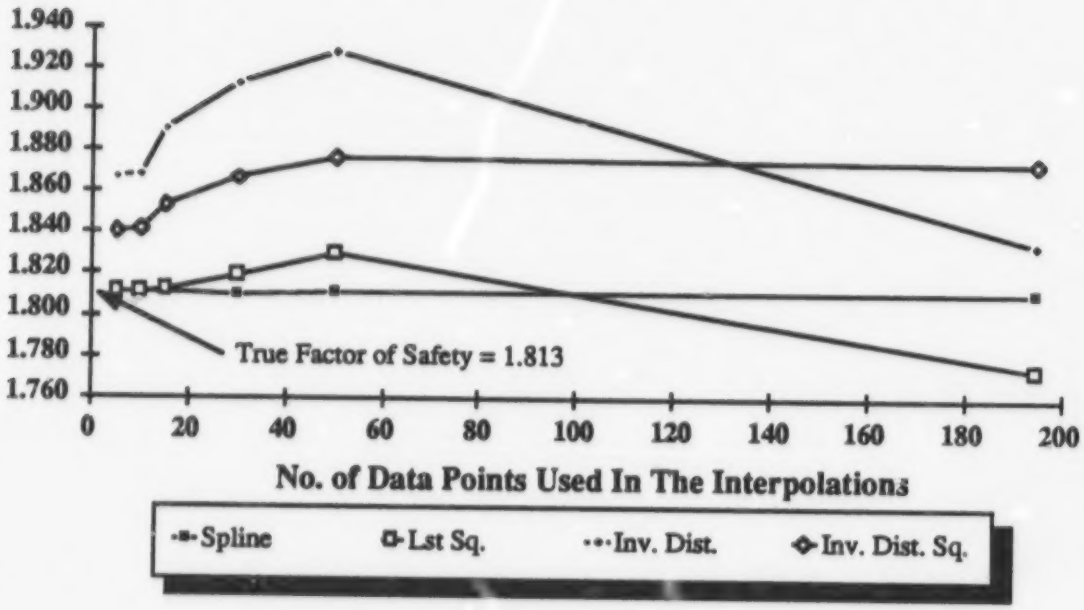

Figure 6 Factors of Safety when using the Spline Interpolation option.

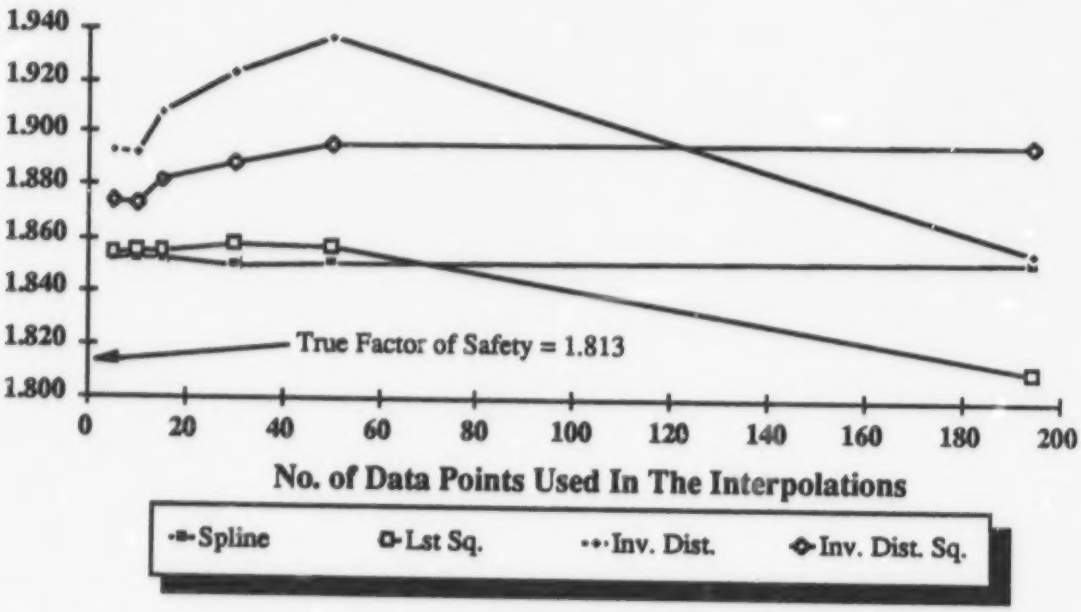

Figure 7 Factors of Safety when using the 4-Way Interpolation option.

The linear least squares method showed favorable factor of safety results when the number of data points used in each interpolation was kept at 15 or lower. In Figure 6, the least squares factor of safety began to deviate from the "true" value when more than 30 points were used. For a neighborhood of data points, the linear least squares estimator is a sloping two dimensional plane. As a result, it would be expected that this sloping plane would be adequate for small neighborhoods but would become a poorer estimate of the true surface as the size of the neighborhood increases. This trend is apparent in the factor of safety results. For example, the computed factor of safety is optimum when the neighborhood of data points is the smallest (i.e., 5 nearest data points) and is the least accurate when the neighborhood is the largest (i.e., all points in the finite element mesh). However, it is probable that a flow problem with large gradients could produce inaccuracies in the least squares method since a planar surface would not be a suitable estimate of the true pore-water pressure surface, even on a small scale. In these cases, the Spline Interpolation method would have a definite advantage over the linear least squares method. The Spline Interpolation method, because of its interpolation properties, is more apt to produce a surface that is a better estimate of the true surface at any scale.

The use of the inverse distance methods to generate grids of representative pore-water pressure heads resulted in the least accurate factor of safety results. The inverse distance method was significantly less accurate than the inverse distance squared method. Both methods showed a tendency to produce poorer estimates as the number of points in the search neighborhood increased which indicates that the interpolation properties of the inverse distance method are not particularly well suited to the spatial properties of the pore-water pressure data.

Figure 7 displays graphically the factors of safety that were computed when using the 4-Way Interpolation method to compute the pore-water pressures along the slip surface from the grids of representative points generated by the four interpolation methods. This exercise verifies the findings of the study conducted by Fredlund et al (1988). In other words, the Spline Interpolation method is superior to the 4-Way Interpolation method on the basis of its estimation accuracy. For almost every type of analysis (i.e., type of interpolation method used to generate the grid and the number of data points used in the interpolations), the use of the Spline Interpolation option in PC-SLOPE resulted in a more accurate factor of safety than when the 4-Way Interpolation option was used. These results also provide justification for the effort that must be expended to interface seepage analyses and slope stability analyses.

When the 4-Way Interpolation method is used to estimate pore-water pressure within a slope stability analysis there is no practical limit to the number of data points that a user can specify. As a result, all pore-water pressure data

from seepage analyses can be incorporated directly into the slope stability analysis. However, if it is desirable to achieve the benefits of the superior estimation capabilities of the Spline Interpolation method, it is important to spend some effort on the interfacing procedure.

Comparison of Computational Time

The time required to compute each grid of estimates was measured. A summary of the times is presented in Table 3 and shown graphically in Figure 8. Both inverse distance methods produced identical times and therefore their results have been summarized under one interpolation method. All tests were performed on a 10 MHz IBM XT compatible computer with a math coprocessor.

Table 3
Comparison of Computing Times Required to Generate The Grids of Pore-Water Pressure Heads

	Method Used to Generate Grid*		
No. of Points	Spline	Least Squares	Inverse Distance
195	329	169	13
50	550	361	36
30	183	135	26
15	49	41	12
10	25	23	12
5	16	14	12

*All times in seconds

The Spline Interpolation method and the linear least squares method require significantly more computing time than does the inverse distance methods. Moreover, the computing time increased more rapidly as the number of data points used in the interpolations increased. The least squares method was significantly faster than the Spline Interpolation method when 50 or more data points were used. However, when 30 or fewer neighboring points were used in the interpolations, the computational time required by both methods was essentially the same. All interpolation methods showed a marked drop in accuracy when all pore-water pressure points were used. In the case of the spline and least squares methods, this is a result of only having to solve for one large set of weighting coefficients as opposed to solving for 49 smaller sets. When all the data points are used in the inverse distance interpolations, the search for neighboring points is not required. As a result, a significant saving in computer time is realized.

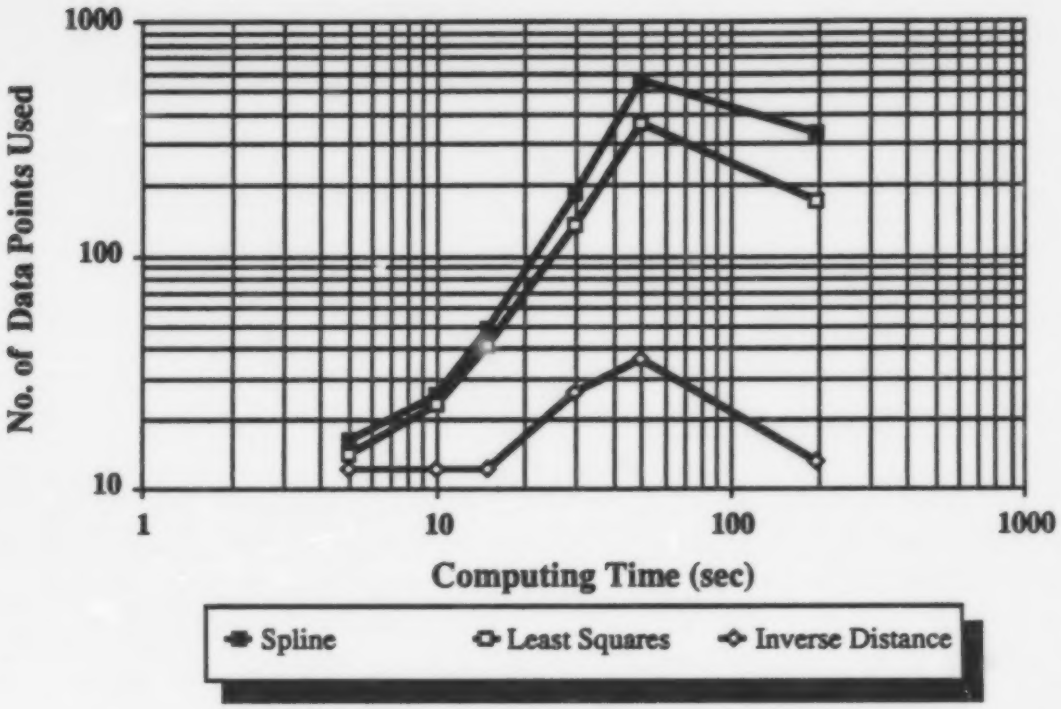

Figure 8 Comparison of computing times by the various interpolation techniques.

CONCLUDING REMARKS

The results of the study show that, on the basis of estimation accuracy and consistency, the inverse distance techniques are inferior to the Spline Interpolation and the linear least squares methods for interfacing seepage and slope stability analyses. The computing time advantage of the inverse distance methods does not offset the less accurate pore-water pressure estimations.

The Spline Interpolation and the linear least squares methods showed comparable results, both in terms of estimation accuracy and computational time. However, the linear least squares method did show a tendency to error as the number of data points used in the interpolations increased. This effect may become more pronounced when pore pressure changes are large and abrupt. It would be desirable to study other more complex flow problems to ascertain whether this is always the case. Based on the consistency of the pore-water pressure estimates over the entire range of data points tested, it can be seen that the Spline Interpolation method is the best interpolation method for interfacing finite element seepage analyses and limit equilibrium slope stability analyses.

REFERENCES

Ahlberg, J. H., Nilson, E. W., and Walsh, J. L., (1967). "The Theory of Splines and Their Applications", Academic Press, New York

Dubrule, O., (1983). "Two Methods With Different Objectives: Splines and Kriging", Mathematical Geology, Vol. 15, No. 2, pp. 245-257

Dubrule, O., (1984). "Comparing Splines and Kriging", Computers and Geosciences, Vol. 10, No. 2-3, pp. 327-338

Duchon, J., (1975). "Fonctions Splines du Type Plaque Mince en Dimension 2" Seminaire D'Analyse Numerique, Université de Grenoble, No. 231, pp 13.

Fredlund, D. G. and Barbour, S. L. (1988). "The Role of Kriging in Slope Stability Analysis" Proceedings of the CSCE Annual Conference, Calgary, Alberta, May, 1988

Fredlund, D.G. and Fredlund, L.D. (1987). "The PC-SLOPE Family of Software for Slope Stability Analysis", The First Canadian Symposium on Microcomputer Applications to Geotechnique, Oct. 22-23, 1987, pp. 173-181.

Krahn, J. (1987). "PC-SEEP User's Manual, A Finite Element Program for Seepage Analysis, S-40", Published by GEO-SLOPE Programming Ltd., Calgary, Alberta, pp. 6-3 to 6-40

Lancaster, P. and Salkauskas, K. (1986). "Curve and Surface Fitting: An Introduction", Academic Press, London

Matheron, G. (1973). "The Intrinsic Random Functions and Their Applications", Advances in Applied Probability, Dec. 1973, No. 5, pp. 439-468.

Matheron, G., (1981), "Splines and Kriging: Their Formal Equivalence", Down to Earth Statistics: Solutions Looking For Geological Problems. Syracuse University, Geology Contribution 8, pp. 77-95.

Ripley, B.D., (1981). "Spatial Statistics", Wiley-InterScience, New York

KR105.SET

```
QUESTION
     EXAMPLE.SET                = DATA FILE NAME
     APPENDIX EXAMPLE
     ONE                 = TRIAL NUMBER
     MARCH 16, 1990   = DATE
     USE OF PC-SEEP FOR -VE PWP
            25,          = # OF SLICES / SLIP SURFACE
        .01000,          = TOLERANCE
        .00000,          = SEISMIC COEFFICIENT
       9.80700,          = UNIT WEIGHT OF WATER
POINT      ,   66
    1,       .000,       6.900
    2,      8.400,       6.900
    3,     15.600,       8.700
    4,     20.400,       9.900
    5,     21.600,      10.200
    6,     26.400,      10.200
    7,     27.600,       9.900
    8,     32.400,       8.700
    9,     39.600,       6.900
   10,     48.000,       6.900
   11,       .000,       4.800
   12,     48.000,       4.800
   13,       .000,        .000
   14,     48.000,        .000
   15,     26.400,      11.400
   16,     31.200,      11.400
   17,     28.200,      15.000
  100,     1.000,     6.900
  101,     0.917,     7.450
  102,     0.833,     8.000
  103,     0.750,     8.550
  104,     0.667,     9.100
  105,     0.583,     9.650
  106,     0.500,     10.200
  107,     3.433,     6.900
  108,     2.997,     7.450
  109,     2.561,     8.000
  110,     2.125,     8.550
  111,     1.689,     9.100
  112,     1.253,     9.650
  113,     0.817,     10.200
  114,     5.867,     6.900
  115,     5.078,     7.450
  116,     4.289,     8.000
  117,     3.500,     8.550
  118,     2.711,     9.100
  119,     1.922,     9.650
  120,     1.133,     10.200
  121,     8.300,     6.900
  122,     7.158,     7.450
  123,     6.017,     8.000
  124,     4.875,     8.550
  125,     3.733,     9.100
  126,     2.592,     9.650
```

```
 127,     1.450,     10.200
 128,    10.733,      6.900
 129,     9.239,     7.450
 130,     7.744,     8.000
 131,     6.250,     8.550
 132,     4.756,     9.100
 133,     3.261,     9.650
 134,     1.767,     10.200
 135,    13.167,      6.900
 136,    11.319,      7.450
 137,     9.472,     8.000
 138,     7.625,     8.550
 139,     5.778,     9.100
 140,     3.931,     9.650
 141,     2.083,     10.200
 142,    15.600,      6.900
 143,    13.400,      7.450
 144,    11.200,      8.000
 145,     9.000,     8.550
 146,     6.800,     9.100
 147,     4.600,     9.650
 148,     2.400,     10.200
LINE      ,    6
  1,  1,  2,  3,  4,  5,  6,  7,  8,  9, 10,  0,  0,  0,  0,  0,  0,  0,  0
  2,  4,  7,  0,  0,  0,  0,  0,  0,  0,  0,  0,  0,  0,  0,  0,  0,  0,  0
  3,  3,  8,  0,  0,  0,  0,  0,  0,  0,  0,  0,  0,  0,  0,  0,  0,  0,  0
  4,  2,  9,  0,  0,  0,  0,  0,  0,  0,  0,  0,  0,  0,  0,  0,  0,  0,  0
  5, 11, 12,  0,  0,  0,  0,  0,  0,  0,  0,  0,  0,  0,  0,  0,  0,  0,  0
  6, 13, 14,  0,  0,  0,  0,  0,  0,  0,  0,  0,  0,  0,  0,  0,  0,  0,  0
SOIL      ,    6
    1,   18.0000,      .0000,    40.0000,      .0000,      .0000,      .0000
     Ballast
    2,   18.0000,     2.5000,    25.0000,    15.0000,      .0000,      .0000
     Sandy Silty Subballast
    3,   18.0000,     2.5000,    10.0000,    10.0000,      .0000,      .0000
     Clay Fill
    4,   18.0000,     5.0000,    10.0000,    10.0000,      .0000,      .0000
     Clay
    5,   18.0000,     5.0000,    15.0000,    15.0000,      .0000,      .0000
     Clay
    6,   18.0000,     5.0000,    20.0000,    15.0000,      .0000,      .0000
     Clay
TENSION   ,    0
GRID
   15,   16,   17
    4,    3
RADIUS
    2,    9
   13,   14
    6
SIDE
    1,                  1-CONSTANT FUNCTION
```

```
LAMBDA      ,     2
      .0000,   999.0000,       .0000,       .0000,       .0000,       .0000
LOAD        ,     0
POGH        ,    49
    100,     -2.09930
    101,     -2.64990
    102,     -3.20390
    103,     -3.76280
    104,     -4.28850
    105,     -4.83770
    106,     -5.37710
    107,     -2.09900
    108,     -2.64920
    109,     -3.21060
    110,     -3.74810
    111,     -4.29500
    112,     -4.83520
    113,     -5.37830
    114,     -2.07290
    115,     -2.64350
    116,     -3.19630
    117,     -3.74470
    118,     -4.29440
    119,     -4.83440
    120,     -5.37750
    121,     -2.09550
    122,     -2.61640
    123,     -3.16030
    124,     -3.73990
    125,     -4.28160
    126,     -4.83250
    127,     -5.37440
    128,     -1.64140
    129,     -2.63330
    130,     -2.89150
    131,     -3.67570
    132,     -4.27760
    133,     -4.84240
    134,     -5.37690
    135,     0.034500
    136,     -1.60270
    137,     -2.13490
    138,     -3.06880
    139,     -4.23230
    140,     -4.81510
    141,     -5.37930
    142,     -1.41000
    143,     0.236700
    144,     -1.89770
    145,     -3.55940
    146,     -4.04330
    147,     -4.71830
    148,     -5.37820
KRIG        ,
     0,
END
```

SAT5.FAC

File name : SAT5.FAC

GEO-SLOPE Ltd. \ P C - S L O P E \ SERIAL NO. 86070
Calgary, Alberta \ Slope Stability Analysis \ PROF. D.G. FREDLUND, PH.D.
\ (C) Copyright, 1987 \

PROJECT NAME ..: APPENDIX EXAMPLE
TRIAL NUMBER .: ONE DATE ..: MARCH 16, 1990
COMMENTS .....: USE OF PC-SEEP FOR -VE PWP

80=NO. OF SLIP SURFACES 4=NO. OF RADII 3=NO. OF FUNCTIONS
.0100=TOLERANCE 1=CONSTANT FUNCTION

SLIP NO.	X-COORD.	Y-COORD.	RADIUS	ITERATION NO.	LAMBDA	FACTOR OF SAFETY (MOMENT)	(FORCE)
1	8.400	11.100	1.165	1	.0000	999.000	999.000
1	8.400	11.100	1.165	2	.0000	999.000	999.000
1	8.400	11.100	1.165	3	.0000	999.000	999.000
2	8.400	11.100	1.485	1	.0000	999.000	999.000
2	8.400	11.100	1.485	2	.0000	999.000	999.000
2	8.400	11.100	1.485	3	.0000	999.000	999.000
3	8.400	11.100	4.881	1	.0000	2.721	3.164
3	8.400	11.100	4.881	10	.0000	2.899	2.578
3	8.400	11.100	4.881	27	.1149	2.900	2.898
4	8.400	11.100	8.627	1	.0000	2.591	3.306
4	8.400	11.100	8.627	10	.0000	3.063	2.400
4	8.400	11.100	8.627	31	.1110	3.068	3.067
5	9.600	11.100	1.831	1	.0000	999.000	999.000
5	9.600	11.100	1.831	2	.0000	999.000	999.000
5	9.600	11.100	1.831	3	.0000	999.000	999.000
6	9.600	11.100	.636	1	.0000	999.000	999.000
6	9.600	11.100	.636	2	.0000	999.000	999.000
6	9.600	11.100	.636	3	.0000	999.000	999.000
7	9.600	11.100	3.883	1	.0000	3.553	3.783
7	9.600	11.100	3.883	7	.0000	3.622	3.440
7	9.600	11.100	3.883	10	.1028	3.626	3.621
8	9.600	11.100	7.524	1	.0000	2.500	3.143
8	9.600	11.100	7.524	10	.0000	2.846	2.280
8	9.600	11.100	7.524	32	.1296	2.850	2.847
9	10.800	11.100	2.496	1	.0000	999.000	999.000
9	10.800	11.100	2.496	2	.0000	999.000	999.000
9	10.800	11.100	2.496	3	.0000	999.000	999.000
10	10.800	11.100	.212	1	.0000	999.000	999.000
10	10.800	11.100	.212	2	.0000	999.000	999.000
10	10.800	11.100	.212	3	.0000	999.000	999.000
11	10.800	11.100	2.884	1	.0000	999.000	999.000
11	10.800	11.100	2.884	2	.0000	999.000	999.000
11	10.800	11.100	2.884	3	.0000	999.000	999.000
12	10.800	11.100	6.421	1	.0000	2.431	2.889
12	10.800	11.100	6.421	9	.0000	2.641	2.255
12	10.800	11.100	6.421	23	.1306	2.645	2.645
13	12.000	11.100	3.162	1	.0000	999.000	999.000
13	12.000	11.100	3.162	2	.0000	999.000	999.000

13	12.000	11.100	3.162	3	.0000	999.000	999.000
14	12.000	11.100	1.061	1	.0000	999.000	999.000
14	12.000	11.100	1.061	2	.0000	999.000	999.000
14	12.000	11.100	1.061	3	.0000	999.000	999.000
15	12.000	11.100	1.886	1	.0000	999.000	999.000
15	12.000	11.100	1.886	2	.0000	999.000	999.000
15	12.000	11.100	1.886	3	.0000	999.000	999.000
16	12.000	11.100	5.318	1	.0000	2.593	2.907
16	12.000	11.100	5.318	7	.0000	2.722	2.447
16	12.000	11.100	5.318	11	.1354	2.723	2.717
17	13.200	11.100	3.828	1	.0000	4.824	4.842
17	13.200	11.100	3.828	5	.0000	4.835	4.825
17	13.200	11.100	3.828	6	.0342	4.835	4.834
18	13.200	11.100	1.909	1	.0000	999.000	999.000
18	13.200	11.100	1.909	2	.0000	999.000	999.000
18	13.200	11.100	1.909	3	.0000	999.000	999.000
19	13.200	11.100	.887	1	.0000	999.000	999.000
19	13.200	11.100	.887	2	.0000	999.000	999.000
19	13.200	11.100	.887	3	.0000	999.000	999.000
20	13.200	11.100	4.215	1	.0000	3.163	3.263
20	13.200	11.100	4.215	5	.0000	3.204	3.119
20	13.200	11.100	4.215	6	.1242	3.204	3.200
21	8.400	12.300	.166	1	.0000	999.000	999.000
21	8.400	12.300	.166	2	.0000	999.000	999.000
21	8.400	12.300	.166	3	.0000	999.000	999.000
22	8.400	12.300	2.333	1	.0000	999.000	999.000
22	8.400	12.300	2.333	2	.0000	999.000	999.000
22	8.400	12.300	2.333	3	.0000	999.000	999.000
23	8.400	12.300	5.547	1	.0000	2.810	3.042
23	8.400	12.300	5.547	7	.0000	2.913	2.725
23	8.400	12.300	5.547	10	.1085	2.914	2.909
24	8.400	12.300	9.100	1	.0000	2.450	3.011
24	8.400	12.300	9.100	8	.0000	2.794	2.281
24	8.400	12.300	9.100	17	.1236	2.797	2.800
25	9.600	12.300	.832	1	.0000	999.000	999.000
25	9.600	12.300	.832	2	.0000	999.000	999.000
25	9.600	12.300	.832	3	.0000	999.000	999.000
26	9.600	12.300	1.485	1	.0000	999.000	999.000
26	9.600	12.300	1.485	2	.0000	999.000	999.000
26	9.600	12.300	1.485	3	.0000	999.000	999.000
27	9.600	12.300	4.549	1	.0000	4.826	4.928
27	9.600	12.300	4.549	6	.0000	4.843	4.762
27	9.600	12.300	4.549	7	.0856	4.845	4.842
28	9.600	12.300	7.997	1	.0000	2.283	2.748
28	9.600	12.300	7.997	7	.0000	2.516	2.109
28	9.600	12.300	7.997	12	.1445	2.518	2.515
29	10.800	12.300	1.498	1	.0000	999.000	999.000
29	10.800	12.300	1.498	2	.0000	999.000	999.000
29	10.800	12.300	1.498	3	.0000	999.000	999.000
30	10.800	12.300	.636	1	.0000	999.000	999.000
30	10.800	12.300	.636	2	.0000	999.000	999.000
30	10.800	12.300	.636	3	.0000	999.000	999.000
31	10.800	12.300	3.550	1	.0000	999.000	999.000

31	10.800	12.300	3.550	2	.0000	999.000	999.000
31	10.800	12.300	3.550	3	.0000	999.000	999.000
32	10.800	12.300	6.894	1	.0000	2.268	2.529
32	10.800	12.300	6.894	7	.0000	2.394	2.165
32	10.800	12.300	6.894	11	.1261	2.395	2.388
33	12.000	12.300	2.163	1	.0000	999.000	999.000
33	12.000	12.300	2.163	2	.0000	999.000	999.000
33	12.000	12.300	2.163	3	.0000	999.000	999.000
34	12.000	12.300	.212	1	.0000	999.000	999.000
34	12.000	12.300	.212	2	.0000	999.000	999.000
34	12.000	12.300	.212	3	.0000	999.000	999.000
35	12.000	12.300	2.552	1	.0000	999.000	999.000
35	12.000	12.300	2.552	2	.0000	999.000	999.000
35	12.000	12.300	2.552	3	.0000	999.000	999.000
36	12.000	12.300	5.791	1	.0000	2.814	2.990
36	12.000	12.300	5.791	5	.0000	2.870	2.715
36	12.000	12.300	5.791	7	.1501	2.872	2.872
37	13.200	12.300	2.829	1	.0000	999.000	999.000
37	13.200	12.300	2.829	2	.0000	999.000	999.000
37	13.200	12.300	2.829	3	.0000	999.000	999.000
38	13.200	12.300	1.061	1	.0000	999.000	999.000
38	13.200	12.300	1.061	2	.0000	999.000	999.000
38	13.200	12.300	1.061	3	.0000	999.000	999.000
39	13.200	12.300	1.553	1	.0000	999.000	999.000
39	13.200	12.300	1.553	2	.0000	999.000	999.000
39	13.200	12.300	1.553	3	.0000	999.000	999.000
40	13.200	12.300	4.688	1	.0000	50.577	50.561
40	13.200	12.300	4.688	5	.0000	50.577	50.595
40	13.200	12.300	4.688	6	-.2007	50.577	50.583
41	8.400	13.500	.832	1	.0000	999.000	999.000
41	8.400	13.500	.832	2	.0000	999.000	999.000
41	8.400	13.500	.832	3	.0000	999.000	999.000
42	8.400	13.500	3.182	1	.0000	999.000	999.000
42	8.400	13.500	3.182	2	.0000	999.000	999.000
42	8.400	13.500	3.182	3	.0000	999.000	999.000
43	8.400	13.500	6.213	1	.0000	3.175	3.309
43	8.400	13.500	6.213	6	.0000	3.233	3.119
43	8.400	13.500	6.213	7	.1043	3.233	3.229
44	8.400	13.500	9.572	1	.0000	2.323	2.751
44	8.400	13.500	9.572	7	.0000	2.566	2.177
44	8.400	13.500	9.572	6	.1337	2.570	2.567
45	9.600	13.500	.166	1	.0000	999.000	999.000
45	9.600	13.500	.166	2	.0000	999.000	999.000
45	9.600	13.500	.166	3	.0000	999.000	999.000
46	9.600	13.500	2.333	1	.0000	999.000	999.000
46	9.600	13.500	2.333	2	.0000	999.000	999.000
46	9.600	13.500	2.333	3	.0000	999.000	999.000
47	9.600	13.500	5.214	1	.0000	12.830	12.853
47	9.600	13.500	5.214	5	.0000	12.825	12.808
47	9.600	13.500	5.214	6	.0338	12.826	12.825
48	9.600	13.500	8.469	1	.0000	1.986	2.244
48	9.600	13.500	8.469	6	.0000	2.135	1.898
48	9.600	13.500	8.469	9	.1397	2.133	2.129
49	10.800	13.500	.499	1	.0000	999.000	999.000
49	10.800	13.500	.499	2	.0000	999.000	999.000
49	10.800	13.500	.499	3	.0000	999.000	999.000

50	10.800	13.500	1.485	1	.0000	999.000	999.000
50	10.800	13.500	1.485	2	.0000	999.000	999.000
50	10.800	13.500	1.485	3	.0000	999.000	999.000
51	10.800	13.500	4.216	1	.0000	999.000	999.000
51	10.800	13.500	4.216	2	.0000	999.000	999.000
51	10.800	13.500	4.216	3	.0000	999.000	999.000
52	10.800	13.500	7.366	1	.0000	2.436	2.599
52	10.800	13.500	7.366	6	.0000	2.501	2.356
52	10.800	13.500	7.366	7	.1321	2.503	2.502
53	12.000	13.500	1.165	1	.0000	999.000	999.000
53	12.000	13.500	1.165	2	.0000	999.000	999.000
53	12.000	13.500	1.165	3	.0000	999.000	999.000
54	12.000	13.500	.636	1	.0000	999.000	999.000
54	12.000	13.500	.636	2	.0000	999.000	999.000
54	12.000	13.500	.636	3	.0000	999.000	999.000
55	12.000	13.500	3.217	1	.0000	999.000	999.000
55	12.000	13.500	3.217	2	.0000	999.000	999.000
55	12.000	13.500	3.217	3	.0000	999.000	999.000
56	12.000	13.500	6.263	1	.0000	3.645	3.689
56	12.000	13.500	6.263	5	.0000	3.652	3.615
56	12.000	13.500	6.263	6	.0980	3.654	3.652
57	13.200	13.500	1.831	1	.0000	999.000	999.000
57	13.200	13.500	1.831	2	.0000	999.000	999.000
57	13.200	13.500	1.831	3	.0000	999.000	999.000
58	13.200	13.500	.212	1	.0000	999.000	999.000
58	13.200	13.500	.212	2	.0000	999.000	999.000
58	13.200	13.500	.212	3	.0000	999.000	999.000
59	13.200	13.500	2.219	1	.0000	999.000	999.000
59	13.200	13.500	2.219	2	.0000	999.000	999.000
59	13.200	13.500	2.219	3	.0000	999.000	999.000
60	13.200	13.500	5.160	1	.0000	999.000	999.000
60	13.200	13.500	5.160	2	.0000	999.000	999.000
60	13.200	13.500	5.160	3	.0000	999.000	999.000
61	8.400	14.700	1.830	1	.0000	999.000	999.000
61	8.400	14.700	1.830	2	.0000	999.000	999.000
61	8.400	14.700	1.830	3	.0000	999.000	999.000
62	8.400	14.700	4.030	1	.0000	999.000	999.000
62	8.400	14.700	4.030	2	.0000	999.000	999.000
62	8.400	14.700	4.030	3	.0000	999.000	999.000
63	8.400	14.700	6.878	1	.0000	4.276	4.343
63	8.400	14.700	6.878	5	.0000	4.303	4.250
63	8.400	14.700	6.878	6	.0784	4.303	4.300
64	8.400	14.700	10.045	1	.0000	2.133	2.420
64	8.400	14.700	10.045	6	.0000	2.297	2.035
64	8.400	14.700	10.045	5	.1329	2.299	2.296
65	9.600	14.700	1.165	1	.0000	999.000	999.000
65	9.600	14.700	1.165	2	.0000	999.000	999.000
65	9.600	14.700	1.165	3	.0000	999.000	999.000
66	9.600	14.700	3.182	1	.0000	999.000	999.000
66	9.600	14.700	3.182	2	.0000	999.000	999.000
66	9.600	14.700	3.182	3	.0000	999.000	999.000
67	9.600	14.700	5.880	1	.0000	999.000	999.000
67	9.600	14.700	5.880	2	.0000	999.000	999.000
67	9.600	14.700	5.880	3	.0000	999.000	999.000

68	9.600	14.700	8.942	1	.0000	2.081	2.268
68	9.600	14.700	8.942	5	.0000	2.181	2.010
68	9.600	14.700	8.942	4	.1567	2.179	2.186
69	10.800	14.700	.499	1	.0000	999.000	999.000
69	10.800	14.700	.499	2	.0000	999.000	999.000
69	10.800	14.700	.499	3	.0000	999.000	999.000
70	10.800	14.700	2.333	1	.0000	999.000	999.000
70	10.800	14.700	2.333	2	.0000	999.000	999.000
70	10.800	14.700	2.333	3	.0000	999.000	999.000
71	10.800	14.700	4.881	1	.0000	999.000	999.000
71	10.800	14.700	4.881	2	.0000	999.000	999.000
71	10.800	14.700	4.881	3	.0000	999.000	999.000
72	10.800	14.700	7.839	1	.0000	2.823	2.893
72	10.800	14.700	7.839	5	.0000	2.839	2.780
72	10.800	14.700	7.839	6	.1036	2.842	2.839
73	12.000	14.700	.167	1	.0000	999.000	999.000
73	12.000	14.700	.167	2	.0000	999.000	999.000
73	12.000	14.700	.167	3	.0000	999.000	999.000
74	12.000	14.700	1.485	1	.0000	999.000	999.000
74	12.000	14.700	1.485	2	.0000	999.000	999.000
74	12.000	14.700	1.485	3	.0000	999.000	999.000
75	12.000	14.700	3.883	1	.0000	999.000	999.000
75	12.000	14.700	3.883	2	.0000	999.000	999.000
75	12.000	14.700	3.883	3	.0000	999.000	999.000
76	12.000	14.700	6.736	1	.0000	55.307	55.317
76	12.000	14.700	6.736	5	.0000	55.308	55.303
76	12.000	14.700	6.736	6	.0238	55.308	55.308
77	13.200	14.700	.832	1	.0000	999.000	999.000
77	13.200	14.700	.832	2	.0000	999.000	999.000
77	13.200	14.700	.832	3	.0000	999.000	999.000
78	13.200	14.700	.636	1	.0000	999.000	999.000
78	13.200	14.700	.636	2	.0000	999.000	999.000
78	13.200	14.700	.636	3	.0000	999.000	999.000
79	13.200	14.700	2.884	1	.0000	999.000	999.000
79	13.200	14.700	2.884	2	.0000	999.000	999.000
79	13.200	14.700	2.884	3	.0000	999.000	999.000
80	13.200	14.700	5.633	1	.0000	999.000	999.000
80	13.200	14.700	5.633	2	.0000	999.000	999.000
80	13.200	14.700	5.633	3	.0000	999.000	999.000

```
----------------------------------------
! SUMMARY OF MINIMUM FACTORS OF SAFETY !
----------------------------------------
MOMENT EQUILIBRIUM: FELLENIUS OR ORDINARY METHOD
      9.6000=X-COOR.      13.5000=Y-COOR.      8.4693=RADIUS          1.986=F.S.
MOMENT EQUILIBRIUM: BISHOP SIMPLIFIED METHOD
      9.6000=X-COOR.      13.5000=Y-COOR.      8.4693=RADIUS          2.135=F.S.
FORCE EQUILIBRIUM: JANBU SIMPLIFIED METHOD (NO fo FACTOR)
      9.6000=X-COOR.      13.5000=Y-COOR.      8.4693=RADIUS          1.898=F.S.
MOMENT AND FORCE EQUILIBRIUM: MORGENSTERN-PRICE OR GLE METHODS
      9.6000=X-COOR.      13.5000=Y-COOR.      8.4693=RADIUS          2.133=F.S.

NORMAL TERMINATION OF SLOPE
```